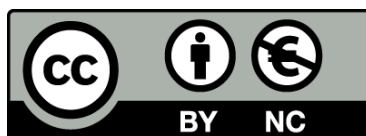




UNIVERSITAT DE  
BARCELONA

## Neuroblastoma cancer stem cells: The role of NXP1 and its receptor $\alpha$ -NRXN1

Lucía Fanlo Escudero



Aquesta tesi doctoral està subjecta a la llicència [Reconeixement- NoComercial 4.0. Espanya de Creative Commons](#).

Esta tesis doctoral está sujeta a la licencia [Reconocimiento - NoComercial 4.0. España de Creative Commons](#).

This doctoral thesis is licensed under the [Creative Commons Attribution-NonCommercial 4.0. Spain License](#).



UNIVERSITAT DE  
BARCELONA



Institut de Biologia Molecular de Barcelona  
Molecular Biology Institute of Barcelona  CSIC

UNIVERSITAT DE BARCELONA

FACULTAD DE FARMÀCIA I CIÈNCIES DE L'ALIMENTACIÓ

# Neuroblastoma cancer stem cells: The role of NXP1 and its receptor $\alpha$ -NRXN1



UNIVERSITAT DE BARCELONA  
FACULTAT DE FARMÀCIA I CIÈNCIES DE L'ALIMENTACIÓ  
PROGRAMA DE DOCTORAT EN BIOMEDICINA

# Neuroblastoma cancer stem cells: The role of NXP1 and its receptor $\alpha$ -NRXN1

Memoria presentada por  
Lucía Fanlo Escudero  
para optar al título de  
Doctora por la Universitat de Barcelona

Este trabajo ha sido realizado bajo la dirección de la Dra. Elisa Martí Gorostiza y del Dr. Gwenvael Le Dréau, en el Instituto de Biología Molecular de Barcelona (IBMB-CSIC)

---

Codirectores:

Dra. Elisa Martí Gorostiza

Dr. Gwenvael Le Dréau

Doctoranda:

Lucía Fanlo Escudero

Tutor:

Dr. Carles Enrich Bastús



[...]

CLARA.- (*Piensa:*) ¿Cómo es posible que alguien quiera dormir cuando hay tanta hermosura en el aire, en las rocas, en los árboles? Yo no quiero dormir nunca, nunca; no quiero perder ni un segundo de vida, por que ahora que he visto la maravilla de esta noche, me figuro que siempre deben estar sucediendo cosas maravillosas. Y si sucede una que no pueda ocurrir más que una vez y yo, por estarme durmiendo, no la veo, no me consolaré en mi vida entera.

Una risita suave responde a los exaltados pensamientos de Clara.

CLARA.- (*Un poco avergonzada, pregunta:*) ¿Quién se ríe de mí?

[...]

Viajes de una gota de agua

María de la O Lejárraga



*A mis padres,  
a mis hermanos,  
a Pablo*



---

## SUMMARY

Neuroblastoma (NB) is a devastating paediatric cancer that originates in the developing sympathetic nervous system. These tumours account for 40% of the cases of cancer diagnosed during the first year of life and 8% of the cases detected overall during childhood. They show a striking clinical diversity, ranging from spontaneous remission to fatal metastatic dissemination. To optimize therapeutic approaches, NB patients have been stratified into risk groups. For the high risk (HR) patients, the 5 years overall survival probability remains below 30-40%. The failure to successfully treat these HR patients mainly results from the therapy-resistance and metastatic potential harboured by these tumours. The large intra-tumour heterogeneity of the HR tumours seems to be a key factor contributing to tumour progression. Thereby, there is an urgent need to understand the biological diversity of the HR-NBs in order to develop efficient therapies for these patients. Interestingly, NBs show a marked scarcity of recurrent genetic changes even during relapse, pointing towards a relevant role of non-genetic sources of tumour heterogeneity. Compelling evidences suggest the existence of cells possessing a tumour-propagating capacity, called cancer stem cells or tumour-propagating cells (CSCs/TPCs), in these HR-NB tumours. Defining the heterogeneity of NBs and their stemness potential is thus fundamental to design new therapies targeting the driving force of the CSCs: their self-renewal ability.

The general aim of this doctoral thesis was to identify a genetic signature for neuroblastoma cancer stem cells (NBcsc), with the ultimate goal of providing new specific molecular markers of these NBcsc and candidate genes that might be useful for the development of future therapeutic strategies targeting the NBcsc in HR-NBs. It is assumed that NBcsc share many similarities with their normal stem cells counterparts, the neural crest cells (NCCs), which represent a transient embryonic population of pluripotent stem cells that give rise to the peripheral nervous system. Therefore, we compared the transcriptomic signature of NCCs with the transcriptomic profiles established for clinically relevant groups of NB patients. Among the candidates identified by our double screening, we retrieved Neurexophilin 1 (NXPH1): an extracellular glycoprotein known to bind to the transmembrane receptors of the alpha-Neurexin ( $\alpha$ -NRXN) family. To determine whether NXPH1/ $\alpha$ -NRXNs activity is effectively related to NBcsc, we analysed their expression in a panel of human NB cell lines in conditions of stem cell enrichment. The marked induction of  $\alpha$ -NRXN1/2 mRNA levels in the stem cell-enriched fraction suggested that they might be NBcsc markers. We identified the existence of a low subpopulation of  $\alpha$ -NRXN1+ cells in samples from human NB cell lines and patient-derived xenografts. We further established that these  $\alpha$ -NRXN1+ cells represent a functionally discrete subpopulation of NB cells characterized by: 1) an active cycling behaviour, 2) an increased self-renewal capacity, and 3) a higher probability to survive upon chemotherapeutic insult. Our data suggest that these  $\alpha$ -NRXN1+ NB cells are endowed with a tumour-propagating capacity and that they are required to sustain tu-

## SUMMARY

---

mour growth *in vivo*. In parallel, we investigated whether NXPH1 is implicated in NB malignancy. Our data revealed that NXPH1 promotes NB growth, possibly by stimulating the proliferation of actively dividing NB cells and by increasing the proportion of NB cells expressing the NCC stem cell marker p75NTR. Finally, we showed that inhibiting NXPH1 or  $\alpha$ -NRXN1 activity abrogates NB tumour growth in xenograft models.

Our work provides the first experimental evidence that NXPH1, probably acting through its receptor  $\alpha$ -NRXN1, exerts a functional role in NB progression. We suggest that NXPH1, present in the tumour microenvironment, controls the tumour-propagating capacity of NBcsc and that its reduced activity might facilitate the malignant progression of these tumours by enabling NBcsc to acquire a metastatic capacity.

---

## RESUMEN

El neuroblastoma (NB) es un tumor pediátrico del sistema nervioso simpático en desarrollo. La probabilidad de supervivencia de los pacientes de alto riesgo no supera el 30-40%. El estudio de la heterogeneidad celular del NB revela la probable existencia de células con capacidad de propagación tumoral (en inglés *cancer stem cells*, *CSCs*). Su identificación y caracterización es fundamental en la búsqueda de nuevos fármacos para dichos pacientes.

El objeto de esta tesis doctoral ha sido la identificación de la huella genética de las *CSCs* en el NB con la finalidad de identificar marcadores moleculares específicos y nuevas dianas terapéuticas. Para ello, partimos de la premisa de que las *CSCs* de los NBs deben de compartir ciertas características con sus equivalentes en el tejido sano, las células de la cresta neural (en inglés *neural crest cells*, *NCCs*), una población embrionaria de células madre que origina el sistema nervioso periférico. Al comparar el transcriptoma de las *NCCs* con el extraído de una comparación entre grupos de pacientes con relevancia clínica, seleccionamos la Neurexofilina 1 (NXP1), un ligando extracelular de las Neurexinas alfa ( $\alpha$ -NRXN). Para determinar si ambos están relacionados con el fenotipo de *CSCs*, analizamos su expresión en una colección de líneas celulares en condiciones de enriquecimiento para dicho fenotipo. El marcado aumento en los niveles de RNA mensajero de  $\alpha$ -NRXN1/2 sugirió que podrían funcionar como marcadores de las *CSCs*. Hemos confirmado la existencia de una población  $\alpha$ -NRXN1+ caracterizada por una mayor capacidad de proliferación, de replicación y de pervivencia a quimioterapia. Las células  $\alpha$ -NRXN1+ presentan características de *CSCs* y son requeridas para el crecimiento tumoral. En paralelo vemos que NXP1 promueve el crecimiento tumoral estimulando la proliferación y la presencia de células p75NTR+, marcador asociado a las *NCCs*. Además, la inhibición de NXP1 o  $\alpha$ -NRXN1 impide el crecimiento tumoral en modelos experimentales.

Este trabajo constituye la primera evidencia funcional del papel de NXP1 en la progresión del NB. Sugerimos que NXP1, probablemente a través de  $\alpha$ -NRXN1, participa en la regulación de la capacidad de propagación tumoral y que su pérdida favorece la adquisición de rasgos asociados a pacientes de alto riesgo.



---

# TABLE OF CONTENTS

ABBREVIATIONS	V
LIST OF FIGURES	VII
LIST OF TABLES	IX
<b>I. INTRODUCTION</b>	<b>1</b>
1. The neural crest	3
1.1. Induction, specification, delamination and migration	3
1.2. NCCs derivatives	5
1.3. Differentiation of the sympathoadrenal lineages	6
1.4. NCC-associated pathologies	8
2. Neuroblastoma: a paediatric tumour deriving from the embryonic sympathoadrenal lineage	8
2.1. Prevalence	8
2.2. Origin	9
2.3. Clinical presentation	9
2.4. Diagnosis	12
2.5. Histology of neuroblastic tumours	13
2.6. Risk factors and pathogenesis	15
2.7. Staging system and prognosis	21
2.8. Treatment	21
3. Cancer stem cells	24
3.1. Origins of tumour heterogeneity	25
3.2. The cancer stem cell concept	31
3.3. The cancer stem cell niche	42
3.4. Therapeutic targeting of the CSCs	43
3.5. CSCs in the context of NB	46
4. NXPH1 and its receptor $\alpha$ -NRXN1	48
4.1. Neurexophilin 1, a neuropeptide-like protein that modulates synaptic maturation	48
4.2. NXPH1 receptors, the $\alpha$ -Neurexins	50

---

II. HYPOTHESIS AND SPECIFIC AIMS.....	53
III. MATERIALS AND METHODS.....	57
1. Gene expression profiling and bioinformatic analysis.....	59
1.1. Genome-wide transcriptomic analysis for primary human NB.....	59
1.2. Genome-wide transcriptomic analysis for NCCs.....	60
1.3. Bioinformatic search for common DEGs in NB and NCCs signatures.....	60
1.4. Bioinformatic analysis of public NB datasets.....	61
2. Cell culture.....	61
2.1. Human cell lines.....	61
2.2. Sub-culturing, cell counting & cryopreservation of cell lines.....	62
2.3. Mycoplasma detection.....	63
2.4. MTT assay.....	63
2.5. BrdU assay.....	64
2.6. Tumour spheroid assay.....	64
2.7. In vitro 2-dimensions (2D) ELDA growth assay.....	65
2.8. Cell culture in the presence of chemotherapeutic drugs.....	66
3. Human NB patient derived xenograft.....	66
4. Generation of transgenic cell lines by lentiviral infection.....	67
4.1. DNA constructs.....	67
4.2. Design of shRNA sequence against target genes.....	70
4.3. Cloning of short-hairpin RNA sequences into pLKO.1-puro plasmid.....	71
4.4. Cloning of short-hairpin RNA sequences into pSLIK-Neo plasmid.....	73
4.5. Bacterial transformation.....	75
4.6. Amplification and purification of DNA constructs (minipreps & midipreps).....	76
4.7. Lentiviral production and transduction.....	76
4.8. Selection of transduced cell lines.....	77
5. Flow cytometry and cell sorting.....	77
5.1. Flow cytometry analysis of transgenic EGFP+ cells.....	78
5.2. Flow cytometry analysis of cell surface antigens in human NB cells.....	78

5.3. Flow cytometry analysis of cell cycle profile in $\alpha$ -NRXN1 positive and negative population..	80
5.4. Cell sorting.....	80
5.5. Data analysis.....	91
6. Animal models.....	81
6.1. Animal care and ethics permission.....	81
6.2. Chorioallantoic membrane (CAM) assay in chick embryos.....	83
6.3. Mouse strains.....	84
6.4. Heterotopic xenograft in mouse.....	85
7. Analysis of gene expression.....	87
7.1. RNA extraction.....	87
7.2. Synthesis of complementary DNA: Reverse-Transcription Polymerase Chain Reaction..	88
7.3. Relative quantification of cDNA: Quantitative Real-Time Polymerase Chain Reaction....	88
8. Histology and immunofluorescence.....	89
8.1. Cell and tissue processing.....	89
8.2. Immunofluorescence staining.....	90
8.3. Image acquisition and processing.....	90
9. Statistical analysis.....	91
<b>IV. RESULTS.....</b>	<b>93</b>
1. Identification of a genetic signature common to NCCs and NB malignancy.....	95
1.1. A double genetic screening identifies 6 genes that are both differentially expressed in clinically-relevant subgroups of NB patients and enriched in the early NCC lineage.....	95
1.2. Selection of <i>NXPH1</i> as a candidate gene for further studies.....	100
1.3. The NXPH1 receptors $\alpha$ -NRXN1 /2 show minimal differences between clinically-relevant subgroups of NB patients.....	100
2. The expression of <i>NXPH1</i> and its receptors $\alpha$ -NRXN1/2 positively correlates with NB stemness <i>in vitro</i> .....	102
3. The expression of $\alpha$ -NRXN1 identifies a subpopulation of NB cells with cancer stem cell-like properties that is required for NB growth.....	106
3.1. $\alpha$ -NRXN1 is expressed by a small subpopulation of cells in human NB cell lines and patient-derived xenografts.....	106
3.2. $\alpha$ -NRXN1 expression identifies a subpopulation of NB cells presenting cancer stem cell-like characteristics <i>in vitro</i> .....	107

---

3.3. Whether $\alpha$ -NRXN1+ cells are endowed with a specific transcriptome remains unknown.....	110
3.4. $\alpha$ -NRXN1+ cells are required for NB growth in vivo.....	110
4. NXP1 and its receptor $\alpha$ -NRXN1 sustain NB growth.....	112
4.1. Increasing NXP1 activity promotes NB growth in vivo.....	112
4.2. Inhibiting <i>NXP1</i> and $\alpha$ -NRXN1 expression impairs NB tumour formation and growth <i>in vivo</i> .....	114
V. DISCUSSION.....	125
1. NXP1 promotes primary NB growth through $\alpha$ -NRXN1+ NBcsc-like cells, but might inhibit metastasis and tumour progression.....	128
1.1. $\alpha$ -NRXN1+ NB cells are tumour-propagating cells.....	128
1.2. NXP1 is required to sustain tumour growth in NB.....	129
1.3. NXP1 expression inversely correlates with bad prognosis and tumour progression...131	
1.4. NXP1 might inhibit NB metastasis and/or tumour dissemination.....	133
2. NB malignant transformation and tumour progression are not a linear process.....	134
2.1. The process of malignant transformation is accompanied by a re-activation of a NCC-like program.....	135
2.2. The process of tumour progression is accompanied by a deactivation of certain NCC features and the loss of the niche-dependency.....	137
2.3. What is known about these other candidate genes in the context of NB and cancer...138	
3. The road ahead: unravelling tumour heterogeneity in the single cell genomics era.....	140
VI. CONCLUSIONS.....	143
VII. REFERENCES.....	147
VIII. APPENDICES.....	179
APPENDIX I.....	181
APPENDIX II.....	187
ACKNOWLEDGEMENTS.....	189

---

## ABBREVIATIONS

<b>ABC:</b>	ATP-binding cassette
<b>BMP:</b>	Bone Morphogenetic Protein
<b>BrdU:</b>	5-bromo-2'-deoxyuridine
<b>BSA:</b>	bovine serum albumin
<b>BSL-2:</b>	biological safety level 2
<b>cCap3+:</b>	activated cleaved-Caspase 3
<b>CNVs:</b>	copy number variations
<b>CRC:</b>	colorectal cancer
<b>CSCs:</b>	cancer stem cells
<b>DAPI:</b>	4',6-diamidino-2-phenylindole
<b>DEGs:</b>	differentially expressed genes
<b>DMSO:</b>	dimethyl sulfoxide
<b>DNAs:</b>	Desoxyribonucleic acids
<b>dsDNA:</b>	double stranded DNA
<b>E10:</b>	embryonic day 10
<b>EFS:</b>	event-free survival
<b>EMT:</b>	epithelial to mesenchymal transition
<b>FC:</b>	fold change
<b>FDR:</b>	false discovery rate
<b>GB:</b>	glioblastoma
<b>GFP:</b>	Green-Fluorescent Protein
<b>GM:</b>	growth media
<b>GN:</b>	ganglioneuroma
<b>GNB:</b>	ganglioneuroblastoma
<b>GPP:</b>	Genetic Perturbation Platform
<b>h:</b>	hours
<b>hESCs:</b>	human embryonic stem cells
<b>HK:</b>	housekeeping
<b>HR:</b>	high risk
<b>HSCs:</b>	haematopoietic stem cells
<b>HSJD:</b>	Hospital Sant Joan de Dèu
<b>INSS:</b>	International Neuroblastoma Staging System
<b>IR:</b>	Intermediate risk
<b>KO:</b>	knockout
<b>LR:</b>	low risk
<b>mg:</b>	miligrams
<b>min:</b>	minutes
<b>ml:</b>	millilitre
<b>mRNA:</b>	messenger RNA
<b>MTX:</b>	mitoxatrone
<b>NB:</b>	neuroblastoma

**NBcsc:** neuroblastoma cancer stem cells,  
**NCCs:** neural crest cells  
**NLG:** neuroligins  
**nc:** nucleotide  
**NT:** neural tube  
**NXPH1:** Neurexophilin 1  
**ON:** overnight  
**opm:** oscillations per minute  
**OS:** overall survival  
**p:** p-value  
**P/S:** penicillin/streptomycin  
**pAdj:** adjusted p-value  
**PBS:** phosphate buffered saline  
**PDX:** patient-derived xenografts  
**PFA:** paraformaldehyde  
**PI:** propidium iodide  
**pLKO.1 puro:** pLKO.1 puromycin  
**PNS:** peripheral nervous system  
**pol:** polymerase  
**pSLIK-Neo:** pSLIK-neomycin  
**RFP:** red-fluorescent protein  
**RMA:** robust multichip averaged  
**RNA:** ribonucleic acid  
**rNXPH1:** recombinant Neurexophilin-1  
**ROS:** reactive oxygen species  
**RT:** room temperature  
**RT-qPCR:** real-time quantitative polymerase reaction chain  
**SA:** sympathoadrenal  
**SCC:** squamous cell carcinoma  
**SCPs:** Schwann-cell precursors  
**sec:** seconds  
**SEs:** super-enhancers  
**SFM:** sphere-forming media  
**sh-RNA:** short-hairpin RNA  
**SN:** supernatant  
**SNPs:** single nucleotide polymorphisms  
**TFs:** transcription factors  
**TIC:** tumour-initiating cell  
**TK:** tyrosine kinases  
**TPCs:** tumour propagating cells  
 **$\alpha$ -DAG:**  $\alpha$ -Dystroglycan  
 **$\alpha$ -NRXNs:**  $\alpha$ -Neurexins  
 **$\mu$ m:** micrometer

---

## LIST OF FIGURES

- Figure-01.** The neural crest cells are a transient, migratory, pluripotent population specified at the neural plate border
- Figure-02.** Regions of the neural crests and embryonic origin of the sympathoadrenal lineage
- Figure-03.** Haematoxylin/eosin histologic preparations of neuroblastic tumours
- Figure-04.** Representative FISH images of human neuroblastoma cells displaying *MYCN* status
- Figure-05.** Graphical representation of genetic predisposition to neuroblastoma
- Figure-06.** Treatment overview of neuroblastoma by risk classification according to the International Neuroblastoma Risk Group Staging System
- Figure-07.** The different models of tumour growth
- Figure-08.** Cell-autonomous versus niche-induced cancer stem cell models
- Figure-09.** Niche dependency and tumour progression in the cancer stem cell model
- Figure-10.** Functional assays to characterize cancer cells with long term self-renewal capacity
- Figure-11.** Genetic engineering for the functional characterization of the tumour-propagating capacity of the CSCs
- Figure-12.** The putative anti-CSCs therapies and their consequences
- Figure-13.** *NXPH1* is an extracellular glycoprotein that modulates  $\alpha$ -*NRXN*s activity
- Figure-14.** pLKO.1 puro vector map and associated sh-RNA
- Figure-15.** Backbone vectors and cloning strategy used for the generation of inducible miR-shRNA
- Figure-16.** Double genetic screening identifies 7 differentially expressed genes shared between the HSJD-19 neuroblastoma cohort and early neural crest lineage
- Figure-17.** The expression of NB/NCC double-screening genes correlates with favourable NB prognosis in HSJD-19 cohort
- Figure-18.** The expression of NB/NCC double-screening genes correlates with NB event free survival in Kocak-649 cohort
- Figure-19.** The changes in the relative expression of  $\alpha$ -*NRXN1/2* receptors between NB subgroups do not exceed the threshold
- Figure-20.** The expression of *NXPH1* and its receptors  $\alpha$ -*NRXN1/2* is independent of the cellular phenotype and of *MYCN* or *ALK* expression
- Figure-21.** The expression of *NXPH1* and its membrane receptors  $\alpha$ -*NRXN1/2* is increased in stem-enrichment conditions
- Figure-22.**  $\alpha$ -*NRXN1*<sup>+</sup> cells are identified in NB cell lines and human NB PDX
- Figure-23.** High  $\alpha$ -*NRXN1* expression identifies NB cells with cancer stem cell-like phenotype in human NB cell lines and PDXs

**Figure-24.** Supervised gene expression analysis of  $\alpha$ -NRXN1<sup>High</sup> compared to  $\alpha$ -NRXN1<sup>Neg</sup> population in NB cell lines and human NB PDXs

**Figure-25.**  $\alpha$ -NRXN1<sup>High</sup> NB cells are required to sustain NB growth

**Figure-26.** Exogenous NXP1 promotes NB growth in CAM assay

**Figure-27.** Exogenous NXP1 increases NB proliferation and the expression of neural crest stem cell marker p75NTR

**Figure-28.** The constitutive inhibition of *NXP1* or  *$\alpha$ -NRXN1* expression prevents permanently NB cell growth *in vitro*

**Figure-29.** The inducible inhibition of *NXP1* or  *$\alpha$ -NRXN1* expression causes mild reduction of NB cell viability *in vitro*

**Figure-30.** The inducible inhibition of *NXP1* or  *$\alpha$ -NRXN1* expression reduces NB growth and tumorigenic potential *in vitro*

**Figure-31.** The inducible inhibition of *NXP1* or  *$\alpha$ -NRXN1* expression reduces subcutaneous NB burden and growth in mouse

**Figure-32.** The inducible inhibition of *NXP1* or  *$\alpha$ -NRXN1* expression does not affect expression of p75NTR or neovascularization of NB tumours xenograft

**Figure-33.** NXP1, through its receptor  $\alpha$ -NRXN1, might control the tumour propagating capacity of NB cells upon metastatic dissemination

**Figure-34.** NXP1 is downregulated along tumour progression

**Figure-35.** Double genetic screening genes are downregulated along tumour progression

**Figure-36.** Working model of NB initiation and progression where the loss of NB/NCC signature might be required for disease progression

---

## LIST OF TABLES

**Table-01.** The procedures used for the diagnosis and staging of NB

**Table-02.** International Neuroblastoma Staging System.

**Table-03.** International Neuroblastoma Risk Group Staging System.

**Table-04.** International Neuroblastoma Risk Group (INRG) consensus pretreatment classification schema

**Table-05.** Isolation of CSCs or TPCs from several tumours using surface markers

**Table-06.** Therapeutic strategies against CSCs

**Table-07.** Identification of cells with tumour propagating capacity in neuroblastoma

**Table-08.** Clinical and biological characteristics of the HSJD NB cohort

**Table-09.** NB expression microarrays used in this thesis and available at the R2 Genomic Analysis and Visualization Platform

**Table-10.** List of human cell lines used in this doctoral thesis

**Table-11.** Generation of sense and antisense oligonucleotide for pLKO.1 puro cloning

**Table-12.** Generation of sense and antisense oligonucleotide for pSLIK-Neo cloning

**Table-13.** Standardised criteria for mice welfare surveillance

**Table-14:** Immunodeficient mouse models used in this doctoral thesis



# I. INTRODUCTION

---



## 1. The neural crest

The neural crest cells (NCCs) represent a transient embryonic population unique to vertebrates. They were first identified by Willheim His (1868) in the chick embryo as a “strip of cells lying between the presumptive epidermis and the neural tube”, but it was Arthur Milner Marshall in 1880 who named them neural crest, as a more anatomically relevant description of their origins (Figure 1A) (Hall, 1999). The NCCs have fascinated developmental biologists for the last 150 years mainly for three reasons:

- o They represent a vertebrate specificity: the emergence of NCCs is considered to be a milestone in chordate evolution since their presence gave rise to changes in the body plan and to the re-organization of the rostral head characteristic of all craniates (Gans and Northcutt, 1983; Northcutt, 2005; Simoes-Costa and Bronner, 2015).
- o They are multipotent: NCCs generate more than 20 different cell types, thereby contributing partially or entirely to the formation of more than 20 different tissues or organs (Crane and Trainor, 2006; Hall, 1999; Simoes-Costa and Bronner, 2015).
- o They are migratory: NCCs delaminate from the developing neural tube (NT) after undergoing an epithelial-to-mesenchymal transition (EMT), they then migrate to the surrounding tissues and colonize distant regions of the embryo where they differentiate into distinct derivatives (Gammill and Bronner-Fraser, 2003; Theveneau and Mayor, 2012).

B.K. Hall called the NCCs the fourth germ layer, given the vast number of different cell identities that they are able to generate and their invaluable contribution to head diversification throughout vertebrate evolution (Hall, 1999).

### 1.1. Induction, specification, delamination and migration.

The formation of the NCCs is a tightly regulated multi-step process that can be subdivided into 3 sequential events with defined regulatory modules: induction, specification and delamination (Figure 1B) (Bronner and LeDouarin, 2012; Simoes-Costa and Bronner, 2015).

The NCCs are induced at the gastrula stage during neurulation, at the border between the neural ectoderm and the adjacent non-neural ectoderm. Cells at this border are co-opted with the competence to give rise to either migratory NCCs, neuroepithelial cells (the primary neural stem cells of the early developing NT) or epithelial cells of the presumptive epidermis. The induction of border cells requires the spatiotemporal integration of three different environmental signals coming from three

different developing tissues: members of the BMP family that are secreted from the neural plate, WNT family members secreted from the ectoderm and ligands of the FGF family released by the paraxial mesoderm. The WNT signalling activity is necessary and sufficient to induce the expression of **the NCC border specifiers**, while intermediate levels of BMP and FGF signalling are mainly required for maintaining the border between neural and non-neural tissues (Simoes-Costa and Bronner, 2015). Collectively, WNTs, BMPs and FGfs trigger the sequential expression of transcription factors (TFs) that will control the specification, delamination, migration and differentiation of the NCCs. These neural plate border specifiers correspond to TFs belonging to the DLX (*DLX5/6*), MSX (*MSX1/2*), ZIC (*ZIC1*) and PAX (*PAX3/7*) families.

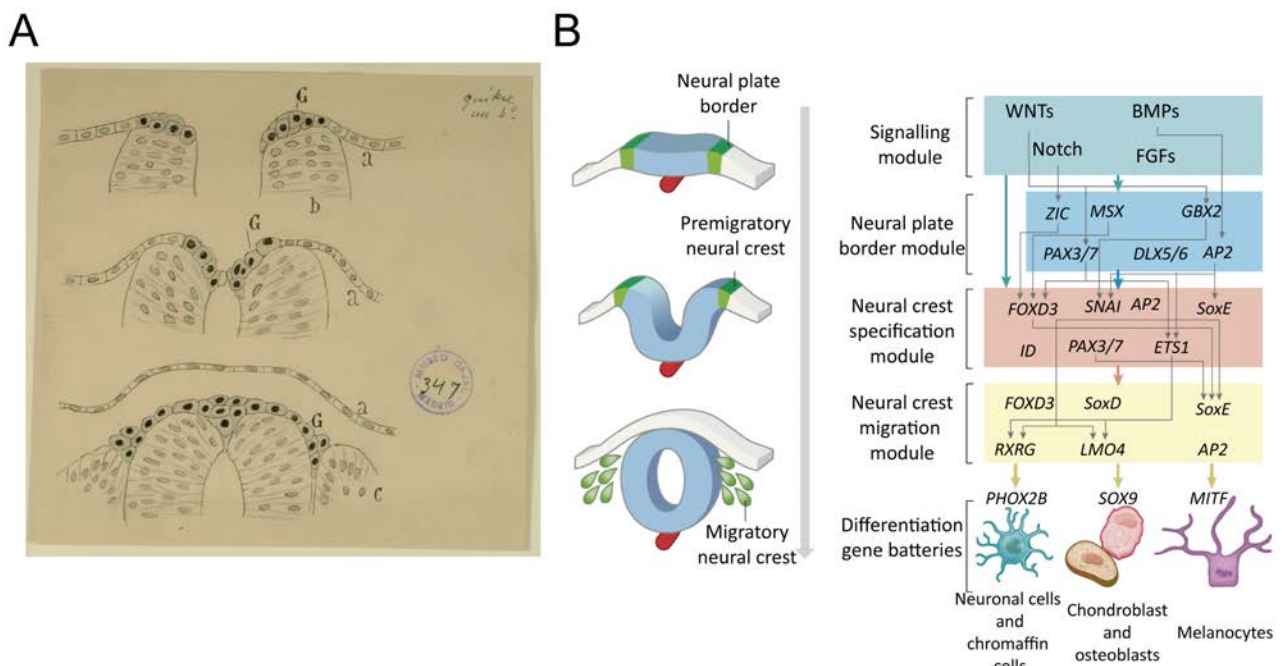


**Figure-01. The neural crest cells are a transient, migratory, pluripotent population specified at the neural plate border**

(A) Cajal's original drawing showing neural crest specification and early migration in a vertebrate embryo. Cajal's Legacy, Instituto Cajal (CSIC), Madrid. (B) Timeline showing different stages in neural crest formation and the gene regulatory network (GRN) that control each stage and endow this cell population with its unique features. The GRN is composed of different modules arranged hierarchically, which control each step of neural crest development. Adapted from (Green *et al.*, 2015). a: ectoderm/presumptive epidermis; b: neural tube; c: somites; G: Neural crest cells.

The precise integration of the transcriptional activities of the NCCs border specifiers drives the expression of **the NCCs specifiers** (also known as NCCs markers): *SOX9/10*, *FOXD3*, *SNAIL1/SLUG* and *MYC* (also known as *C-MYC*). Expressed in pre-migratory and/or migratory NCCs, these NCCs specifiers confer to the NCCs the ability to undergo EMT, delaminate, migrate and subsequently differentiate into diverse derivatives. Mechanistically, the NCC specifiers repress the expression of the neural progenitor marker *SOX2*, while activating the expression of **final effector genes** such as *CDH11*, *CDH7* and different Rho GTPases, which promote the changes in cell adhesion and polarity that are required for EMT (Bronner and LeDouarin, 2012; Sauka-Spengler and Bronner-Fraser, 2008; Simoes-Costa and

Bronner, 2015). The molecular changes promoting delamination include a switch in the expression of type I cadherins (*CDH2*, *N-cadherin*), which mediate strong cell-cell adhesion, to the expression of type II cadherins (*CDH7* and *CDH11*) that favour weak cell-cell adhesion. They also induce the expression of  $\beta 1$ -*integrin* (Simoes-Costa and Bronner, 2015; Theveneau and Mayor, 2012). Importantly, the NCCs represent a paradigmatic example of cells undergoing an EMT, during which presumptive NCCs convert from tightly adherent cells integrated in the neuroepithelium to motile mesenchymal cells that delaminate from the NT. Notably, NCCs can be morphologically identified only after EMT (Bronner & LeDouarin, 2013; Simoes-Costa & Bronner, 2015).

After delamination, the NCCs migrate towards their destinations following stereotypical pathways. Different migratory behaviours have been described at distinct axial levels and in different species, ranging from individual migratory cells using only focal adhesions to compact migratory chains. Hence, several questions remain open regarding the molecular control of the different behaviours observed during the migration of NCCs, making of this event an area of intense research (Gammill and Roffers-Agarwal, 2010; Theveneau and Mayor, 2012).

Remarkably, most of the molecular machinery implicated in NCC formation has been conserved throughout vertebrate evolution (at least in the animal models studied so far). However, some differences have been identified in the case of the mouse embryo, and the underlying reasons of these differences between the mouse and the other species remain elusive (Barriga *et al.*, 2015; Theveneau and Mayor, 2012).

## 1.2. NCCs derivatives

Studies that performed clonal analyses (Bronner-Fraser and Fraser, 1988), and more recently experiments conducted with an elegant confetti-mouse model (Baggiolini *et al.*, 2015), showed that early migratory NCCs are multipotent progenitors. Cell-cell interactions and environmental signals progressively restrain the lineage potential of NCCs until they settle in diverse and distant destinations where they differentiate into numerous lineages. How and when the NCCs multipotentiality is initially determined is a matter of debate. Two opposed models exist: either the NCCs “gain” their potential during or prior to EMT, or they retain it from early embryonic stages. Although the two hypotheses are not exclusive, recent data in *Xenopus* suggest that the NCCs potential shows substantial similarities to that of the blastula-stage animal pole cells (Buitrago-Delgado *et al.*, 2015). Nevertheless, early inter-species grafts and fate mapping analyses demonstrated that the cell fates derived from NCCs arising at different axial levels are regionalized (Bronner and LeDouarin, 2012). Based on the findings obtained using the chick embryo as a model organism, the NCCs have been subdivided into four main axial groups that contribute to different anatomical territories and cell lineages along the antero-

posterior axis (Figure 2A)(Hall, 1999):

- o Cranial NCCs: committed NCCs arising from the anterior region of the NT to the otic vesicle. These NCCs give rise to the ciliary and cranial sensory ganglia, the thymic stroma, the odontoblasts of the tooth primordia, the bone of the middle ear and jaw and also contribute to the craniofacial mesenchyme.
- o Cardiac NCCs: committed NCCs arising from the otic vesicle to the 3<sup>rd</sup> somite. These NCCs give rise to melanocytes, neurons, the cartilage and connective tissue of the 3<sup>rd</sup>, 4<sup>th</sup> and 6<sup>th</sup> pharyngeal arches and to the muscular connective tissue of the outflow tracks of the heart and to the cardiac septum.
- o Vagal and lumbosacral NCCs: committed NCCs arising from the somites 1 to 7 and those from the region posterior to somite 28. They give rise to the enteric nervous system.
- o Trunk NCCs: committed NCCs arising between the somites 8 and 28. These NCCs give rise to the peripheral nervous system, the medulla of the adrenal gland, the sympathetic extra-adrenal paraganglia and melanocytes.

### 1.3. Differentiation of the sympathoadrenal lineages

In the classical model of development of the sympathoadrenal (SA) lineage, p75NTR<sup>+</sup>/HNK1<sup>+</sup>/SOX10<sup>+</sup> trunk NCCs migrate ventrally to para-aortic positions to form the sympathetic primordia. BMPs (mainly BMP2/4), secreted from the dorsal aorta and the para-aortic mesenchyme, instruct the expression of the TFs MASH1/ASCL1 and PHOX2B in the sympathetic primordia, together with the concomitant upregulation of PHOX2A, dHAND and GATA2/3. These TFs constitute the core regulatory unit that instructs the NCCs present at the sympathetic primordia to become SA progenitors. MASH1 and PHOX2B activate a gene regulatory network that induces the expression of tyrosine hydroxylase (TH) and dopamine β-hydroxylase (DBH), two key enzymes involved in the synthesis of catecholamines (Huber, 2006; Simoes-Costa and Bronner, 2015). Interestingly, a detailed spatiotemporal dissection of the early murine neural crest development carried out using lineage tracing and single cell RNA-seq, recently demonstrated that PHOX2B is the master transcriptional regulator that drives the segregation of the NCCs committed to the autonomic nervous system lineage (Soldatov *et al.*, 2019). The specification of SA progenitors occurs in parallel to the aggregation of the sympathetic primordia into primary sympathetic ganglion. Then, a second wave of migration splits SA progenitors into the ones that will give rise to the sympathetic ganglia dorsally and those committed to form the adrenal medulla more ventrally (Figure 2B, left panel)(Bolande, 1974; Turkel and Itabashi, 1974). The generation of the neurons forming the sympathetic ganglia depends on their active differentiation in

response to FGF signalling and their selective survival which is controlled by neurotrophic signalling through the family of TRK receptors (Huber et al., 2009; Mora and Gerald, 2004). By contrast, the nature and origin of the signal controlling the differentiation of SA progenitors into the chromaffin cells of the adrenal medulla remains unknown. These chromaffin cells produce and secrete catecholamines, and are characterized by the expression of TH, CHGA, DLK1, B2M and PNMT (Huber, 2006; Unsicker *et al.*, 2013).

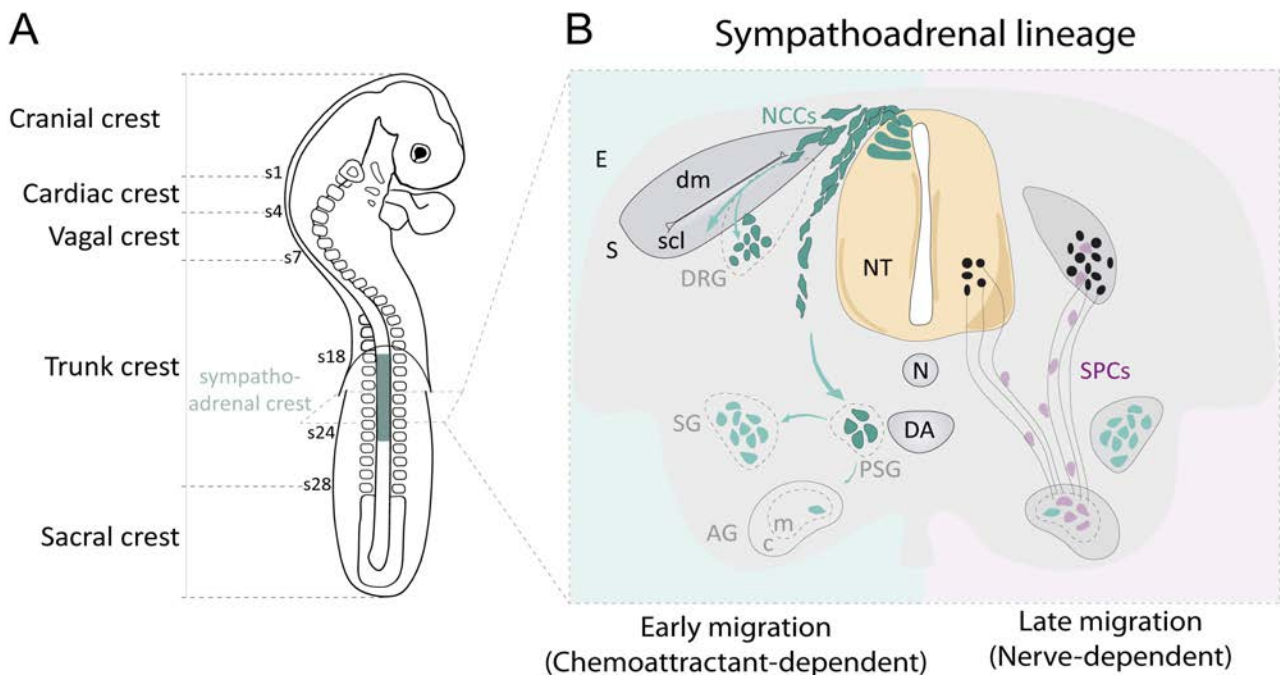


**Figure-02. Regions of the neural crests and embryonic origin of the sympathoadrenal lineage**

(A) Regions of the neural crest along the anterior-posterior axis of the chick embryo. Each region contributes to different lineages. Adapted from (Gilbert, 2000). (B) Distinct embryonic origins of the sympathoadrenal lineage. (Left panel) Early NCC migratory cells following chemotactic cues, contribute to the presumptive DRG and the SP. A second migratory wave lead SP cells towards their final locations at the presumptive SG (most part) and the medulla of the AG (few). (Right panel) The majority of the adrenal gland cells (around 80%) are derived from late-migratory neural crest cells (called Schwann Cell Precursors) that migrate along the preganglionic nerves innervating the presumptive adrenal gland. Adapted from (Tsubota & Kadomatsu, 2018). AG: adrenal gland; c: cortex; DA: dorsal aorta; dm: dermomyotome; DRG: dorsal root ganglia; E: epidermis; m: medulla; N: notochord; NCCs: neural crest cells; NT: neural tube; PSG: primary sympathetic ganglion; S: somite; scl: sclerotome; SPCs: Schwann cell precursors; SP: sympathetic primordia.

This classical model of development of the SA lineage has been challenged by recent studies that propose an alternative origin for the chromaffin cells (Figure 2B, right panel)(Furlan *et al.*, 2017). By combining lineage tracing and cell ablation techniques in different transgenic models, these studies revealed for the first time that NCC-derived Schwann cell precursors (SCPs) migrating along the preganglionic sympathetic nerve fibres into the adrenal gland constitute the main source of chromaffin cells in the mouse embryo. After colonizing the adrenal medulla and the paraganglia, SCPs (SOX10+, S100 $\beta$ +) transit through an intermediate state, the bridge cells (SOX10-, PHOX2B+, TH-), to give rise to chromaffin cells (SOX10-, PHOX2B+, TH+, CHGB+). Thereby, this model proposes that the diversifica-

tion of the SA lineage between sympathetic neurons and chromaffin cells occurs soon after completion of NCC migration (Furlan *et al.*, 2017; Kastriti *et al.*, 2019). Importantly, these new findings suggest an unexpected cellular origin for developmental disorders derived from malformations of the adrenergic system, such as neuroblastoma (NB) and pheocromocytoma.

## 1.4. NCC-associated pathologies

Errors occurring during NCCs development can result in a plethora of heterogenic developmental disorders known generally as neurocristopathies (Bolande, 1974). Neurocristopathies can originate from perturbations that affect NCCs at different axial levels and during distinct events such as NCC induction, specification, migration and/or differentiation. Neurocristopathies comprise neoplasms or malformations presented as simple or syndromic disorders (Etchevers *et al.*, 2006; Vega-Lopez *et al.*, 2018; Watt, 2014). For instance, errors occurring during the development of the SA lineage can result in neuroblastic tumours, a highly heterogeneous group of paediatric tumours among which NB is the most frequent and aggressive form (Mora and Gerald, 2004).

## 2. Neuroblastoma: a paediatric tumour deriving from the embryonic sympathoadrenal lineage

NB is a devastating paediatric cancer that originates in the developing sympathetic nervous system. The first reference to NB tumours dates from 1864, when the physician Dr. Rudolf Virchow described the presence of an abdominal solid tumour that he called “glioma” (Virchow, 1864,1865). More than 40 years later, the pathologist Dr. James Wright recapped clinical information from other colleagues and came up with the term “neuroblastoma” based on the similarities that these tumour cells share with immature cells from the adrenal medulla and sympathetic neuroblasts (Wright, 1910).

### 2.1. Prevalence

NB is the most common extracranial solid tumour diagnosed during childhood and is responsible for almost 15% of cancer-related paediatric deaths. The incidence rates are age-dependent, with 40% of the cases detected during the first year of life and 95% before the age of 10. Strikingly, NB is the most common cancer among infants younger than 12 months, with an incidence rate of 55 per million infants while leukaemia accounts for 44 per million infants (Linabery and Ross, 2008; Program, 2019). It is also slightly more frequent in boys than girls (Goodman, 1999). Approximately 80 cases are

diagnosed each year in Spain in children under 14, accounting for 8.4% of the total childhood tumours (Pardo Romaguera, 2018). The age at the time of diagnosis is related with prognosis and is used as a staging criterion. The median age at diagnosis is 17.3 months and patients diagnosed under 18 months show generally a better outcome (London *et al.*, 2005). The clinical presentation and prognosis of these tumours are extremely heterogeneous: they can range from a tumour that will undergo a spontaneous regression to an aggressive metastatic tumour refractory to multimodal chemotherapy and that can lead to death. This clinical diversity correlates with numerous clinical and biological factors, including the age of the patient, the stage of the disease and a variety of cellular, molecular and genetic traits and reflects the “embryonic/immature” environment in which NBs arise (Brodeur, 2003; Maris and Denny, 2002).

## 2.2. Origin

The primary localisation of NB tumours, the expression of cellular markers associated to SA development and the role of PHOX2B, MYCN and ALK in the process of malignant transformation altogether support the notion that neuroblastic tumours arise consequently to errors occurring during SA development (Mora and Gerald, 2004; Tolbert *et al.*, 2017; Tsubota and Kadomatsu, 2018). As explained above, cells of the SA lineage derive from trunk NCCs. The trunk NCCs get progressively restricted towards the SA lineage while migrating and colonizing ventral territories close to the foetal dorsal aorta. Later on during development, the NCC-derived SCPs migrate along the nerve fibres and colonize the adrenal medulla and the paraganglia to become the major source of chromaffin cells (see section 1 for further detailed) (Furlan *et al.*, 2017; Kastriti *et al.*, 2019). In the light of recent discoveries that revealed the early segregation between the sympathetic and chromaffin lineages, the malignant transformation leading to NB formation could be initiated at different steps of the normal development, early within the migratory SA progenitors to late in the nerve-dependent migratory SCPs (Delloye-Bourgeois and Castellani, 2019; Furlan and Adameyko, 2018). Hence, more work is still needed to clearly identify the cell of origin of NBs.

## 2.3. Clinical presentation

Nearly 50% of the primary NBs arise in the adrenal medulla, while the remaining 50% appear in the sympathetic ganglia of the abdomen (24%), thorax (15%), pelvis (3%) or neck (3%). In approximately 1% of the cases, the primary location cannot be identified. Interestingly, the location of the primary tumour is related with prognosis and might reflect distinct cellular origins (Tsubota and Kadomatsu, 2018; Vo *et al.*, 2014). The clinical symptoms identified at diagnosis reflect the location of the primary tumour, the extent of the metastatic spreading (if present) and the presence of paraneoplastic syn-

dromes (Maris *et al.*, 2007). In rare cases NB patients presenting a local or metastatic disease develop paraneoplastic syndromes such as intractable watery diarrhoea (due to the autonomous secretion of vasoactive intestinal peptide by NB cells) and opsoclonus-myoclonus syndrome (rapid eye movement, ataxia and irregular muscle movement)(Maris *et al.*, 2007; Matthay *et al.*, 2016). Thereby, the clinical presentation can range from asymptomatic to systemic affectations.

### 2.3.1. Localised neuroblastoma

Around 40% of the newly diagnosed patients present a localized tumour. Localised NBs are most frequent in patients under 18 months and are generally associated with an excellent outcome, especially when they do not present *MYCN* amplification. The 5 years event-free survival (EFS) rate is over 75% and the 5 years overall survival (OS) rate is 90-100% (Maris *et al.*, 2007; Nakagawara *et al.*, 2018). Better outcomes are associated with patients presenting thoracic or neck tumours, whereas the poorest outcomes to those presenting adrenal tumours, independently of their age, the tumour classification and the status of *MYCN* gene (Vo *et al.*, 2014). Distinct clinical symptoms are associated with the location of the tumour mass. Large abdominal tumours can result in bowel or bladder compression and hamper venous and lymphatic drainage. Thoracic tumours can cause a deviation or narrowing of the trachea and Horner syndrome<sup>1</sup>. Paraspinal tumours in the thorax, abdomen or pelvis are observed in 5-15% of the patients. These tumours can grow along the spinal nerves and invade the neural foramina, causing symptoms related to the compression of nerve roots and spinal cord such as motor weakness, pain and sensory loss (Maris *et al.*, 2007; Matthay *et al.*, 2016).

A subset of patients presenting a localised NB frequently shows a spontaneous. In that case, the patients only require clinical surveillance without major interventions (Brodeur, 2018; Tolbert and Matthay, 2018). Although localized tumours can be very large and locally invasive, most are successfully treated with surgery alone and metastatic recurrences are rare (Tolbert and Matthay, 2018).

### 2.3.2. Metastatic neuroblastoma

NB metastatic spreading is detected in nearly 60% of the cases of NB and differs according to the patient age and the primary tumour site (DuBois *et al.*, 1999; Park *et al.*, 2017; Vo *et al.*, 2014). NB metastasizes through lymphatic and haematogenous routes, invading the bone marrow (74-70%), the bones (61-56%), the lymph nodes (34-31%), the liver (30%-18%), intracranial or orbital locations (18%), and less frequently the skin (4-3%), the lungs (3%) and the central nervous system (3-0.6%). The presence of metastases in the lungs and central nervous system is symptomatic of an end-stage

<sup>1</sup> Among the most frequent clinical symptoms that characterise the **Horner syndrome** are: ptosis (the drooping of the upper eyelid), miosis (a persistently small pupil), anisocoria (an evident difference in pupil size between the two eyes) and anhidrosis (little or no sweating)

disease (DuBois *et al.*, 1999; Vo *et al.*, 2014). The prognosis depends on whether the patient presents metastases at distant sites or a locoregional spreading to adjacent lymph nodes (Maris *et al.*, 2007). The adrenal primary tumours show higher proportions of metastases in the bone marrow (77%), bones (65%) and liver (20%), whereas patients with neck, pelvic or thoracic primary tumours present lower rates of bone metastasis (45-50%) (Vo *et al.*, 2014).

The metastatic dissemination usually causes broad symptoms such as bone pain, fever, weight loss or pallor from anaemia and thrombocytopenia. The infiltration of the tumour in the periorbital bones can cause ptosis, proptosis and periorbital ecchymosis (the latter is also known as “raccoon eyes” and is described in 15% of NB patients). Finally, a frequent and visual manifestation of the NB metastatic spreading to the skin is the appearance of firm bluish-red subcutaneous nodules that can be distributed over the entire body. These lesions appear in 30% of the children presenting a congenital NB (Maris *et al.*, 2007; Matthay *et al.*, 2016).

### 2.3.3. Special metastatic NB (4S disease)

The clinical phenotype called stage 4S (S standing for special) refers to infants up to 18 months presenting small localized primary tumours with extensive metastasis in the liver and skin but no or minimal spreading to the bone marrow. It corresponds to 5-10% of the cases of NB (D’Angio *et al.*, 1971; Evans *et al.*, 1971; Monclair *et al.*, 2009). The 4S NB spontaneously regresses with minimal or no treatment (D’Angio *et al.*, 1971; Evans *et al.*, 1971). Most of these patients are near-triploid, do not show segmental chromosomal aberrations or *MYCN* amplification and present a favourable histology (Lavarino *et al.*, 2009; Maris *et al.*, 2007). They also present a specific transcriptomic signature and a distinct DNA methylome compared to stage 4 NBs (Benard *et al.*, 2008; Gomez *et al.*, 2015). Their 5year-EFS rate is over 75% and the 5year-OS rate is 90-100% (Nakagawara *et al.*, 2018). Spontaneous regression seems to occur due to massive cell death however, the underlying reasons are uncertain and suggest the contribution of different mechanisms. A TRKA-mediated apoptosis, a shortening of the telomeres, an immune response and/or an epigenetic regulation are seen as solid candidates that might mediate spontaneous NB regression (Brodeur, 2018; Brodeur and Bagatell, 2014).

The distinctive multifocal spreading of 4S NBs has been a matter of intense debate among the scientific community. Two hypotheses still persist on whether they derive from genetically identical malignant cells that metastasize or if they are instead truly multifocal tumours coming simultaneously from different malignant populations (van Noesel, 2012). Interestingly, NCC-derived SOX10<sup>+</sup>/p75NTR<sup>+</sup> precursors of the glial and melanocyte lineages are naturally found in the liver, skin and bone marrow (Nagoshi *et al.*, 2008; Wong *et al.*, 2006), thereby supporting the hypothesis of a multifocal origin for 4S NBs.

## 2.4. Diagnosis

The differential diagnosis of NB requires a range of tests that includes biochemical and genetic laboratory tests and imaging and histological analyses (Table-01).

Laboratory tests	Complete blood count and platelet count Prothrombin time and partial thromboplastin time Electrolyte, creatinine and uric acid levels and liver function Ferritin and lactate dehydrogenase levels Urine vanillylmandelic acid, homovanillic acid and dopamine levels
Imaging techniques	CT or MRI of the primary site, chest, abdomen and pelvis CT or MRI of the head and neck if clinically involved <sup>123</sup> I-MIBG scan and then <sup>18</sup> F-PET scan if the tumour is not MIBG-avid
Pathological evaluation	Tumour biopsy with immunohistochemistry and the International Neuroblastoma Pathology Committee Classification Fluorescence <i>in situ</i> hybridization for <i>MYCN</i> Array comparative genomic hybridization or other study for segmental chromosomal alterations DNA index (ploidy) Bilateral bone marrow aspirate and biopsy with immunohistochemistry Optional: genomic analysis for <i>ALK</i> mutations or other mutations

**Table-01.** The procedures used for the diagnosis and staging of NB. CT: Computed tomography; MRI: Magnetic resonance Imaging; <sup>123</sup>I-MIBG: <sup>123</sup>I-Meta-iodobenzylguanidine; <sup>18</sup>F-PET: 18-Fluorodeoxyglucose-Positron emission tomography. Adapted from (Matthay et al., 2016).

### 2.4.1. Laboratory tests: urine catecholamines

NBs are neuroendocrine tumours and as such, NB cells produce catecholamines (dopamine, epinephrine and norepinephrine). Both catecholamines and their metabolites (homovanillic acid and vanillylmandelic acid) can be detected in the serum and urine and are used for diagnosis and disease monitoring over time (Matthay *et al.*, 2016).

### 2.4.2. Imaging techniques

Ultrasonography, computed tomography, magnetic resonance or <sup>123</sup>I-MIBG scan<sup>2</sup> are used to determine the primary tumour location and the presence of tumour infiltration and metastatic spreading. A complete evaluation by imaging is required for optimal staging and risk classification of NB patients (Matthay *et al.*, 2016).

### 2.4.3. Histopathological evaluation

The histological evaluation is required to establish a definitive diagnosis. The histopathological features of the tumour correlate with patient's prognosis. The possible spreading to the bone marrow is

<sup>2</sup> <sup>123</sup>I-MIBG scan refers to a radiographic scanning technique based on the administration of the norepinephrine analogue <sup>123</sup>I-Meta-iodobenzylguanidine to the patients. This molecule binds to the norepinephrine transporter expressed by sympathetic nervous tissues and NB cells, and allows the evaluation of metastatic bone disease (Vik *et al.*, 2009).

additionally confirmed through a bilateral bone marrow biopsy and /or aspirate (Matthay *et al.*, 2016).

#### 2.4.4. Genetic and genomic characterization

The samples from the tumour tissue and/or NB-positive bone marrow are then subjected to a genetic screening (evaluation of the *MYCN* status, presence of segmental chromosomal aberrations and DNA ploidy)(Matthay *et al.*, 2016).

### 2.5. Histology of neuroblastic tumours

The heterogenic nature of the neuroblastic tumours is also reflected at the cellular level. Neuroblastic tumours present 2 distinct cellular types: the neuronal (N) cells and the Schwann (S) cells. Cells from the N-type resemble primitive or maturing neuroblasts or even ganglionic cells, whereas S-type cells resemble immature Schwann precursors or mature Schwann cells. The balance between N-type and S-type components and their degree of differentiation are used to further classify neuroblastic tumours and are predictive of the patient's outcome (Figure 3)(Shimada *et al.*, 1999).

#### 2.5.1. Neuroblastoma

NBs correspond to the neuroblastic tumours that present a poor Schwannian stroma that never exceeds 50% of the tumour tissue. 97% of the neuroblastic tumours are NBs (Shimada *et al.*, 1999). Based on the degree of differentiation of the tumour cells, NBs are further sub-classified as:

- **Undifferentiated:** all the neuroblasts show an immature morphology characterized by a round shape with a rounded-to-elongated nucleus and nearly indiscernible cytoplasmic borders. Rosettes or neuropils (thin neuritic processes) cannot be identified. They present a minimal or no stromal component (Shimada *et al.*, 1999).
- **Poorly differentiated:** no more than 5% of the neuroblasts show cytomorphological features of differentiation toward ganglionic cells such as neuropils or rosettes. They present a minimal or no stromal component (Figure 3A)(Shimada *et al.*, 1999).
- **Differentiating:** at least 5% of the tumour cells show synchronous cytomorphological features of differentiation toward ganglion cells, including an enlarged and eccentric nucleus with a single nucleolus and a conspicuous cytoplasm. In these tumours, the neuroblasts usually have abundant neuropils. The schwannian stromal component is commonly present in the septa between contiguous lobules of neuroblastic cells, but still represents less than 50% of the tumour (Shimada *et al.*, 1999).

### 2.5.2. Ganglioneuroblastoma

Ganglioneuroblastoma (GNB) are neuroblastic tumours presenting a rich Schwannian stroma, although the proportion of the stromal component does not exceed 50% of the total tumour area. In these tumours, the neuroblasts appear at various stages of differentiation and are clustered together as nests or nodules intermixed with the Schwannian stroma. Neuropils are easily identified. The GNB generally present an intermediate level of malignancy (Shimada *et al.*, 1999).

GNBs are classified as the nodular subtype when the neuroblastic component is detected as distinct macroscopic haemorrhagic nodules in stroma-poor areas coexisting with stroma-rich areas (Figure 3B). By contrast, when the neuroblastic nests are scattered through the tumour area as multiple foci, GNBs are classified as the intermixed subtype (Figure 3C)(Shimada *et al.*, 1999).

### 2.5.3. Ganglioneuroma

Ganglioneuroma (GN) correspond to the neuroblastic tumours in which the Schwannian stroma is dominant, with maturing and fully mature ganglion cells individually scattered. These tumours are more frequently detected in patients around 5 to 7 years of age. GNBs can metastasize, although they are considered to be benign and hence show an excellent prognosis (Figure 3D)(Shimada *et al.*, 1999).

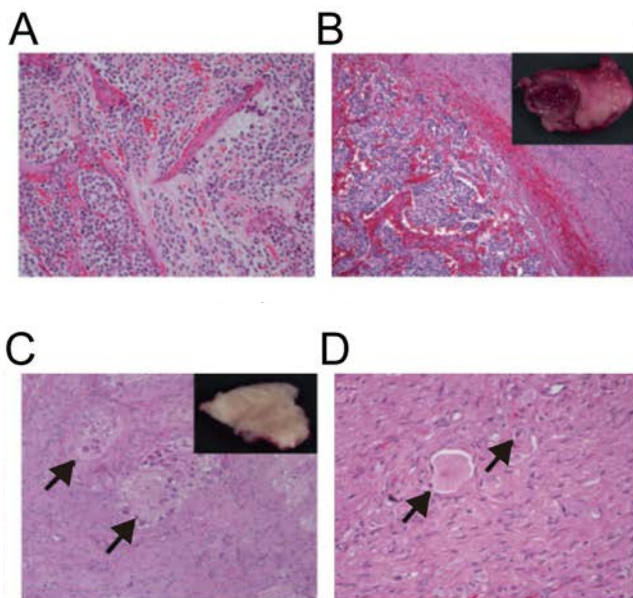


**Figure-03. Haematoxylin/eosin histologic preparations of neuroblastic tumours**

(A) Poorly differentiated neuroblastoma, with nest of neuroblasts in a background of light pink fibrillary neuropil (magnification  $\times 100$ ). (B) Nodular ganglioneuroblastoma, defined by the presence of a grossly visible haemorrhagic nodule (inset). Histologic examination reveals an expansive haemorrhagic nodule of neuroblastoma (lower left) in a background of Schwannian stroma (right side of the image) (magnification  $\times 40$ ). (C) Intermixed ganglioneuroblastoma, defined by the absence of 'gross' nodularity and an homogenous appearance (inset). Histologic examination reveals microscopic nests of neuroblastoma (arrow), embedded in Schwannian stroma (magnification  $\times 100$ ). (D) Ganglioneuroma, composed of Schwannian stroma and scattered maturing ganglion cells (arrow) (magnification  $\times 200$ ). Adapted from <https://oncohemakey.com/neuroblastoma-5/>.

## 2.6. Risk factors and pathogenesis

The causative factors for NB formation are not well defined. Environmental risk factors seem unlikely, while genetic or genomic changes are frequent but show a low recurrence rate (Cheung and Dyer, 2013; Tolbert *et al.*, 2017). **Familial** NBs account for 1-2% of the cases and appear to be inherited in an autosomal-dominant pattern, although the penetrance is variable (Cheung and Dyer, 2013; Tolbert *et al.*, 2017). Germline mutations in *ALK* and *PHOX2B* are found in 80% and 10% of the familial cases, respectively (Mosse *et al.*, 2004; Mosse *et al.*, 2008; Trochet *et al.*, 2004). Interestingly, mutations causing a loss of function of *PHOX2B* predispose to the majority of the syndromic NB cases, in which the formation of NB is accompanied by a central congenital hypoventilation syndrome and/or a Hirschsprung disease (Bachetti and Ceccherini, 2019). Germline mutations in other loci such as *TP53*, *SDHB*, *PTPN11*, *APC* and *NF1* have also been reported in a few cases. Thus, the familial predisposition to NB formation remains only partially understood (Tolbert *et al.*, 2017). Familial cases are usually diagnosed earlier (the mean age at diagnoses is 9 months) and a large proportion of the patients present bilateral adrenal tumours or multifocal tumour presentation (Kushner *et al.*, 1986).

The vast majority of NBs are **sporadic** and do not correlate with any specific germline mutation. The sequential accumulation of multiple genetic/genomic alterations occurring before the terminal differentiation of the SA derivatives can cooperate and contribute to NB tumorigenesis. However, different *MYCN*-driven transgenic models have shown that the temporal window during which an oncogenic-driving event such as *MYCN* amplification can induce malignant transformation might be incredibly narrow and mainly restricted to pre-natal development (Hansford *et al.*, 2004; Mobley *et al.*, 2015; Weiss *et al.*, 1997). Although several genetic alterations are recurrently found in NB patients, the penetrance of the phenotypes and their recurrence rate are low and variable. Therefore, a plausible explanation of the sequence of events that led to the malignant transformation is still lacking for most of the patients.

### 2.6.1. Recurrent genomic abnormalities

#### 2.6.1.1. DNA Ploidy

The total DNA content (DNA ploidy or index) is used as a prognostic indicator. NBs tumours with a DNA index >1 correspond to hyperdiploid or near-triploid NBs that present altered numbers of chromosomes (ranging from 58 to 80 chromosomes). These tumours are usually of low stage and are associated with good prognosis. By contrast, NB tumours harbouring a DNA index =1 (44 to 57 chromosomes) correspond to diploid or nearly diploid tumours that present structural chromosomal gains or losses. These tumours are usually of high stage and are associated with bad prognosis (Lavarino *et*

*al.*, 2008; Mora *et al.*, 2001; Mora *et al.*, 2007). Alterations in the total DNA content presumably result in mitotic dysfunction. However, it is not known whether the DNA ploidy could also be related to the process of maturation of the NB cells (Matthay *et al.*, 2016; Nakagawara *et al.*, 2018).

### 2.6.1.2. Amplification of the oncogene *MYCN*

*MYCN* (*v-myc myelocytomatosis related oncogene, neuroblastoma derived*) belongs to the family of *MYC* oncogenes, together with *L-MYC* and *C-MYC*. It encodes a basic helix-loop-helix (bHLH) transcription factor that possesses a bi-modal (activator/repressor) activity. Unlike *C-MYC*, *N-MYC* is specifically expressed during embryonic development, mainly in the developing central nervous system. It acts as a transducer of multiple signalling pathways and regulates cell proliferation, differentiation and survival (Huang and Weiss, 2013).

*MYCN* is mapped to the short arm of chromosome 2, at the position 2p24-23. The amplification of this region results in persistently high levels of *MYCN* protein. *MYCN* amplification occurs in 25% of all NB patients and in 50% of the patients showing metastasis (Figure 04). *MYCN* amplified-tumours usually consist of undifferentiated or poorly differentiated neuroblasts and present an aggressive behaviour. Indeed, *MYCN* amplification is the only factor that classifies a NB tumour as high risk independently of the age of the patient and the tumour clinical stage (Brodeur *et al.*, 1988; Cohn *et al.*, 2009; Matthay *et al.*, 2016). The transgenic overexpression of *MYCN* in SA precursors (under the control of the tyrosine hydroxylase promoter) in zebrafish or mouse causes NB formation. However, it does not recapitulate the metastatic spreading (Weiss *et al.*, 1997; Zhu *et al.*, 2012).

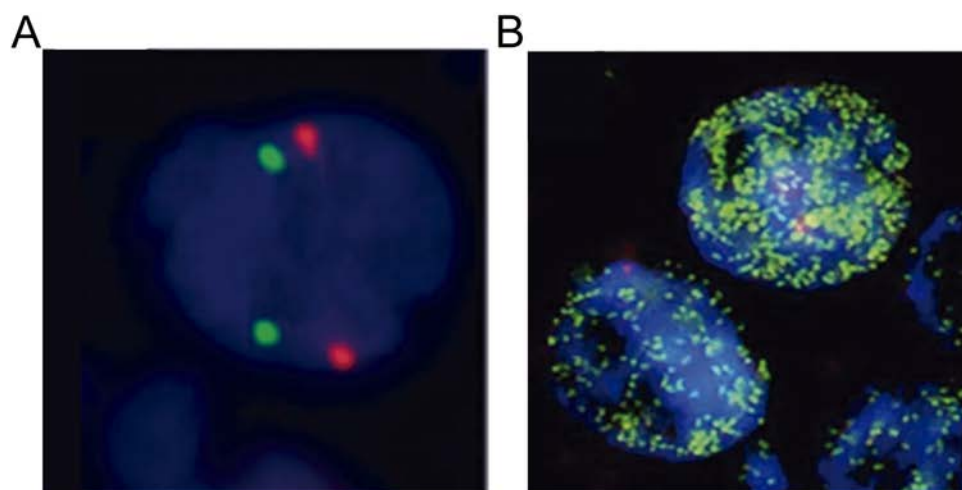


**Figure-04. Representative FISH images of human neuroblastoma cells displaying *MYCN* status**

(A) Neuroblastoma cells without *MYCN* amplification. (B) Neuroblastoma cells with amplified *MYCN*. *MYCN* probe (green). Centromeric *CEP2* probe (red). Nuclei are counterstained with DAPI (magnification x1000). Adapted from (Wang *et al.*, 2013).

The molecular mechanisms underlying *MYCN* amplification remain poorly understood. The most plausible explanation suggests an initial aberrant amplification of the *MYCN* locus as extra-chromosomal elements of different sizes (double minutes), that are then linearly integrated as reiterated amplicons within its chromosomal site (Amler and Schwab, 1989; Brodeur and Seeger, 1986; Yoshimoto *et al.*, 1999).

Interestingly the human *MYCN* locus encodes a cis-antisense transcript, *MYCNOS*. *MYCNOS* encodes the N-CYM protein, which promotes *MYCN* protein stabilization by inhibiting GSK3- $\beta$  activity. *MYCNOS* is always amplified together with *MYCN* in human NBs. Importantly, a double transgenic mouse model for *MYCN* and *MYCNOS* presents frequent metastases (Suenaga *et al.*, 2014).

#### 2.6.1.3. Loss of chromosome 1p (1p36)

The loss of the chromosomal region 1p36 is detected in one third of the primary NBs. This abnormality is positively correlated with *MYCN* amplification and is associated with poor prognosis (Attiyeh *et al.*, 2005).

Several candidate tumour suppressor genes are located in 1p36 such as *CHD5*, *CAMTA1*, *KIF1B*, *CASZ1* and mir-34A, suggesting that the deletion of 1p36 might acts as a tumour driver (Bagchi *et al.*, 2007; Henrich *et al.*, 2012). Recently, the clonal selection of *CHD5* mutant alleles was reported by whole-exome sequencing as the first proof of concept that *CHD5* acts as an haploinsufficient tumour suppressor in NB (Schramm *et al.*, 2015).

#### 2.6.1.4. Gain of chromosome 17

The numerical or segmental gain of chromosome 17 is the most frequent genomic aberration found in NBs and is detected in 70% of the NBs at diagnosis (Plantaz *et al.*, 1997). The segmental gain of 17q is detected in 50% of the NB patients and is associated with poor prognosis (Bown *et al.*, 1999). At least 3 candidate oncogenes are located in 17q: *BIRC5* (*Survivin*), *NM23A* and *PPM1D*. These candidates might be responsible for the selective advantages brought by unbalanced copies of 17q (Godfried *et al.*, 2002; Islam *et al.*, 2000).

Loss of 1p and gain of 17q correlate with *MYCN* amplification and poor prognosis (Bown *et al.*, 1999).

#### 2.6.1.5. Loss of chromosome 11q

The loss of chromosome 11q is present in one third of high risk NB patients. It is inversely correlated with *MYCN* amplification and the loss of 1p36 and it is associated with an aggressive phenotype

(Attiyeh *et al.*, 2005). Together with *MYCN* amplification, it is the only genetic alteration that is consistently assessed for risk stratification of NB patients (Cohn *et al.*, 2009). The putative tumour suppressor gene *TSCL1* is located in 11q23 (Ando *et al.*, 2008).

#### 2.6.1.6. Others

Other segmental chromosomal aberrations commonly found in NB patients include the gains of 1q and 2p and the loss of 3p, 4p and 14q. However, their association with patients' prognosis is less clear (Jiang *et al.*, 2011; Matthay *et al.*, 2016; Nakagawara *et al.*, 2018).

*TERT* re-arrangements are present in 25% of high risk NBs and strongly associate with bad prognosis. They are usually found in *MYCN* non-amplified tumours carrying *ATRX* mutations (Peifer *et al.*, 2015; Valentijn *et al.*, 2015).

Finally, chromothripsis (a local shredding of the chromosomes) has also been detected in nearly 20% of high risk NBs. Its putative clinical meaning is however still unknown (Boeva *et al.*, 2013; Molenaar *et al.*, 2012).

### 2.6.2. Recurrent genetic abnormalities

#### 2.6.2.1. *ALK* (Anaplastic lymphoma kinase)

The *ALK* oncogene encodes an orphan tyrosine kinase (TK) receptor expressed in the developing nervous system. Germline mutations in *ALK* are present in nearly 80% of the familial NBs, while somatically acquired mutations are found in 10% of the sporadic NBs (Chen *et al.*, 2008; George *et al.*, 2008; Janoueix-Lerosey *et al.*, 2008; Mosse *et al.*, 2008). The frequency of activating mutations in *ALK* is increased in relapses (Schleiermacher *et al.*, 2014). Point mutations usually affect the catalytic domain of *ALK*, increasing its kinase activity by autophosphorylation. The hyperactivation of *ALK* leads to an increased signalling through PI3K, RAS/MAPK and RET pathways and contributes to oncogenic transformation (Chen *et al.*, 2008; George *et al.*, 2008; Janoueix-Lerosey *et al.*, 2008; Mosse *et al.*, 2008). In addition, *ALK* is located at 2p23 and is thus co-amplified with *MYCN* in some cases (Chen *et al.*, 2008; Janoueix-Lerosey *et al.*, 2008).

#### 2.6.2.2. *ATRX* ( $\alpha$ -Thalassaemia/mental retardation syndrome X-linked).

*ATRX* encodes a SWI/SNF chromatin-remodelling ATP-dependent helicase. Mutations in *ATRX* causing its loss of function are found in 10% of the NB patients (Cheung *et al.*, 2012; Molenaar *et al.*, 2012). The frequency of mutation of *ATRX* increases with the age of the patient and is associated to

bad prognosis. The *ATRX* mutations inversely correlate with *MYCN* amplification (Cheung *et al.*, 2012).

### 2.6.3. Genetic susceptibility to NB

In the last decade, genome-wide association studies have discovered multiple single nucleotide polymorphisms (SNPs, both in gene-coding and non-coding sequences) and copy-number variations (CNVs) that might act as oncogenic drivers for NB formation such as: *LIN28*, *LMO1*, *BARD1*, *TP53* or copy number variation in *16p*. However, their individual contribution to NB predisposition is very low (Figure 05) (Capasso *et al.*, 2009; Diskin *et al.*, 2012; Nguyen le *et al.*, 2011; Oldridge *et al.*, 2015; Pugh *et al.*, 2013; Sausen *et al.*, 2013; Tolbert *et al.*, 2017).

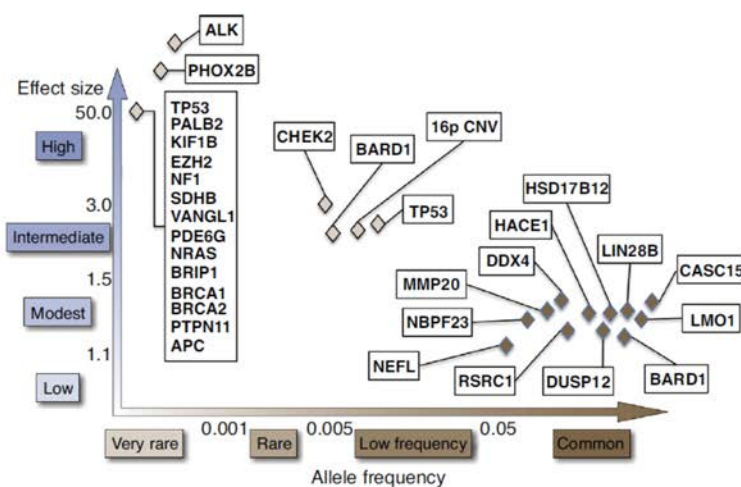


Figure-05. Graphical representation of genetic predisposition to neuroblastoma

Known familial and sporadic predisposition genes compiled into one summary figure across multiple studies. The familial mutations are shown in the top left of the graph representing a very rare allele frequency and high effect size. GWAS-discovered variations are in the bottom right corner representing a higher allele frequency with a lower effect size. Adapted from (Tolbert *et al.*, 2017).

### 2.6.4. Epigenetic modifications in neuroblastoma

The remarkable scarcity of recurrent mutations at the time of diagnosis and the key role of the epigenetic regulation in the differentiation process, have led to the notion that an epigenetic unbalance and/or rewiring might be an important mechanism driving tumorigenesis. In this regard, genome-wide epigenetic alterations and mutations in epigenetic regulators have been described in NB tumours and are suspected to cooperate to the malignant transformation and/or the acquisition of aggressive traits (such as therapy-resistance or metastatic behaviour) (Decock *et al.*, 2011; Durinck and Speleman, 2018; Flavahan *et al.*, 2017). The main epigenetic changes reported so far in NBs are included hereafter:

First, genome-wide changes in the **DNA methylation pattern** have been detected in several NB cohorts and are proposed to have prognostic value. Current data suggest that the hypermethylation of the CpG promoter regions together with the genome-wide hypomethylation of the non-CpG regions contribute to tumour progression and to the acquisition of unfavourable clinical features by promoting aberrant oncogene activation (for example *TERT*), tumour suppressor silencing (for example

*CASP8*), and genomic instability (Alaminos *et al.*, 2004; Decock *et al.*, 2016a; Decock *et al.*, 2016b; Decock *et al.*, 2016c; Gomez *et al.*, 2015; Mayol *et al.*, 2012; Olsson *et al.*, 2016).

Second, changes in the **post-transcriptional modification of histones** (mainly their acetylation and methylation status) seem also to play a role in NB malignancy. The overexpression of the histone deacetylase *HDAC8* significantly correlates with poor patient prognosis (Oehme *et al.*, 2009a; Oehme *et al.*, 2009b), and different HDACs can cooperate with MYCN to repress its target genes (Fabian *et al.*, 2014; Fabian *et al.*, 2016; Lodrini *et al.*, 2013). In parallel, changes in the expression levels of different histone methyltransferases and demethylases have been described mainly in relation with MYCN activity. The overexpression of *DOTL1*, *WDR5* or that of the core components of the Polycomb Repressive Complexes 1 & 2 (for example *EZH2* and *BMI1*) cooperate with MYCN in regulating transcription and correlates with poor patients' survival (Cui *et al.*, 2007; Huang *et al.*, 2011; Sun *et al.*, 2015; Wong *et al.*, 2017).

Third, the expression of **epigenetic chromatin readers** and that of components of the **chromatin-remodelling complexes** is also affected in NBs. For example *BPTF*, a chromatin reader able to recognize histone acetylation marks, is amplified in 55% of the NBs, due to the chromosomal gain of the locus 17q24 (Buganim *et al.*, 2010). Additionally, the loss of *CHD5* expression (caused by the loss of the locus 1p36 or by promoter methylation) and the mutation or deletion of the components of the SWI-SNF complex *ARID1A/B*, all associate with poor patient prognosis and high risk stage (Koyama *et al.*, 2012; Lavarino *et al.*, 2008; Lee *et al.*, 2017; Sausen *et al.*, 2013).

Finally, a read-out of the epigenetic status of a cell is the activity of the **super-enhancers** (SEs). SEs are a cluster of highly active enhancers coupled to genes encoding master TFs, whose final aim is to instruct the cellular identity (Pott and Lieb, 2015). The combinatorial effect of some of the above mentioned epigenetic changes might cause an epigenetic reprogramming in the tumour cells that change the activity of the super-enhancers compared to that of the non-malignant cells. Therefore, the intra- and inter-tumour heterogeneity has been recently studied in the light of SEs regulatory circuitries. NB tumours consist in a heterogeneous mixture of two main interconvertible cell states: the adrenergic cell state (controlled by *GATA3* and *HAND1*) and the mesenchymal cell state (controlled by *MEX1/2* and *SOX9*). The mesenchymal cell state is proposed to mimic NCC identity (van Groningen *et al.*, 2017). A parallel approach described the existence of other 3 main cellular subtypes based on the activity of super-enhancers: the sympathetic noradrenergic cell subtype (controlled by *PHOX2B*), the NCC-like subtype (controlled by *AP1*) and the mixed transiting subtype (Boeva *et al.*, 2017).

Collectively, these data suggest that a better understanding of epigenetic plasticity and tumour-specific dependency on epigenetic regulation might help to get a deeper insight into the intra-/inter-tumour heterogeneity and should be taken into account as novel therapeutic strategies.

## 2.7. Staging system and prognosis

Due to the large heterogeneity displayed by NB tumours in terms of distinct clinical behaviours and biological features, the definition of risk groups has been the main goal of international consortiums. The stratification of patients into risk groups aims to cluster patients into therapeutically meaningful subgroups. For the last 3 decades, the most widely used staging systems have been the International Neuroblastoma Staging System (INSS) and the International Neuroblastoma Risk Group Staging System (INRGSS).

### 2.7.1. The International Neuroblastoma Staging System (INSS)

The INSS was first established in 1988 and stratifies the patients according to the post-surgical criteria (Brodeur *et al.*, 1993; Brodeur *et al.*, 1988). A detailed definition of the stages established by the INSS is included in Table-02.

### 2.7.2. The International Neuroblastoma Risk Group Staging System (INRGSS)

To establish a consensus and facilitate the comparisons of clinical trials across different international cooperative consortiums, the International Neuroblastoma Risk Group developed the INRGSS for pre-treatment risk classification based on image-defined risk factors (IDRFs) and clinical and biological features of the tumours (Table-03)(Cohn *et al.*, 2009; Monclair *et al.*, 2009).

The age of the patient at the time of diagnosis, the stage of the disease and the presence of *MYCN* amplification in NB cells are the three strongest determinants of clinical outcome. These determinants, combined with the loss of chromosome 11q, the tumour histology and the DNA ploidy, are the defining criteria of NB risk-group stratification by the INRGSS system (Table-04) (Monclair *et al.*, 2009).

## 2.8. Treatment

The treatment of NB patients remains a challenge due to the diverse clinical course of the disease and to the infant or child development. Thus, the therapeutic strategies are determined based on the risk stratification of NB patients, by trying to optimize both the efficiency and the specificity of the treatment. After diagnosis and risk classification, each risk group is managed according with specific protocols (Figure 06).

Stage	Definition
1	Localized tumour with complete gross excision, with or without microscopic residual disease; representative ipsilateral lymph nodes negative for tumour microscopically (nodes attached to and removed with the primary tumour may be positive).
2A	Localized tumour with incomplete gross excision; representative ipsilateral nonadherent lymph node negative for tumour
2B	Localized tumour with or with our incomplete gross excision; representative ipsilateral non adherent lymph node positive for tumour. Enlarged contralateral lymph nodes must be negative microscopically
3	Unresectable unilateral tumour infiltrating across the midline, * with or without regional lymph node involvement; or midline tumour with bilateral extension by infiltration (unresectable) or by lymph node involvement
4	Any primary tumour with dissemination to distant lymph nodes, bone, bone marrow, liver, skin, and/or other organ (except as defined for 4S).
4S	Localized primary tumour (as defined for stage 1, 2A or 2B) with dissemination limited to skin, liver, and/or bone marrow** (limited to infants < 1 year of age)

NOTE. Multifocal primary tumour (for example bilateral adrenal primary tumours) should be staged according to the greatest extent of disease, as defined above, and followed by a subscript letter M (for example 3<sub>M</sub>)

\*The midline is defined as the vertebral column. Tumours originating on one side and crossing the midline must infiltrate to or beyond the opposite side of the vertebral column.

\*\*Marrow involvement in stage 4S should be less than 10% of the total nucleated cells identified as malignant on bone marrow biopsy or on marrow aspirate. More extensive marrow involvement would be considered to be stage 4. The MIBG scan (if performed) should be negative in the marrow.

**Table-02. International Neuroblastoma Staging System.** Adapted from (Brodeur *et al.*, 1993).

Stage	Description
L1	Localized tumour not involving vital structures as defined by the list of image-defined risk factors and confined to one body compartment
L2	Locoregional tumour with presence of one or more image-defined risk factors
M	Distant metastatic disease (except stage MS)
MS	Metastatic disease in children younger than 18 months with metastases confined to skin, liver and/or bone marrow

NOTE. Patients with multifocal primary tumours should be staged according to the greatest extent of disease as defined in the table.

**Table-03. International Neuroblastoma Risk Group Staging System.** Adapted from (Monclair *et al.*, 2009).

### Very low risk and low risk

Very low risk and low risk (LR) NB patients present a 5 year(y)-EFS above 75% and a 5y-OS rate of 90-100%. The standard treatment for these patients is limited mainly to clinical observation, although the surgical resection of the primary tumour might be required in some cases (Matthay *et al.*, 2016; Nakagawara *et al.*, 2018).

INRG stage*	Age (months)	Histologic category	Grade of tumour differentiation	MYCN status	11q aberration	Ploidy	Pretreatment risk group
L1/L2		GN maturing; GNB intermixed					Very low
L1		Any, except GN maturing or GNB intermixed		NA			Very low
				A			High
L2	< 18	Any, except GN maturing or GNB intermixed		NA	No		Low
					Yes		Intermediate
	> 18	GNB nodular; NB	Differentiating	NA	No		Low
					Yes		Intermediate
		Poorly differentiated or undifferentiated	NA			High	
				A			High
M	< 18			NA		Hyperdiploid	Low
	< 12			NA		Diploid	Intermediate
	12 to <18			NA		Diploid	Intermediate
	<18			A			High
	>18						High
MS	<18			NA	No		Very Low
					Yes		High
				A			High

\* See table 03 for detailed explanation

**Table-04. International Neuroblastoma Risk Group (INRG) consensus pretreatment classification schema.** A: Amplified; GN: Ganglioneuroma; GNB: Ganglioneuroblastoma; NA: Non-Amplified; NB: Neuroblastoma. Adapted from (Cohn *et al.*, 2009).

### Intermediate risk

Intermediate risk (IR) NB patients have a 5y-EFS of 50-75% and a 5y-OS rate of 60-85%. These patients require the surgical resection of the primary tumour (when possible), plus chemotherapy and radiotherapy (Matthay *et al.*, 2016; Nakagawara *et al.*, 2018).

### High risk

High risk (HR) NB patients have a 5y-EFS rate of 30-50% and require a multimodal therapeutic strategy that consists of 4 consecutive phases: induction chemotherapy, surgery, consolidation therapy and maintenance therapy. The induction chemotherapy consists of 2-8 cycles of a high-dose cocktail of chemotherapeutic compounds (named COJEC and consisting of cisplatin, vincristine, carboplatin, etoposide and cyclophosphamide) that aims to shrink the primary tumour and reduce metastases. The consolidation therapy consists of a myelo-ablative chemotherapy followed by an autologous hematopoietic stem cell transplantation (AH SCT) and radiotherapy. The maintenance therapy is aimed to eradicate the minimal residual disease using immunotherapy (using dinutuximab<sup>3</sup> with or without cytokines) and/or differentiation therapy (using 13-cis-retinoic acid also known as isotretinoin) (Matthay *et al.*, 2016; Nakagawara *et al.*, 2018).

Despite this aggressive therapeutic regimen, 50% of the high-risk NB patients relapse and the 5y- OS remains below 30% for those presenting certain clinical-biological features such as patients older than 18 months, with metastatic dissemination and amplification of *MYCN* (Cohn *et al.*, 2009;

<sup>3</sup> **Dinutuximab** is a chimeric monoclonal antibody against the disialoganglioside GD2, a cell-surface tumour associated antigen highly expressed by NB cells.

Nakagawara *et al.*, 2018). Thereby, there is an urgent need to discover and develop novel therapeutic targets or strategies in order to optimize the treatment of high-risk NBs and improve their outcome.

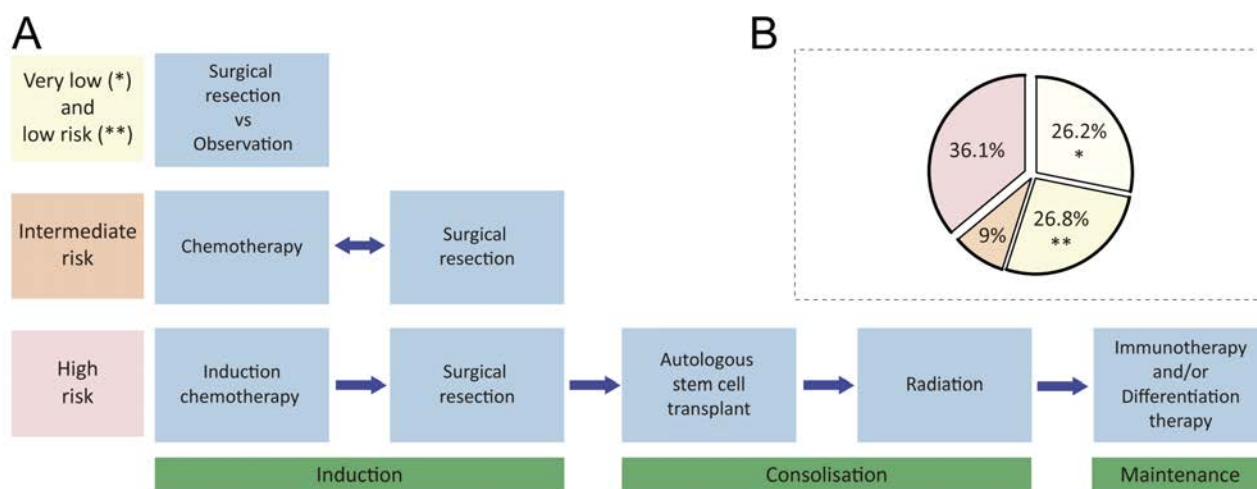


**Figure-06. Treatment overview of neuroblastoma by risk classification according to the International Neuroblastoma Risk Group Staging System**

(A) Patients with very low and low risk are often managed with surgical resection or observation alone with tumours likely to spontaneously regress that are not causing symptoms. Intermediate patients are treated with chemotherapy with the number of cycles dependent on their response as well as surgical resection of the primary tumour. High risk disease requires intensive multimodal therapy including chemotherapy, myeloablation, radiation, immunotherapy and differentiation therapy. (B) Proportion of NB patients diagnosed according to each risk category. Adapted from (Tolbert and Matthay, 2018; Cohn *et al.*, 2009).

### 3. Cancer stem cells

The origins of the term ‘stem cell’ can be traced back to the late 19<sup>th</sup> century when Ernst Haeckel used the term ‘Stammzellen’ (‘stem cell’) to describe ‘the fertilized egg cell as the cell of origin of all other cells of an animal or human organism’ (Maehle, 2011). Soon the term was adopted by the embryology field. Already in 1892, the zoologist T. Boveri described as ‘Stammzellen’ the cells which derive from the fertilized egg cell and lead to the primordial germ cell and from which various primordial somatic cells branch off. Boveri defined precisely the two essential characteristics of a stem cell that persist to date: their self-renewal capacity and their multipotency or ability to give rise to different lineages (Maehle, 2011). In parallel to Haeckel’s work on the ‘Stammzellen’, M. Askanazy and others conducted pioneering studies on the nature of teratomas: tumours deriving from the germ cells. Askanazy described for the first time the heterogenic composition of teratomas, where he found multiple cell lineages from the 3 germ-layers (Askanazy, 1907). Their resemblance to aberrant ‘embryos’ led him and others to use the term Stammzellen to name the teratoma tumour cells, and to propose that the well differentiated benign somatic teratoma cells might develop by differentiation from multipotent stem cell(s) (Askanazy, 1907). These early studies settle the bases for the cellular analysis of

tumour heterogeneity with the landmark work of B.G. Pierce in the 1960's (Kleinsmith and Pierce, 1964; Pierce and Wallace, 1971). Using *in vivo* radiolabelling approaches, Pierce described how the undifferentiated teratoma cells were labelled by short incubations, while the well differentiated areas of the tumour were preferentially labelled after longer exposures. Interestingly, the latter were unable to form secondary tumours when transplanted into a syngeneic host (Pierce and Wallace, 1971). These findings led Pierce to propose that tumours are a caricature of normal embryonic development and to state the first preliminary definition of a cancer stem cell: '[...] A tumour is a dynamic system composed of malignant stem cells and their well differentiated and benign progeny, admixed to form a caricature of the tissue of origin. Malignant stem cells are responsive to environmental controls, an observation that should make us rethink the concept of progression and autonomy [...]' (Pierce, 1974).

However, the discovery of oncogenes and tumour suppressor genes changed the focus of interest in the cancer field. The clonal evolution theory of tumour growth and tumour heterogeneity was broadly accepted by the scientific community, and Pierce's cancer stem cell hypothesis of tumour heterogeneity was abandoned for almost 25 years (Clevers, 2011; Nowell, 1976).

### 3.1. Origins of tumour heterogeneity

Tumours are composed by a heterogenic cell population. This heterogeneity is revealed by differences in the cellular morphology, proliferative capacity, genetic/ epigenetic changes, response upon treatment and metastatic behaviour (Greaves and Maley, 2012). Tumour heterogeneity mainly comes from the tumour cells *per se* and from their interaction with the tumour microenvironment (Hannahan and Weinberg, 2011). Throughout the 20<sup>th</sup> century, two main models have been proposed to explain cancer growth and tumour heterogeneity at the cellular level (Clevers, 2011; Nowell, 1976; Pierce, 1974): **the stochastic and the cancer stem cell model** of tumour growth (Nowell, 1976; Pierce, 1974). Superimposed on these models, tumours undergo clonal evolution as a result of genetic instability (Figure 07) (Greaves and Maley, 2012; McGranahan and Swanton, 2017). This means that new tumour clones progressively appear and whenever the new genetic variant constitutes a selective advantage over the pre-existing population, the new clone will be the precursor of the next predominant tumour subpopulation (Greaves and Maley, 2012; McGranahan and Swanton, 2017). Finally, tumour cells recruit fibroblasts, immune cells and endothelial cells to create a favourable microenvironment that fosters tumour progression and contributes to tumour heterogeneity (Joyce and Pollard, 2009; Plaks *et al.*, 2015).

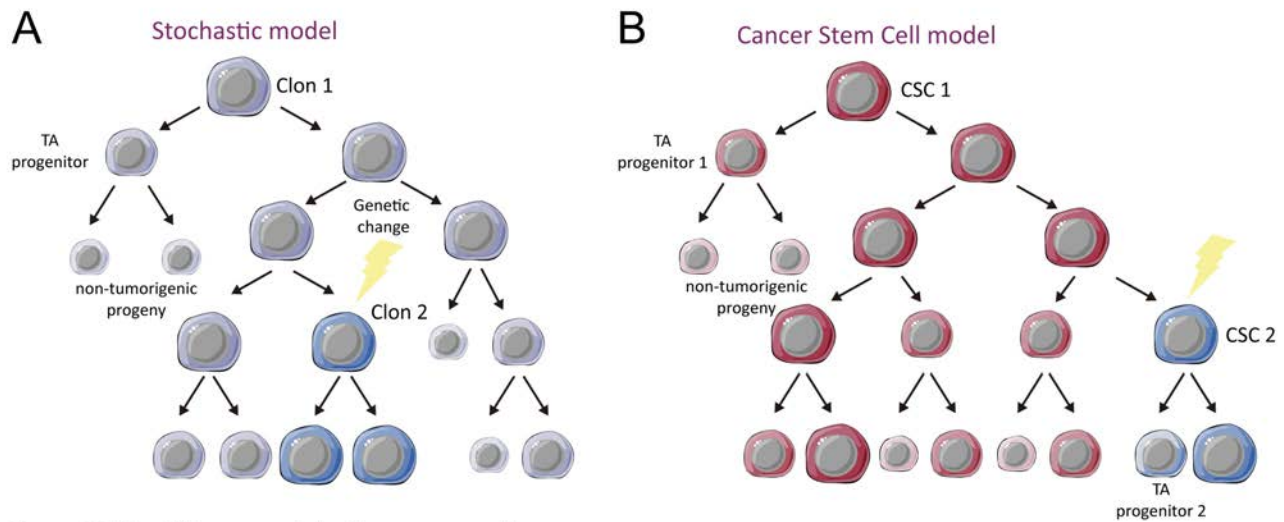


**Figure-07. The different models of tumour growth**

(A) In the stochastic model of tumour growth, all cells are equipotent and stochastically self-renew or differentiate into transient amplifying (TA) progenitors or non-tumorigenic cancer cells, leading to tumour heterogeneity. (B) In the cancer stem cell (CSC) model of tumour growth, only a subset of tumour cells has the ability for long-term self-renewal and these cells give rise to TA progenitors with limited self-renewal potential and to non-tumorigenic 'differentiated' progeny. In both models, new genetic changes due to genome instability generate new clones/CSCs that might present selective advantages over the previous population, increasing tumour heterogeneity. Adapted from (Beck and Blanpain, 2013).

### 3.1.1. The stochastic model

The stochastic model states that all tumour cells are equipotent and stochastically a proportion of them proliferate to fuel tumour growth while the other tumour cells differentiate. Hence, in this model each tumour cell appears as the minimal unit for tumour evolution. As a result of genetic instability, somatic mutations and chromosomal changes might occur in any tumour cell, increasing tumour heterogeneity. Whenever the new variant provides a survival advantage over the pre-existing population, the cell will become the next predominant clonal population. This dynamic and constant clonal evolution renders tumours increasingly abnormal and more aggressive over time (Cairns, 1975; Greaves and Maley, 2012; Nowell, 1976; Sun *et al.*, 2018).

The use of single-cell sequencing has confirmed the existence of a clonal architecture in different cancers (such as triple negative breast cancer, colon cancer, EGFR-amplified glioblastoma, acute myeloid leukaemia and paediatric lymphoblastic leukaemia) and even the clonal history of each patient has been established when possible (Anderson *et al.*, 2011; Francis *et al.*, 2014; Gao *et al.*, 2016; Niemoller *et al.*, 2016; Wang *et al.*, 2014; Yu *et al.*, 2014). Clonal diversity and therapy-driven clonal evolution have also been found in two cohorts of NB patients composed by pair samples of primary tumours and their relapse. The authors show the emergence of new genetic subclonal population at relapse showing recurrent mutations driving RAS-MAPK pathway activation. However, it remains unknown whether it depends on the acquisition of *de novo* mutations or on the expansion of previously existing rare subclones (Eleveld *et al.*, 2015; Schramm *et al.*, 2015).

### 3.1.2. The cancer stem cell model

The cancer stem cell model states that tumours are hierarchically organized, similarly to normal tissues, and that tumour growth is fuelled by a subpopulation of dedicated tumorigenic cancer cells called cancer stem cells (CSCs) (Pierce, 1974; Wang and Dick, 2005). Hence tumours are composed mainly of 'immature' CSCs and their non-tumorigenic progeny, the non-CSCs. As described by Pierce, CSCs are defined by their capacity to self-renew and to give rise to a multilineage progeny that recapitulates the tumour heterogeneity (Kreso and Dick, 2014; Pierce, 1974; Wang and Dick, 2005). Thereby, the widespread interest in the CSC model is that it can comprehensibly explain clinical observations that are poorly understood, such as: 1) the almost inevitable recurrence of tumours after an initially successful chemotherapy and/or radiation therapy (Kreso *et al.*, 2013); 2) tumour dormancy (Giancotti, 2013; Pece *et al.*, 2010; Roesch *et al.*, 2010); 3) metastasis (Oskarsson *et al.*, 2014) and 4) the presence of tumour cells at different stages of differentiation within the same tumour (as it happens in teratoma and NB tumours) (Kleinsmith and Pierce, 1964; Shimada *et al.*, 1999).

The recent rise of the CSC model is closely related to advances in our understanding of haematopoiesis and haematological malignancies (Batlle and Clevers, 2017; Clevers, 2011; Wang and Dick, 2005). Early studies in haematological malignancies reported that the proliferative capacity of leukemic cells was heterogenic and described a hierarchical organization that resembled that of normal haematopoietic stem cells (Clarkson, 1969). In addition, leukemic stem-like cells were found to re-enter cell cycle after chemotherapy as shown by *in vivo* radiolabelling of human patients (Clarkson *et al.*, 1970; Killmann *et al.*, 1963). The development of secondary leukaemia after xenotransplantation of CD34<sup>+</sup>CD38<sup>-</sup> leukemic cells into immunodeficient mice is considered to be the first identification of a CSC population (Dick *et al.*, 1997; Lapidot *et al.*, 1994; Uckun *et al.*, 1995). Interestingly, this combination of biological markers (CD34<sup>+</sup>CD38<sup>-</sup>) is the same that identifies normal haematopoietic stem cells (HSCs) (Bonnet and Dick, 1997; Lapidot *et al.*, 1994; Uckun *et al.*, 1995). The identification of CD44<sup>+</sup>CD24<sup>-/low</sup> as breast cancer CSCs using a similar approach started the discovery of CSCs or CSC-like subpopulations in many other types of solid tumours (Al-Hajj *et al.*, 2003).

#### 3.1.2.1. The divergent behavior of CSCs

Multiple evidences demonstrate the relevance of the CSC model to explain tumour growth and relapse in many tumour types (Batlle and Clevers, 2017; Nassar and Blanpain, 2016). Nevertheless, the past two decades of research in the field have revealed some caveats in the original CSC model (hereafter called the standard hardwired CSC model) and the need of new experimental approaches such as lineage-tracing and cell ablation techniques to accurately unravel CSC identity and behaviour (Figure 8) (Batlle and Clevers, 2017; Clevers, 2011; Magee *et al.*, 2012; Medema, 2013).

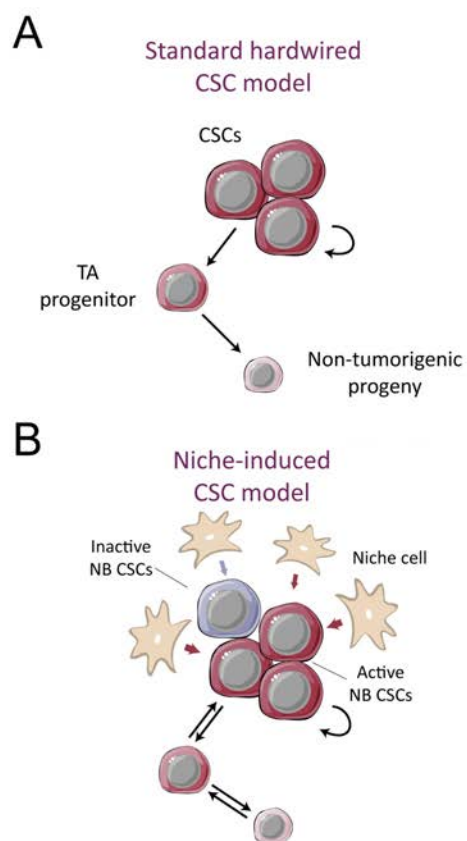


**Figure-08. Cell-autonomous versus niche-induced cancer stem cell models**

(A) Canonical hardwired cancer stem cell (CSC) hierarchy. In this type of hierarchy self-renewal capacity is a cell-autonomous property of the CSCs. Upon asymmetric division, CSCs give rise to one CSC and one transit amplifying (TA) tumour cells. TA cells divide rapidly originating non-tumorigenic 'differentiated' progeny. (B) Niche-induced CSC hierarchy. In this type of hierarchy the CSC phenotype can be instructed by extracellular cues. CSCs can divide symmetrically or asymmetrically. TA cells and 'differentiated' cells display variable plasticity and can trans-differentiated into CSCs upon environmental signals. Adapted from (Batlle and Clevers, 2017).

### 3.1.2.1.1. The standard hardwired CSC model

The classical CSC model adopted most of the features established for the HSCs and haematological malignancies (Batlle and Clevers, 2017; Clevers, 2011; Wang and Dick, 2005). First, it established that a substantial fraction of tumour heterogeneity results from its hierarchical organization, which is usually reminiscent of the one of the tissue of origin but superimposed on underlying genetic aberrations. Second, it states that the tumour hierarchy consists of rare slow-cycling CSCs located at the apex of the hierarchy and that divide asymmetrically into progenitor daughter cells and new quiescent CSCs. The non-CSC progeny could divide symmetrically for a limited number of rounds before giving rise to the non-dividing 'terminally-differentiated' tumour cells (Figure 8A). Third, this tumour cell hierarchy is rigidly hardwired due to the fact that non-CSCs hardly initiate tumours after transplantation. Therefore, the cell founder of the tumour has to be a normal stem cell that stochastically undergoes malignant transformation. Finally, this classical model supposes that the relapse depends on the survival of quiescent CSCs that are unlikely to be affected by the chemotherapeutic treatment, since it targets more efficiently the fast-cycling non-CSCs (Batlle and Clevers, 2017; Clevers, 2011; Wang and Dick, 2005).

Several of these features have been proved for certain types of cancer. For example, the histological and transcriptomic analysis of colorectal cancer (CRC) revealed that their hierarchical organization seems to be reminiscent of the organisation of the normal colonic epithelium (Dalerba *et al.*, 2011; Merlos-Suarez *et al.*, 2011). However, the stability of the CSC phenotype and the existence of a rigid

and unidirectional hierarchy might not be applicable for most CSC-driven tumours and led to a revision of the model (Kreso and Dick, 2014).

### 3.1.2.1.2. The niche-induced CSC model

Glioblastoma (GB) and melanoma represent two enlightening examples of the caveats that emerged against the hardwired CSC model. GBs are brain tumours in which the existence of hierarchical organization is widely accepted. GB cancer stem cells (GBcsc) are responsible of the long-term tumour growth (Chen *et al.*, 2010) and the relapse after therapy (Bao *et al.*, 2006; Chen *et al.*, 2012a; Kondo *et al.*, 2004). In this regard, several therapeutic strategies targeting GBcsc have been developed pre-clinically (Chen *et al.*, 2012a; Piccirillo *et al.*, 2015). However, at least 5 different markers of GBcsc-like subpopulations, including CD133, CD15, NESTIN, SSEA1, EPHA2 and EPHA3, have been described so far and it is unclear whether they identify the same GBcsc population or different subtypes of GBcsc (Binda *et al.*, 2012; Chen *et al.*, 2010; Chen *et al.*, 2012b; Day *et al.*, 2013; Kim *et al.*, 2013; Singh *et al.*, 2004; Son *et al.*, 2009). In addition, the transdifferentiation of GB non cancer stem cells (non-CSCs) into GBcsc has been proposed (Suva *et al.*, 2014) and the oncogenic transformation of mature neuron and/or astrocytes can induce their dedifferentiation into immature GBcsc-like cells (Friedmann-Morvinski *et al.*, 2012). Hence any mature cell from the CNS can potentially become the substrate of malignant transformation and GB initiation.

On the contrary, melanomas are tumours with no recognized hierarchy. Most of the melanoma tumour cells present tumour-propagating capacities and the expression of surface markers seems highly plastic (Quintana *et al.*, 2010; Quintana *et al.*, 2008; Shackleton *et al.*, 2009).

These two examples illustrate the obvious disparities that can exist in regards to the rigid unidirectional CSC hierarchy and led to the refining of the CSC model to take into account this dynamic and plastic reality (Greaves, 2013; Kreso and Dick, 2014; Magee *et al.*, 2012; Medema, 2013). The **niche-induced CSC model** proposes a plastic hierarchical organization whereby the phenotypic interconversion between CSCs and the more differentiated non-CSCs is possible and contributes to tumour evolution (Figure 8B). Whether this happens by neutral competition<sup>4</sup>, or if it is regulated by the microenvironment through paracrine signalling, is likely to depend on each type of tumours and on its genetic background (Batlle and Clevers, 2017; Beck and Blanpain, 2013; Medema, 2013). Additionally, the plasticity of the tumour hierarchy in the niche-induced CSC model suggests that any cell of a tissue could become the cell-of-origin of a tumour (also known as the tumour-initiating cell,

<sup>4</sup> The notion of **neutral competition** refers to a dynamic model of stem cell growth where the stem cells can be lost and replaced stochastically by asymmetric or symmetric division of any other stem cell of the niche. (Stine *et al.*, 2013). The neutral competition dynamics have been described in epithelial tissues such as the epidermis, the stomach and the intestinal crypts as well as in breast cancer cells and for the CSCs population in squamous skin cancer (Doupe *et al.*, 2010; Driessens *et al.*, 2012; Gupta *et al.*, 2011; Leushacke *et al.*, 2013; Lopez-Garcia *et al.*, 2010; Snippert *et al.*, 2010).

TIC) after undergoing malignant transformation (Blanpain, 2013; Visvader, 2011). Finally, in the niche-induced CSC model, the tumour growth might be fuelled by CSCs undergoing symmetric or asymmetric divisions and the fate of their progeny (whether they generate 0, 1 or 2 daughter CSCs) might be determined by neutral competition, similarly to the adult stem cell dynamics (Batlle and Clevers, 2017; Beck and Blanpain, 2013).

### 3.1.3. The clonal evolution of CSCs

In the current view about tumour growth, the tumour heterogeneity can arise from different tumour cells presenting distinct mutations in combination with an aberrant but hierarchical organization that shows a variable degree of plasticity and niche dependency (Greaves and Maley, 2012; Kreso and Dick, 2014; Marjanovic *et al.*, 2013; Meacham and Morrison, 2013). Accordingly, mutations might affect the tumour-propagating capacity of any tumour cell and dictate to what extent the tumour growth depends on niche signals (Greaves and Maley, 2012; Kreso and Dick, 2014). For example, the analysis of clonal dynamics during serial transplantation of pancreatic cancer samples indicated that long-term growth is driven by the successive activation of transiently active tumour-propagating cells<sup>5</sup> carrying different genetic alterations (Ball *et al.*, 2017). However, the plasticity of the tumour hierarchy and the influence of the tumour microenvironment might dictate to what extent mutations can influence the behaviour of the non-CSC progeny (Plaks *et al.*, 2015). Activating mutations in the WNT/ $\beta$ -catenin signalling pathway drive CRC in the colonic epithelium, but the intracellular activity of the pathway in CRC cells depends on microenvironmental signals (Brabletz *et al.*, 2001; Vermeulen *et al.*, 2010). Either way, the genetic instability occurring at different levels of the tumour hierarchy might direct clonal evolution throughout tumour progression, thereby unifying the tumour-propagating capacities of most of the tumour cells of the hierarchy and making the tumour cells progressively insensitive to the niche signals (Figure 9) (Batlle and Clevers, 2017; Greaves and Maley, 2012; Kreso and Dick, 2014; Medema, 2013). Independently of the predominant tumour organization (either hierarchical or genetically-driven), it is worth noting that tumour cells might develop specific vulnerabilities and requirements at different moments of the tumour progression, such as during minimal residual disease<sup>6</sup> or metastasis initiation. For instance, the regeneration of Lgr5<sup>+</sup> CRCcsc from Lgr5<sup>-</sup> non-CSCs occurs in the primary tumour but not in the liver metastasis (de Sousa e Melo *et al.*, 2017).

---

5 Along this doctoral thesis the notion of **tumour propagating cells (TPCs)** refer to the tumour cells that present self-renewal capacity and drive tumour growth despite not fitting to the CSC definition. These type of cells are expected to drive the growth of tumours where there is no hierarchical organization of the tumour cells such as pancreatic cancer and melanoma (Ball *et al.*, 2017; Held *et al.*, 2010; Quintana *et al.*, 2010; Quintana *et al.*, 2008; Shackelton *et al.*, 2009).

6 The notion of **minimal residual disease** refers to a small and undetectable population of tumour cells that persists during the chemotherapeutic treatment in an environmentally-induced drug-tolerant state and that resume tumour growth after therapy. Thereby, these cells are the ultimate responsible of the tumour relapse (Meads *et al.*, 2009)

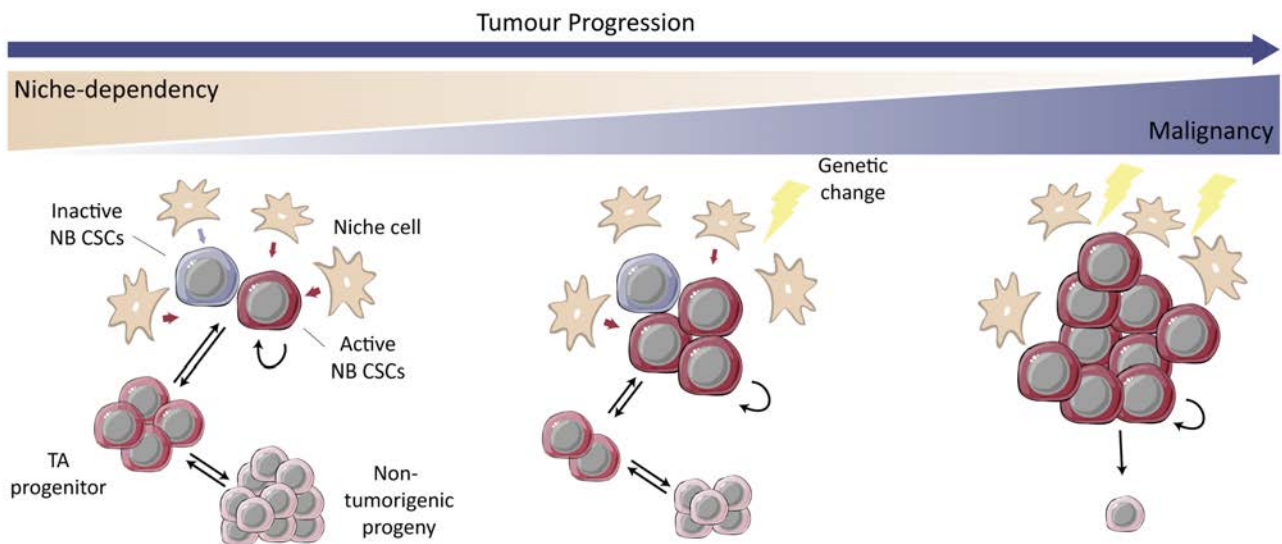


**Figure-09. Niche dependency and tumour progression in the cancer stem cell model**

(A) In the niche induced cancer stem cell (CSC) model, genetic and epigenetic changes render CSCs progressively independent of niche signals. As a consequence, the cell-autonomous CSC phenotype impedes 'differentiation', resulting in a shallow hierarchy with many CSCs and few non-CSCs. NB: neuroblastoma; TA progenitor: transit amplifying progenitor. Adapted from (Batlle and Clevers, 2017).

## 3.2. The cancer stem cell concept

The existence and clinical relevance of CSCs has been further validated in certain tumour types with the recent development of lineage tracing and cell ablation techniques (Batlle and Clevers, 2017; Nassar and Blanpain, 2016). It is now evident that the CSC concept refers to malignant cells with diverse and plastic behaviours but characterized by their self-renewal ability and their multi-lineage potential. Nevertheless, other interesting traits have been used to identify CSCs/CSCs-like subpopulations and to understand their biological relevance for tumour progression (Batlle and Clevers, 2017).

### 3.2.1. CSCs properties

#### 3.2.1.1. Functional parallels between normal SCs and CSCs

The CSCs and the cells with tumour-propagating capacities might share certain characteristics with their normal SC counterparts of the tissue of origin, including a common transcriptomic and/or epigenomic profile and their similar biological response to regulatory signalling pathways (see the next section for further details) (Magee *et al.*, 2012; Matsui, 2016; Reya *et al.*, 2001). As mentioned before, the hierarchical organization of CRC might reflect that of the normal colonic epithelium with Lgr5<sup>+</sup> CSCs/SCs at the apex of the hierarchy (Dalerba *et al.*, 2011; Merlos-Suarez *et al.*, 2011). Similarly, a common transcriptomic signature has been identified for breast CSCs and an embryonic subpopula-

tion of mammary stem cells (Pece *et al.*, 2010; Spike *et al.*, 2012). Additionally, recent evidences have shown the epigenetic reprogramming of cancer cells towards an embryonic-like state upon chemotherapy (Boeva *et al.*, 2017; Rambow *et al.*, 2018; van Groningen *et al.*, 2017). Melanoma and NB are two different types of tumours that both derive from the malignant transformation of different NCC derivatives: the terminally differentiated melanocytes and the developing SA lineage, respectively. In a model of minimal residual disease of melanoma, the transdifferentiation of melanoma cells towards a NCC-like state favours their resistance to treatment and their relapse (Rambow *et al.*, 2018).

### 3.2.1.2. Self-renewal capacity

All CSCs has the unique capacity to self-renew (Kreso and Dick, 2014). Regulation of their self-renewal capacity might depend on the same signalling pathways that control proliferation of normal stem cells such as WNT, Hedgehog, FGF and Notch. However, the different genetic and/or epigenetic changes harboured by the CSCs might cause the constitutive activation or an aberrant regulation of these pathways, leading to an uncontrolled growth (Matsui, 2016; Reya *et al.*, 2001). For instance, WNT/ $\beta$ -catenin signalling as well as the of the Polycomb group member BMI1 are required to maintain the self-renewal capacity of the adult HSCs and the leukemic stem cells in certain subtypes of leukaemia (Lessard and Sauvageau, 2003; Park *et al.*, 2003; Zhao *et al.*, 2007). On the contrary, WNT/ $\beta$ -catenin signalling is required to maintain the self-renewal capacity of the CSCs in a mouse model of squamous cell carcinoma (SCC) but not for epidermal stem cell maintenance, thus representing a putative therapeutic target for SCC (Malanchi *et al.*, 2008). In addition, several evidences suggest a relevant role of the microenvironment in regulating the self-renewal capacity of CSCs. In this regard, the self-renewal of CD133<sup>+</sup> GBcsc in the vascular niche is regulated by VEGF-A secreted from the endothelium and by the oxygen levels through the HIF1- $\alpha$ /2- $\alpha$  TFs (Calabrese *et al.*, 2007; Li *et al.*, 2009; Soeda *et al.*, 2009). In CRC, the secretion of IL-17A by cancer-associated fibroblasts maintains the self-renewal capacity of CD44<sup>+</sup> CRCcsc-like cells during chemotherapy (Lotti *et al.*, 2013).

### 3.2.1.3. Plasticity

The ability to generate a multi-lineage progeny that recapitulates the original tumour heterogeneity is the second defining feature of a *bona fide* CSC (Batlle and Clevers, 2017; Kreso and Dick, 2014; Nassar and Blanpain, 2016). As detailed in the previous section, in many solid neoplasms the CSC hierarchy accounts for a certain degree of plasticity, and the epigenetic reprogramming of the non-CSC subpopulation into CSCs might happen under certain conditions (Batlle and Clevers, 2017; Nassar and Blanpain, 2016). These interconversions could be driven stochastically or regulated by environmental signals (Batlle and Clevers, 2017; Chaffer *et al.*, 2011; Chaffer *et al.*, 2013; Gupta *et al.*, 2011; Nassar and Blanpain, 2016). Remarkably, the interconversion from non-CSCs to CSCs might sustain tumour

growth and suggest that CSCs-targeted therapies used alone might fail in controlling tumour growth (de Sousa e Melo *et al.*, 2017).

#### 3.2.1.4. Resistance to therapy

The use of radio-labelled isotopes in human leukaemia showed that slow-cycling leukemic stem cells re-enter into the cell cycle after chemotherapy, causing tumour relapse (Clarkson *et al.*, 1970; Killmann *et al.*, 1963). This early result suggested that the resistance to chemotherapy and radiation therapies was an intrinsic property of CSCs (Wang and Dick, 2005). Lineage tracing experiments in genetic mouse models of GB and SCC have demonstrated the persistence of quiescent CSCs after chemotherapy that are latter on responsible of tumour relapse (Chen *et al.*, 2012b; Oshimori *et al.*, 2015). Several independent mechanisms have been described and might contribute to the acquired resistance of CSCs to chemotherapy and radiation therapy (Cojoc *et al.*, 2015; Zhou *et al.*, 2009). The main strategies include:

- o The increased expression of drug efflux pumps such as the ATP-binding Cassette (ABC) transporter superfamily (Bleau *et al.*, 2009).
- o The increased expression of anti-apoptotic genes or the activation of survival pathways (Zhang *et al.*, 2010b).
- o An enhanced DNA-repair capacity (Bao *et al.*, 2006).
- o An enhanced protection against reactive oxygen species (ROS) (Diehn *et al.*, 2009).
- o The entry into quiescence or plastic cell cycle kinetics (Liau *et al.*, 2017).

#### 3.2.1.5. Metastasis, EMT and CSCs

Metastasis is a complex multistep process that requires tumour cells to leave the primary tissue, reach a distant site (either through the blood or the lymphatic circulation) and colonize a secondary location to initiate a new tumour (Oskarsson *et al.*, 2014). The CSCs are defined as the only cells in the tumour with a self-renewal capacity, which implies that they are the only ones that could be responsible for metastasis initiation (Batlle and Clevers, 2017; Oskarsson *et al.*, 2014). Several evidences have supported this notion. For instance, the high expression of SCs/CSCs-related markers in primary colorectal and breast tumours is associated with poor prognosis and metastatic relapse (Dalerba *et al.*, 2011; Merlos-Suarez *et al.*, 2011; Pece *et al.*, 2010). Additionally, circulating tumour cells expressing CSC-related markers isolated from the blood of breast cancer patients were able to generate bone, liver and lung metastases when transplanted into immunodeficient mice (Baccelli *et al.*, 2013).

Nevertheless, the connection between the CSC phenotype and the EMT remains controversial. Initial data suggested that the EMT might be required to sustain the CSC phenotype and reinforced the notion that the CSC phenotype was essential for metastatic spreading (Puisieux *et al.*, 2014). The EMT process and its role in NCC formation were briefly introduced in section 1.1. The same TFs that control the embryonic EMT (such as Snail1/Slug, ZEB1/2, TWIST1/2, PRRX1 among others) drive the EMT program in epithelial tumour cells. They seem to induce a transient mesenchymal-like migratory phenotype that might coincide with other malignant features such as a lengthening of the cell cycle, an increased chemoresistance capacity and the upregulation of stemness-associated TFs and markers (Thiery *et al.*, 2009). Whether the EMT program is required to sustain the CSC phenotype has been a matter of intense debate (Batlle and Clevers, 2017; Beerling *et al.*, 2016; Brabletz, 2012; Puisieux *et al.*, 2014). At present, the most plausible scenario includes the EMT program as another source of tumour plasticity that can generate (in certain contexts) CSC-like states that contribute to tumour progression (Batlle and Clevers, 2017; Oskarsson *et al.*, 2014). As an example, the TF ZEB1 seems to regulate the interconversion between non-CSCs and CSCs in response to environmental TGF- $\beta$  signaling in the basal type of breast cancer (Chaffer *et al.*, 2013), while the TF PRRX1 suppresses stemness<sup>7</sup> properties and has to be downregulated after metastatic colonization to allow the formation of secondary tumours (Ocana *et al.*, 2012).

As suggested by current evidences, the metastatic process might be a complex interplay between multiple elements such as: the CSCs and the non-CSC populations and their dependency on micro-environmental signals, the co-existence of distinct genetic/epigenetic tumour subclones and other cellular populations that compose the tumour niche in the primary and the receiving tissues (for further details see section 3.1.3 from the Introduction) (Batlle and Clevers, 2017; Beck and Blanpain, 2013; Nassar and Blanpain, 2016; Oskarsson *et al.*, 2014). In this regard, the CSCs with metastatic capacity could be just a subset of the original CSC population of the primary tumour, or even a specific subpopulation of CSCs that is dispensable for primary tumour growth but required for metastatic dissemination (de Sousa e Melo *et al.*, 2017; Hermann *et al.*, 2007; Pascual *et al.*, 2017). As such, the Lgr5+ CRCcsc might be dispensable for primary growth but required for colonization and growth in the liver (de Sousa e Melo *et al.*, 2017).

### 3.2.1.6. Other features attributed to CSCs

Certain inconsistencies in the CSC concept come from the inadequate generalization of conclusions extracted from the haematopoietic stem cell field (Batlle and Clevers, 2017). The study of the different adult SC populations has shown that several characteristics that were once associated to the functional characterization of a SC population (such as their low frequency, their ability to divide

---

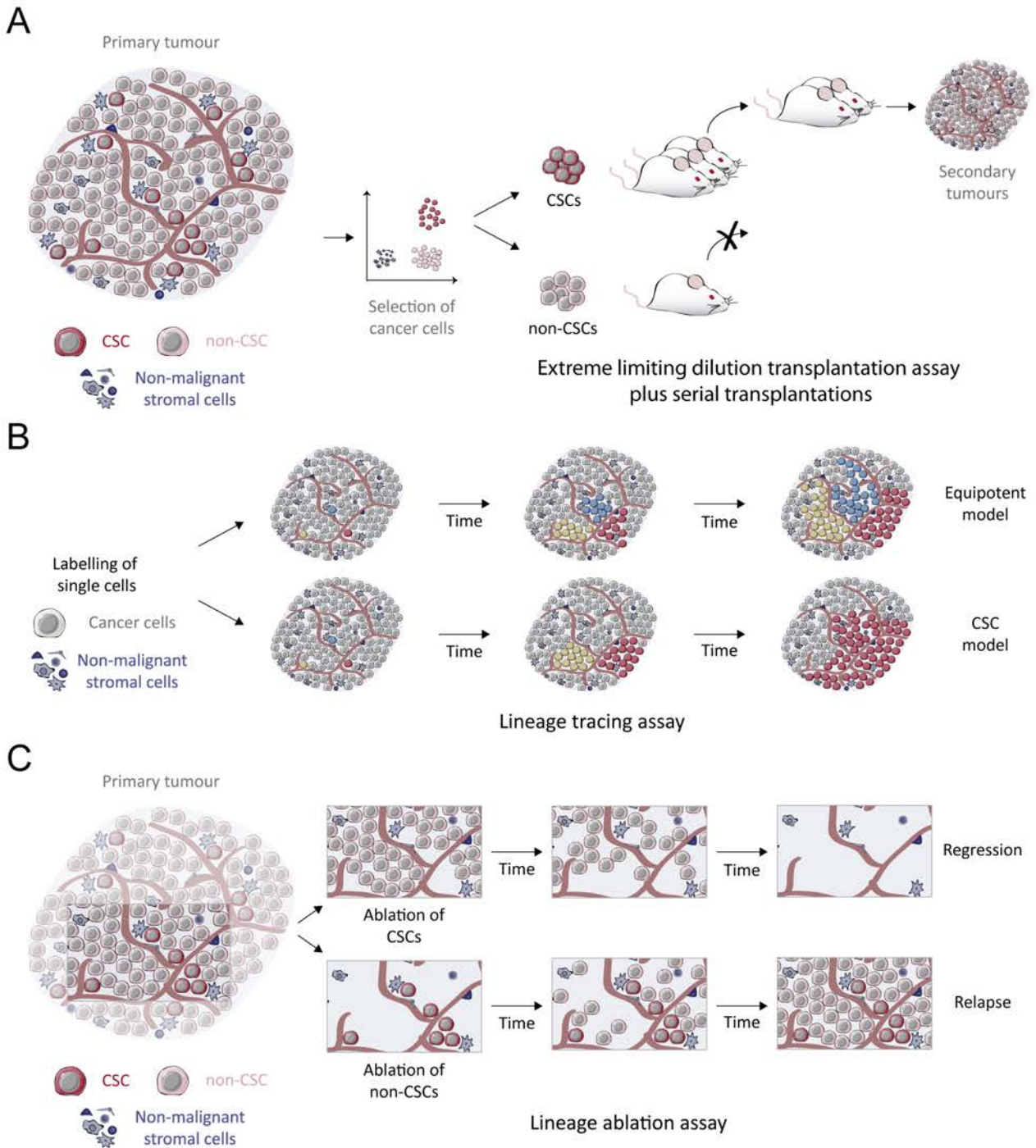
<sup>7</sup> The notion of **stemness** refers collectively to the integrated functioning of molecular programs that govern and maintain the stem cell state (Kreso and Dick, 2014).

symmetrically, their glycolytic metabolism and their ability to enter into quiescence), are not shared by most of the different adult SC populations (Clevers, 2015). Thereby, just as the SCs from the different tissues are functionally different, the above-mentioned parameters cannot be all successfully used to properly identify the CSCs in all the different types of cancers. Instead, the behaviour of each CSC population in terms of cell cycle status, metabolism, plasticity or frequency has to be defined experimentally for each type of tumour and might or might not differ from that of their non-CSC counterparts (Batlle and Clevers, 2017; Magee *et al.*, 2012; Meacham and Morrison, 2013). Due to the plastic nature of the CSCs, the phenotype of this population might vary greatly depending on the tumour type or the metastatic location and can be also influenced by the experimental settings (Batlle and Clevers, 2017; Nassar and Blanpain, 2016; Oskarsson *et al.*, 2014).

### 3.2.2. Identification of the CSCs

Since their original identification in haematopoietic tumours (Bonnet and Dick, 1997; Lapidot *et al.*, 1994; Uckun *et al.*, 1995), the existence of CSCs and of a hierarchical tumour organization have been confirmed in many types of solid tumours, including breast (Al-Hajj *et al.*, 2003), head and neck SCC (Prince *et al.*, 2007), sarcoma (Wu *et al.*, 2007), colon (Dalerba *et al.*, 2007; O'Brien *et al.*, 2007; Ricci-Vitiani *et al.*, 2007), brain (Singh *et al.*, 2004), skin (Malanchi *et al.*, 2008), lung (Eramo *et al.*, 2008), ovarian (Zhang *et al.*, 2008) and prostate cancers (Collins *et al.*, 2005; Patrawala *et al.*, 2006). Still, the current data cannot conclude whether other cancers such as pancreatic cancer or NB are hierarchically organized (Ball *et al.*, 2017; Hermann *et al.*, 2007; Li *et al.*, 2007; Tomolonis *et al.*, 2018).

The prototypic approach to decipher whether the CSC concept applies for a given cell subpopulation within a tumour depends on its capacity to form secondary tumours after transplantation into a immunocompromised mouse (Bruce and Van Der Gaag, 1963; Dick *et al.*, 1997; Kreso *et al.*, 2013). This approach thus requires cells to be sorted by FACS according to the heterogenic expression of a cell surface marker. The development of the genetic lineage tracing and cell ablation techniques has overcome the major drawbacks of this classical approach (Figure 10) (Batlle and Clevers, 2017; Nassar and Blanpain, 2016). Additionally, the FACS-sorted 'CSC' subpopulation can be functionally characterized by a combination of different *in vitro* functional assays (Podberezin *et al.*, 2013). This section includes a brief description of the main approaches used to identify and characterize CSCs.



### 3.2.2.1. Cell surface markers

The use of heterogeneously expressed cell surface markers has been instrumental for the identification of CSC subpopulations. Most of the so-called CSC markers are also expressed (either exclusively or in combination) by the embryonic or adult stem populations of the tissue of origin. In other cases, they were arbitrarily selected based on previous data obtained in other tumour types (Batlle and Clevers, 2017). In very few cases the functional role of the markers is well defined. This is the case of Lgr5+, a CRCcsc marker that acts as a co-receptor of WNT ligands in the WNT/ $\beta$ -catenin canonical

### Figure-10. Functional assays to characterize cancer cells with long term self-renewal capacity (previous page)

(A) The transplantation assay relies on the dissociation of tumour cells into single cells and on the FACS isolation of different tumour subpopulations followed by their transplantation into immunodeficient mice. Transplantation of limiting dilutions allows the estimation of the proportion of tumour-propagating cells (TPCs) in each tumour subpopulation. Cancer stem cells (CSCs) should be more enriched in TPCs compared with non-CSCs. CSCs should present higher self-renewal properties compared with non-CSCs in serial transplantations. Secondary tumours should recapitulate the tumour heterogeneity of the primary tumour. (B) Clonal analysis using lineage-tracing experiments relies on the labelling of single cancer cells using the Cre recombinase system with a reporter gene, DNA barcoding, or lentiviral transduction. The fate of the labelled cells is then followed during cancer progression. If the tumour grows in a hierarchical manner, labelled CSCs will show long-term renewal and important clonal expansion, whereas transit amplifying (TA) cells will show limited proliferative potential and finally differentiate into non proliferative cells. If the tumour growth is mediated by equipotent cancer cells, all labelled cells will participate equally in tumour growth. (C) Lineage ablation allows for specific elimination of a subpopulation of cancer cells using targeted expression of suicide genes. In tumours that are maintained by CSCs, if CSCs are eliminated, the remaining non-CSCs will not be capable of sustaining tumour growth, inducing tumour regression. If non-CSCs are ablated, CSCs will sustain tumour growth, and no long-term regression will be observed. Adapted from (Nassar & Blanpain, 2016.)

pathway (Kumar *et al.*, 2014). On the contrary, the function of most of them is poorly characterized and/or seems to involve multiple signalling pathways as happen for the CD133 (Jang *et al.*, 2017). A detailed list of the most used CSC markers is included in Table-05. Importantly, the expression of surface markers can be dynamically regulated; hence the simple presence or absence of a given marker or a combination of markers at the surface of some tumour cells does not necessarily imply that these cells are CSCs (Beck and Blanpain, 2013).

Tumour type	CSC or TPC markers	Reference
Acyte myeloid leukaemia	CD34+, CD38-	Lapidot <i>et al.</i> , 1994
Brain	CD15+, CD133+, CD44+, CD49f+, EPHA2+, EPHA3+, SSEA1+	Binda <i>et al.</i> , 2012; Singh <i>et al.</i> , 2004; Chen <i>et al.</i> , 2010; Day <i>et al.</i> , 2013; Son <i>et al.</i> , 2009; Pietras <i>et al.</i> , 2014
Breast	CD44+, CD24 <sup>Neg/Low</sup> , EpCAM <sup>High</sup> , ALDH+, DNER+, CD49f+	al-Hajj <i>et al.</i> , 2003; Mani <i>et al.</i> , 2008; Pece <i>et al.</i> , 2010
Colon	CD133+, CD44+, CD44v6+, CD166+, EpCAM+, CD24+, Lgr5+, EphB2+	Dalerba <i>et al.</i> , 2007, Merlos-Suarez <i>et al.</i> , 2011; O'Brien <i>et al.</i> , 2007, Ricci-Vitiani <i>et al.</i> , 2007, Scherpers <i>et al.</i> , 2012, Todaro <i>et al.</i> , 2014
Gastric	ALDH1, CD24/CD44, CD54/CD44, EpCAM/CD44, CD71 <sup>Neg</sup> , CD90, CD133, ANCB1, ABCG2	Katsuno <i>et al.</i> , 2012; Takaishi <i>et al.</i> , 2009; Chen <i>et al.</i> , 2012; Han <i>et al.</i> , 2011; Jiang <i>et al.</i> , 2012; Ohkuma <i>et al.</i> , 2012; Jiang <i>et al.</i> , 2012; Hashimoto <i>et al.</i> , 2014
Head and Neck	CD44+, CD24 <sup>Neg/low</sup> , EpCAM+, ALDH+, DNER+, CD49f+	Prince <i>et al.</i> , 2007
Liver	CD90+	Yang <i>et al.</i> , 2008
Lung	CD133+	Eramo <i>et al.</i> , 2008
Pancreatic	ESA+CD44+CD24+	Hermann <i>et al.</i> , 2007
Prostate	CD133+, CD44+, CD24 <sup>Neg</sup>	Collins <i>et al.</i> , 2005; Patrawala <i>et al.</i> , 2006, Wang <i>et al.</i> , 2009
Skin	CD34+	Malanchi <i>et al.</i> , 2008
Ovarian	CD133+	Curley <i>et al.</i> , 2009; Zhang <i>et al.</i> , 2008; Alvero <i>et al.</i> , 2009; Stewart <i>et al.</i> , 2007

Table-05. Isolation of CSCs or TPCs from several tumours using surface markers

### 3.2.2.2. Transplantation

The transplantation of cancer cells into a secondary recipient animal was performed for the first time by Furth and Kahn in 1937 with leukemic cells (Furth, 1937). Afterwards, the frequency of leukemic cells that was able to propagate the disease upon transplantation, was established in 1 every  $10^3$  to  $10^7$  leukemic cells (Bruce and Van Der Gaag, 1963; Hewitt, 1958; Makino, 1956). Since then, it has become the gold-standard assay for assessing CSC activity (Batlle and Clevers, 2017; Clevers, 2011; Kreso and Dick, 2014). The prototypic CSC transplantation assay consists in sorting the putative CSC subpopulation based on the differential expression of one or more surface markers, and their subsequent transplantation into immunocompromised mice at numbers sufficiently low to avoid tumour growth by the bulk tumour cell population (that is used as a reference) (Figure 10A) (Batlle and Clevers, 2017). The capacity of a cell subpopulation to propagate tumour growth under these conditions over serial passages is considered as a proof of the presence of CSCs within this subpopulation (Al-Hajj *et al.*, 2003; Alvero *et al.*, 2009; Bonnet and Dick, 1997; Curley *et al.*, 2009; Dalerba *et al.*, 2007; Eramo *et al.*, 2008; Hermann *et al.*, 2007; Li *et al.*, 2007; Mani *et al.*, 2008; Merlos-Suarez *et al.*, 2011; O'Brien *et al.*, 2007; Pece *et al.*, 2010; Ricci-Vitiani *et al.*, 2007; Schepers *et al.*, 2012; Singh *et al.*, 2004; Stewart *et al.*, 2011; Uckun *et al.*, 1995; Wang *et al.*, 2009; Zhang *et al.*, 2008).

Nevertheless, this transplantation assay presents two major drawbacks, especially when working with solid tumours. First, it requires the dissociation of the tumour into single cells, thereby removing the original niche components. Second, due to the possible inherent plasticity of the tumour hierarchy, the transplantation assay might not reveal the real fate of the cells in their original environment (Batlle and Clevers, 2017; Beck and Blanpain, 2013; Clevers, 2011; Meacham and Morrison, 2013; Medema, 2013; Nassar and Blanpain, 2016). Overall, whether the CSCs identified using the transplantation assay are the ones that drive growth in the primary tumour remains unclear (Batlle and Clevers, 2017; Beck and Blanpain, 2013; Nassar and Blanpain, 2016). The development of lineage tracing models and cell ablation approaches are contributing to unveil this question (Batlle and Clevers, 2017; Nassar and Blanpain, 2016).

### 3.2.2.3. Lineage-tracing strategies

Lineage-tracing approaches allow the unequivocal tracking of the cellular ontogeny of a population of interest while preserving tissue integrity (Blanpain and Simons, 2013; Kretzschmar and Watt, 2012). The development of genetic lineage-tracing models is being instrumental to study how proliferation and fate specification are coordinated *in situ* starting from a single cell (Blanpain and Simons, 2013; Kretzschmar and Watt, 2012). This technique is based on the identification of a specific marker gene that is used to drive the expression of a recombinase (typically Cre recombinase), which in turn triggers the stable expression of a reporter gene (preferentially coding for a fluorescent protein)

(Kretzschmar and Watt, 2012) (Figure 11A). The expression of the reporter gene will then be stably passed on to all the progeny generated over time. The persistence, the size and the composition of the clones allow the evaluation of the CSC potential of the tracked subpopulation (Figure 10B) (Batlle and Clevers, 2017; Blanpain, 2013; Blanpain and Simons, 2013; Kretzschmar and Watt, 2012). Several

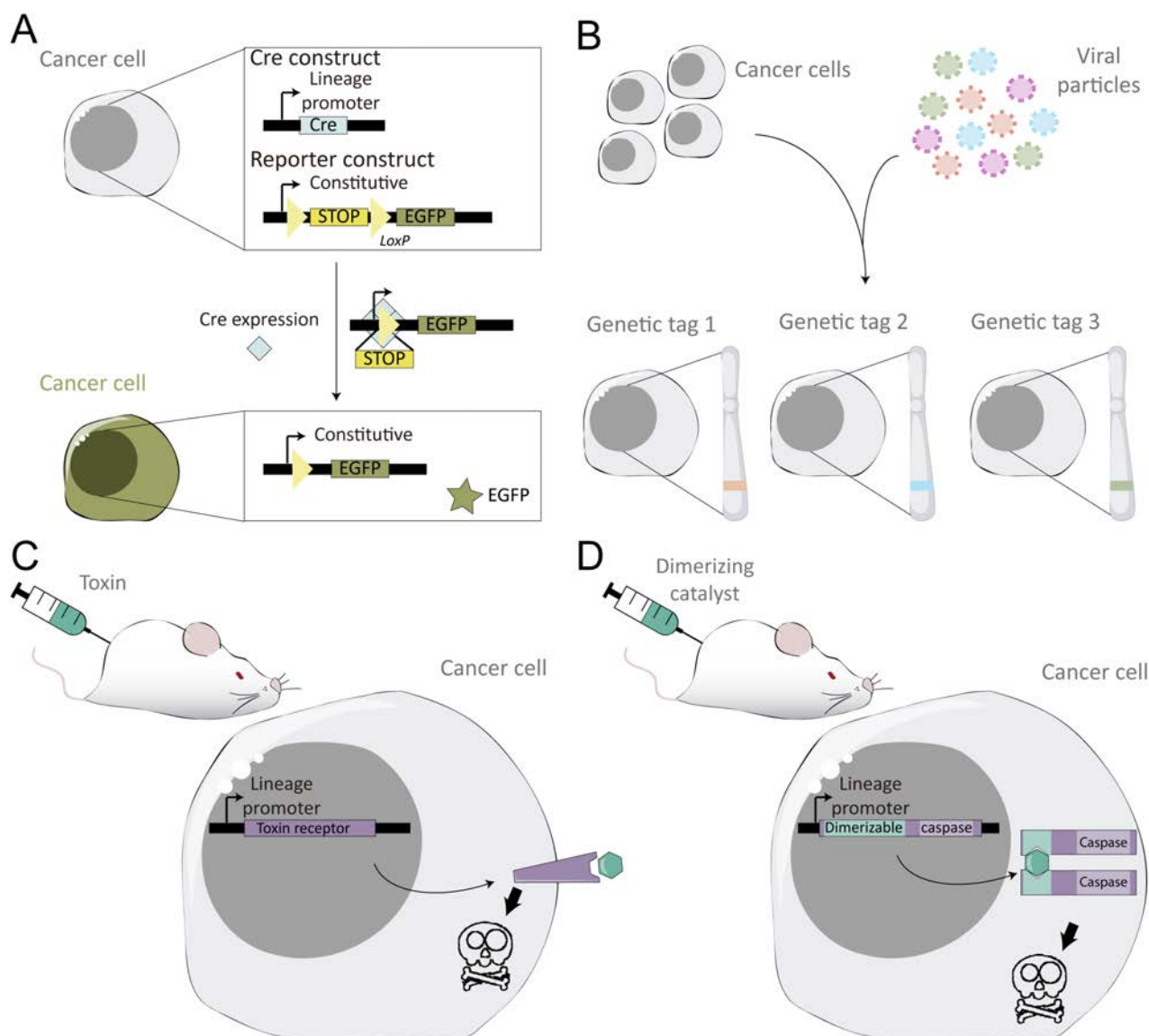


**Figure-11. Genetic engineering for the functional characterization of the tumour-propagating capacity of the CSCs**

(A) Schematic representation of the genetic elements in the Cre-loxP system. Cre recombinase is constitutively expressed under the control of a CSC-specific promoter. Cre recombinase remove STOP cassette at loxP sites in the ubiquitously expressed reporter construct allowing the expression of a fluorescence reporter (for example EGFP) in these cells and all their progeny. Adapted from (Kretzschmar and Watt, 2016). (B) Genetic tagging of individual cancer cells using viral infection. Viral genome or DNA barcode sequences are randomly inserted into the cancer cells' genome and in vivo cell growth allow the different clones to expand, which can be track by PCR-based or sequencing methods. (C, D) Scheme of the distinct mechanisms for the induction of cell death. (C) Targeted cytotoxic effect through the expression of a toxin receptor, which induces cell death upon administration of their respective toxin. (D) Targeted cell death through the expression of a modified dimerizable caspase, which induces the endogenous apoptotic pathway upon administration of the dimerizing catalyst. Adapted from (Gregoire and Kmita, 2014).

genetic mouse models have already validated *in situ* the existence and contribution of CSCs to tumour growth. For instance, the analysis of clonal population dynamics has confirmed a predominant hierarchical organization in benign skin papilloma, SCC and mammary tumours (Driessens *et al.*, 2012; Oshimori *et al.*, 2015; Zomer *et al.*, 2013). A second approach for genetic lineage-tracing of tumour cells is based on lentiviral infections to integrate DNA barcodes into the nuclear genome. The genetic tags will be then passed into the cell progeny allowing for clonal population dynamic analysis and for the identification of cells with tumour propagating capacity, as shown in CRC (Figure 11B) (Kreso and Dick, 2014; Kreso *et al.*, 2013).

#### 3.2.2.4. Lineage ablation strategies

Cell ablation techniques allow the selective elimination of a specific cell population. Hence it is a powerful approach to study the physiological relevance of a particular lineage in homeostasis and/or disease (Gregoire and Kmita, 2014). Theoretically, if the CSCs are responsible for the long-term growth of a tumour, the targeted ablation of these CSCs should cause the regression of the tumour (Figure 10C) (Batlle and Clevers, 2017; Nassar and Blanpain, 2016). Genetic cell lineage strategies use CRISPR/Cas9 to engineer the targeted expression of pro-apoptotic genes (such as an inducible caspase 9) (Shimokawa *et al.*, 2017) or of activation-dependent toxic elements (such as the diphtheria toxin receptor or a modified version of the herpes simple virus thymidine kinase) (Figure 11B) (Boumahdi *et al.*, 2014; Chen *et al.*, 2012a; de Sousa e Melo *et al.*, 2017). A pioneering study revealed that the induction of apoptosis in the NESTIN<sup>+</sup> GB cells, the putative GBcsc, halted tumour growth. A similar result was found after ablation of the Sox2<sup>+</sup> CD34<sup>+</sup> cells in a genetic mouse model of SCC (Boumahdi *et al.*, 2014).

#### 3.2.2.5. *In vitro* functional assays

Several *in vitro* approaches are used to assess the stemness potential of a putative CSC population. Although they must be considered as indirect read-outs of the presence of CSCs in a population of interest, they are valuable tools for preclinical studies, especially in the absence of defined specific surface markers (Podberezin *et al.*, 2013). The most widely used functional assays are detailed hereafter and include: the tumour sphere-forming assay, the soft-agar colony formation assay, the side population assay, the measurement of the activity of metabolic regulators such as ALDH1.

##### 3.2.2.5.1. Tumour sphere-forming assay

This assay was developed to maintain mammalian neural stem cells in culture (Reynolds *et al.*, 1992; Reynolds and Weiss, 1992). This free-floating spheroid assay is based on the premise that only cells with self-renewal capabilities can survive and proliferate when grown in suspension in the ab-

sence of growth factors, while the most 'differentiated' non-tumorigenic cells cannot contribute to the long-term growth of the tumour sphere (Weiswald *et al.*, 2015). Thus, this assay can be used to expand the stem cell population of an original sample and enrich it in stem cells or to assess the stemness potential of a FACS-sorted population. In addition, the spheres can be dissociated and replated for a secondary spheroid culture to evaluate long-term self-renewal potential (Weiswald *et al.*, 2015). In the cancer field it has been shown that the cells with higher sphere-forming capacity usually show higher tumorigenic potential upon transplantation, as described for glioma, colorectal, breast, ovarian and lung cancers among others (Eramo *et al.*, 2008; Mani *et al.*, 2008; Ricci-Vitiani *et al.*, 2007; Singh *et al.*, 2004; Zhang *et al.*, 2008).

#### 3.2.2.5.2. Soft agar colony formation assay

The soft agar colony formation assay is another culture assay widely used to evaluate the self-renewal capacity of a cell population (Rajendran and Jain, 2018). It was the first assay designed to directly quantify the effects of different radiation doses on the survival and proliferative capacity of tumour cells (Puck and Marcus, 1956). Since then, it has been widely used to assess the cytotoxic effects of multiple treatments, including chemotherapeutic drugs and ionizing radiation. The rationale behind it also allows an interesting application in the cancer stem cell field (Borowicz *et al.*, 2014). In the absence of an extracellular matrix or adhesive surface, normal cells cannot proliferate and undergo a specific type of programmed cell death called anoikis (Frisch and Francis, 1994). Conversely, cells with tumorigenic potential can proliferate independently of an adhesive surface (Taddei *et al.*, 2012). In this assay, the tumour cells are embedded as single cells in a soft agarose gel and grown in the presence of a complete growth medium. Hence, the cells that can divide in the absence of cell-cell and cell-substrate contacts will form clonogenic tumour spheroids (Hamburger and Salmon, 1977). The number and size of the tumour spheroids serve as an indirect estimation of the tumorigenic potential of the cells that are tested (Rafehi *et al.*, 2011).

#### 3.2.2.5.3. Side population assay

The expression of efflux pumps of the ATP-binding cassette (ABC) superfamily at the surface is a feature shared by different cell subpopulations (Chen *et al.*, 2016). These pumps are responsible for the active efflux of multiple xenobiotic compounds. Therefore, the cells that express ABC transporters are more resistant to chemotherapeutic drugs, which has been associated to a stem-like phenotype (Challen and Little, 2006). The side population (SP) assay is based on the ability of these transporters to pump out fluorescent lipophilic vital dyes such as Hoechst 33342. The simultaneous measurement of the dye fluorescence at 2 wavelengths (450nm and >670nm in the case of Hoechst 33342) by flow cytometry allows the identification of a weakly fluorescent cell fraction, the SP. This assay was first

used to identify a rare subset of HSCs with increased expression of MDR pumps (Goodell *et al.*, 1996). SP cells have been detected in human cancer cell lines and in primary samples in a percentage ranging from 0 to 20% (Hirschmann-Jax *et al.*, 2004; Kondo *et al.*, 2004; Patrawala *et al.*, 2005; Szotek *et al.*, 2006; Wu *et al.*, 2007).

Compared to non-SP cells, the SP fraction shows an increased expression of stem-like genes and an increased tumorigenic potential upon transplantation. It remains however unclear whether the SP fraction consistently contributes to long-term tumour growth (Wu and Alman, 2008).

#### 3.2.2.5.4. ALDH assay

The aldehyde hydrogenases (ALDH) are enzymes responsible for the oxidation of aldehydes into carboxylic acids. They participate in the synthesis of retinoic acid, in the inactivation of aldehydes derived from physiological metabolic processes or xenobiotic compounds and in the inactivation of reactive oxygen species. Hence, high levels of ALDH activity have been associated to an increased drug resistance (Vasiliou and Nebert, 2005). Both the activity and the surface expression of ALDH1 have been linked to the CSC phenotype; however there are contradictory results about the individual contribution of each of the 3 isoforms of the ALDH1 gene (Marcato *et al.*, 2011). The contribution of ALDH1 activity to therapy resistance was first described for leukemic cells upon cyclophosphamide exposure (Hilton, 1984). Later on, high ALDH1 activity was described in CSC/CSC-like cells from liver, breast or lung cancers among others (Ginestier *et al.*, 2007; Huang *et al.*, 2013a; Ma *et al.*, 2008).

### 3.3. The cancer stem cell niche

As seen for normal adult SCs, the CSC niche is a dedicated microenvironment that provides all the regulatory elements required for CSC activity (Morrison and Spradling, 2008; Plaks *et al.*, 2015). The CSC niche might be formed by extracellular matrix components (such as periostin, tenascin C or osteopontin) and cellular elements such as endothelial cells, fibroblasts/myofibroblasts, immune cells and even other tumour cells (either CSCs and non-CSCs) (Plaks *et al.*, 2015). The prominent role played by the tumour microenvironment in cancer progression and therapy response is already undeniable. In the context of the CSC model, data supporting the plasticity of the hierarchical organization has focused all the attention in understanding the biological pathways that control the activation and plasticity of the CSC (Oskarsson *et al.*, 2014). Interestingly, recent data support the notion of a bidirectional interplay between the CSCs and the components of niche.

Endothelial cells appear to play a pivotal role in the regulation of the activity of the CSCs. CD133+ GBcsc are primarily located in close contact with blood vessels and induce neo-angiogenesis through the secretion of VEGF and SDF1, while the GBcsc phenotype is reinforced by different secreted factors

from the vascular niche that activate bFGF or Notch signalling (Bao *et al.*, 2006; Calabrese *et al.*, 2007; Charles *et al.*, 2010; Fessler *et al.*, 2015; Folkins *et al.*, 2009; Li *et al.*, 2009). Remarkably, vascular mimicry (i.e: the transdifferentiation of tumour cells into functional endothelial cells) has been described at least in GB and NB tumours and might also contribute to tumour progression (Pezzolo *et al.*, 2007; Ribatti *et al.*, 2006; Ricci-Vitiani *et al.*, 2010).

Cancer-associated fibroblasts also influence CSC behaviour. Multiple studies demonstrated how paracrine signalling from cancer-associated fibroblasts enhance the self-renewal and tumorigenic potentials of CSCs. They can even promote the conversion of non-CSCs into CSCs in preclinical models of breast, ovarian, colon, prostate or lung cancers (Chen *et al.*, 2014; Geary *et al.*, 2014; Hu *et al.*, 2015; Huynh *et al.*, 2016; Lau *et al.*, 2016; Li *et al.*, 2012; Lotti *et al.*, 2013; Tsuyada *et al.*, 2012; Valenti *et al.*, 2017; Vermeulen *et al.*, 2010; Yasuda *et al.*, 2014).

Throughout tumour progression, the CSCs encounter new and different microenvironments in the secondary organs targeted by the metastatic spreading. This suggests that the requirements and the relations between the CSCs and their niche might change in these different contexts (de Sousa e Melo *et al.*, 2017; McGranahan and Swanton, 2017; Oskarsson *et al.*, 2011). Cell ablation experiments have shown that the conversion of Lgr5<sup>-</sup> tumour cells into Lgr5<sup>+</sup> CSCs only happens in the primary tumour, demonstrating that the plasticity of non-CSCs is differentially regulated in the primary tumour and in the metastatic site (de Sousa e Melo *et al.*, 2017). Tenascin C, a component of the extracellular matrix, is not required for the primary tumour growth of breast cancer cells but is secreted by the breast metastasis-initiating cells and enhances the CSC phenotype of the tumour cells in the micrometastatic lesions in the lung (Oskarsson *et al.*, 2011).

### 3.4. Therapeutic targeting of the CSCs

The discovery of CSCs has dramatically redefined the therapeutic opportunities for cancer patients (Boesch *et al.*, 2016; Ramos *et al.*, 2017; Talukdar *et al.*, 2016; Zhou *et al.*, 2009). The CSCs emerged as specific targets that drive tumour progression. So far, the 3 main strategies to combat the CSCs have been: (1) the **direct targeting of the CSC population**; (2) **therapies directed towards the CSC state**; (3) the **targeting of the CSC niche** that controls the activity of the CSCs (Figure 12)(Boesch *et al.*, 2016; Ramos *et al.*, 2017; Talukdar *et al.*, 2016; Zhou *et al.*, 2009).

Several attempts have been done to target CSCs using antibodies conjugated with toxic agents (Table-06). Up to date, none of them has however reported a clear benefit in the clinical trials (de Goeij and Lambert, 2016; Laszlo *et al.*, 2014). An interesting option might be the development of bi-specific antibodies that bring into close contact the immune cells with the CSCs. Recent data showed the efficiency of bi-specific CD3 and CD133 antibody to bind cytokine-induced CD3<sup>+</sup> killer cells to

CD133+ CSC-like cells in preclinical models of pancreas and hepatic cancers (Huang *et al.*, 2013b). However, in the absence of a rigid hierarchical organization, CSCs might be continuously recovered by other cells of the tumour hierarchy. The therapeutic approaches targeting CSCs might be pointless under this reality.

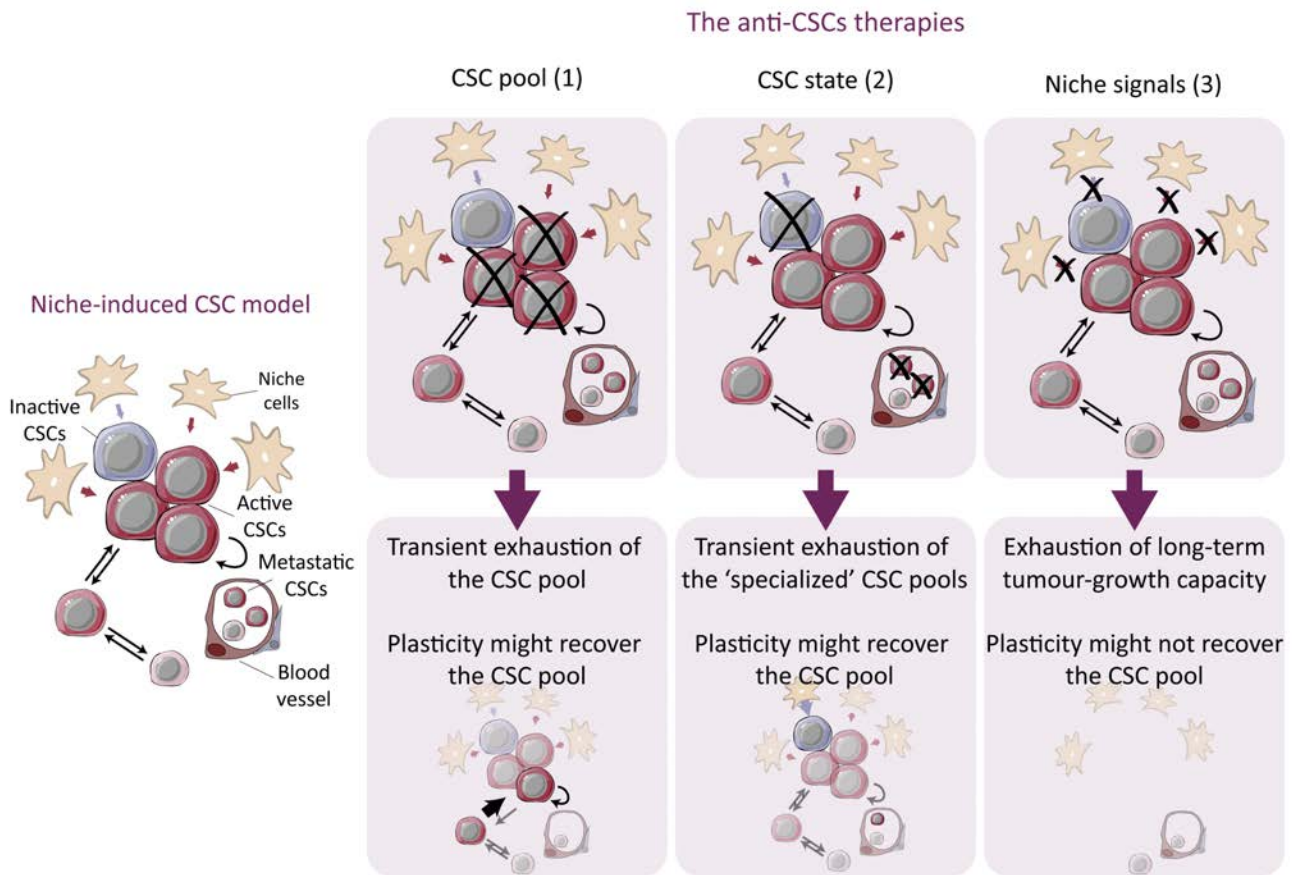


**Figure-12. The putative anti-CSCs therapies and their consequences**

In tumours displaying a niche-induced CSC hierarchy, at least three different therapeutic approaches might target the CSCs: the direct ablation of the CSC pool (strategy 1); the targeting of the CSC phenotype through the blockade of specific dependencies such as their metabolic requirements or their epigenetic regulators (strategy 2) and; the inhibition of the key CSC signalling pathways (strategy 3). The outcome of the distinct strategies could be transient if the plasticity of the hierarchy manages to recover the CSC pool. Adapted from (Batlle and Clevers, 2017).

Another approach consists in the use of drugs that control the CSC state, by waking the CSCs up from quiescence, avoiding their entry into quiescence (Kurtova *et al.*, 2015; Takeishi *et al.*, 2013) or promoting their differentiation (Table-06). The use of differentiation-inducing therapies was first established for acute promyelocytic leukaemia in the 1980's (Breitman *et al.*, 1981; Daenen *et al.*, 1986; Huang *et al.*, 1987; Nilsson, 1984). Remarkably, retinoic derivatives are currently part of the standard of care for NB, acute promyelocytic leukaemia and other haematological malignancies (for further details see section 2.8 from the Introduction) (Matthay *et al.*, 1999; Nowak *et al.*, 2009; Stahl *et al.*, 2016).

More recently, the attention has turned towards the regulatory role of the CSC niche and of the signalling pathways regulating the activity or plasticity of the CSCs (Table-06) (Boesch *et al.*, 2016; Ramos *et al.*, 2017; Talukdar *et al.*, 2016). In this regard, WNT, Notch and Hedgehog signalling pathways (among others) are known to be implicated in the regulation of CSCs in different types of cancer and might represent a powerful target to block the activity of the CSCs in a broad range of cancer types (Ramos *et al.*, 2017; Reya *et al.*, 2001). Several drugs targeting these CSC pathways are already available and under clinical trials (Ramos *et al.*, 2017).

Therapy	Potential drawbacks and limitations	Target	Progress to clinic
CSC ablation (using ADCs)	<p>Toxicity associated with ADCs</p> <p>Lack of CSC-specific markers</p> <p>Depletion of normal stem cells that share surface markers with CSC</p> <p>Regeneration of the CSC pool by plasticity of non-CSCs upon treatment cessation</p> <p>Intratour heterogeneity in CSC surface-marker expression</p>	Several CSC surface markers, including CD33, LGR5, CD133, and DLL3	<p>ADC directed against CD33+ leukemic stem cells in AML was given FDA approval but it was later withdrawn due to toxicity</p> <p>Strategies base on <i>bona fide</i> CSC markers (for example LGR5) remain at preclinical phases</p>
Targetting the CSC state (Epigenetic therapies)	<p>Toxicity owing to misregulation of gene expression in healthy stem cells</p> <p>Knowledge of the epigenetic regulation of CSCs in solid tumours is sparse</p>	Multiple epigenetic regulators, including BMI1, LSD1, HDACs, DOT1L, BET proteins, and IDH1/2	<p>Differentiation therapy by all-trans retinoic acid is standard of care in NB and APLM</p> <p>HDAC inhibitors approved by FDA for several malignancies.</p> <p>Large number of other epigenetic regulator inhibitors in phase I-III trials for hematological and solid malignancies, some of which potentially target CSCs</p>
	Regeneration of the CSC pool by plasticity of non-CSCs upon treatment cessation	Blockade of specific dependencies, such as metabolic requirements (for example anti-CD36 or inhibitors of oxidative phosphorylation)	Preclinical research
Inhibition of key CSC signalling pathways	Side effects on healthy stem cells that depend on the equivalent signals	WNT pathway	<p>Inhibitors of upstream WNT-signalling components (PORCN, FZD, anti-RSPO3) in clinical phase for CRC, pancreas and other tumour types</p> <p>PRI-724, an inhibitor of <math>\beta</math>-catenin/CBP interaction in phase I trials for several malignancies</p>
	Acquisition of resistance mechanisms	NOTCH pathway	Several inhibitors of $\gamma$ -secretase, NOTCH receptor or NOTCH ligands in distinct clinical phases for multiple cancer types
	Regeneration of the CSC pool by plasticity of non-CSCs upon treatment cessation	JAK/STAT3 pathway	Inhibitors of STAT3 in preclinical research for NB

**Table-06. Therapeutic strategies against CSCs.** ADCs: antibody-drug conjugates; AML: acute myeloid leukaemia; APLM: acute promyelocytic leukaemia; CRC: colorectal cancer; CSC: cancer stem cell; FDA: Food and Drug Administration; HDAC: Histone deacetylases; NB: neuroblastoma. Adapted from (Batlle and Clevers, 2017).

To sum up, the development of new drugs targeting CSC activity foresees a promising future in clinical oncology. Yet, the tumour evolution is designed to continually fit growth upon a changing environment. Thereby, the astonishing plasticity of the CSC and non-CSC populations might require a

combined approach whereby new targeted drugs would tackle the CSCs while classical chemotherapeutic agents shrink the non-CSC compartment and avoid the recovery of the CSC pool (Boesch *et al.*, 2016; Ramos *et al.*, 2017; Talukdar *et al.*, 2016; Zhou *et al.*, 2009).

### 3.5. CSCs in the context of NB

NBs are paediatric tumours that arise due to errors occurring during the development of the SA lineage (see chapter 2 for further details). 85-90% of these patients present metastases at diagnosis and despite the attempts to improve the treatment of HR patients using multimodal strategies, half of them suffer relapse due to therapeutic failure (Morgenstern *et al.*, 2019). The relative paucity of recurrent somatic mutations in HR tumours challenges the possibilities to find particular genetic changes susceptible to be exploited as therapeutic targets (Pugh *et al.*, 2013). This reality points towards rare germline variants, copy number alteration and epigenetic modifications as the putative drivers of HR-NBs tumorigenesis, and reinforce the notion that the non-genetic functional diversity of HR-NBs might hide new promising therapeutic options. In this regard, a striking intra-tumour heterogeneity and plasticity has been observed in NB cell lines, patient-derived-xenografts and even in primary samples (Boeva *et al.*, 2017; Ciccarone *et al.*, 1989; Hansford *et al.*, 2007; Hirschmann-Jax *et al.*, 2004; Hsu *et al.*, 2013; Newton *et al.*, 2010; Ross and Spengler, 2007; Ross *et al.*, 1983; Ross *et al.*, 2015; van Groningen *et al.*, 2017; Walton *et al.*, 2004).

Initial data showed the phenotypic heterogeneity within the human NB cell lines, which are composed of 3 different morphological and biochemical cell subtypes: the N (neuroblastic), the S (substrate-adherent) and the I (intermediate) types. While N-type cells exhibit short neuritic processes and express markers of noradrenergic neurons, S-type cells lack neural characteristics and exhibit an extensive cytoplasm and high expression of vimentin. The I-type cells show an intermediate morphology, which led to the idea that they represent a transitional state between N- and S-type cells or more immature precursors (Ciccarone *et al.*, 1989; Ross *et al.*, 1983). Interestingly, NB cells of the I-type are able to transdifferentiate into S-type or N-type cells in the presence of BrdU or retinoic acid. They also show higher expression levels of stem-like markers (such as CD133, NESTIN and KIT) and a higher tumorigenic potential (Ross and Spengler, 2007; Ross *et al.*, 2015; Walton *et al.*, 2004).

The progressive advances in the CSC field in other solid tumours led the incipient analysis of the stemness potential of NB cells (Table-07). A first study focuses on the identification of 'drug-resistant' SP cells, as putative responsible for therapeutic failure. A variable SP fraction were found increased in a paired analysis using pre- and post-treatment sample; however, a formal confirmation of *in vivo* self-renewal capacity was never achieved (Hirschmann-Jax *et al.*, 2004; Newton *et al.*, 2010). Then, the tumour spheroid assay was used to compare the self-renewal capacity of primary NB cells isolated

from LR and HR patients. LR-and HR-derived samples showed different long-term growth capacity when forced to grow as tumour spheres. While the NB cells from LR patients did not survive longer than 1 passage, the cells derived from HR patients were maintained as spheroid cultures up to 34 passages, indicating that the NB cells from HR patients present a longer self-renewal capacity (Hansford *et al.*, 2007). In parallel different markers were used to identified particular NB subpopulations and analyse their tumour propagating capacity (Table-07). The resemblance of the putative NBcsc/TPCs populations to the NCCs have been inferred based on the expression of distinct markers previously associated to NCCs or to the SA lineage (Ross *et al.*, 1995; Tomolonis *et al.*, 2018). Nevertheless, most of the markers analysed so far were chosen based on previous results on other tumour types and none of them are expressed in the NCCs, their SCs counterparts. Thereby, these data support the notion that the functional diversity of NBs might depend on the heterogenic distribution within the tumour population of the tumour propagating potential. Similarly it suggests that the NB cells harbouring an enhanced tumour propagating capacity seem to express markers related with the embryonic NCCs.

Feature	Marker or phenotype	Reference
Cell surface markers	CD133+	Cournoyer <i>et al.</i> , 2012; Mahller <i>et al.</i> , 2009; Takenobu <i>et al.</i> , 2011; van Groninger <i>et al.</i> , 2017; Walton <i>et al.</i> , 2004; Xing <i>et al.</i> , 2015; Zhong <i>et al.</i> , 2018
	CD114 (GCSFR)+	Hsu <i>et al.</i> , 2013
	CD117 (KIT)+	Mahller <i>et al.</i> , 2009; Walton <i>et al.</i> , 2004; Xing <i>et al.</i> , 2015
	ABCG2+	Hirschmann-Jax <i>et al.</i> , 2004; Mahller <i>et al.</i> , 2009; Xing <i>et al.</i> , 2015
Cytoplasmic and nuclear proteins	Nestin	Xing <i>et al.</i> , 2015
	FZD6	Cantilena <i>et al.</i> , 2011
Other properties/enzymes	Tumour spheroids	Hansford <i>et al.</i> , 2007; Hirschmann-Jax <i>et al.</i> , 2004; Mahller <i>et al.</i> , 2009; Xing <i>et al.</i> , 2015
	SP	Hirschmann-Jax <i>et al.</i> , 2004; Komuro <i>et al.</i> , 2007; Mahller <i>et al.</i> , 2009; Newton <i>et al.</i> , 2004; Xing <i>et al.</i> , 2015
	ALDH	Hartomo <i>et al.</i> , 2015
	Morphology (I-subtype)	Ross and Spengler, 2007; Ross <i>et al.</i> , 1983; Ross <i>et al.</i> , 1995; Ross <i>et al.</i> , 2015; Ross <i>et al.</i> , 2013

**Table-07. Identification of cells with tumour propagating capacity in neuroblastoma.** SP: side population. Adapted from (Garner and Beierle, 2016).

Additionally, it remains unclear whether NB tumours are hierarchically organized or whether various populations of NBcsc/TPCs coexist simultaneously within the tumour, maybe supporting tumour growth in distinct specialized niches or upon certain environmental stressors. The latter is supported by two recent genome-wide studies that revealed the coexistence of different super-enhancer-driven NB cellular states that can interconvert between each other (Boeva *et al.*, 2017; van Groningen *et al.*, 2017). Interestingly, the gene expression profiles of some of the detected cellular states were closely related to that of human NCC samples. It is noteworthy that the acquisition of therapy resistance favours the transition toward these NCC-related subtypes, suggesting that the transdifferentiation of NB cells toward a more immature state might play a pivotal role in the acquisition of aggressive features and disease progression (Boeva *et al.*, 2017; van Groningen *et al.*, 2017).

## 4. *NXPH1* and its receptor $\alpha$ -*NRXN1*

### 4.1. Neurexophilin 1, a neuropeptide-like protein that modulates synaptic maturation

#### 4.1.1. The *NXPH1* protein

Neurexophilin 1 (*NXPH1*) is a small extracellular glycoprotein that belongs to the Neurexophilin family. This gene family comprises 4 members that are only found in vertebrates. *NXPH1* was identified in a screening searching for the  $\alpha$ -Latrotoxin receptor (Petrenko *et al.*, 1996). *NXPH1*, *NXPH2* and *NXPH3* show a high sequence homology, while the coding sequence of *NXPH4* is more divergent (Missler *et al.*, 1998; Missler and Sudhof, 1998; Petrenko *et al.*, 1996). The human *NXPH1* gene maps to the chromosomal location 7p21.3 and codes for an immature form of the multi-domain *NXPH1* protein. This immature multi-domain protein structure consists of: 1) an N-terminal signal peptide, 2) an N-terminal variable domain, 3) a conserved central domain that contains 3 N-glycosylation sites, 4) a small linker region and finally, 5) a conserved C-terminal domain that contains six cysteine residues. The maturation of *NXPH1* requires an N-glycosylation on 4 residues, followed by the proteolytic cleavage of both the N-terminal signal peptide and the N-terminal variable domain. The mature *NXPH1* thus corresponds to a 29KDa glycosylated protein that is transported to the cell surface by the secretory pathway (Missler and Sudhof, 1998).

#### 4.1.2. Functions of *NXPH1*

*NXPH1* is mainly expressed in the nervous system, although it has also been detected in protein extracts of non-neural tissues (Missler and Sudhof, 1998). The fact that *NXPH1* is a secreted glycoprotein of small size that is mainly expressed in the nervous system led its discoverers to propose that *NXPH1* and its related family members represent a new class of neuropeptide-like proteins (Missler and Sudhof, 1998).

To date, *NXPH1* is known to bind to a single family of transmembrane receptors, the  $\alpha$ -Neurexins ( $\alpha$ -*NRXNs*) (Missler *et al.*, 1998; Petrenko *et al.*, 1996; Reissner *et al.*, 2014). There are some evidences suggesting that the binding of *NXPH1* to  $\alpha$ -*NRXNs* takes place during the maturation process, in the secretory pathway. Hence, the mature *NXPH1* protein might be directly released bound in a complex with its receptors  $\alpha$ -*NRXNs* (Missler *et al.*, 1998; Reissner *et al.*, 2014).

$\alpha$ -*NRXNs* play key roles in synaptogenesis and synaptic neurotransmission (Sudhof, 2017). Through

its direct binding to  $\alpha$ -NRXNs, *NXPH1* plays a role in modulating these processes, mainly by regulating the interactions of the  $\alpha$ -NRXNs with their post-synaptic partners such as  $\alpha$ -dystroglycan ( $\alpha$ -DAG) or neuroligins (NLG). Structural studies showed that *NXPH1* and  $\alpha$ -DAG partially bind to the same domain of the extracellular region of  $\alpha$ -NRXN1, thereby suggesting that their binding to  $\alpha$ -NRXN1 is mutually exclusive (Reissner *et al.*, 2014). Apart from regulating the accessibility of other ligands to  $\alpha$ -NRXNs, so far there is no evidence that *NXPH1* plays other functions nor that its binding to  $\alpha$ -NRXNs modulate any intracellular signalling (Born *et al.*, 2014). Of note, mice presenting a knockout (KO) of *NXPH1* are viable and show no obvious anatomical, physiological nor behavioural abnormalities (Born *et al.*, 2014; Missler *et al.*, 1998).

Interestingly, the binding of *NXPH1* to  $\alpha$ -NRXN1 has been reported to inhibit the haematopoietic progenitor cell proliferation in the spleen (Kinzfogel *et al.*, 2011). The same authors detected high levels of human *NXPH1* in the umbilical cord blood plasma ( $460 \pm 60$  ng/ml) but low levels in the adult peripheral blood plasma ( $6 \pm 1$  ng/ml), suggesting a putative role of *NXPH1* during embryonic or early postnatal development (Kinzfogel *et al.*, 2011). The cellular source of this circulating *NXPH1* remains unknown.

#### 4.1.3. *NXPH1* and related pathologies

So far, no genetic variation in the *NXPH1* gene has been related to human mendelian disorders (OMIM, 2019). It has been described the loss of *NXPH1* expression along cancer progression for breast cancer, pancreatic ductal adenocarcinoma and NB (Decock *et al.*, 2016a; Faryna *et al.*, 2012; Hong *et al.*, 2012; Jin and Tsai, 2016; Tommasi *et al.*, 2009; Warnat *et al.*, 2007). In some cases, the authors detected a correlation between the hypermethylation of the *NXPH1* CpG promoter regions and tumour progression, when different malignant stages were compared by genome-wide methylation screening (Decock *et al.*, 2016a; Faryna *et al.*, 2012; Hong *et al.*, 2012; Tommasi *et al.*, 2009). However, the downregulation of *NXPH1* protein has only been confirmed for breast cancer and pancreatic ductal adenocarcinoma by immunohistochemistry (Faryna *et al.*, 2012; Jin and Tsai, 2016). Whether *NXPH1* plays a causal role in the context of these cancers remains unknown.

## 4.2. NXPH1 receptors, the $\alpha$ -Neurexins

### 4.2.1. NRXN proteins

In mammals, the highly conserved neurexin (NRXN) family consists of 3 genes: *neurexin 1*, *neurexin 2* and *neurexin 3*. The NRXNs were initially identified as part of the endogenous receptor complex for  $\alpha$ -Latrotoxin (Geppert *et al.*, 1992; Giancotti, 2013; Petrenko *et al.*, 1991; Ushkaryov *et al.*, 1994; Ushkaryov *et al.*, 1992; Ushkaryov and Sudhof, 1993). Each *NRXN* gene possesses two independent promoters driving the expression of 2 different isoforms: alpha ( $\alpha$ )- and beta ( $\beta$ )-NRXNs. All the NRXN isoforms are type I membrane proteins containing an isoform-specific extracellular domain followed by a single transmembrane region and a short cytoplasmic PDZ (for PSD-95, Disc Large, Zona Occludens 1) domain. The extracellular domain of  $\alpha$ -NRXN is composed of 6 LNS (for Laminin/Neurexin/Sex-hormone-binding globulin) domains and 3 interspersed EGF-like (for Epidermal Growth Factor-like) repeats, followed by an O-linked sugar modification sequence and a short cysteine-loop sequence. The  $\beta$ -NRXNs represent an N-terminal truncated form of  $\alpha$ -NRXNs with a specific short N-terminal sequence (Sudhof, 2017). Recently, a second internal promoter was identified in the *NRXN1* gene, controlling the expression of a shorter isoform named *gamma* ( $\gamma$ )-*NRXN1*.  $\gamma$ -NRXN1 is also an N-terminal truncated form of  $\alpha$ -NRXN1 with a specific N-terminal  $\gamma$ -neurexin sequence (Sterky *et al.*, 2017).

The total number of NRXN protein variants is under intense research, due to the massive diversification caused by alternative splicing (Schreiner *et al.*, 2014; Treutlein *et al.*, 2014; Ullrich *et al.*, 1995). The sequence coding for the extracellular domain of the  $\alpha$ -NRXNs contains 6 canonical splicing sites (referred to as SS1 to SS6), while the truncated  $\beta$ -NRXN and  $\gamma$ -NRXN1 isoforms contain respectively only 2 (SS4 and SS6) and 1 (SS6) splicing site (Sudhof, 2017). As an example, up to 399 different  $\alpha$ -NRXN1 transcripts have been identified by deep sequencing in the mouse brain (Schreiner *et al.*, 2014). How the alternative splicing of NRXNs is regulated remains elusive, but it seems clear that expression of the different splicing variants does not follow an “all or nothing” strategy, but rather the multiple isoforms are expressed at different levels. Despite this, the final  $\alpha$ -NRXN1 repertoires are, at least partially, cell-type specific (Schreiner *et al.*, 2014).

### 4.2.2. Functions of NRXNs

NRXNs are widely expressed in the nervous system, where all three genes (NRXN1-3) are transcribed at similar levels. By contrast,  $\alpha$ -NRXNs are much more abundant than  $\beta$ -NRXNs (Schreiner *et al.*, 2014). NRXNs play a key role in synaptic formation and neurotransmission. Both  $\alpha$ - and  $\beta$ -NRXNs are located at the synaptic cleft where they constitute trans-synaptic signalling complexes together with different pre- and post-synaptic ligands. Presynaptic NRXNs send instructive signal that induce

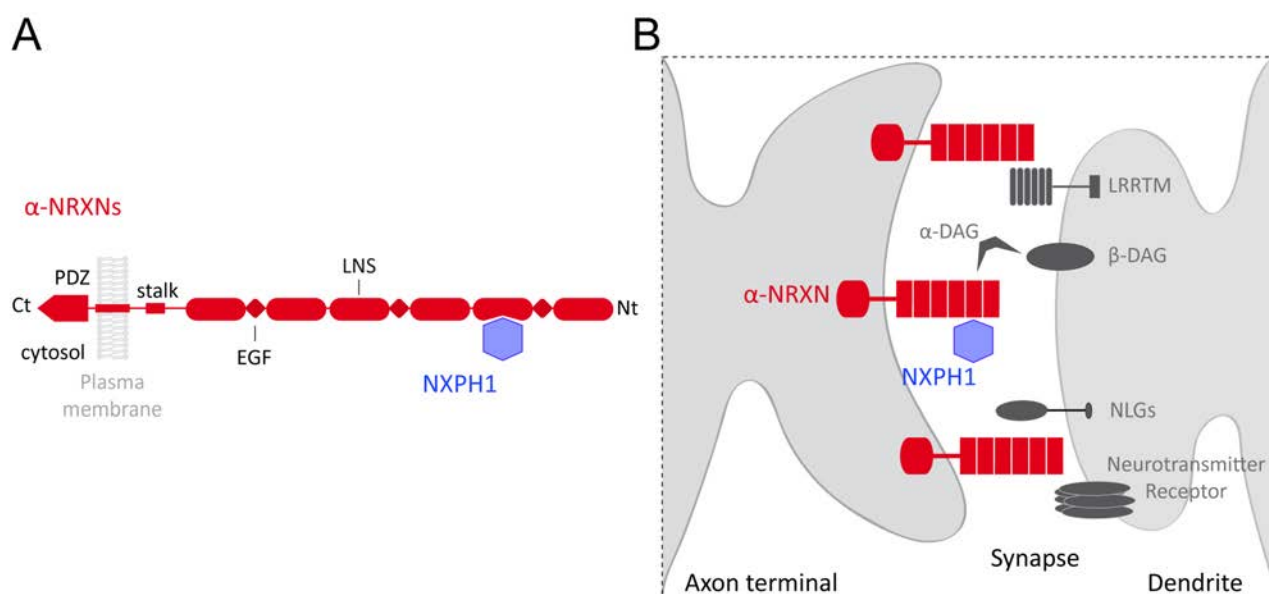


**Figure-13. NXP1 is an extracellular glycoprotein that modulates  $\alpha$ -NRXNs activity**

(A) NXP1 (purple) binds to the 2nd LNS domain of the extracellular region of the three  $\alpha$ -NRXNs (1/2/3) (red). (B)  $\alpha$ -NRXNs are transmembrane proteins expressed at the pre-synaptic terminals of synapses that have been shown to modulate the activity of diverse families of post-synaptic transmembrane proteins including neurotransmitter receptors, Leucine-rich-repeat transmembrane proteins (LRRTM), Neuroligins (NLGs) and  $\beta$ -Dystroglycan ( $\beta$ -DAG). The activity of the  $\alpha$ -NRXNs can be modulated by extracellular proteins such as  $\alpha$ -Dystroglycan ( $\alpha$ -DAG) or NXP1.

the initial organization of the post-synaptic bottom and subsequently contribute to synaptic refining in a neuron sub-type specific manner (Sudhof, 2017).

In the last decade, multiple ligands have been described for the NRXNs. Structural studies have determined 3 ligand-binding regions in their large extracellular domain: 1) the LNS2 domain that is specific for  $\alpha$ -NRXNs, 2) the LNS6 domain and 3) the juxta-membranous sequence. These last two domains are both shared by  $\alpha$ - and  $\beta$ -NRXNs. Examples of ligands binding to different regions are: NXP1s and  $\alpha$ -DAG, which bind to LNS2 (Missler *et al.*, 1998; Petrenko *et al.*, 1996; Reissner *et al.*, 2014; Sudhof, 2017);  $\alpha$ -DAG, NLGs, LRRTMs, LPHNs, GABA<sub>A</sub> receptors, CLSTNs and CBLNs, which all bind to LNS6 (Boucard *et al.*, 2012; de Wit *et al.*, 2009; Ichtchenko *et al.*, 1995; Ichtchenko *et al.*, 1996; Ko *et al.*, 2009; Pettem *et al.*, 2013; Reissner *et al.*, 2014; Sugita *et al.*, 2001; Uemura *et al.*, 2010; Zhang *et al.*, 2010a); and CA10/11 and C1q1s, which bind to the juxta-membranous domain (Matsuda *et al.*, 2016; Sterky *et al.*, 2017). It is noteworthy that the presence of a ligand bound to a given region is exclusive for the binding of other ligands to the same region, whereas the simultaneous binding of 2 ligands to different binding regions is possible (Reissner *et al.*, 2014). Naturally, alternative splicing has been shown to modulate the binding of NRXNs with their ligands (Sudhof, 2017). In this regard, the binding of NXP1 to the LNS2 domain is unaffected by alternative splicing (Reissner *et al.*, 2014). In addition, all NRXNs isoforms share an intracellular PDZ domain that is known to bind to CASK (Hata *et al.*, 1996; Mukherjee *et al.*, 2008), Mints (Biederer and Sudhof, 2000) and FERM-domain proteins

such as protein 4.1 (Biederer and Sudhof, 2001). To date, no intracellular signalling through the different PDZ interactors has been identified, an exciting possibility that should be explored.

The triple  $\alpha$ -NRXN and double  $\alpha$ -NRXN1/3 KO mouse models die after birth due to dysfunction of the neural circuits controlling breathing, while the single and double  $\alpha$ -NRXN1/2 or  $\alpha$ -NRXN2/3 KOs mouse models survive longer but show impaired  $\text{Ca}^{2+}$  channel activity and neurotransmitter release at the presynaptic terminal of brainstem and neocortex neurons (Missler *et al.*, 2003). Outside of its neural functions,  $\alpha$ -NRXN1 has also been detected in pancreatic  $\beta$ -cells and in haematopoietic stem cells (Kinzfogel *et al.*, 2011; Mosedale *et al.*, 2012; Suckow *et al.*, 2008). However, currently no one has investigated whether the single or combinatorial  $\alpha$ -NRXN KO mice models present any possible extra-neural affectation (Chen *et al.*, 2017; Missler *et al.*, 2003).

#### 4.2.3. NRXNs and related pathologies

Consistent with their relevant role in synaptic neurotransmission, multiple alterations have been identified in the NRXN genes and associated with the development of spontaneous or familial forms of neuropsychiatric disorders such as schizophrenia, autism spectrum disorders and, intellectual disability (Sudhof, 2017). As an example, the OMIM database details the causal relation between  $\alpha$ -NRXN1 haploinsufficiency and 2 different congenital conditions: Pitt-Hopkins-like Syndrome 2 and Susceptibility to schizophrenia-17 (OMIM, 2019).

## II. HYPOTHESIS AND SPECIFIC AIMS

---



---

The general aim of this doctoral thesis was to identify a genetic signature for the NBcsc, with the ultimate goal of providing new specific molecular markers of these NBcsc and candidate genes that might be useful for the development of future therapeutic strategies targeting NBcsc in high risk NBs.

My work was based on the key hypothesis that cancer stem cells of a particular tissue share many properties with their normal stem cell counterparts, including a partial common genetic signature. We adapted this concept to NBcsc and their normal stem-like counterparts, the NCCs, hypothesizing that these two cell populations share a common genetic signature and that the genes from this common signature might play a crucial role in NB formation or malignancy. In order to tackle this hypothesis, the specific objectives of my doctoral thesis were:

**-Aim-1:** To identify a genetic signature common to NCCs and NB malignancy

**-Aim-2:** To study the role of one candidate gene, *NXPH1*, in controlling NB stem cell potential and malignancy. More specifically:

- o -Aim-2A: To study whether the *NXPH1* receptor  $\alpha$ -NRXN1 is a marker of NBcsc
- o -Aim-2B: To define the role of *NXPH1* and its receptor  $\alpha$ -NRXN1 in NB malignancy



## III. MATERIALS AND METHODS

---



## 1. Gene expression profiling and bioinformatic analysis

Gene expression profiling consists in the simultaneous measurement of the activity of thousands of genes. In microarray-based gene expression profiling the activity of thousands of previously known genes is monitored and changes in gene expression are obtained when comparing different experimental conditions. In this doctoral thesis, differentially expressed genes (DEGs) from two different DNA microarray datasets were compared to retrieve common DEGs for both datasets.

### 1.1. Genome-wide transcriptomic analysis for primary human NB

The NB expression profiling array was previously done and published by our collaborator Dr. Lavarino (Gomez *et al.*, 2015). All the NB samples included in this expression screening were obtained at the time of diagnosis from patients attended at Hospital Sant Joan de Déu (HSJD, Barcelona, Spain). Tumours were evaluated by a pathologist and only 19 snap frozen pre-treatment samples with at least 70% viable tumour content, were included in the study. NB risk assessment was defined by the International Neuroblastoma Staging System (INSS) (Table-08) (Brodeur *et al.*, 1993). Total RNA from frozen samples was extracted by TRIzol® Reagent. High quality RNA was hybridized to Human Genome U219 microarray plates (Affymetrix, Inc, Santa Clara, California, USA) at the Functional Genomic

Sample name	Risk group	INSS	MYCN status
NB1	LR	1	NA
NB2	LR	4s	NA
NB8	LR	1	NA
NB14	LR	3	NA
NB18	LR	1	NA
NB20	LR	1	NA
NB24	LR	4s	NA
NB25	LR	3	NA
NB32	LR	4s	NA
NB4	HR	4	NA
NB13	HR	4	NA
NB23	HR	4	NA
NB26	HR	4	NA
NB30	HR	4	NA
NB10	HR	1	A
NB19	HR	4	A
NB27	HR	4	A
NB28	HR	4	A
NB33	HR	4	A
DEGs per pair-wise comparison	54/46500	235/46500	238/46500

**Table-08. Clinical and biological characteristics of the HSJD NB cohort.** HR (high risk) refers to MYCN amplified (A) or MYCN non-amplified (NA) & INSS 4. LR (low risk) refers to MYCN NA & INSS 1,2,3 or 4S. INSS: International Neuroblastoma Staging System.

Unit, Institut d'Investigacions Biomèdiques August Pi i Sunyer (IDIBAPS, Barcelona, Spain) according to Affymetrix standard protocols. Data was processed through an adapted method from computational methods/target prediction algorithms (using RMA algorithm and R-packages R/Bioconductor) (Kulis *et al.*, 2012; Gautier *et al.*, 2004). Pair-wise comparisons between clinically and biologically relevant parameters for NB tumours prognosis led to the identification of sets of DEGs between patients' subgroups. Standard deviation density plots were used to determine the cut-off value for gene expression analyses. The results were filtered using thresholds of  $[\log_2FC]>1$  and adjusted P-value  $<0.01$ . Microarray data was deposited in NCBI GSE54720.

## 1.2. Genome-wide transcriptomic analysis for NCCs

Our group conducted in the past a lineage tracing study for the NCCs during early development (Feronha *et al.*, 2013; Rabadan *et al.*, 2013). Of the genetic lineage tracing of chick NCCs, plasmid DNAs encoding for bone-morphogenetic-protein (BMP) reporter (BRE-tk-EGFP) and a constitutively expressed form of histone-H2B fused to RFP (H2B-RFP) were co-electroporated in HH10 chick embryos and the NT was dissected out of the embryos 24h later. Neural tissue was dissociated to single cells and GFP and RFP fluorescent cells were sorted out using MoFlo flow cytometer (DakoCytomation, Fort Collins, Colorado, USA). 4 biological replicates of either RFP+GFP- cells or RFP+GFP+ cells were obtained, and total RNA was extracted from the resulting cell sorted populations following standard TriZol™ Reagent protocol. Subsequently, high quality RNA was hybridized to GeneChip Chicken Genome Array (Affymetrix, Inc) at the Functional Genomics Unit of the Institut de Recerca Biomèdica (Barcelona, Spain) according to Affymetrix standard protocols. For statistical analysis, the data from four biological replicates of each experimental condition were averaged and microarray data was analysed using Bioconductor software, and a false discovery rate (FDR) with a p-value  $<0.05$ . The quality of the data was assessed, normalized with the robust multichip averaged (RMA) algorithm and differentially expressed genes were selected. The results were filtered using thresholds of  $[\log_2FC]>0.5849$  and p-value  $<0.05$ . Microarray data was deposited in NCBI GSE81717.

## 1.3. Bioinformatic search for common DEGs in NB and NCCs signatures

The comparison between BRE embryonic NCC and human NB datasets was conducted by our collaborator Soledad Gómez (Dr. Lavarino's group, IRSJD). The Unigene gene symbol provided by Affymetrix (when available) was used as link for both datasets.

## 1.4. Bioinformatic analysis of public NB datasets

Publically available human NB patient microarrays were obtained from the R2: genome analysis and visualization platform (R2-server, 2019). R2-web based application was used to generate Kaplan Meier survival curves. The query parameter was event-free survival and the average *gene* expression was always used as cut-off value for all survival analysis. Significance was calculated via the website interface. In addition R2-web based application was also used to compare expression levels of NXP1 receptors,  $\alpha$ -NRXNs among different NB prognosis groups. In this regard, R2 Tview tool was used to verify probesets specificity for  $\alpha$ -NRXN1/2 or 3 isoform. The only 3 datasets that contained specific probeset for these isoforms were chosen for further analysis. Raw data was downloaded and statistical significance was assessed using GraphPad Prism v8 (GraphPad Software, Inc) (see section 9, from Materials and Methods). All public NB datasets used during this doctoral thesis are listed in Table 09.

NCBI GEO ID	Title	R2 internal identifier	Common name	Reference
GSE45547	Hox-C9 activates the intrinsic pathway of apoptosis and is associated with spontaneous regression in neuroblastoma	ps_avgpres_gse45547geo649_ag44kcwolf	Kocak dataset	Kocak et al., 2013
GSE19274	Expression profiling in Neuroblastoma Primary tumors and Cell lines	ps_avgpres_nbil100_ilmnhwg6v2	Jagannathan dataset	Cole et al., 2011
GSE62564	An Investigation of Biomarkers Derived from Legacy Microarray Data for Their Utility in the RNA-Seq Era	ps_avgpres_gse62564geo498_seqcnb1	SEQC dataset	Su et al., 2014
Not available	Not available	ps_avgpres_gse27608geop47_huex10p	Khan dataset	Not available
Not available	Not available	ps_avgpres_targett161_ensh37e59t	TARGET dataset	Not available

**Table-09. NB expression microarrays used in this thesis and available at the R2 Genomic Analysis and Visualization Platform**

## 2. Cell culture

### 2.1. Human cell lines

Short term *in vitro* culture of NB cells started in the 2<sup>nd</sup> half of the XX century using fresh biopsies from primary tumours, bone marrow aspirates or even peripheral blood. Ever since, NB cell lines have become an invaluable material to study genetic changes and phenotypic plasticity of NB tumour cells (Thiele, 1998).

During this thesis, the SK-N-SH cell line was the main cellular model used for *in vitro* and *in vivo* experiments. This cell line derives from a bone marrow aspirate of a metastatic chemotherapy-resistant NB that was primary located at a thoracic paraganglia (Biedler *et al.*, 1973). SK-N-SH cell line contains

all 3 (N-, S- & I-) morphological cell subtypes described in NB cell lines (hence we call it mixed, M- or parental cell line); this makes it particularly interesting for studies approaching stemness potential of NB. Together with SK-N-SH, other 9 human NB cell lines (LAN-1, IMR-5, SK-N-LP, SK-N-JD, IMR-32, LAI-5-S, SK-N-AS, SK-N-Be(2)c and SH-SY5Y) were also used for tumour spheroid screening. This panel of 10 cell lines recapitulates genetic, genomic and biological diversity of human NB tumours (Table-10). In addition, HEK293T cell line was used to generate lentiviral particles.

Cell lines were grown in complete growth medium (GM) containing RPMI-1640 Glutamax™ or DMEM. Glutamax™ supplemented with 10% or 20% inactivated foetal bovine serum (FBS) and 1% penicillin/streptomycin (P/S) (Table-10) and kept at 37°C, 95% humidity, 5% CO<sub>2</sub> pressure as standard culture conditions. In order to degrade complement proteins naturally present in FBS, FBS stock was heated at 56°C during 30min, prior to complete GM preparation.

Cell line	RRID identifier	Growth media	source
HEK 293	CVCL_0045	DMEM Glutamax®-10%FBS-1%P/S	Marian Martínez-Balbás Lab (IBMB-CSIC)
SK-N-SH	CVCL_0531	RPMI 1640 Glutamax®-20%FBS-1%P/S	Joaquín Lopez-Soriano Lab (VHIR)
SK-N-Be(2)c	CVCL_0529		
IMR-32	CVCL_0346		
LAN-1	CVCL_1827	RPMI 1640 Glutamax®-10%FBS-1%P/S	Cinzia Lavarino Lab (IRSJD)
IMR-5	CVCL_1306		
SH-SY5Y	CVCL_0019		
SK-N-AS	CVCL_1700		
SK-N-JD	CVCL_WH12		
SK-N-LP	CVCL_WH13		
LA-I-5s	not available		

**Table-10. List of human cell lines used in this doctoral thesis.** FBS: foetal bovine serum; P/S:penicillin/streptomycine.

## 2.2. Sub-culturing, cell counting & cryopreservation of cell lines

All cell lines were cultured in polystyrene-coated culture dishes. To avoid induction of neural-like differentiation by cell-to-cell contacts once cell density reached 50-70% of dish surface, cells were detached and seeded in new plate. Briefly, plates were washed with pre-warmed PBS1x and cells were detached from the plate using 0.25% trypsin/EDTA (5min incubation, at 37°C). Trypsin activity was stopped by adding 2 volumes of complete growth medium. Detached cells were recovered, centrifuged (300g, 5min, RT), and resuspended in 1ml complete GM. Total cell number was estimated, when needed, using trypan blue and Countess II FL Automated Cell Counter (ThermoFisher SCIENTIFIC), following manufacturer's protocol. Cell lines were sub-cultured twice a week and GM was renewed every 3 days. Cell lines were kept on culture no longer than 12-14 passages.

To maintain continuous stocks of cell lines, cells can be stored through cryopreservation.  $4 \cdot 10^6$  cells

from early passage plates were resuspended in 1ml GM containing 5% DMSO. Cryogenic vials (Corning, Inc.) were gradually frozen (-1°C/min) using a home-made porexpan container to avoid formation of ice crystals that could perforate cell membrane. Cryopreserved cell lines were stored at -80°C &/or in liquid nitrogen (Parc Cientific de Barcelona). To start cell cultures from cryopreserved cell lines, cells have to be thawed and DMSO has to be removed as fast as possible to avoid DMSO-mediated toxicity. Briefly, cryogenic vials were thawed in 37°C water bath while swirling. Immediately after complete thawing, cells (1ml) were diluted into 9ml GM and spun down (300g, 5min, RT). Supernatant (SN) was carefully removed and cells resuspended to single cell suspension in 1ml GM. Plates were washed and GM renewed 24h after seeding in order to remove cellular debris and DMSO residues.

### 2.3. *Mycoplasma* detection

Biological contamination of cell culture is a frequent problem in cell culture facilities. Certain species from the genus of *Mycoplasma* are responsible for persistent contaminations due to their slow growing rate and small size (less than 1 µm). In addition, antibiotics that are routinely added to home-made GM formulation could mask mycoplasma contamination by keeping mycoplasma levels below limits of detection. Therefore, the presence of *Mycoplasma* has to be periodically tested.

For assessment of *Mycoplasma* contamination,  $2 \cdot 10^4$  cells were seeded into 8 well Permanox® Nunc® Lab-Teck® chamber slide™ system and cultured with GM without P/S. After 3 days of growing, cells were fixed, permeabilized and DNA was stained with 4',6-diamidino-2-phenylindole (DAPI) (for a detailed explanation see section 8.2, from Materials and Methods). Whenever there is *Mycoplasma contamination*, tiny bacteria can be detected as small DAPI+ dots inside the cytosol of the eukaryotic cells using a fluorescent microscope.

### 2.4. MTT assay

Cell viability assessment is a classical approach to evaluate whether different stimuli altered the growing rate or survival capability of a cell line. Proper mitochondrial function is essential for cellular fitness, and a direct read-out of the cell viability. The MTT reduction assay is a colorimetric method that quantifies mitochondrial function, giving an indirect estimation of cell viability. MTT assay is based on the activity of mitochondrial NADH-dehydrogenases. MTT (3-(4,5-dimethylthiazol-2-yl)-2,5-diphenyltetrazolium bromide) is a yellowish soluble salt that is reduced to formazan by mitochondrial NADH-dehydrogenases. Formazan has a purple-to-black colour and form insoluble crystals in aqueous solutions that are solved with DMSO. The amount of formazan is indicative of mitochondrial activity and cell viability.

To assess cell viability cells were seeded in quadruplicates on 96 wells plates ( $8 \cdot 10^3$  cells/well) in a final volume of 100  $\mu$ l. At desired time points (normally 24h, 48h, 72h and 96h), 10 $\mu$ l of 5mg/ml MTT solution was added to each well and the plates were incubated at 37°C for 4h. After removal of GM, formazan crystals were dissolved with 100 $\mu$ l DMSO by shaking on a bench rocker (100 oscillations per minute, opm) for 15min, covered with aluminium foil. Optic density at 570nm ( $OD_{570}$ ) was read in a microplate reader.  $OD_{570}$  from wells with GM were used to define the background signal.

## 2.5. BrdU assay

Evaluation of cell proliferation and estimation of the replicating fraction of a cell culture or a tissue have been of major interest in cancer studies. Progression through the cell cycle is a tightly regulated process, with specific signalling cascades controlling major cell cycle transitions. Those cells that overcome G1 checkpoint start DNA replication that span over the whole S-phase length. Therefore, the detection of replicating cells is a direct estimation of the proliferative fraction during a define time period.

BrdU (5-bromo-2'-deoxyuridine) is an analogue of the nucleoside thymidine that is incorporated into replicating DNA and can be detected using anti-BrdU antibodies. The detection of integrated BrdU needs to unwind DNA to facilitate the access of anti-BrdU antibodies. The use of DNase I type II to open DNA allows the combination of proliferation studies together with cell immunophenotyping or detection of transgenic fluorescent proteins (such as GFP).

For all our studies a 10  $\mu$ M BrdU solution was added to SK-N-SH cells growing in monolayers. Length of the incubation period was adapted to the aim of every experimental design: for routine estimation of cells in S-phase (BrdU incorporation assay) a 2h incubation at 37°C was performed; for *in vivo* evaluation of proliferating cells after recombinant NXPH1 (rNXPH1) treatment (BrdU retention assay) 24h incubation at 37°C was used.

## 2.6. Tumour spheroid assay

The ability to grow as tumour spheroids of cancer cells has been conventionally used as an *in vitro* surrogate of their tumorigenic potential (for further details see section 3.2.2.5.1 from Introduction).

For tumour spheres assays, cells were grown in sphere-forming-media (SFM) (see Appendix I for the detailed formulation).

For **CSC screening**,  $3 \cdot 10^6$  cells were cultured in uncoated 60mmx15mm plates or in ultra-low attachment surface plates and were fed with fresh SFM weekly (2ml per plate). Spheres were allowed to

grow for 5 weeks and photographed using an inverted bright-field microscope (Leica DMIRBE). Then spheres were recovered and processed for RNA extraction as described in the standard protocol (see section 7, from Materials and Methods).

For **evaluation of tumorigenic potential of  $\alpha$ -NRXN1<sup>High/Low/Neg</sup> populations**,  $2 \cdot 10^3$  single cells from each population were sorted in quadruplicates directly into pre-coated 12 well plates (see also section 5.2, from Materials and Methods). Previously, each well was coated with 450 $\mu$ l sterile 0.5% agarose solution to avoid cell adhesion to the plate surface. Plates were monitored every two days and spheroids were allowed to grow for 1 week. For enable discrimination of viable spheres, plates were incubated for 3h (37°C) in the presence of 100 $\mu$ l MTT (5mg/ml stock). Finally, viable spheres (black coloured) were manually counted using an inverted bright-field microscope (Leica DMIRBE).

This protocol was adapted from (Hansford *et al.*, 2007; Ikegaki *et al.*, 2013; Takenobu *et al.*, 2011).

## 2.7. *In vitro* 2-dimensions (2D) ELDA growth assay

When grown in conventional adherent cultures, cell density influences cell proliferation by means of cell-to-cell contacts and paracrine signalling. Cell culture under extreme limiting dilution conditions (extreme limiting dilution assay, ELDA) is used to test proliferative potential independently of those extracellular stimuli.

For 2D ELDA growth assay, defined cell numbers of  $\alpha$ -NRXN1<sup>High/Neg</sup> subpopulations and parental SK-N-SH cell line were sorted in triplicates into 96 well plates using a BD FACSAria™ Fusion sorter (BD Bioscience, Franklin Lakes, New Jersey, USA). The ending point was established whenever cells, at any of the conditions, managed to fully cover the well surface (approximately, 2 weeks after seeding). Each well contained 100 $\mu$ l GM and half of the volume was renewed after 1 week of culture. Then, GM was removed and cells were fixed with 4%PFA for 15min (RT). After washing with PBS1x, 50 $\mu$ l of 0.5% crystal violet solution was added to each well and incubated for 20 min (RT) on a bench rocker (20-30 opm). Dye was washed out by gently washing the plate in a stream of tap water at least 4 times. Plates were inverted on filter paper and air-dry for at least 2 hours (RT). To permeabilize the cells and dissolve crystal violet staining, 200 $\mu$ l methanol was added to each well and incubated for 20min (RT) on a bench rocker (20-30 opm). Finally, OD<sub>570</sub> was measure with a microplate reader (POWER WAVE XS Microplate Spectrophotometer). OD<sub>570</sub> from wells without cells were used to define the background of the staining method.

This protocol was adapted from (Bahena-Ocampo *et al.*, 2016; Feoktistova *et al.*, 2016).

## 2.8. Cell culture in the presence of chemotherapeutic drugs

The expression of xenobiotic transporters on the plasmatic membrane and slower cell cycle rates protect stem cells from standard chemotherapeutic drugs that normally tackle fast-cycling populations. This is due to the fact that most of these drugs are designed to block DNA replicative machinery and induce irreversible DNA damage.

For this thesis cisplatin and mitoxantrone (MTX) were used to test chemoresistance capacity of NB cells. Cisplatin belongs to a platinum-based antineoplastic family of medications. It binds to DNA nucleotides (nc, mainly to guanines), crosslinking DNA and interfering with DNA synthesis. Damaged DNA activates apoptosis when repair proves impossible. Cisplatin is currently used as standard of care for IR and HR NB patients (Tolbert and Matthay, 2018). MTX is an anthracenedione antineoplastic drug that intercalates into DNA, inhibiting type II topoisomerase. The final outcome is similar to the one previously described for cisplatin since it disrupts DNA synthesis and repair, inducing apoptosis of tumour cells. MTX is used in paediatric cancer as standard of care for acute lymphoblastic leukaemia patients.

To assess whether  $\alpha$ -NRXN1+ cells persist during drug treatment,  $0.5$  to  $1 \cdot 10^6$  SK-N-SH cells were seeded into 100mm x 20mm (p100) plates. The optimal drug concentration was determined as the one that cause a 70-80% reduction in MTT cell viability assay after 4 days (data not shown). Cisplatin ( $3\mu\text{M}$ ) or MTX (5ng/ml) was added to each plate 7, 3 or 1 day before analysis of surviving  $\alpha$ -NRXN1+ cells by flow cytometry (BD FACSAria™ Fusion). For the recovery condition, cells were seeded in the presence of the drugs for 3 days. Afterwards, plates were washed carefully with PBS1x and let grow for another 4 days with normal GM. Staining of viable cells with anti- $\alpha$ NRXN1-ATTO488 antibody and detection of  $\alpha$ -NRXN1+ cells by flow cytometry are detailed later on (see section 5.2, from Material and Methods).

## 3. Human NB patient derived xenograft

Despite the usefulness of established tumour cell lines as pre-clinical models, a major restriction is their poor predictive response for the drug pharma industry. It has been seen that the therapeutic response in these pre-clinical models has a very low correlation with drug activity in phase II clinical trial (Johnson *et al.*, 2011). To circumvent conventional cell lines limitations the development of patient-derived xenografts (PDXs) as advanced preclinical models has re-gained interest during the last decade (Hidalgo *et al.*, 2014). A significant effort to established and characterized NB PDX models together with others paediatric PDXs has been recently done (Braekeveldt *et al.*, 2015; Stewart *et al.*,

2017). Although engraftment rate is relatively low (around 24% for orthotopic implantation), successfully engrafted NB PDXs retain genomic and phenotypic features of the original patient's tumours, exhibit an aggressive behaviour typical of high risk NBs and are useful platforms to validate new therapeutic strategies (Braekeveldt *et al.*, 2015; Monterrubio *et al.*, 2017; Monterrubio *et al.*, 2015; Stewart *et al.*, 2017).

NB PDX models were established from patient biopsies at HSJD under an Institutional Review Board-approved protocol. The NN PDX models HSJD-NB-007 and HSJD-NB-011 were derived from patients refractory to all treatments. HSJD-NB-007 was established from a 5 year old male with progressive stage 4 disease, amplification of *MYCN* gene and no mutations in *TP53* and *ALK*. HSJD-NB-011 was from a 2.5 year old male with progressive stage 4 disease, amplification of *MYCN* gene, *TP53* wild type and *ALK*-mutated (I1171N).

The HSJD-NB-007 and HSJD-NB-011 were used for previous publications (Boeva *et al.*, 2017; Monterrubio *et al.*, 2017). The HSJD-NB-012 has not been characterized yet and has not been included in previous publications so far.

Subcutaneous grafting of human NB PDX is described later on (see section 6.4, from Materials and Methods).

## 4. Generation of transgenic cell lines by lentiviral infection

Self-inactivating lentiviral and retroviral vectors are basic tools for transgenic delivery and are frequently used for the manipulation of expression levels of genes of interest. Retroviral –based vectors depend of active cell division to effectively integrate into host genome, while lentiviral vectors could integrate into the host genome in the absence of cell division. Throughout this thesis lentiviral vectors were used for selective inhibition of *NXPH1* or  $\alpha$ -*NRXN1* gene expression in SK-N-SH (using constitutive or inducible short-hairpin RNA (sh-RNA)).

### 4.1. DNA constructs

#### 4.1.1. Transfer vectors

Transfer vectors contain the gen or DNA sequence of interest together with specific sequences that are required to incorporate the region of interest to the lentiviral particles and to integrate it into the host genome of the target cells.



- o It allows tetracycline-regulated expression of miR-shRNAs (Tet-ON conditional expression) thanks to a third-generation reverse Tet transactivator (rtTA) and a Tetracycline-Tight Responsive Element (TRE-tight) promoter. Constitutive stable silencing of genes implicated in cell proliferation or survival readily results in a dramatic drop of cell culture viability and growth, reducing experimental possibilities. Even a cytotoxic effect of the shRNA, which could be not apparent in the initial post-transduction period, might generate a negative selection pressure against effective gene silencing during prolonged cell culture (Fish and Kruithof, 2004).
- o It allows the concomitant and coordinated expression of a transgene (for example *EGFP*), coupled to miR-shRNA expression, allowing the straightforward identification of miR-shRNA expressing cells.

These technical improvements made pSLIK system an attractive option for the regulated knock-down of *NXPH1* or  $\alpha$ -*NRXN1*. For this purpose, pSLIK-Neomycine (pSLIK-Neo) (Figure 15A) and a donor plasmid for gateway recombination cloning, pEN\_TTGmiRc2 (Figure 15B), were purchased from Addgene. The cloning of specific shRNAs against human *NXPH1* or  $\alpha$ -*NRXN1* genes was done for this doctoral thesis (for further details see section 4.4 from Materials and Methods).

#### 4.1.2. Viral constructs

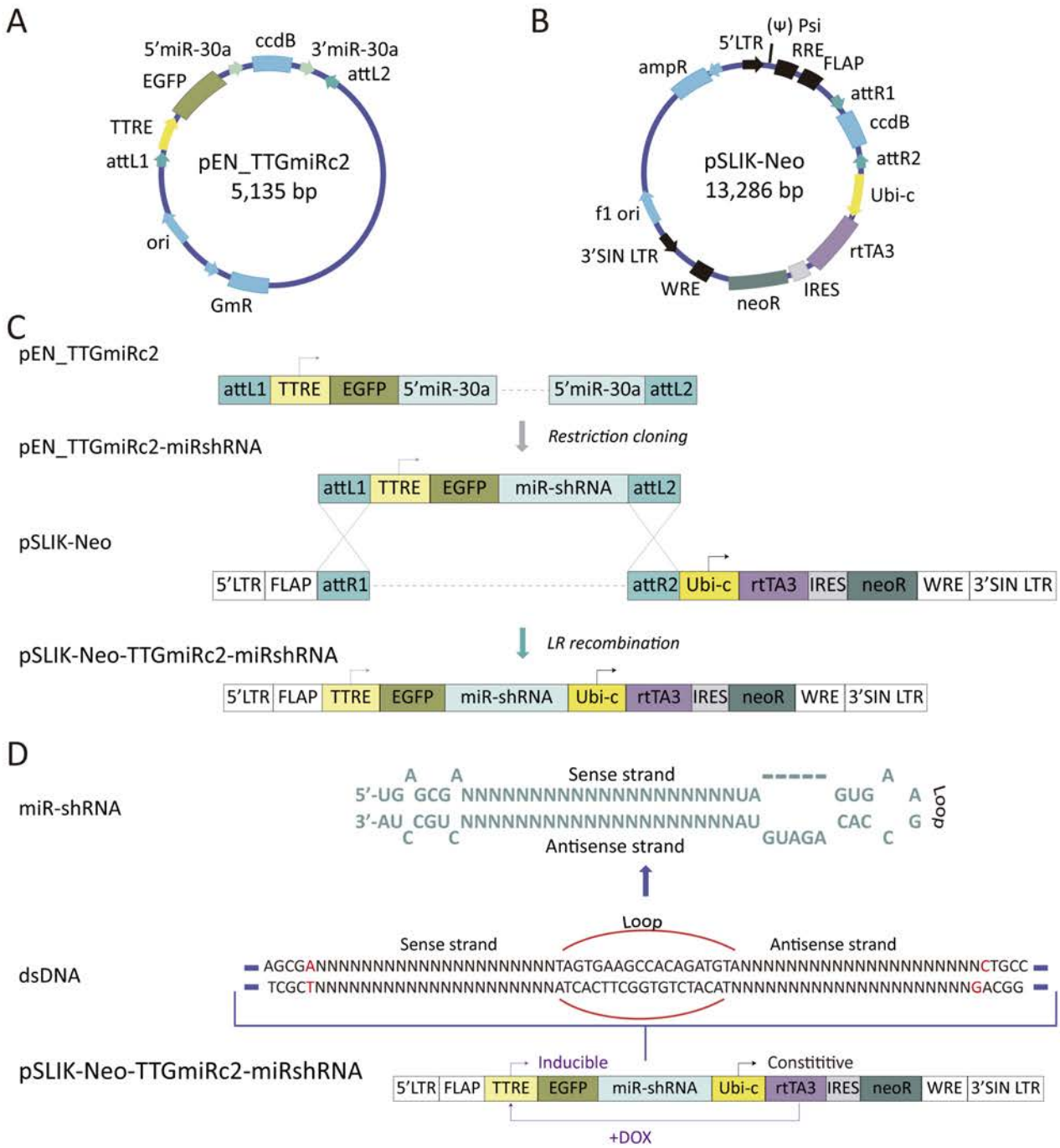
Both viral constructs pMD2.G & psPAX2 were a kind gift of Dr. Marian Martínez-Balbás (IBMB-CSIC, Spain).

##### 4.1.2.1. pM2D.G

pM2D.G is a 2<sup>nd</sup> generation envelop vector, that codes for the Vesicular Stomatitis Virus G Glycoprotein (*vsv-g*), necessary for viral penetration of the plasma membrane of the target cells.

##### 4.1.2.2. psPAX2

psPAX2 is a 2<sup>nd</sup> generation packaging vector, that codes for HIV-1 viral capsid precursor protein (*gag*), retrotranscriptase and integrase precursor protein (*pol*), RNA-binding protein (*rev*) and transactivator protein (*tat*). These four genes are required for lentiviral replication and for the assembling of new lentiviral particles.



## 4.2. Design of shRNA sequence against target genes

Searching and selection of gene-specific shRNA sequences was done using the Genetic Perturbation Platform (GPP)-web based tool, generated by the Broad Institute. GPP web portal applies an algorithm for the ranking of potential 21mer targets within each RefSeq transcript. The algorithm is constantly revisited based on current literature. For this thesis rule set 9 of GPP algorithm was used to get a list of candidate shRNA sequences. The following rules were considered for the ultimate selection of shRNA sequences from the GPP-generated list:

**Figure-15. Backbone vectors and cloning strategy used for the generation of inducible miR-shRNA**

(A) Schematic representation of entry backbone vector pEN\_TTGmiR2 carrying inducible TTRE promoter, controlling EGFP and human miR30a adaptor sequence, plus attL recombination sites. (B) Schematic representation of destination backbone vector pSLIK-Neo carrying constitutive Ubi-c promoter, controlling rTA3 and neoR expression, plus attR recombination sites. (C) Diagram showing cloning strategy used to generate pSLIK-Neo-TTGmiRc2-miRshRNA. First shRNA was introduced to entry vector pEN\_TTGmiR2 by restriction cloning, then inducible TTRE-EGFP-miRshRNA cassette was translocated to destination vector pSLIK-Neo by left-right recombination. (D) Integrative region of pSLIK-Neo-TTGmiRc2-miRshRNA showing predictive constitutive (rTA3-IRES-neoR) and doxycycline-inducible (EGFP-miRshRNA) transcripts. miR-like shRNA structure is transcribed from a dsDNA sequence cloned downstream EGFP transgene. 3'SIN LTR: 3' self-inactivating long terminal repeat; 5'LTR: 5' long terminal repeat; 3'miR30a: 3' end of human miR-30a; 5'miR30a: 5' end of human miR-30a; ampR: ampicillin resistance gene; attL1/attL2 sites: recombination sites entry vector; attR1/attR2 sites: recombination sites destination vector; ccdB: DH5a toxin; DOX: doxycycline; dsDNA: double-stranded DNA; EGFP: enhanced-green-fluorescent-protein; fl ori: f1 bacterial origin of replication; FLAP: region that contains central polypurine tract (cPPT/CTS); GmR: gentamycin resistance gene; IRES: internal ribosome entry site; miR-sh-RNA: miR-like short hairpin RNA; neoR: neomycin/G418 resistance gene; ori: bacterial origin of replication; ( $\psi$ ) Psi: RNA target site; RRE: Rev response element; rTA3: 3rd generation reverse tetracycline transactivator element; TTRE: tight tetracycline repressor element; Ubi-c: Human ubiquitin-c promoter; WRE: Woodchuck hepatitis virus post-transcriptional regulatory element. Adapted from (Shin *et al.*, 2006).

- o Regions within 50-100nt of the start codon and the termination codon were avoided
- o Intronic regions were avoided
- o Stretches of 4 or more bases (AAAA,CCCC...) were avoided
- o Repeats (for example G/C) and SNP sites were avoided
- o BLAST homology search had to give none off-target binding to other gene or sequences

Final shRNA sequences for constitutive or inducible gene knockdown through pLKO.1 puro or pSLIK-Neo respectively are shown in Table B (Appendix I).

### 4.3. Cloning of short-hairpin RNA sequences into pLKO.1-puro plasmid

Unless specified, all the enzymes required for molecular biology techniques were purchased from ThermoFisher SCIENTIFIC. The suppliers and catalog numbers of the rest of the reagents are detailed in Table E (Appendix I).

Cloning of shRNA sequences into pLKO.1-puro proceeded as follow:

#### *STEP 1: Adapt original target sequences to pLKO.1 puro system*

Gene-specific shRNA sequences were adapted to pLKO.1 puro cloning (for further details see Table B-Appendix I) and unphosphorylated sense and antisense oligonucleotides were ordered to SIGMA-

ALDRICH. Adaptation of sh1-NXPH1 sequence to pLKO.1 puro system is used as an example (Table-11):

1. To generate the sense oligonucleotide, start from a 21-mer gene-specific target sequence: 5'-GCCCTTTAAGGTGATCTGTAT-3'
2. Add 5' flanking sequence at 5' end (seen in blue): 5'-CCGGGCCCTTTAAGGTGATCTGTAT-3'
3. Add the PstI internal loop sequence at 3' end (seen in green): 5'-CCGGGCCCTTTAAGGTGATCTGTATCTGCAG-3'
4. Add reverse complement sequence of the 21nc sequence at 3' end (seen in black). 5'-CCGGGCCCTTTAAGGTGATCTGTATCTGCAGATACAGATCACCTTAAAGGGC-3'
5. Add 3' flanking sequence at 3' end (seen in blue). This is the sense oligonucleotide: 5'-CCGGGCCCTTTAAGGTGATCTGTATCTGCAGATACAGATCACCTTAAAGGGCTTTTGG-3'
6. To generate the antisense oligonucleotide, start from a 21-mer gene-specific target sequence: 5'-GCCCTTTAAGGTGATCTGTAT-3'
7. Add 5' flanking sequence at 5' end (seen in blue): 5'-AATTCAAAAAGCCCTTTAAGGTGATCTGTAT-3'
8. Add the PstI internal loop sequence at 3' end (seen in green): 5'-AATTCAAAAAGCCCTTTAAGGTGATCTGTATCTGCAG-3'
9. Add reverse complement sequence of the 21-mer sequence at 3' end (seen in black). This is the antisense oligonucleotide: 5'-AATTCAAAAAGCCCTTTAAGGTGATCTGTATCTGCAGATACAGATCACCTTAAAGGGC-3'

**Table-11. Generation of sense and antisense oligonucleotide for pLKO.1 puro cloning**

*STEP 2: Linearization of destination vector (pLKO.1-puro cloning vector)*

1. Digestion of 3µg of pLKO.1-puro cloning vector with EcoRI and AgeI in 20 µl final volume. Tubes were incubated for 3h (37°C), adding fresh buffer and enzyme after 1.5h

Dephosphorylation of EcoRI/AgeI-open vector adding 1µl FastAP per 1µg DNA (30min incubation, at 37°C). Final vector concentration was around 200-500 ng/µl

2. Verification of complete pLKO.1-puro linearization by 0.7% agarose electrophoresis
3. Linear dephosphorylated pLKO.1-puro was purified using illustra™ GFX™ PCR DNA and Gel Band Purification kit following manufacturer's instructions

*STEP 3: Generation of phosphorylated double stranded DNA*

1. Oligonucleotides were resuspended in H2O MQ to a final concentration of 3µg/µl
2. Sense and antisense oligonucleotides were diluted together in annealing buffer (for further details see Table B-Appendix I). Final concentration of oligonucleotides was 60ng/µl
3. Stable annealing of sense and antisense oligonucleotides was achieved through 3 sequential incubation steps: 4min 90°C → 10min 70°C → turn off thermoblock and let it cold down till 25°C. Double stranded DNA (dsDNA) stock are store at 4°C
4. Phosphorylation of dsDNA duplex by T4PNK following manufacturer's instructions. Final concentration of phospho-dsDNA was 12 ng/µl

#### STEP 4: Ligation

Ligation was done using T-4 Ligase, following manufacturer's instructions. Linear dephosphorylated vector (50ng) was ligated with phospho-dsDNA keeping a 1:3 molar ratio. A re-ligation tube of the linear vector alone was always included as a control.

#### STEP 5: Transformation

Home-made competent DH5 $\alpha$  *E.coli* (100 $\mu$ l) were mixed with 3 $\mu$ l of ligation mix and transformed by thermic shock (see section 4.5, from Materials and Methods). Ligation tubes were seeded in ampicillin plates.

#### STEP 6: Colony diagnosis

1. Re-ligation control was checked to evaluate ligation efficacy
2. Selected colonies were seeded in 4ml LB media (for a detailed formulation see Table A-Appendix I) with ampicillin (37°C, ON)
3. Plasmid DNA was extracted (see section 4.6, from Materials and Methods)
4. Screen for positive clones by digesting 200-500ng plasmid DNA with BamHI/PstI:

Negative colonies (1 BamHI site): single band (7050bp)

Positive colonies (1 BamHI and 1 PstI sites): two bands(6332bp+752bp)

5. Sequencing of positive clones with pLKO.1-puro sequencing primer (GATC sequencing service). pLKO.1 sequencing primer sequence is detailed in Table B-Appendix I

### 4.4. Cloning of short-hairpin RNA sequences into pSLIK-Neo plasmid

The cloning of shRNA sequences into pSLIK-Neo requires two sequential protocols (Figure 15C-D). In the first part the dsDNA is introduced into the donor plasmid pEN\_TTGmiRc2 by restriction digestion and ligation. The donor plasmid pEN\_TTGmiRc2 contains all the elements of the functional inducible cassette and the 5' and 3' ends of human miR30 surrounding two BfuA1 restriction sites (Figure 15C). In the second part the inducible cassette (containing TRE promoter upstream EGFP transgene and miR30-shRNA sequence) is translocated by gateway recombination into pSLIK-Neo destination plasmid (Figure 15C,D).

## 4.4.1. Restriction cloning of miR30-shRNA into donor plasmid pEN\_TTmiRc2

*STEP 1: Adapt original target sequences to pSLIK-Neo system*

Gene-specific target sequences were adapted to pSLIK-Neo cloning (Table-12) and unphosphorylated sense and antisense oligonucleotides were ordered to SIGMA-ALDRICH. Adaptation of sh1-NX-PH1 sequence to pSLIK-Neo system is used as an example (Table-12):

1. To generate the sense oligonucleotide, start from a 20-mer gene-specific target sequence: 5'-CCCTTTAAGGTGATCTGTATT-3'
2. Insert one uncomplementary nc at the 5' end (seen in red): 5'-ACCTTTAAGGTGATCTGTATT-3'
3. Insert miR30 flanking sequence at 5' end (seen in blue): 5'-AGCGACCTTTAAGGTGATCTGTATT-3'
4. Insert the internal loop sequence et 3' end (seen in green): 5'-AGCGACCTTTAAGGTGATCTGTATTAGTGAAGCCACAGATGTA-3'
5. Insert reverse complement sequence of the 21-mer sequence at 3' end (seen in black) and an extra uncomplementary nc to generate a mismatched (seen in red). This is the sense oligonucleotide: 5'-AGCGACCTTTAAGGTGATCTGTATTAGTGAAGCCACAGATGTAATACAGATCACCTTAAAGGGC-3'
6. To generate the antisense oligonucleotide, generate the reverse complement sequence of the sense oligo: 5'-GCCCTTTAAGGTGATCTGTATTAGTGAAGCCACAGATGTAATACAGATCACCTTAAAGGGTCGCT-3'
7. Delete the las 4 nc of the 3' end: 5'-GCCCTTTAAGGTGATCTGTATTAGTGAAGCCACAGATGTAATACAGATCACCTTAAAGGGT-3'
8. Insert 5'-GGCA-3' sequence at 5' end (seen in blue). This is the antisense oligonucleotide: 5'-GGCAGCCCTTTAAGGTGATCTGTATTAGTGAAGCCACAGATGTAATACAGATCACCTTAAAGGGT-3'

**Table-12. Generation of sense and antisense oligonucleotide for pSLIK-Neo cloning**

*STEP 2: Linearization of donor plasmid*

- Digestion of 3µg of donor vector (pEN\_TTGmiRc2) with BfuA1 in 20µl final volume. Tubes were incubated for 3h (37°C), adding fresh buffer and enzyme after 1.5h. Digestion with BfuA1 removes the ccdB cassette (toxic for DH5α *E.coli* strain)
- Verification of complete pEN\_TTGmiRc2 linearization by 1% agarose electrophoresis
- Linear donor plasmid was purified using illustra™ GFX™ PCR DNA and Gel Band Purification kit following manufacturer's instructions. Optimal final vector concentration was around 200-500 ng/µl

*STEP 3: Generation of phosphorylated dsDNA*

Proceed as in STEP 3 from section 4.3 (Materials and Methods)

*STEP 4: Ligation*

Proceed as in STEP 4 from section 4.3 (Materials and Methods)

### STEP 5: Transformation

Proceed as in STEP 5 from section 4.3 (Materials and Methods). In this case ligation tubes were seeded in neomycin/G418 plates.

### STEP 6: Colony diagnosis

1. Select and grow colonies as in STEP 6 from section 4.3 (Material and Methods). In this case 5µg/ml neomycin/G418 was used as selection antibiotic
2. Ligation could result in empty plasmids by pEN\_TTG\_miR2 vector recircularization (negative colonies) or plasmids where the phospho-dsDNA was efficiently incorporated (positive colonies). Due to the small difference in size between both plasmids, screening for positive colonies was done by direct sequencing of plasmid DNA with EGFP-C sequencing primer (GATC sequencing service). EGFP-C sequencing primer sequence is detailed in Table C- Appendix I

#### 4.4.2. Gateway recombination of TTRE-EGFP-miRshRNA cassette into destination plasmid pSLIK-Neo

The TTRE-EGFP-miRshRNA cassette was introduced into destination plasmid pSLIK-Neo by left-right gateway *in vitro* recombination (Figure 15C,D). LR Gateway recombination and subsequent bacterial transformation was performed using LR Clonase™ II kit and following manufacturer's instructions. In this way plasmids containing inducible TTRE-EGFP-miRshRNA cassette and constitutive bicistronic Ubi c-rtTA3-IRES-EGFP cassette were generated (Figure 15C,D)

## 4.5. Bacterial transformation

Plasmid DNAs were incorporated into home-made competent DH5α *E.coli* bacteria, in order to amplify them for different experimental purposes. To facilitate plasmid DNA internalization, bacterial wall and membrane needs to be destabilized. Among available protocols, the classical thermic shock method is a robust procedure for bacterial wall and membrane destabilization. Briefly, competent DH5α *E.coli* (100µl) were slowly thawed in ice and gently mixed with plasmid DNA (ratio 10: 1, in volume). Tubes containing bacteria and plasmid DNA were incubated 20min in ice, followed by 75sec at 42°C and 2min back in ice. For bacterial recovery, 1ml LB without antibiotic was added to each tube that was then incubated for 1h at 37°C. Finally, bacteria were spun down (16,000g, 30seg), resuspended in 200µl LB and seeded in antibiotic-containing plates.

#### 4.6. Amplification and purification of DNA constructs (minipreps & midipreps)

Extraction of plasmid DNA for cloning and cloning diagnosis purposes was done following a home-made low purity protocol (minipreps). Briefly, on the previous day 4ml LB tubes with proper antibiotic were inoculated with desired colonies or bacterial glycerol stocks and were grown overnight (ON) at 37°C. On the next morning bacteria were spun down (1min, 16,000g) and the SN was removed. Pellets were resuspended in 100µl P1 resuspension buffer by gentle agitation. Then, 100µl of P2 lysis buffer was added to each tube and mixed by inversion. Again, 100µl P3 neutralization buffer were added and content was mixed by inversion. Tubes were centrifuged (6min at 16,000g) and SNs were recovered in clean tubes. Finally DNA pellets were washed with 600µl ice-cold absolute ethanol. After centrifugation (16,000g, 5min, 4°C), SNs were carefully removed and DNA pellets were allowed to dry completely. Plasmid DNAs were resuspended in 50µl sterile H<sub>2</sub>O MQ and stored at -20°C until needed.

High purity extraction of plasmid DNA for HEK293T transfection and lentiviral production purposes (midipreps) was performed using NucleoBond® Xtra Midi kit following manufacturer's instructions.

In order to check for the plasmid DNA quality and purity, vectors were routinely checked by restriction digestion.

#### 4.7. Lentiviral production and transduction

In this thesis, 2<sup>nd</sup> generation lentiviral particles were used and produced as described by Didier Trono's Lab. Lentivirus production and handling were done under biological safety level 2 (BSL-2) area. Disposal of all the contaminated material was also conducted as specified for BSL-2 organisms.

Lentiviral particles were produced by transfecting HEK293T cell line with 15µg transfer plasmid, 10µg packaging psPAX2 plasmid, and 5µg envelop pM2D.G plasmid using Lipofectamine 2000, a soluble cationic lipid agent. Briefly, HEK293T cells were seeded at high density ( $6.5 \cdot 10^6$  Cells/p100) in complete GM and let adhere ON. To allow Lipofectamine 2000-DNA complex formation, 50µl Lipofectamine 2000 were diluted in 700µl Optimen minimal growth media and incubated for 5min (RT). In parallel, the indicated amounts of the 3 vectors were diluted in Optimen (up to 750µl). Lipofectamine 2000 and DNA solutions were mixed and incubated for 20min (RT). HEK293T plates were washed gently twice with pre-warmed PBS1x and refilled with 7ml DMEM-10%FBS per plate. Then, 1.5ml of liposomes were added to each plate and was then return to the incubator for 6-8h (37°C). Finally, liposomes media was replaced with 5.5ml complete GM and transfected cells were allowed to generate lentivirus particles. After 48h, lentivirus-bearing SN was recovered, centrifuged (300g, 5min) and filtered through 45µm Millex-HV PVDF syringe filter. SNs were immediately used or stored at -80°C until needed.

Lentiviral transduction of target cells was normally performed readily after lentivirus recovery. Briefly, target cell line (SK-N-SH in this project), was seeded at low density ( $0.7 \cdot 10^6$  Cells/p100) in complete GM and let adhere for 24h. Then, GM was replaced by fresh GM plus lentivirus SN (dilution range from 1/4 to 1/10). SK-N-SH cells were incubated with the lentiviral particles for 48h, This period was enough for stable transgene integration and expression in the target cells. Following this protocol infection efficiency in SK-N-SH NB cell line reached 70-90%.

#### 4.8. Selection of transduced cell lines

Selection of transduced cells started 48h after infection and was done according to each vector specifications. Host cells were not used for any experimental procedures until selection was completed.

Puromycin ( $2 \mu\text{g}/\text{ml}$ ) was used for selection of pLKO.1-puro SK-N-SH host cells. To determine puromycin working concentration, a killing curve was done with concentrations ranging from 0 to  $4.5 \mu\text{g}/\text{ml}$  (one point every  $0.5 \mu\text{g}$ ). The lowest concentration of puromycin that killed all wild-type SK-N-SH in 3 days was selected as working concentration.

Neomycin (also known as G418) (SIGMA-ALDRICH) ( $600 \mu\text{g}/\text{ml}$ ) was used for selection of pSLIK-Neo SK-N-SH host cells. To determine neomycin working concentration, a killing curve was done with concentrations ranging from 0 to  $10^3 \mu\text{g}/\text{ml}$  (one point every  $100 \mu\text{g}$ ). The lowest concentration of neomycin that killed all wild-type SK-N-SH in 7 days was selected as working concentration.

Antibiotic toxicity in killing curve assays was evaluated using a wide field optical LEICA DR IMBE epifluorescence microscope (LEICA, Wetzlar, Germany). Puromycin and neomycin were freshly added twice a week to the GM media of the host cells. The transgenic cells were grown with antibiotic for at least one month.

### 5. Flow cytometry and cell sorting

All the experiments were conducted at the Cytometry Core Facility (Centres Científics i Tecnològics, Universitat de Barcelona). Sorting tubes,  $70 \mu\text{m}$  mesh filter and DNA-binding and vital dyes were provided by the Cytometry Core Facility. Unless specified, vital DNA-binding dyes as DAPI (at  $0.1 \mu\text{g}/\text{ml}$ ) or propidium iodide (PI) (at  $2 \mu\text{g}/\text{ml}$ ) were always used for discarding damaged and dying cells.

As a general consideration, cells were kept on ice along the complete protocol and flow cytometer microfluidic system and collector device (when needed) were also maintained at  $4^\circ\text{C}$  to prevent cell

death. Single cell suspensions were analysed with a BD FACSAria™ Fusion according to the following criteria:

- o Cell debris was discarded by FSC-A/SSC-A gating
- o Cell aggregates were discarded by FSC-A/FSC-W gating
- o Live cells were selected by DAPI or PI negative signal (violet channel 450V or far red channel 610V, respectively)
- o Cell subpopulations positive for the antibodies or fluorophores of interest were detected (cytometer lasers and detectors were adapted to every different fluorophore)

## 5.1. Flow cytometry analysis of transgenic EGFP+ cells

In this project sorting of EGFP+ transgenic cells was done in order to purified pSLIK-Neo transgenic SK-N-SH cells where EGFP-miRshRNA cassette was efficiently induced. Dox-induced EGFP-miRshRNA+ cells from subconfluent plates were trypsinized, and resuspended in 1ml ice-cold DMEM-5%FBS (FACS buffer) to a final density of  $10^6$  cells /ml (see section 2.2, from Materials and Methods).

Cell suspensions were analysed with a BD FACSAria™ Fusion as described above. EGFP+ cells were selected by Blue B (530V) positive signal.

## 5.2. Flow cytometry analysis of cell surface antigens in human NB cells

The protocol used for immunophenotyping of alive cells by flow cytometry was adjusted for samples coming from *in vitro* culture or for cells coming from tumour xenografts:

For immunophenotyping of cell lines expanded *in vitro*, cells were plated sub-confluently and allowed to grow for 4 days prior to FACS experiment. On the day of the experiment, plates were washed with pre-warmed PBS1x and cells were detached from the plate using pre-warmed StemPro Accutase Cell Dissociation Reagent (20min, 37°C). Accutase activity was blocked with 2 volumes ice-cold complete GM and cells were recovered by centrifugation (300g, 5min, 4°C). For immunophenotyping of SK-N-SH cells growing as subcutaneous xenograft tumours or NB cells from PDX tumours, xenograft tumours were processed and dissociated to single cell suspension as described later on (see section 6.4, from Materials and Methods). Single cell suspensions were prepared in FACS buffer at the desired cell density (see section 2.2, from Materials and Methods).

For immunofluorescent staining, cell concentration was adjusted to  $10^7$  Cells/ml. At least 250,000

cells were incubated with primary or fluorescent-conjugated antibodies (see Table D-Appendix I) for 60min (in ice and protected from the light). Whenever a secondary fluorescent-conjugated antibody was required, cells were washed once with 10 volumes ice-cold FACS buffer and resuspended at  $10^7$  Cells/ml in FACS buffer containing  $2\mu\text{g/ml}$  fluorescently-labelled secondary antibody (see Table D Appendix I)(45min incubation,  $4^\circ\text{C}$ , protected from the light). Finally, cells were washed twice with 10 volumes ice-cold FACS washing buffer and resuspended at  $5\cdot 10^6$  cells /ml in ice-cold FACS buffer. DAPI or PI was chosen as vital dyes depending on the fluorophore combination.

Cell suspensions were analysed with a BD FACSAria™ Fusion as described above.

### *General considerations for the identification of $\alpha\text{-NRXN1+}$ cells deriving from tumour xenograft using flow cytometry*

Tumours contain a heterogeneous cell population broadly composed by cancerous cells and non-malignant niche cells (endothelial cells, immune cells and cancer-associated-fibroblasts). Therefore, cytometric identification of human cancer cells deriving from tumour xenografts requires a double selection strategy: a negative selection of niche cells and a positive selection of tumour cells. In this project all xenograft tumours were grafted subcutaneously in Nude or NOD/SCID immunocompromised mouse models. Nude animals are characterized by the lack of T cells, while NOD/SCID animal lack T cells and B cells. In addition, presence of cancer-associated- fibroblast in subcutaneous tumour models is considered negligible. Consequently in the tumour xenografts used for this project niche cells mainly consist of endothelial cells and certain myeloid immune cells. Identification of human NB cells in dissociated tumour xenografts was done following this double-selection strategy: after gating for viable cells by DAPI exclusion, murine endothelial cells (PECy7-CD31+) and myeloid cells (PECy7-CD11b+) were discarded by the far red channel while human NB cells (A647-GD2+ or A647-HLA (A,B,C)+) were selected by the red channel. Analysis of ATTO488- $\alpha\text{NRXN1+}$  population was then assessed over the PECy7-A647+ cells using the green channel.

$\alpha\text{-NRXN1+}$  tumour populations were defined as follows:  $\alpha\text{-NRXN1+}$  cells were considered the brightest 10-12% of original NB population and  $\alpha\text{-NRXN1-cells}$  were considered the 40-20% most negative NB population. When required,  $\alpha\text{-NRXN1}^{\text{High}}$  cells were established as the brightest 0.5-1% of the  $\alpha\text{-NRXN1+}$  population and  $\alpha\text{-NRXN1}^{\text{Low}}$  cells were considered the 10-20%  $\alpha\text{-NRXN1+}$  cells whose mean fluorescent intensity (MFI) was 3 to 4 times lower than the  $\alpha\text{NRXN1}^{\text{High}}$  population. For depletion of  $\alpha\text{-NRXN1+}$  cells prior to *in vivo* grafting, the 10-15% ATTO488-brightest pool was discarded allowing recovery of the remaining 80-85% population.

The gating strategy for detection and purification of  $\alpha\text{-NRXN1}$  subpopulations was adapted from (Merlos-Suarez *et al.*, 2011).

### 5.3. Flow cytometry analysis of cell cycle profile in $\alpha$ -NRXN1 positive and negative population

Flow cytometry analysis of DNA content allows a quantitative evaluation of cell cycle distribution. Combinatorial analysis of DNA content & cell-surface immunophenotyping gives real-time information about the cycling behaviour of the different cell subpopulations from a sample. DNA content quantification in live cells is done by Hoescht 33342 incubation. Hoescht 33342 binds to A-T base pairs and could be excited with UV or violet lasers. Fluorescence emission at 460nm gives a snapshot of cell cycle status among 3 distinct groups: cells in  $G_0/G_1$ -phases (DNA content  $2n$ ), cells in S-phase (DNA content  $\geq 2n, \leq 4n$ ) and finally those in G2/M-phases (DNA content  $4n$ ).

For the analysis of DNA content, cells were plated sub-confluently and allowed to grow. After 96h, cells were detached with StemPro Accutase Dissociation Reagent (20min, 37°C) and resuspended in pre-warmed DMEM-10% FBS ( $10^6$  cells/ml). Hoescht33342 (5 $\mu$ g/ml) was added and incubated for 45min, at 37°C, protected from the light. Cells were then concentrated (300g, 5min, 4°C) to  $10^7$  cells/ml in ice-cold FACS buffer with 5 $\mu$ g/ml Hoescht 33342 and transferred to ice bucket. Immunophenotyping of  $\alpha$ -NRXN1+ population was done as specified above (see section 5.2, from Materials and Methods)

Cell suspensions were analysed with a BD FACSAria™ Fusion as described above. For cell cycle analysis cytometer flow rate never exceed 1.5. ATTO488 emission was assessed using the Blue B (530V) detector. Then, fluorescent emission of Hoescht-33342 in ATTO488- $\alpha$ NRXN1+/- populations was measured at 450/50V.

### 5.4. Cell sorting

Isolation and purification of cell populations of interest was done by fluorescent-activated-cell-sorting (FACS). As general considerations: (1) single cell suspensions were filtered through 70 $\mu$ m mesh filter prior to cell sorting to avoid cytometer clotting and, (2) whenever long sorting times were expected, 10 $\mu$ M Rock Inhibitor (SIGMA-ALDRICH) was added to FACS buffer or collection buffer to block apoptosis. Cell recovery procedure was adjusted to the different experimental purposes as detailed hereafter:

- For subsequent ***in vitro* expansion** of sorted population, up to  $3 \cdot 10^6$  cells were sorted into 15ml-Falcon tube containing 5ml FACS buffer plus 10 $\mu$ M Rock inhibitor. After cell sorting, cells were centrifuged (300g, 5min, 4°C), resuspended and seeded under standard conditions (see 2.2 section, from Materials and Methods).

- For subsequent **tumour spheroid assay** or 2D ELDA growth assay, indicated cell numbers were directly sorted into multi-well dishes containing appropriate growth media (see section 2.6 and 2.7, from Materials and Methods). After cell sorting, plates were directly placed in the incubator.
- For subsequent **in vivo grafting** (both subcutaneous xenograft and CAM assay), indicated cell numbers were sorted into 1.5ml-Eppendorf tube containing 500 $\mu$ l FACS buffer plus 10 $\mu$ M Rock inhibitor. After cell sorting, cells were centrifuged (300g, 5min, 4°C), resuspended in appropriate volume of grafting media and grafted (see sections 6.2 and 6.4, from Materials and Methods).
- For subsequent **RNA extraction by picoprofiling**, up to 2 $\cdot$ 10<sup>3</sup> cells were sorted into 1.5ml-Eppendorf tube containing 45 $\mu$ l lysis buffer 2x. Immediately after cell sorting, tubes were mixed, spun down and incubated for 15min at 60°C to facilitate cell lysis. Then, tubes were frozen in dry ice and store at -80°C (see section 7.1, from Materials and Methods).
- For subsequent **RNA extraction by TriZol™ Reagent**, up to 5 $\cdot$ 10<sup>4</sup> cells were sorted into 1.5ml-Eppendorf tube containing 500 $\mu$ l TriZol™ Reagent. Immediately after cell sorting, tubes were mixed, spun down and incubated for 5min at RT to facilitate cell lysis. Then, tubes were frozen in dry ice and store at -80°C (see section 7.1, from Materials and Methods).

## 5.5. Data analysis

Analysis of flow cytometry files was done using Flow Jo v7.6.5 and FlowJo v10.6.1 (Tree Star, San Carlos, CA, USA). Cell cycle profiles were computed by MultiCycle software (Phoenix Flow Systems, San Diego, CA, USA)

# 6. Animal models

## 6.1. Animal care and ethics permission

In this project two main animal models (chicken embryos and adult mice) were used for different experimental purposes.

Fertilized white **Leghorn chicken** (*Gallus gallus domesticus*) **eggs** were provided by Granja Gibert, Rambla Regueral, S/N, 43850Cambrils, Spain. Eggs were incubated in a humidified atmosphere at 38°C in a Javier Masalles 240N incubator for the appropriate duration and staged according to the method of Hamburger and Hamilton (Hamburger and Hamilton, 1951). Following animal care guide-

lines in Spain, no approval was required to perform the experiments described here. Sex was not identified at these stages.

Two **immunocompromised adult mouse** (*Mus musculus*) strains were purchased from different suppliers (see section 6.3, from Materials and Methods). All mice were housed under a regimen of 12 h light/12 h dark cycles and specific pathogen-free conditions. Unless indicated, sterile dry pellets and water was administered *ad libitum*. Once experimental designs reached end point or when required by ethic reasons, animals were sacrificed by cervical dislocation or CO<sub>2</sub> administration. All procedures were evaluated and approved by the CEEA (Ethical Committee for Animal Experimentation) of the Government of Catalonia (number CEEA-10-225).

### 6.1.1. Surveillance procedure for animal welfare

Mice welfare was supervised twice a week under the following standardised criteria (Table-13):

A) Physical appearance:	0) Normal 1) Coat in poor condition 2) Coat in poor condition (dermatitis, alopecia, itching) 3) Ulcerous dermatitis
B) Weight loss:	0) Normal weight 1) Weight loss under 10% 2) Weight loss between 10% to 15% 3) Weight loss higher than 20%
C) Hydration status:	0) Normal 1) Mild dehydration (5-6%) 2) Moderate dehydration (7-10%), abnormal colour loss from mucous membranes 3) Severe dehydration ( $\geq 10\%$ )
D) Tumour appearance:	0) Normal 3) Ulcerous or necrotic
E) Tumour volume (total tumour volume from the same animal):	0) $\leq 500\text{mm}^3$ 1) $< 1000\text{mm}^3$ 2) $< 1500\text{mm}^3$ 3) $\geq 1500\text{mm}^3$

**Table-13. Standardised criteria for mice welfare surveillance**

General overall score can range from 0 to 15 points. Final mouse score after careful evaluation implies:

- o Low severity:  $< 4$  points
- o Moderate severity:  $\geq 4 \leq 8$  points, implies daily animal surveillance
- o High severity ( $\geq 8$ ) or 3-points at any criteria implies animal euthanasia

### 6.1.2. Mice identification

Ear notches were used as unique identifiers for mice within a cage. An ear punch was used to make ear notches in anesthetized animals.

## 6.2. Chorioallantoic membrane (CAM) assay in chick embryos

The chicken egg has been used to study tumorigenic behaviour of mammalian tumours for more than one century (Rashidi and Sottile, 2009). The implantation of mammalian tumour cells onto chick CAM is used to evaluate the growth and the metastatic seeding properties of the cancer cells. Indeed, this model is considered an efficient *in vivo* system to monitor tumour growth alone or in response to putative therapeutic compounds. The main limitation however is its short length since the experimental window is reduced to 7 days.

In this project the implantation of SK-N-SH cell line onto the CAM was done as detailed hereafter. Eggs were incubated horizontally and after 48h, 3ml of albumin were evacuated from the egg using an 18-gauge syringe. At embryonic day 10 (E10), a small window was created by cutting the egg shell using a sterile scalpel. Then, 10 $\mu$ l single cell suspension was implanted onto the surface of the CAM (one graft per egg) by gently scraping the upper CAM layer at the desired implantation site. Egg windows were sealed with conventional plastic tape and incubated for 7 additional days (until E17). Egg manipulation and cell grafting was performed in a laminar flow cabinet to minimize contamination probability.

For assessment of recombinant proteins effect over tumour growth: parental SK-N-SH cells were plated subconfluently and allow growing. After 96h, cells were trypsinized to single cell suspension (see section 2.2, from Materials and Methods) and resuspended in grafting media-bearing indicated amounts of recombinant proteins or 100 $\mu$ g/ml BSA (for the catalog numbers see Table E-Appendix I). Final cell concentration was set up at 5 $\cdot$ 10<sup>5</sup> cells per 10 $\mu$ l of grafting media. For *in vivo* BrdU-retention assay, SK-N-SH cells growing in cell monolayers were incubated for 24h in the presence of 10 $\mu$ M BrdU (see section 2.5, from Materials and Methods). Then cells were trypsinized and prepared as described above.

Recombinant proteins were resuspended in sterile PBS1x following manufacturer's instructions. Recombinant rat NXPH1 (rNXPH1)(4208-Nx, R&D Systems) contains Ala22-Gly271 immature recombinant NXPH1 (29.4kDa) and Arg107-Gly271 mature recombinant NXPH1 (19 kDa). Recombinant rat  $\alpha$ -NRXN1 (4485-Nx, R&D Systems) contains Leu31-Thr1431 soluble recombinant form of the extracellular domain of rat  $\alpha$ -NRXN1 (165-175 kDa). When used as a recombinant form, the extracellular domain of a transmembrane protein could be used as a decoy. Decoy receptors bind a ligand, prevent-

ing it from binding to its normal receptor. Hence, recombinant rat  $\alpha$ -NRXN1 is a decoy form of full-length  $\alpha$ -NRXN1 that might prevent the binding of extracellular ligands to transmembrane  $\alpha$ -NRXN1. Both recombinant proteins present a 6 His-tag in the C-terminal domain, derived from NS0-mouse myeloma cell line and were purified by HPLC followed by SDS-PAGE.

For *in vivo*  $\alpha$ -NRXN1 depletion CAM assay: alive parental SK-N-SH or  $\alpha$ -NRXN1 depleted pools were sorted (see 5.2 section, from Materials and Methods) and resuspended in grafting media at a final concentration of  $5 \cdot 10^5$  cells per  $10 \mu\text{l}$ .

Tumour collection was done by removing tumours from the CAM using sterile scissors under a stereoscope microscope (LEICA). Tumours were readily weighted, photographed and measured (length, depth, width) using a digital calliper (VWR™, Radnor, PA, USA) Final tumour volume (V) was calculated using the following formula:  $V = (4/3) \cdot \pi \cdot \text{length} \cdot \text{depth} \cdot \text{width}$ . Tumours were then fixed in PFA4% (1h30min, 4°C, agitation) and store in PBS1x waiting for further processing (see section 8, from Materials and Methods).

### 6.3. Mouse strains

Immunocompromised mouse models are the most widely used animal models in oncology research. These models enable long experimental windows, given the option to study tumour progression and response to different experimental settings. Tumour progression could be mimicked through orthotopic or heterotopic xenograft of human cell lines or PDXs into appropriate immunodeficient models. However, the broad variety of genetic backgrounds and the degree of endogenous immune system functionality require a thorough understanding of the available ones. Nevertheless, immunodeficient models disregard the important role of immune system in tumour progression and therapeutic response. This has to be kept in mind when drawing conclusions using these models. In this project, 2 different immunodeficient models were used (Table-14):

Mouse strain		Fur	Immune system status			Source
Common name	Name		T cells	B cells	NK cells	
Athymic nude	Nu/Nu Nude	Hairless, albino background	NO	YES	YES	Envigo
NOD.SCID	NOD.CB17-Prkdc <sup>scid</sup> /NCrHsd	white	NO	NO	ALTERED	Envigo

**Table-14: Immunodeficient mouse models used in this doctoral thesis**

- o Athymic nude mice (Nu/Nu Nude): This model presents a homozygous null mutation in *Foxn1* gene (*Foxn1<sup>nu</sup>*). *Foxn1* encodes a transcription factor required for both hair follicle and thymic development. The *Foxn1<sup>nu</sup>* mutation is commonly known as nude. The mice lack thymus, so they are

unable to produce T cells. However certain extrathymic T cell function is developed with age. They present normal B cells and intact innate immunity: macrophages, NK cells and antigen-presenting cells (APCs). Subcutaneous tumour growth is easily assessed since they are hairless.

Athymic nude mice were used to establish and maintain human NB PDX models by Dr. Ángel M. Carcaboso (IRSJD). This model was purchased from Envigo (Huntingdon, Cambridgeshire, UK).

- o NOD.SCID mice (NOD.CB17-Prkdc<sup>scid</sup>/NCrHsd): This model presents a homozygous *scid* mutation in *Prkdc* gene. *Prkdc* gene encodes the catalytic subunit of a DNA-dependent protein kinase that is required for DNA repair and for sealing the double-stranded DNA breaks that occur during somatic recombination of T cell receptor and immunoglobulin genes. The *scid* mutation in the *Prkdc* gene stands for severe combined immunodeficient. They lack functional T and B cells. Due to the non-obese-diabetic (NOD) background, their innate immunity is impaired although not completely absent. Therefore they support higher levels of engraftment than nude mice. However, they suffer a high incidence of thymic lymphoma, which limits their life span to approximately 30 weeks (Shultz *et al.*, 1995).

NOD.SCID mice were used to compare *in vivo* tumour growth capacity of SK-N-SH cells after conditional knockdown of *NXPH1* or  $\alpha$ -NRXN1 expression. This model was purchased from Envigo.

## 6.4. Heterotopic xenograft in mouse

### 6.4.1. Subcutaneous grafting of human NB-PDX

Human NB-PDX models were established and maintained by Dr. Ángel M. Carcaboso. Experimental manipulation of NB-PDX was conducted in the IRSJD under the supervision of Dr. Ángel M. Carcaboso. For initial engraftment of NB PDX, tumour fragments (25–50 mm<sup>3</sup>) coming from fresh biopsies, were subcutaneously transplanted to the flank of athymic nude mice. Successfully engrafted tumours were expanded as PDXs for 2 generations. Then, small tumour fragments were cryopreserved.

For *in vivo* studies, fragments from cryopreserved or actively growing NB PDXs were engrafted to the flank of as many new athymic mice as required for each experimental designed. Tumour growth was monitored with an electronic calliper once a week. Once, tumours reached exponential growth, they were excised and processed for subsequent experiments. During this doctoral thesis NB PDXs from different passages were used (from 2<sup>nd</sup> to 8<sup>th</sup> passage).

Whenever NB PDX dissociation to single cells was required, tumours were dissociated following recommended protocol from Brain Tumour Dissociation Kit. After red blood cells lysis with home-

made ACK buffer (for the detailed formulation see Table A-Appendix I), single cell suspension was re-suspended at  $10^7$  Cells/ml in FACS buffer plus  $10\mu\text{M}$  Rock inhibitor and used for desired experimental purposes

#### 6.4.2. Subcutaneous grafting of human NB cell lines

Subcutaneous grafting was used to evaluate whether *NXPH1* or  $\alpha$ -NRXN1 expression is required for *in vivo* tumour growth. In order to do so, transgenic SK-N-SH cell sublines carrying a conditional knockdown of *NXPH1* or  $\alpha$ -NRXN1 expression were grafted subcutaneously into NOD.SCID mice. Transgenic SK-N-SH sublines carrying inducible EGFP-miRshCtl (hereafter sh-Ctl), EGFP-miRshNXPH1 (hereafter sh-NXPH1) or EGFP-miRsh $\alpha$ NRXN-1 (hereafter sh- $\alpha$ NRXN1) cassette were generated as described above (see section 4, from Materials and Methods). Prior to *in vivo* grafting, transgene expression in SK-N-SH sublines was induced *in vitro* by treating for 96h with 1mg/ml doxycycline. Then,  $4 \cdot 10^6$  GFP+ cells coming from sh-Ctl, sh-NXPH1 and sh- $\alpha$ NRXN1 were sorted into different tubes. GFP+ sorted pools were spun down (300g, 5min, 4°C) and resuspended in 800 $\mu\text{l}$  grafting media plus  $10\mu\text{M}$  Rock inhibitor. Final cell concentration was  $0.5 \cdot 10^6$  cells per 100 $\mu\text{l}$ . 5 weeks old female NOD.SCID were used as immunodeficient model. To keep transgene activation *in vivo*, dox was administered *ad libitum* in drinking water. Dox solution contained 2mg/ml dox dissolved in 5% sucrose-bearing sterile water. Fresh dox solution was prepared every two days and store in dark feeding bottles to prevent light toxicity. *in vivo* dox administration started 2 days prior to cell implantation.

To facilitate subcutaneous grafting, mice were anesthetized using inhaled anaesthesia (isoflurane) and back fur was shaved using an electric razor. Then, 100 $\mu\text{l}$  cell suspension was grafted subcutaneously using a 0.5ml BD Micro-Fine 29G insulin syringe. Each animal received 2 grafts (on the right and left flanks). Mice were allowed to recover spontaneously from the anaesthesia. Once they could actively move, they were returned to their cage.

Mouse weight and tumour growth was monitored twice a week, until tumour growth was detected. Then tumour volume was measured every two days with a digital calliper. Mice were sacrificed once tumour volume reached ethical permission limit. Tumours were resected, weighted and photographed prior to further processing. Afterwards, tumours were cut in half. One piece was cryopreserved for future analysis. The second piece was readily fixed in PFA4% (4°C, ON) and reserved for histological analysis (see section 8, from Materials and Methods).

## 7. Analysis of gene expression

### 7.1. RNA extraction

Total RNA from NB cell lines or xenografts was extracted with TRIzol™ Reagent following manufacturer's recommended protocol. Briefly, 500µl TRIzol was added to each tube and sample was homogenized by pipetting up and down. After 5min incubation (RT), 100µl chloroform was added to each tube and mixed using vortex (15 seconds). Samples were then incubated 15min (RT) and phase separation was done by centrifugation (12,000g, 15min, 4°C). The mixture separates into a lower red phenol-chloroform phase (that retains the DNA), interphase (that retains the proteins) and a colourless upper aqueous phase (that retains the RNA). Therefore, aqueous phase was recovered into a clean Eppendorf tube. For RNA precipitation, 250µl isopropanol was added to the aqueous phase, incubated for 10min (RT) and allowed to precipitate by ON incubation (-20°C). Then, tubes were centrifuged (12,000g, 8min, 4°C). For the final washing step, SN was removed and RNA pellets were washed with 1ml 75% ethanol by brief vortex and centrifugation (7,500g, 8min, 4°C). RNA pellets were air dry for 5-10min and resuspended in 20-50µl pre-warmed RNase-free water. For complete resuspension, tubes were finally incubated 10min at 55°C.

Genomic DNA traces were removed with AMBION® DNA-free™ DNase Treatment and Removal Reagents, following manufacturer's instructions for routine DNase treatment. Briefly, a master mix containing, 0.1 vol of 10x DNase I Buffer and 1µl DNase I per RNA sample, was prepared and mixed. Each RNA tube received 0.12 vol of the master mix. Tubes were incubated for 25min (37°C). DNase I was removed from the samples using 0.1 vol DNase Inactivation Reagent and incubating 2min (RT). A final centrifugation (10,000g, 1.5min, RT) allowed the recovery of DNA-free RNA samples to a fresh tube. RNA tubes were kept in ice from now on or were store at -80°C.

When the starting sample was small (0.2-0.5·10<sup>6</sup> cells), 2µl Pellet Paint Co-precipitant was added to each tube after homogenization in TRIzol™ Reagent. Pellet Paint Co-precipitant works as a carrier for the precipitation of nucleic acids, increasing RNA yield and facilitating RNA pellet detection thanks to its pink colour.

For RNA extraction from α-NRXN1 populations purified by cell sorting, 1·10<sup>3</sup> to 2·10<sup>3</sup> cells were recovered per each experimental condition (see sections 5.2 and 5.5, from Materials and Methods). RNA extraction and retrotranscription was done by the Functional Genomics Unit of the IRB according to in-house protocol (Gonzalez-Roca *et al.*, 2010).

## 7.2. Synthesis of complementary DNA: Reverse-Transcription Polymerase Chain Reaction (RT-PCR)

DNA-free RNA was used to synthesize its copy DNA (cDNA) by retrotranscription reaction. Equal amounts of DNA-free RNA were used in each experiment to allow gene expression comparison among different samples. RNA was quantified by measuring sample absorbance at 260nm using NanoDrop™1000 Spectrophotometer (ThermoFisher SCIENTIFIC).

Between 300ng to 1.5µg of DNA-free RNA was used to synthesize copy DNA (cDNA) using High-Capacity cDNA Reverse Transcription Kit according to manufacturer's instructions. Briefly, up to 10µl DNA-free RNA were retrotranscribed using random primers. A master mix was prepared containing 0.1 vol 10x RT reaction buffer, 0.1 vol 10x RT random primers, 4mM dNTPs mix, 1U RNase Inhibitor, 0.05 vol MultiScribe RT and up to 10µl nuclease-free water. Final volume was 20µl containing 10 µl master mix and up to 10µl of RNA. Retrotranscription was performed using a Thermal cycler (Eppendorf, Hamburg, Germany) programmed for: 10min at 25°C, 120min at 37°C and 5min at 85°C. Once retrotranscription finished, 20µl nuclease-free water were added to each tube (final cDNA stock volume: 40µl) and samples were stored at -20°C.

## 7.3. Relative quantification of cDNA: Real-Time Quantitative Polymerase Chain Reaction

The Real-Time Quantitative Polymerase Chain Reaction (RT-qPCR) is a relative quantification technique that allows quantification of cDNA levels of genes of interest relative to cDNA levels of housekeeping (HK) control genes. HK genes are those genes that codify for proteins that participate in basic cellular processes, therefore mRNA levels of HK genes are expected to be similar among different samples. Genes used as HK controls have to be adapted to every experimental field, since key cellular processes could vary among different cell types, tissues or organisms. In this project *18SrRNA* or *TATA-binding-protein (TBP)* genes were used as HK control genes for the different experiments. Relative cDNA levels were calculated using the efficiency-corrected  $\Delta C_t$  method, which compares values of genes of interest to that of housekeeping genes, on corresponding cDNA (Bookout *et al.*, 2006). Unless indicated, primers were design using UCSC Genome browser server and Primer3Plus online software.

RT-qPCR was done using SYBR Green 2x and a Roche Lightcycler®480 Real-Time PCR System (Roche) with a 96-wells plate format. For every gene of interest, a standard dilution curve was prepared to allow estimation of reaction efficiency. In addition, samples were loaded in duplicates. Each well contained a final volume of 10µl: 0.5vol SYBR Green2x, 0.1vol forward and reverse primer mix (6µM)

(qPCR primer sequences are detailed in Table C-Appendix I), 2µl nuclease-free water and 2µl cDNA (dilution 1:3 to 1:9 for the cDNA stock). Once 96-wells PCR plates were loaded with reaction volumes of housekeeping genes and genes of interest, plates were taken to Lightcycler®480. Lightcycler® 480 was previously programmed for 5min at 95°C, followed by 40 cycles of 15sec at 95°C plus a final minute at 60°C. Once reaction finished, Ct values were exported and analysed using Microsoft® Office Excel, as specified above.

## 8. Histology and immunofluorescence

In this project fluorescent microscopy and fluorescent confocal microscopy were used to evaluate and quantify various cellular parameters such as cell proliferation, apoptosis or expression of different markers of interest. SK-N-SH cells growing *in vitro* or as a xenograft were processed and analysed by microscopy as detailed below:

### 8.1. Cell and tissue processing

Whenever cell lines growing *in vitro* were subjected to immunostaining, cells were cultured on 8 well Permanox® Nunc® Lab-Teck® chamber slide™ system. Around  $2 \cdot 10^4$  cells were seeded per well, conditions were seeded at least in duplicates. At desired time points, cells were washed with PBS1X, fixed PFA4% for 15 min (RT) and subsequently used for immunostaining.

For histological analysis of CAM or xenograft NB tumours, tumours were harvested and fixed in PFA4%, 1.5-3h, RT (see section 6, from Materials and Methods). Tumours were then washed in PBS1x and prepared for cryosection. To avoid tissue damage while freezing, tumours were consecutively submerged into 15% sucrose and 30% sucrose PBS1x solutions and incubated at 4°C with constant oscillation. Sinking into the bottom of the tube denoted that sucrose had efficiently penetrated into the whole tissue. Then, small cubical tumour pieces (5mm·5mm·5 mm approx.), were embedded in Tissue-tek® optimum cutting temperature (OCT) and frozen in dry ice. Tumour pieces were sectioned on a cryostat (Leica). Tumour sections (16µm) were recovered in home-made TESPA pre-coated slides and distributed serially. Tumour slides were stored at -20°C.

## 8.2. Immunofluorescence staining

Fixed samples were used for immunofluorescence staining following standard protocol:

Samples were permeabilized with 0.1% Triton-PBS1x (0.1% PBT) for 15 minutes. The unspecific staining was blocked for 30 min with blocking buffer. Primary antibodies were incubated ON at 4°C and fluorescence-conjugated secondary antibodies were incubated for 2 hours at room temperature. Sections were finally stained with 1 µg/ml DAPI and mounted in home-made Mowiol.

For BrdU immunostaining, after cell fixation and permeabilization, samples were balanced with Milli-Q® H<sub>2</sub>O and washed with DNase buffer before addition of 5U/ml DNase I type II prepared in DNase buffer. Following 15min incubation at RT, DNase was removed and samples were washed twice with 0.5% bovine serum albumin (BSA) (SIGMA-ALDRICH)-PBS1x solution. Immunofluorescence staining continued from the blockade step as described above.

## 8.3. Image acquisition and processing

Optical sections of fixed NB CAM or xenograft tumours were acquired at RT with two different confocal microscopes:

- with the Leica LAS software, in a **Leica TCS SP5 confocal microscope** using 20x (dry/HC PL APO 20x/0.70 CS ∞/0.17/C) or 40x (oil /HCX PL APO 40X/1.25-0.75 OIL CS ∞/0.17/D) objective lenses
- with LSM Software ZEN 2.1, in a **ZEISS Lsm780 confocal microscope** using 25x (oil,w,Glic, NA 0.8, Plan-Apochromat/ImmKorr) or 40x (oil/NA 1.3/Plan-Apochromat/(UV)VIS-IR).

To image whole sections of CAM NB tumours, large images were acquired as tile scans using the motorized XY stage. Tiles were directly stitched into a single mosaic by the microscope software. Maximal projections obtained from 3µm Z-stack images were processed in ImageJ for image merging, resizing and cell counting. Cell counting in NB CAM or xenograft tumours was performed in a minimum of 3 sections per tumour.

NB cell lines immunofluorescence were image with a Leica LAS\_X (2016) software, in an **Automated Inverted Leica AF7000 wide-field microscope** using 20x (Dry/NA 0.5/HC PL APO/0.70 CS ∞/0.17/C) or 40x (oil/NA 1.25-0.75/HCX PL APO Lbd Blue ∞/0.17/D). Cell counting was done in at least 4 independent images per well.

## 9. Statistical analysis

No statistical methods were used to predetermine sample size. The experiments were not randomized. I was not blinded to allocation during experiments and outcome assessment. Unless indicated otherwise, all *in vitro* experiments were repeated at least three times independently. In the case of *in vivo* experiments, n values correspond to different tumours or animals. Statistical analyses were performed using the GraphPad Prism 8 software (GraphPad Software, Inc.). The normal distribution of the values was assessed by the Shapiro-Wilk normality test.

To compare differences in a variable between two experimental conditions significance was assessed with a two sided unpaired t-test for data presenting normal distribution or alternatively with the non-parametric Mann-Whitney test.

To compare differences in a variable among 3 or more experimental conditions significance was assessed with parametric one-way ANOVA +Tukey's test or non-parametric Kruskal-Wallis test + Dunn's test for multiple comparison analysis.

To compare differences in a variable along time, among 2 or more experimental conditions, significance was assessed with parametric two-way ANOVA + Sidak's, Dunnet's or Tukey's test.

For correlation analysis between 2 independent variables, the non-parametric Spearman r correlation coefficient was calculated.

For survival analysis of mouse xenograft experiments, Kaplan-Meier method was used to create survival curves from raw data, and statistically significant differences among survival curves were assessed using the logrank test

The following convention was used: n.s, non-significant; \*P<0.05, \*\*P<0.01, \*\*\*P<0.001. The detailed information related to quantifications is included in the figure legends.



## IV. RESULTS

---



## 1. Identification of a genetic signature common to NCCs and NB malignancy

### 1.1. A double genetic screening identifies 6 genes that are both differentially expressed in clinically-relevant subgroups of NB patients and enriched in the early NCC lineage

To identify the genes enriched in the neural crest cell lineage that might play a crucial role in NB formation or malignancy, we combined two complementary genome-wide transcriptomic studies. A first study, conducted by our collaborator Dr Cinzia Lavarino (Institut de Recerca Sant Joan de Dèu, Hospital Sant Joan de Dèu, HSJD, Barcelona, Spain), was set to identify the DEGs between clinically and biologically relevant subgroups of NB patients. This transcriptomic analysis was done using pre-treatment primary tumour samples from a cohort of 19 NB patients diagnosed and monitored at HSJD (from now on, HSJD-19 dataset/cohort), using Affymetrix Human genome U219 microarray plates and applying a processing adapted from computational methods/target prediction algorithms (Gautier *et al.*, 2004; Gomez *et al.*, 2015; Kulis *et al.*, 2012). Supervised pair-wise comparisons were performed between: 1) Low Risk (LR, stages 1/2/3/4s without *MYCN* amplification) vs High Risk (HR, stage 4 and non-stage 4 with *MYCN* amplification), 2) *MYCN* non-amplified (*MYCN*-NA) vs *MYCN* amplified (*MYCN*-A) and 3) Loco-regional (LcR, corresponding to the INSS stages 1/2/3/4s) vs Metastatic (Met, stage 4) NB tumour samples. These three comparisons identified respectively 54, 238 and 235 differentially expressed probes out of 46,498, above the threshold criteria ( $FC > 2.0$ ,  $p_{Adj} \leq 0.01$ , Figure 16A), which represented 0.12%, 0.51% and 0.51% of the total number of probes present in the U219 microarray plate, respectively (Gomez *et al.*, 2015). This analysis thereby identified novel candidate genes potentially relevant to NB malignancy (Gomez *et al.*, 2015).

We wished to identify among these candidate genes the ones that might play a more specific role in regulating NB stemness potential and/or whose expression might be correlated to the presence of putative NB cancer stem cells (NBcsc). To this aim, we took advantage of a second genome-wide transcriptomic analysis previously done in our group and which identified the genetic signature of pre-migratory and early migratory chick NCCs (Figure 16B). This lineage-tracing was performed by electroporating *in ovo* the neural tube of HH10 chicken embryos with a fluorescent reporter (BRE-tk-EGFP) of the canonical BMP pathway, whose activity specifically identifies cells of the NCC lineage and of the most dorsal part of the developing NT during the early stages of neural patterning and NCCs specification (see Materials and Methods section 1.1.2) (Ferronha *et al.*, 2013; Le Dreau *et al.*, 2012; Rabadan *et al.*, 2013). The genome-wide transcriptomic profile of BRE-tk-EGFP<sup>+</sup>;H2B-RFP<sup>+</sup> pre-migratory and early migratory NCCs was compared to the profile of BRE-tk-EGFP<sup>+</sup>;H2B-RFP<sup>+</sup> neuroepi-

thelial progenitor cells. This analysis identified a set of 413 genes above the threshold criteria ( $FC > 1.5$ ,  $p < 0.05$ ), whose expression is enriched or repressed in pre-migratory and early migratory chick NCCs as compared to spinal progenitors (Figure 16B) (Ferronha *et al.*, 2013; Rabadan *et al.*, 2013). The proteins encoded by these genes are thus likely to play a role in NCC formation, possibly in the acquisition of the migratory and/or multipotent lineage potential of these embryonic stem cells from which NBs originate.

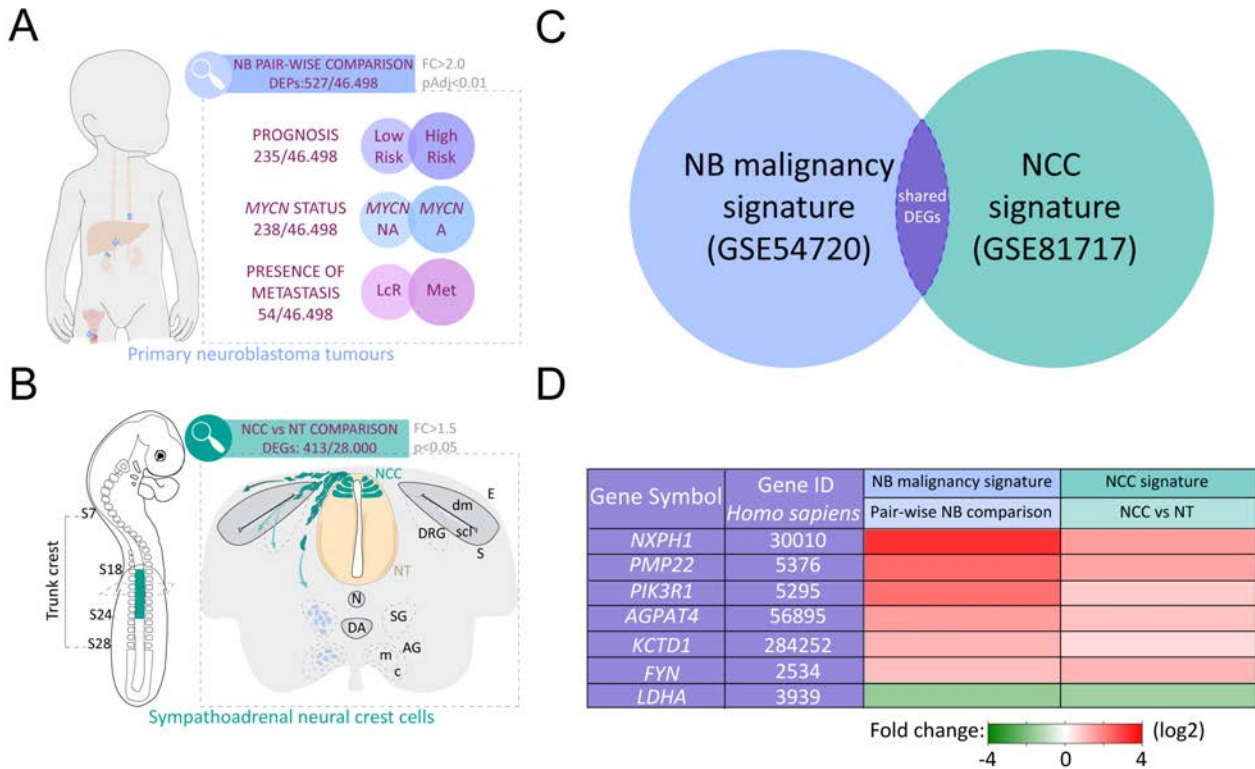


**Figure-16. Double genetic screening identifies 7 differentially expressed genes shared between the HSJD-19 neuroblastoma cohort and early neural crest lineage**

(A) Methodology used to identify genes differentially expressed in clinically relevant NB subgroups. A supervised pair-wise comparison was done to find genes that might be implicated in NB malignancy [Risk groups: low risk vs high risk; MYCN status: MYCN non-amplified (NA) vs MYCN A (amplified), and presence of metastasis: loco-regional (LcR) vs metastatic tumours (Met)]. (B) Methodology used to identify genes differentially expressed by early NCCs. The transcriptome of early migratory and pre-migratory NCCs (green) was compared to that of neuroepithelial cells (yellow) in early stage chicken embryos. (C) The comparison of NB and NCC screenings identifies common genes (shown in purple) that are both differentially expressed in the HSJD-19 NB cohort (GSE4720, shown in blue) and in early neural crest cells (GSE81717, shown in green). (D) The heatmap shows fold-changes of each candidate gene in the two genome-wide transcriptomic analyses. For the DEGs retrieve in more than 1 NB comparison, the highest fold change is depicted in the heatmap. A: amplified; AG: adrenal gland; c: cortex; Ct: C terminal; DA: dorsal aorta; DEPs: differentially expressed probes; DEGs: differentially expressed genes; dm: dermomyotome; DRG: dorsal root ganglia; E: epidermis; LcR: loco-regional; m: medulla; Met: metastatic; N: notochord; NA: non-amplified; NCC: neural crest cells; NT: neural tube; S: somite; scl: sclerotome; SG: sympathetic ganglia.

Comparing the genetic signatures of these two independent genome-wide transcriptomic studies identified 6 genes that are both differentially expressed between clinically-relevant NB subgroups and enriched in early NCCs (neurexophilin 1, *NXP1*; peripheral myelin protein 22 *PMP22*; phosphoinosit-

ide-3-kinase regulatory subunit 1, *PIK3R1*; 1-acylglycerol-3-phosphate O-acyltransferase 4, *AGPAT4*; potassium channel tetramerization domain containing 1, *KCTD1* and *FYN* proto-oncogen, Src family tyrosine kinase, *FYN*; Figure 16C,D). A seventh gene (lactate dehydrogenase A, *LDHA*) was retrieved due to its repressed expression in early NCCs and was thus ruled out for further studies (Figure 16D). These 6 candidate genes code for a secreted protein (*NXPH1*), a transmembrane protein (*PMP22*), a kinase protein and a kinase regulatory subunit (*FYN* and *PIK3R1* respectively), an enzyme of lipid metabolism (*AGPAT4*) and a transcription factor (*KCTD1*). To date, most of these candidate genes have not been firmly associated to NB specifically nor to cancer biology in general, except the kinase *FYN* and the kinase regulatory subunit *PIK3R1* (Berwanger *et al.*, 2002; Fransson *et al.*, 2013; Gururajan *et al.*, 2015; Lu *et al.*, 2009; Posadas *et al.*, 2009; Ross *et al.*, 2013; Urick *et al.*, 2011).

*NXPH1* was the sole candidate gene that passed the restrictive threshold criteria ( $FC > 2$ ,  $pAdj < 0.01$ ) in 2 out of the 3 different comparisons between clinically-relevant NB subgroups ( $FC$ : 7.3 in LR vs HR and 9.4 in *MCYN*-NA vs *MCYN*-A and  $pAdj < 0.01$ ; Figure 17A). Interestingly, *NXPH1* came out differentially expressed ( $FC > 2$ ,  $pAdj < 0.05$ ) in the 3 different comparisons (Figure 17A). The other 5 candidates were only retrieved by the LR vs HR comparison (*PMP22*  $FC$ : 4.88, *PIK3R1*  $FC$ : 3.64, *AGPAT4*  $FC$  2.93, *KCTD1*  $FC$ : 2.48, *FYN*  $FC$  2.24 and  $pAdj < 0.01$ ; Figure 17B-F). For these 5 genes, significant differences ( $FC > 2$ ,  $pAdj < 0.05$ ) only appeared in 2 of the 3 comparisons. *PMP22* was found differentially expressed between *MYCN* NA vs A subgroups ( $FC$ : 5.57,  $pAdj > 0.05$ ; Figure 17B). The 4 others came out in the LcR vs Met comparison (*PIK3R1*  $FC$ : 2.96, *AGPAT4*  $FC$ : 2.95, *KCTD1*  $FC$ : 2.34 and *FYN*  $FC$ : 2.10 and  $pAdj < 0.05$ ; Figure 17C-F). Surprisingly, the results obtained using the HSDJ-19 cohort dataset revealed that the expression of all our 6 candidate genes is inversely correlated to NB malignancy.

To confirm this correlation, I took advantage of the R2 Genomic analysis and visualization platform, a web-based server that allows analyses across various publically available datasets of different types of cancer, including NB (R2-server, 2019). Among the different NB datasets proposed in the platform, we chose the Kocak-649 dataset since it accounts for the largest cohort and contains specific probes for all the genes retrieved by our double screening. For each of our candidate genes, we analysed the EFS probability after dividing the patient samples based on their expression level of a defined gene (Figure 18). These Kaplan-Meier analyses revealed that the expression of all our candidate genes is prognostic for NB EFS progression. For each of these 6 candidate genes, the EFS probability is remarkably higher for the group of patients that presents a higher expression level compared to the one presenting a lower expression level (5-year EFS for high vs low expression for *NXPH1*: 0.9 vs 0.45,  $p = 1.5 \cdot 10^{-16}$ ; for *PMP22*: 0.9 vs 0.45,  $p = 1.5 \cdot 10^{-18}$ ; for *PI3KR1* 0.85 vs 0.5;  $p = 3.0 \cdot 10^{-14}$ ; for *AGPAT4*: 0.85 vs 0.45,  $p = 1.2 \cdot 10^{-14}$ ; for *KCTD1*: 0.8 vs 0.55,  $p = 1.1 \cdot 10^{-5}$ ; for *FYN*: 0.85 vs 0.5,  $p = 7.4 \cdot 10^{-12}$ , Figure 18A-F). A similar correlation was established using *CHD5* as a discriminating gene (5-year EFS for high vs low expression: 0.85 vs 0.45,  $p = 2.7 \cdot 10^{-16}$ ; Figure 18G). *CHD5* is a marker of good NB prognosis which

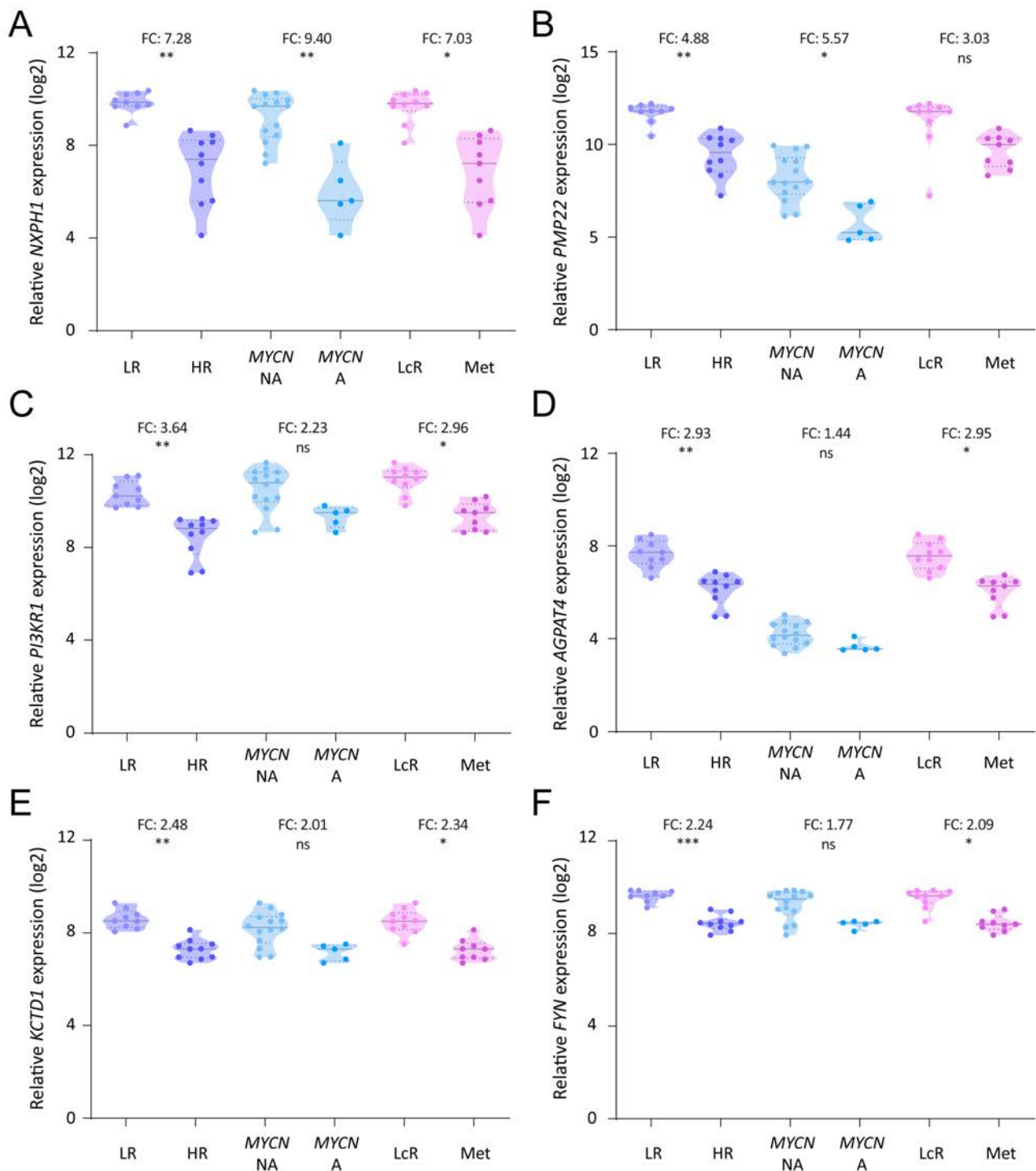


**Figure-17. The expression of NB/NCC double-screening genes correlates with favourable NB prognosis in HSJD-19 cohort**

(A-F) Violin plots showing *NXPH1* (A), *PMP22* (B), *PI3KR1* (C), *AGPAT4* (D), *KCTD1* (E) and *FYN* (F) expression levels in clinically-relevant NB subgroups of HSJD-19 cohort. Significance was assessed with the parametric T-test during microarray data processing. \*pAdj<0.05, \*\*pAdj<0.01, \*\*\*pAdj>0.001. HR: High Risk; INSS: international neuroblastoma Staging System; LcR: Loco-regional tumours; Met: Metastatic tumours; LR: Low Risk; *MYCN* A: *MYCN* amplified; *MYCN* NA: *MYCN* non-amplified; pAdj: p-value adjusted for multiple testing.

forms together with *PAFAH1B1* and *NME1* a 3-gene predictor model used for clinical NB risk stratification (Garcia *et al.*, 2012). Therefore, the Kaplan-Meier analysis conducted with the Kocak-649 dataset confirmed the strong and positive correlation between the expression levels of our 6 candidate genes and NB patient's outcome.

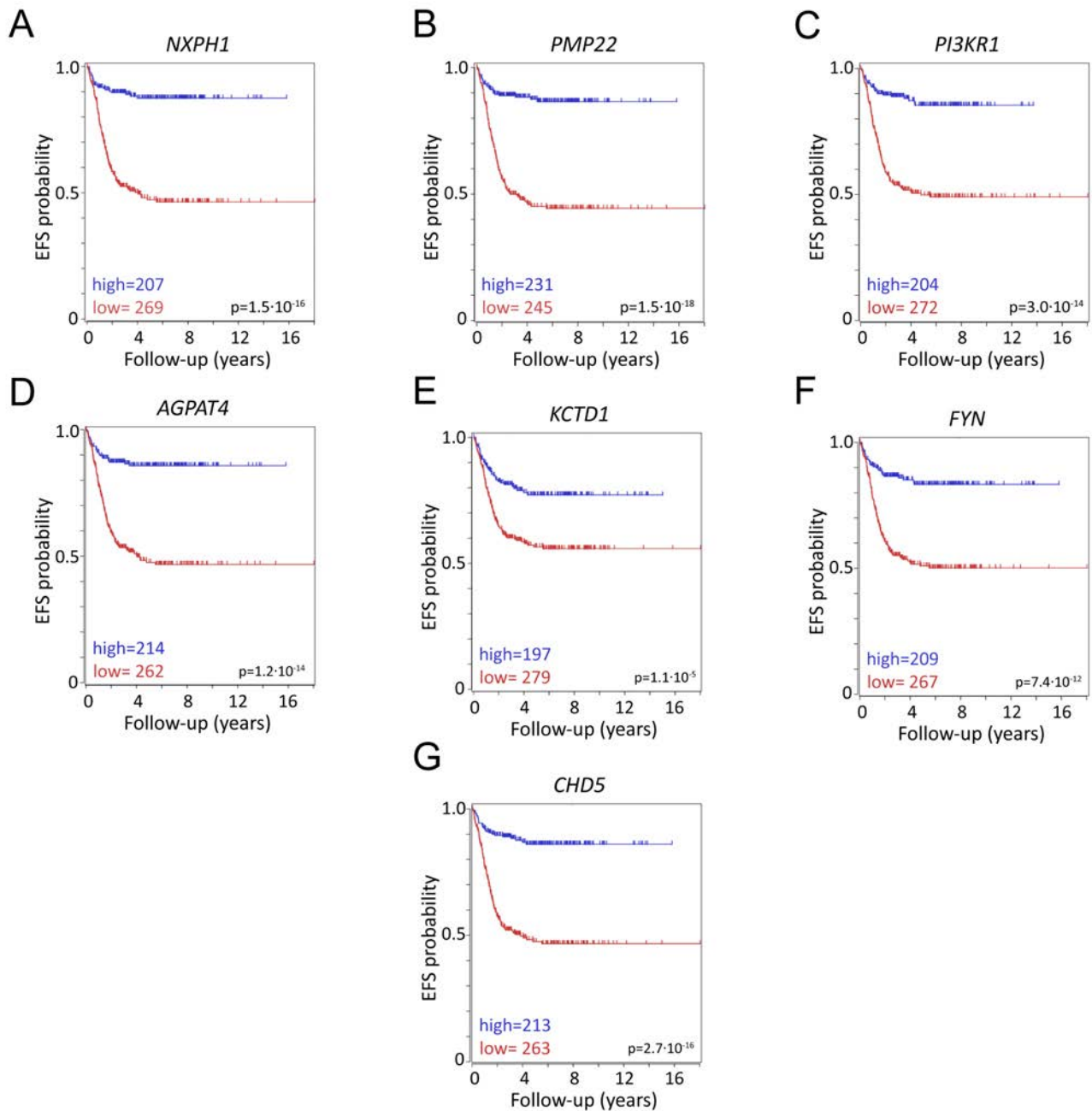


**Figure-18. The expression of NB/NCC double-screening genes correlates with NB event free survival in Kocak-649 cohort**

(A) Kaplan-Meier event free survival analysis of *NXPH1* (A), *PMP22* (B), *PI3KR1* (C), *AGPAT4* (D), *KCTD1* (E), *FYN* (F), and *CHD5* (G) in Kocak-649 NB dataset. Mean gene expression was used to group Kocak-649 cohort and statistical significance of survival analysis was automatically assessed by R2-server using logrank test. EFS: event-free survival.

## 1.2. Selection of *NXPH1* as a candidate gene for further studies

We decided to continue this work by focusing on the putative role of *NXPH1* in regulating NB stemness potential and malignancy. Among our 7 candidate genes *NXPH1* was selected for the following reasons:

1- *NXPH1* is the only candidate gene that came out differentially expressed in the 3 comparisons between clinically-relevant NB subgroups (Figure 16D and Figure 17A).

2- *NXPH1* is also the candidate gene that presented the highest enrichment in the NCC signature (FC: 2.9 in “NCC vs non-NCC”, Figure 16D).

3- *NXPH1* codes for an extracellular ligand, whose activity might be easily modulated pharmacologically (Missler and Sudhof, 1998; Petrenko *et al.*, 1996).

4- *NXPH1* is known to bind specifically to a single family of receptors, the  $\alpha$ -neurexins ( $\alpha$ -NRXNs) (Missler *et al.*, 1998; Petrenko *et al.*, 1996).

5- *NXPH1* acts as a potent inhibitor of the proliferation of hematopoietic progenitor cells by binding to  $\alpha$ -NRXN1 (Kinzfogel *et al.*, 2011).

6- The putative roles of *NXPH1* and of its receptors  $\alpha$ -NRXNs in NB malignancy have never been reported so far.

## 1.3. The *NXPH1* receptors $\alpha$ -NRXN1 /2 show minimal differences between clinically-relevant subgroups of NB patients

Based on the literature, a putative role of *NXPH1* in regulating NB stemness potential and malignancy would be mediated by its receptors of the  $\alpha$ -NRXNs family (Missler *et al.*, 1998; Petrenko *et al.*, 1996; Reissner *et al.*, 2014). We thus assessed the expression of the 3  $\alpha$ -NRXN receptors in datasets of NB patient samples. The 3 human *NRXN* genes present at least 3 different promoters and are subjected to extensive alternative splicing, encoding multiple variants (for further details see section 4.2 from Introduction). Unfortunately, there were no specific  $\alpha$ -NRXNs probes in the Affymetrix U219 microarray used to analyse the transcriptomic profiles of the HSJD-19 cohort, nor in the Kocak-649 dataset used previously. Therefore, we searched within the R2 platform the NB datasets containing specific probes against  $\alpha$ -NRXNs. Probes specific for  $\alpha$ -NRXN1 and  $\alpha$ -NRXN3 were found in the Jagannathan-100 dataset, while probes specific for  $\alpha$ -NRXN2 were found in the datasets TARGET-161 and Khan-47 (Figure 19A). As done previously, the data were categorized according to risk prognosis (LR vs HR), *MYCN* status (*MYCN*-NA vs A) or the INSS stage (INSS1 vs INSS 4). The expression of  $\alpha$ -NRXN1

came out different in each of these 3 comparisons (FC: 1.19,  $p < 0.05$  in LR vs HR; FC: 1.27,  $p < 0.001$  in MYCN-NA vs A; FC: 1.22,  $p < 0.05$  in INSS 1 vs INSS 4; Figure 19B). Similarly,  $\alpha$ -NRXN2 came out differentially expressed in the two comparisons available (FC: 1.49,  $p < 0.01$  in MYCN-NA vs A; and FC: 1.39,  $p < 0.05$  in INSS1 vs INSS4; Figure 19C). By contrast, no significant difference was found for  $\alpha$ -NRXN3 expression in any of the 3 clinically-relevant categories in the Jagannathan-100 dataset (Figure 19D).

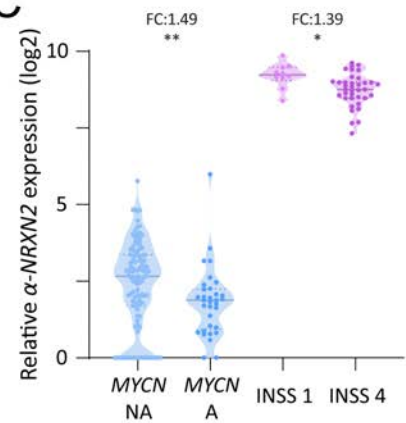
However, none of the probes for  $\alpha$ -NRXN1/2 reached the cut-off threshold for our NB screening (FC>2,  $p > 0.01$ ) and the differences were considered consistent but marginal. Unfortunately, none of the datasets interrogated for  $\alpha$ -NRXN1-3 expression allowed for the analysis of the event-free survival probability.

Altogether these results suggest that NXPH1 might play a role in regulating NB malignancy.

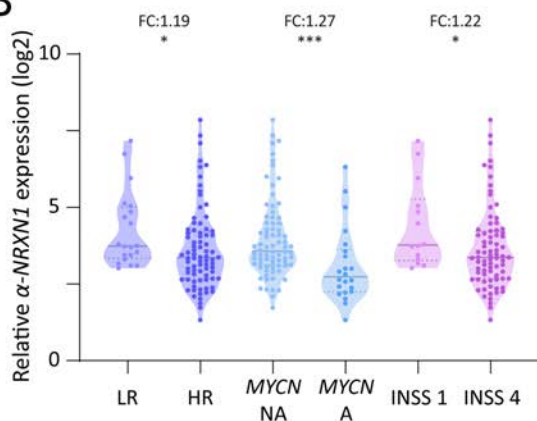
A

NRXN gene	Common name	GEO ID	Probe ID
$\alpha$ -NRXN1	Jagannathan dataset	GSE19274	ILMN1673152
$\alpha$ -NRXN2	Khan dataset	Not available	3376944
	TARGET dataset	Not available	ENST486057
$\alpha$ -NRXN3	Jagannathan dataset	GSE19274	ILMN1700657

C



B



D

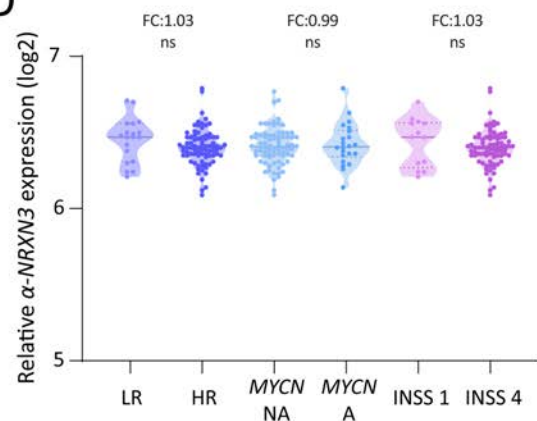


**Figure-19. The changes in the relative expression of  $\alpha$ -NRXN1/2 receptors between NB subgroups do not exceed the threshold**

(A) Public NB datasets and specific probes used to perform  $\alpha$ -NRXNs expression analysis in clinically-relevant NB subgroups using R2 platform. (B) Violin plot showing  $\alpha$ -NRXN1 expression in clinically-relevant NB subgroups from Jagannathan-100 dataset. (C) Violin plot showing  $\alpha$ -NRXN2 expression in clinically-relevant NB subgroups from TARGET-161 dataset (MYCN status comparison) and Khan-47 dataset (INSS comparison). (D) Violin plot showing  $\alpha$ -NRXN3 expression in clinically-relevant NB subgroups from Jagannathan-100 dataset. Significance was assessed with the non-parametric Mann-Whitney test (B, C MYCN status comparison and D risk groups and INSS comparison) or with the parametric unpaired T-test (C INSS comparison and D MYCN status). \* $p < 0.05$ , \*\* $p < 0.01$ , \*\*\* $p > 0.001$ . HR: High Risk; INSS: international neuroblastoma Staging System; LR: Low Risk; MYCN A: MYCN amplified; MYCN NA: MYCN non-amplified.

## 2. The expression of *NXPH1* and its receptors $\alpha$ -*NRXN1/2* positively correlates with NB stemness *in vitro*

To test whether *NXPH1*/ $\alpha$ -*NRXN* signalling plays a role in NB malignancy, we first analysed the expression of *NXPH1* and of its receptors  $\alpha$ -*NRXN1/2/3* in a panel of 10 human NB cell lines. We selected established and commonly used human NB cell lines that present different molecular and morphological signatures defined as mixed (M-type: SK-N-SH, SK-N-Be(2)C and IMR-32), neuronal (N-type: LAN-1, IMR-5 and SH-SY5Y), intermediate (I-type: SK-N-JD and SK-N-LP) or stromal (S-type: SK-N-AS and LA1-5s) phenotypes (Figure 20A and (Thiele, 1998)). These cell lines also present distinct profiles of genetic alterations with demonstrated clinical implications in NB oncogenesis, including *MYCN* amplification and/or the activating F1174L *ALK* mutation (Figure 20A and (Boeva *et al.*, 2017; Cellosaurus, 2019; Thiele, 1998)). 7 of these cell lines present a *MYCN* amplification (SK-N-Be(2)c, IMR-32, LAN-1, IMR-5, SK-N-JD, SK-N-LP and, LA1-5s), while the activating F1174L *ALK* mutation has been reported for 4 of them (SK-N-SH, LAN-1, SH-SY5Y and, LA1-5s) (Boeva *et al.*, 2017; Cellosaurus, 2019; Thiele, 1998)). Our panel of NB cell lines thereby contains all possible combinations of *MYCN* amplification and *ALK* mutation status (Figure 20A).

In basal culture conditions, the mRNA expression levels of *NXPH1* and  $\alpha$ -*NRXN1/2* in our panel of human NB cell lines were overall low, while the levels of  $\alpha$ -*NRXN3* transcripts were below the detection threshold (Figure 20A). A Z-score analysis of *NXPH1* and  $\alpha$ -*NRXN1/2* expression highlighted the cell lines with relatively higher or lower expression levels compared to the average expression in the panel (Figure 20A). No obvious correlation was observed between the expression levels of *NXPH1* and its receptors. The highest relative expression levels of *NXPH1*,  $\alpha$ -*NRXN1* and  $\alpha$ -*NRXN2* were respectively detected in the IMR-32 and SK-N-Be(2)c (z-score= 1.84 and 1.46), SK-N-JD and IMR-32 (z-score= 1.29 and 1.28), and LA1-5s and SK-N-JD cell lines (z-score= 1.59 and, 1.25; Figure 20A). The lowest relative expression levels of *NXPH1*,  $\alpha$ -*NRXN1* and  $\alpha$ -*NRXN2* were respectively detected in the LA1-5s and SK-N-LP (z-score=-3.02 and -3.01), SK-N-AS and SH-SY5Y (z-score=-2.39 and -2.11) and SK-N-LP and SK-N-Be(2)c cell lines (z-score=-2.33 and -1.92; Figure 20A). To assess whether the relative expression levels of *NXPH1* and  $\alpha$ -*NRXN1/2* could be related to a particular NB subtype, the NB cell lines were categorized by phenotypic subgroups (M, N, I or S-type) and the average expression levels of *NXPH1* or  $\alpha$ -*NRXN1/2* compared between the four different NB subtypes. However, no obvious correlation was either observed between the expression levels of *NXPH1* or  $\alpha$ -*NRXN1/2* and the morphological NB phenotype (Figure 20B). No clear correlation was either observed between the expression levels of *NXPH1* and *MYCN* (Spearman r: 0.539, p=0.1139; Figure 20C), nor between the expression of *NXPH1* and *ALK* (Figure 20D). Thus, we did not find any obvious correlation associating the expression of *NXPH1* or that of its receptors  $\alpha$ -*NRXN1/2* with the morphological and genetic features of these

human NB cell lines in basal culture conditions.

A

NB cell Lines				Endogenous mRNA levels [Z-score (log2)]			
Name	subtype	MYCN status	ALK status	<i>NXPH1</i>	$\alpha$ - <i>NRXN1</i>	$\alpha$ - <i>NRXN2</i>	$\alpha$ - <i>NRXN3</i>
SK-N-SH	M	NA	F1174L	Green	Green	Green	Grey
SK-N-Be(2)c	M	A	WT	Red	White	Green	Grey
IMR-32	M	A	WT	Red	Red	White	Grey
LAN-1	N	A	F1174L	Green	Green	Red	Grey
IMR-5	N	A	WT	Green	Green	Green	Grey
SH-SY5Y	N	NA	F1174L	Green	Green	Green	Grey
SK-N-AS	S	NA	WT	Green	Green	Green	Grey
SK-N-JD	I	A	n.d.	Green	Red	Red	Grey
SK-N-LP	I	A	n.d.	Dark Green	Green	Green	Grey
LA1-5s	S	A	F1174L	Dark Green	Red	Red	Grey

Z-score: (log2)    Grey not detected

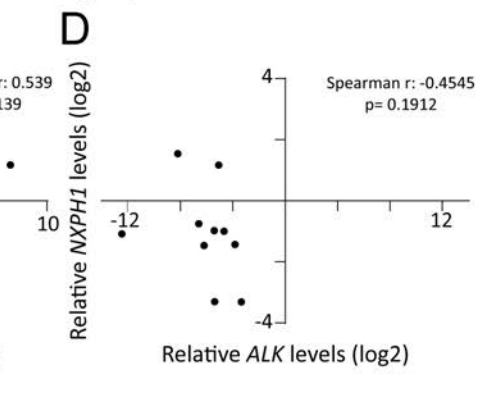
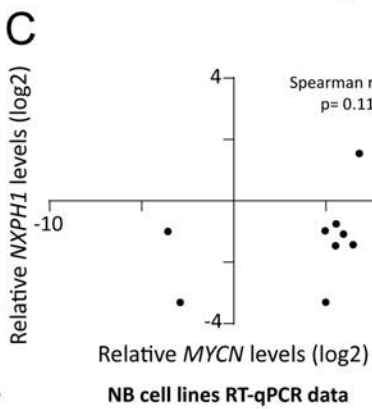
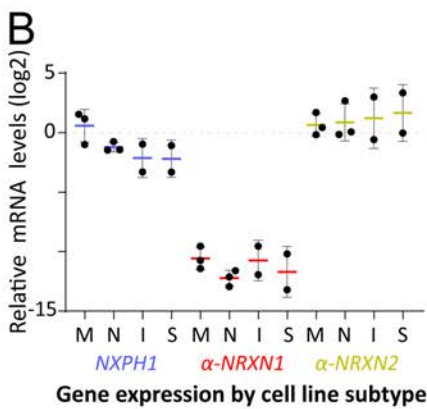


Figure-20. The expression of *NXPH1* and its receptors  $\alpha$ -*NRXN1/2* is independent of the cellular phenotype and of *MYCN* or *ALK* expression

(A) Table presenting the characteristics of our panel of human NB cell lines, including their cell morphology (M: mixed; N: neuronal; I: intermediate; S: stromal), their *MYCN* status (A: amplified; NA: non-amplified) and their *ALK* status (F1174L: activating mutation; n.d.: non-determined; wt: wild-type) as previously described in the literature. The heatmap shows the endogenous basal levels of *NXPH1* and  $\alpha$ -*NRXNs* calculated as a Z-score of their relative mRNA levels. (B) Relative expression level of *NXPH1* and  $\alpha$ -*NRXN1/2* genes in the 4 phenotypic subgroups of NB cell lines. (C-D) Correlation analysis between *NXPH1* and *MYCN* (C) or *ALK* (D) relative levels quantified by RT-qPCR in our panel of human NB cell lines. Significance was assessed with the non-parametric Kruskal-Wallis test (B) or the Spearman  $r$  correlation method (C-D).

We next decided to test whether the expression of *NXPH1* or that of its receptors  $\alpha$ -*NRXN1/2* might be correlated to the stemness potential of our NB cell lines. Growing NB cell lines in restrictive culture conditions for 5 weeks can cause cell detachment and formation of sphere-like structures which are progressively enriched in cells with stem cell characteristics (Hansford *et al.*, 2007; Ikegaki *et al.*, 2013; Takenobu *et al.*, 2011). We thus submitted all the cell lines of our panel to restrictive culture conditions and assessed their stem cell enrichment (Figure 21A).

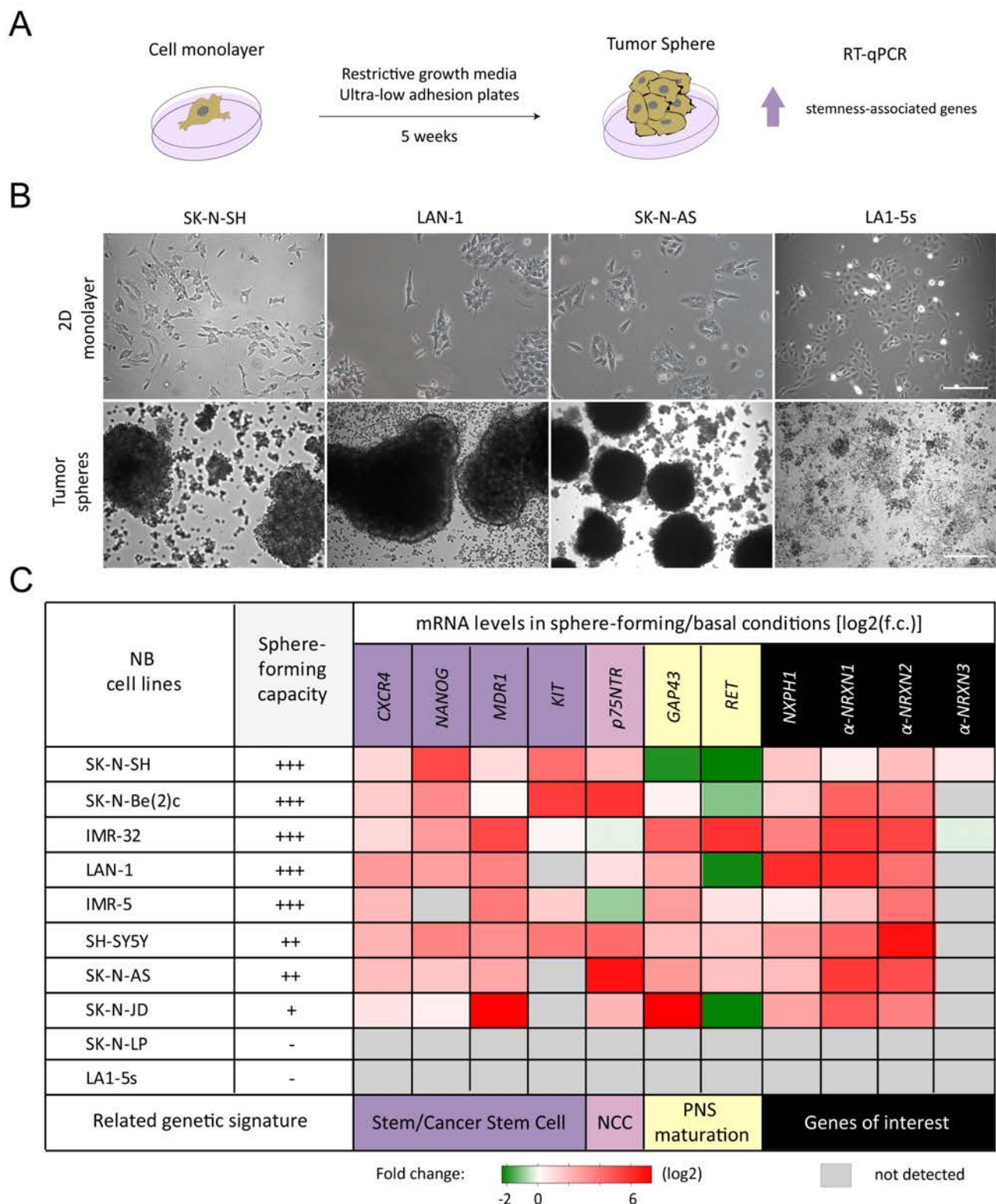


Figure-21. The expression of *NXPH1* and its membrane receptors  $\alpha$ -*NRXN1/2* is increased in stem-enrichment conditions

(A) Schematic representation of tumour sphere-forming protocol. Cells are grown under restrictive conditions (absence of growth factors & impaired substrate adhesion) for 5 weeks. Spheroids are then imaged and processed for RT-qPCR. (B) The cellular morphologies observed for the SK-N-SH, LAN-1, SK-N-AS and LA1-5s human NB cells cultured in basal or restrictive conditions for 5 weeks. (C) The sphere-forming capacity of our human NB cell lines and the heatmap showing the related changes in the mRNA levels of general stem cell markers (purple: *CXCR4*, *NANOG*, *MDR1*, *KIT*), NCC-associated marker (pink: *p75NTR*), neural-differentiation markers (yellow: *GAP43*, *RET*) and those of candidate gene *NXPH1* and their receptors  $\alpha$ -*NRXNs* (n=2). Scale bar: 100 $\mu$ m.

The sphere-forming capacity of the different lines was initially evaluated by bright field microscopy (Figure 21B) and confirmed by RT-qPCR whenever viable and growing spheroids were detected (Figure 21C). The increased expression of general (*CXCR4*, *NANOG*) or neural crest-specific (*p75NTR*) stemness markers validated a stem cell enrichment for 8 out of the 10 NB cell lines tested (Figure 21C). Notably, when NB spheroids were compared to their respective control monolayers, the up-regulation of *CXCR4*, *NANOG* and *p75NTR* mRNA expression was detected in almost all the cell lines that showed the capacity to grow as spheres over 5 weeks. The relative levels of *CXCR4*, *NANOG* and *p75NTR* were increased up to 7.4 and 113 folds respectively (except for *NANOG* in IMR-5 cells and *p75NTR* in IMR-32 and IMR-5, where their relative expression decreased). An increase up to 153 and 47 folds in the transcript levels of *MDR1* and *KIT*, two genes that have been respectively related with chemotherapy resistance and stem cell proliferation (Foster et al., 2018; Hirschmann-Jax et al., 2004), was also observed in most of the cell lines presenting a sphere-forming capacity (Figure 21C). The restrictive culture conditions also resulted in the decreased expression of *GAP43* and *RET*, two genes whose expression is classically associated to neuronal differentiation (Avantaggiato et al., 1994; Skene et al., 1986; Tahira et al., 1991), in a few cell lines such as the SK-N-SH line (Figure 21C). Remarkably, an increase in the transcript levels of *NXP1* and  $\alpha$ -*NRXN1/2* was detected in all the cell lines that showed the capacity to grow as stem cell-enriched spheres (Figure 21C). The low-to-almost undetectable levels of *NXP1*,  $\alpha$ -*NRXN1* and  $\alpha$ -*NRXN2* transcripts quantified in basal culture conditions were increased up to 64, 61 and 113 folds in these sphere-forming conditions, respectively (Figure 21C). By contrast, in most cases the levels of  $\alpha$ -*NRXN3* did not change significantly in response to the stem cell enrichment protocol. Together, these results revealed a strong and positive correlation between the expression of *NXP1* and  $\alpha$ -*NRXN1/2* and NB stemness *in vitro*.

On the basis of these first results, we decided to follow this study by addressing in parallel two complementary questions:

- o To determine whether the expression of the NXP1 receptors  $\alpha$ -NRXN1/2 identifies NB cancer stem cells (section 3)
- o To define how NXP1/ $\alpha$ -NRXN signalling modulates NB malignancy (section 4)

### 3. The expression of $\alpha$ -NRXN1 identifies a subpopulation of NB cells with cancer stem cell-like properties that is required for NB growth

The results previously obtained demonstrated that the low expression levels of the *NXPH1* transmembrane receptors  $\alpha$ -NRXN1/2 quantified in our panel of NB cell lines grown in basal culture conditions, are strongly increased in stem-cell enrichment conditions. This led us to hypothesize that  $\alpha$ -NRXN1 and  $\alpha$ -NRXN2 might be specifically expressed by NBsc.

To test this hypothesis, we took advantage of a commercially available fluorescence-conjugated antibody specifically recognizing the extracellular region of human  $\alpha$ -NRXN1 (see the Material and Methods section 5.2). No such tool was available to detect  $\alpha$ -NRXN2, which led us to focus this approach on  $\alpha$ -NRXN1.

#### 3.1. $\alpha$ -NRXN1 is expressed by a small subpopulation of cells in human NB cell lines and patient-derived xenografts

Using a commercial fluorescence-conjugated antibody recognizing the extracellular region of human  $\alpha$ -NRXN1, we assessed by FACS the presence of  $\alpha$ -NRXN1<sup>+</sup> cells in living human NB cells from various sources (Figure 22A,B). The 3 human NB cell lines that showed the highest sphere-forming capacity (SK-N-SH, SK-N-Be(2)c and IMR-32; Figure 21C) all contained a small subpopulation of cells expressing detectable levels of  $\alpha$ -NRXN1 protein (<2%) (Figure 22C), in agreement with the low levels of  $\alpha$ -NRXN1 transcripts quantified by RT-qPCR. In addition, we analysed  $\alpha$ -NRXN1 expression in dissociated cell samples obtained from 3 different NB PDXs, Similarly to what was observed in the cell lines, all 3 PDXs presented a low proportion of  $\alpha$ -NRXN1<sup>+</sup> cells (<1%; Figure 22C).

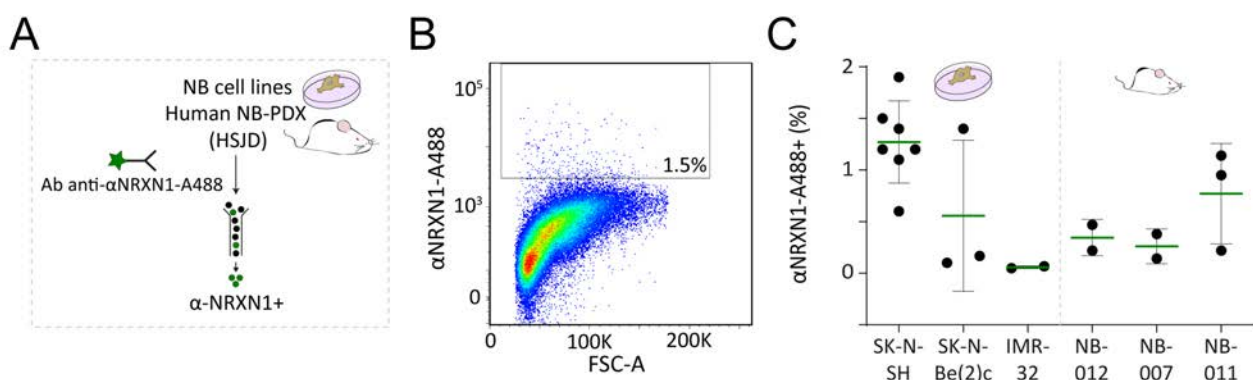


**Figure-22.  $\alpha$ -NRXN1<sup>+</sup> cells are identified in NB cell lines and human NB PDX**

(A) Methodology used to FACS-sort human NB cell lines and patient-derived-xenograft (PDXs) samples based on  $\alpha$ -NRXN1 expression. (B) Flow cytometry plot showing the proportion of  $\alpha$ -NRXN1<sup>+</sup> cells identified within the parental SK-N-SH cells. (C) Mean percentage of  $\alpha$ -NRXN1<sup>+</sup> cells identified within 3 human established cell lines and 3 PDX samples  $\pm$  SD.

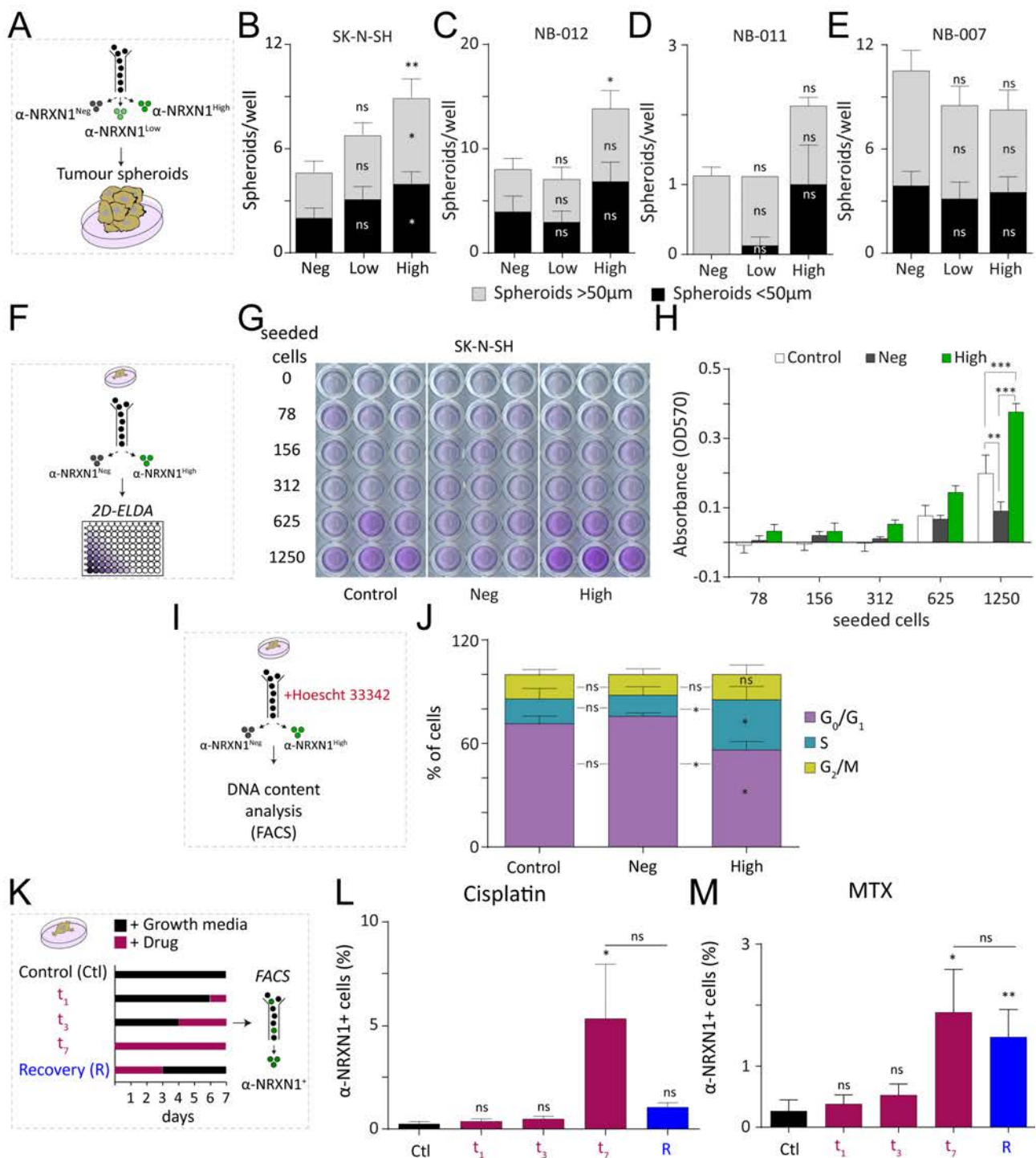
### 3.2. $\alpha$ -NRXN1 expression identifies a subpopulation of NB cells presenting cancer stem cell-like characteristics *in vitro*

The detection of  $\alpha$ -NRXN1 at the surface of a subpopulation of NB cells allowed us to purify these  $\alpha$ -NRXN1<sup>+</sup> cells by FACS and further test whether they possess the biological properties typically harboured by cancer stem cells such as sphere-forming capacity, proliferative ability in conditions of extreme dilution and chemotherapy-resistance (Batlle and Clevers, 2017).

First, we evaluated the ability of  $\alpha$ -NRXN1<sup>+</sup> cells, further subdivided into  $\alpha$ -NRXN1<sup>High</sup> and  $\alpha$ -NRXN1<sup>Low</sup>, purified from the SK-N-SH cell line or from NB PDXs to generate tumour spheroids when grown for 1 week in restrictive culture conditions (Figure 23A). Compared to  $\alpha$ -NRXN1<sup>Neg</sup> and  $\alpha$ -NRXN1<sup>Low</sup> cells,  $\alpha$ -NRXN1<sup>High</sup> cells from the SK-N-SH cell line generated twice as much spheroids (Figure 23B). This increase in the number of spheroids was observed both for the spheroids smaller than 50 $\mu$ m and the ones larger than 50 $\mu$ m. An enhanced sphere-forming capacity was also observed for the  $\alpha$ -NRXN1<sup>High</sup> cells deriving from the PDXs NB-012 and NB-011 (Figure 23C,D), demonstrating that  $\alpha$ -NRXN1<sup>High</sup> cells purified from various sources possess an enhanced spheroid-forming capacity compared to their sister cells. This increased ability was however not observed in all the samples tested:  $\alpha$ -NRXN1<sup>Neg</sup>,  $\alpha$ -NRXN1<sup>Low</sup> and  $\alpha$ -NRXN1<sup>High</sup> cells purified from the PDX NB-007 generated spheroids in comparable numbers (Figure 23E), suggesting that the enhanced sphere-forming capacity of  $\alpha$ -NRXN1<sup>High</sup> cells is regulated by a mechanism unidentified so far.

Second, we assessed the ability of  $\alpha$ -NRXN1<sup>High</sup> cells to grow in conditions of extreme limiting dilution (ELDA 2D assay) (Figure 23F).  $\alpha$ -NRXN1<sup>High</sup> cells, purified from the SK-N-SH cell line and seeded at low density after serial dilutions, presented an enhanced proliferative capacity compared to both purified  $\alpha$ -NRXN1<sup>Neg</sup> cells and unsorted parental SK-N-SH cells (Figure 23G,H). To determine whether this enhanced proliferative capacity results from differences in cell cycle progression, the DNA content of unsorted parental SK-N-SH cells and purified  $\alpha$ -NRXN1<sup>High</sup> and  $\alpha$ -NRXN1<sup>Neg</sup> cells was estimated by FACS after Hoechst incorporation (Figure 23I). Compared to  $\alpha$ -NRXN1<sup>Neg</sup> and unsorted SK-N-SH cells which harboured similar profiles,  $\alpha$ -NRXN1<sup>High</sup> cells contained a smaller proportion of cells presenting a 2n content (cells in the G<sub>0</sub>/G<sub>1</sub>-phase) and a larger proportion of cells with a 2n-4n content (cells transiting through S-phase, Figure 23J). This finding demonstrated that  $\alpha$ -NRXN1<sup>High</sup> cells are cycling more actively than  $\alpha$ -NRXN1<sup>Neg</sup> cells in these conditions, whether  $\alpha$ -NRXN1<sup>High</sup> cells present an overall shorter cell cycle (i.e a shorter G<sub>1</sub> phase) or if a higher proportion of  $\alpha$ -NRXN1<sup>High</sup> cells is actively cycling (i.e, not in the quiescent G<sub>0</sub> state).

Third, we estimated the chemotherapy-resistance potential of  $\alpha$ -NRXN1<sup>+</sup> cells by examining their persistence upon a toxic insult (Figure 23K). SK-N-SH cells were exposed to cisplatin, a platinum-based drug used in NB chemotherapies (Tolbert and Matthay, 2018) or to MTX, a chemotherapeutic drug



classically used in experimental models of chemoresistance (Golebiewska *et al.*, 2011). After 7 days of treatment with sub-lethal doses of cisplatin or MTX, the proportion of  $\alpha$ -NRXN1<sup>+</sup> cells quantified by FACS was increased by 21 and 7-folds, respectively (Figure 23L,M). These results suggest that  $\alpha$ -NRXN1<sup>+</sup> cells are more resistant than  $\alpha$ -NRXN1<sup>Neg</sup> cells to cisplatin/MTX-induced cell death, as it is described for certain cancer stem cells (Batlle and Clevers, 2017). Alternatively, these cytotoxic treatments might have caused an up-regulation of  $\alpha$ -NRXN1 expression. Interestingly, the proportion of  $\alpha$ -NRXN1<sup>+</sup> cells was restored to normal levels or reduced when cisplatin or MTX were removed from the medium for the last 3 days, arguing for a certain degree of plasticity of  $\alpha$ -NRXN1 expression by NB cells (Figure 23L,M).

**Figure-23. High  $\alpha$ -NRXN1 expression identifies NB cells with cancer stem cell-like phenotype in human NB cell lines and PDXs (previous page)**

(A) Methodology used to FACS-sort NB cells based on endogenous  $\alpha$ -NRXN1 levels ( $\alpha$ -NRXN1<sup>Neg</sup>,  $\alpha$ -NRXN1<sup>Low</sup> and  $\alpha$ -NRXN1<sup>High</sup>) for subsequent comparison of their tumorigenic potential by sphere-forming assay. (B-E) Mean number of spheroids  $\pm$  SEM generated by FACS-sorted  $\alpha$ -NRXN1<sup>Neg</sup>,  $\alpha$ -NRXN1<sup>Low</sup> and  $\alpha$ -NRXN1<sup>High</sup> cells from SK-N-SH (B) and human PDX NB-012 (C), NB-011 (D) and, NB-007 (E). Spheroid diameter (below or above 50 $\mu$ m) was taking into consideration during spheroid quantification. Error bars represent SEM interval of 4 biological (B) or technical replicates (C-E). (F) The proliferative capacity of  $\alpha$ -NRXN1<sup>+</sup> cells under extreme dilution conditions was compared to that of  $\alpha$ -NRXN1<sup>Neg</sup> or to a control SK-N-SH sample. (G-H) Plates were stained with crystal violet (G) and cell density was quantified by measuring optic density at 570nm (OD570), shown as mean OD570  $\pm$  SEM (n=3 biological replicates) (H). (I-J) DNA content of  $\alpha$ -NRXN1<sup>+</sup>,  $\alpha$ -NRXN1<sup>Neg</sup> cells and control SK-N-SH cells was quantified by FACS after Hoescht incorporation (I) and used to estimate and compare cell cycle distribution among the 3 different populations, shown as mean percentage of cells  $\pm$  SEM (n=3 biological replicates) (J). (K-M) Response of  $\alpha$ -NRXN1<sup>+</sup> cells to cytotoxic insults was evaluated by exposing SK-N-SH cells to 3 $\mu$ M Cisplatin (L), 5ng/ml Mitoxantrone (M) or its vehicle during increasing time periods. 3 days drug exposure followed by 4 days incubation in control growth media was used as a recovery condition. Percentage of  $\alpha$ -NRXN1<sup>+</sup> cells was quantified by FACS (L-M). Mean percentage of  $\alpha$ -NRXN1<sup>+</sup> cells  $\pm$  SEM in Cisplatin-treated and Mitoxantrone-treated (M) conditions (n=4 biological replicates). Significance was assessed with the non-parametric Kruskal-Wallis test + Dunn's test (B-E, L, M), the two-way ANOVA + Tukey's test (H), and non-parametric the Mann-Whitney test (J) \*p<0.05, \*\*p<0.01, \*\*\*p<0.001. NB: neuroblastoma; Neg: negative.

Taken together, these data obtained *in vitro* demonstrated that  $\alpha$ -NRXN1<sup>+</sup> NB cells present several biological properties classically assigned to cancer stem cells. We thus concluded that the expression of  $\alpha$ -NRXN1 identifies a subpopulation of NB cells presenting cancer stem cell-like characteristics *in vitro*.

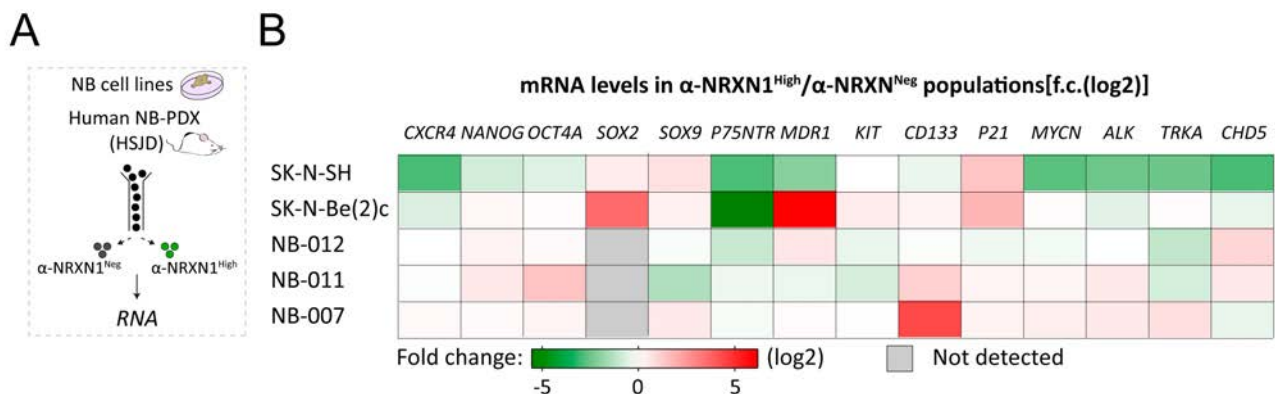


**Figure-24. Supervised gene expression analysis of  $\alpha$ -NRXN1<sup>High</sup> compared to  $\alpha$ -NRXN1<sup>Neg</sup> population in NB cell lines and human NB PDXs**

(A) Methodology used to FACS-sort human NB cell lines and patient-derived-xenografts (PDXs) samples based on  $\alpha$ -NRXN1 expression for subsequent RNA analysis. (B) The heatmap shows gene expression profile (RT-qPCR) of FACS-sorted  $\alpha$ -NRXN1<sup>High</sup> cells in relation to  $\alpha$ -NRXN1<sup>Neg</sup> cells from 2 NB cell lines (SK-N-SH and SK-N-Be(2)c, n=4 biological replicates) and 3 human NB-PDXs (NB-012, NB-011 & NB-007, n=1 biological replicate). f.c.: fold change; NB: neuroblastoma; Neg: negative.

### 3.3. Whether $\alpha$ -NRXN1<sup>+</sup> cells are endowed with a specific transcriptome remains unknown

To better understand the molecular signature underlying the biological features of  $\alpha$ -NRXN1<sup>+</sup> cells, we conducted a supervised gene expression analysis and compared by RT-qPCR the expression levels of selected genes in  $\alpha$ -NRXN1<sup>+</sup> cells and  $\alpha$ -NRXN1<sup>Neg</sup> cells purified from two human NB cell lines (SK-N-SH and SK-N-Be(2)c) and from 3 NB PDXs (Figure 24A). We quantified the transcript levels of 13 genes which were selected based on the literature: 3 genes associated with pluripotency (*NANOG*, *OCT4A*, *SOX2*), 4 general cancer-stem cell markers (*CXCR4*, *MDR1*, *KIT* and *CD133*), 2 neural crest cells markers (*SOX9* and *p75NTR*), 1 gen related to cell cycle (*P21*) together with 4 genes related to a bad (*MYCN* and *ALK*) or a good NB clinical prognosis (*TRKA* and *CHD5*). A differential expression between  $\alpha$ -NRXN1<sup>+</sup> cells and  $\alpha$ -NRXN1<sup>Neg</sup> cells was observed for certain genes in different samples, but none of these 13 genes showed a consistent expression profile in all the samples (Figure 24B). Therefore, whether  $\alpha$ -NRXN1<sup>+</sup> cells are endowed with a specific transcriptomic signature that accounts for their CSC-like behaviour remains unknown to date.

### 3.4. $\alpha$ -NRXN1<sup>+</sup> cells are required for NB growth *in vivo*

Next, we wondered how the subpopulation of  $\alpha$ -NRXN1<sup>+</sup> cells affects NB malignancy. To address this question, we performed a chick chorioallantoic membrane (CAM) tumour assay. The CAM assay has been successfully used to study NB tumour growth and/or metastatic behaviour *in vivo* (Rashidi and Sottile, 2009). In this assay, cells are embedded in matrigel and subsequently grafted *in ovo* on top of the richly vascularised CAM of 10 days-old chicken embryos. The putative growth of tumours derived from the engrafted cells is evaluated after 7 days of incubation. For our purpose, we thus set up an *in vivo* CAM assay in which we compared the growth potential of FACS-purified SK-N-SH cells depending on the presence or deprivation (by discarding the 10-12% of cells presenting the highest  $\alpha$ -NRXN1 expression levels) of their  $\alpha$ -NRXN1<sup>+</sup> subpopulation (Figure 25A). One week after grafting, NB tumours were carefully removed and analysed. Compared to their control containing  $\alpha$ -NRXN1<sup>+</sup> cells, the grafts seeded with SK-N-SH cells deprived of their  $\alpha$ -NRXN1<sup>+</sup> subpopulation showed a 2-fold reduction in the final tumour volume and a concomitant 1.5 fold decrease in tumour weight (Figure 25B,C). Moreover, the grafts seeded with SK-N-SH cells deprived of their  $\alpha$ -NRXN1<sup>+</sup> subpopulation showed numbers of NB tumour (HuNu<sup>+</sup>) cells per section and per area that were reduced to half the numbers quantified in tumour areas of similar size in the control grafts (Figure 25D-G). These results, although not statistically significant due to the low sample size, demonstrate the importance of the  $\alpha$ -NRXN1<sup>+</sup> cell subpopulation for localized NB tumour growth *in vivo*.

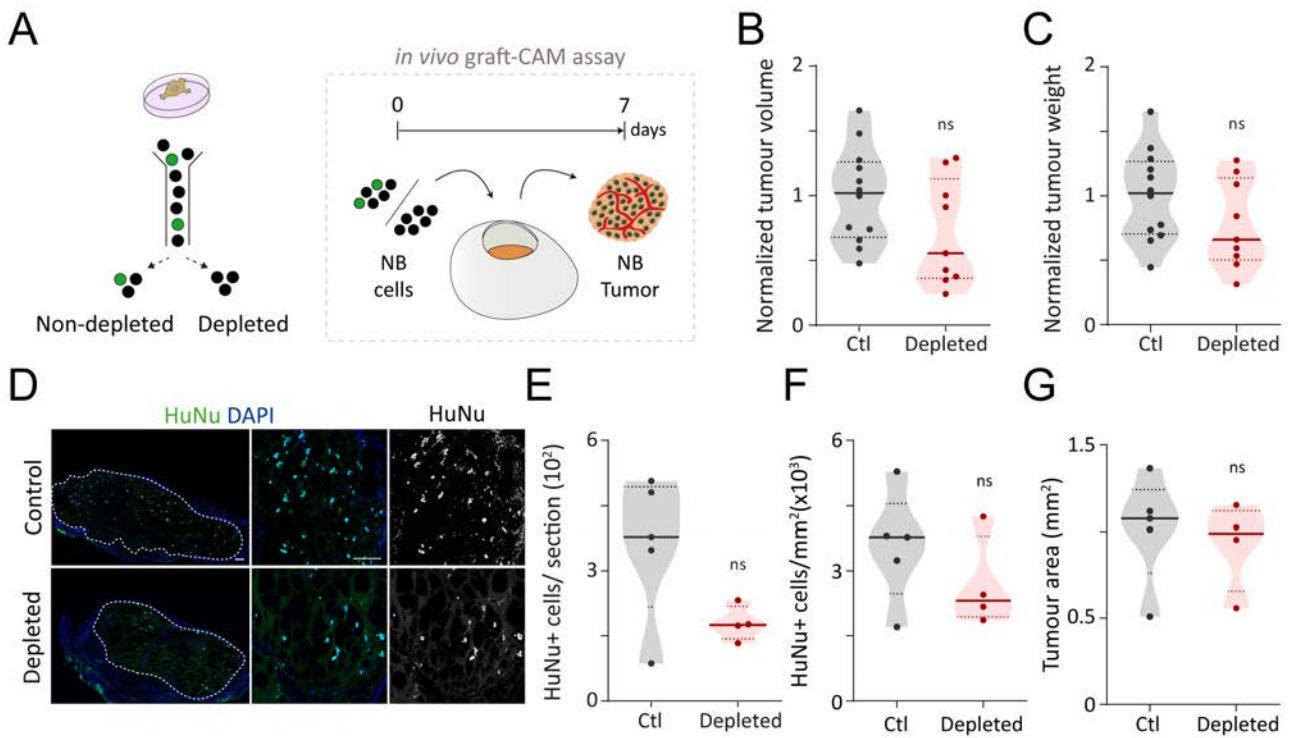


**Figure-25.  $\alpha$ -NRXN1<sup>High</sup> NB cells are required to sustain NB growth**

(A) Methodology used for depleting  $\alpha$ -NRXN1<sup>+</sup> cells from SK-N-SH parental cell line (Depleted) prior to in vivo grafting onto chorioallantoic membrane of chick embryos (CAM assay). Depleted and non-depleted (control, Ctl) CAM tumours were analysed by immunofluorescence. (B-C) The median normalized tumour volume (B) and the median normalized tumour weight (B) in Depleted CAM tumours and their controls, obtained from 9-12 tumours per experimental condition. (D-G) The HuNu immunoreactivity in Depleted tumours and its controls (D), and the median HuNu+ cells per confocal section (E), the median HuNu+ cells per tumour area in mm<sup>2</sup> (F) and the median tumour area per confocal section (G) in Depleted CAM tumours and their controls. Each dot results from the quantification of 6-12 independent confocal sections obtained from 4-5 tumours per experimental condition. Significance was assessed with the non-parametric Mann-Whitney test. Scale bar: 100 $\mu$ m. Ctl: control.

Taken altogether, the results presented in this section demonstrate that NB tumours contain a small subpopulation of cells expressing the NXP1 transmembrane receptor  $\alpha$ -NRXN1, and that these cells present cancer stem cell-like characteristics. Importantly, these  $\alpha$ -NRXN1<sup>+</sup> NBcsc-like cells appear to be crucial for NB growth and thus malignancy.

## 4. NXPH1 and its receptor $\alpha$ -NRXN1 sustain NB growth

We next wished to define how NXPH1/ $\alpha$ -NRXN signalling modulates NB malignancy. Since we previously established that  $\alpha$ -NRXN1 expression identifies a subpopulation of NBcsc-like cells with relevance for NB growth, we focused on this member of the  $\alpha$ -NRXN family. We thus developed both gain- and loss-function strategies to modulate NXPH1 and  $\alpha$ -NRXN1 activity and tested the consequences of these modulations on NB growth *in vitro* and *in vivo*.

### 4.1. Increasing NXPH1 activity promotes NB growth *in vivo*

#### 4.1.1. The addition of rNXPH1 promotes NB growth in the CAM assay

In a first approach, we took advantage of the CAM assay (see the Results' section 3.4 and Materials and Methods) to explore how increasing NXPH1 activity would affect NB growth *in vivo*. To do so, SK-N-SH cells were grafted in matrigel in the presence of recombinant human NXPH1 (rNXPH1) or its vehicle (an equivalent concentration of BSA) and seeded on top of the richly vascularised CAM of 10 days-old chicken embryos, which were then incubated for 7 days without receiving any further treatment. The recombinant human NXPH1 protein used in this work was purchased commercially and has been reported to be biologically active (Kinzfogel *et al.*, 2011). One week after grafting, the tumours that had formed were carefully removed and analysed (Figure 26A,B). While none of the 3 different doses of rNXPH1 used to treat SK-N-SH cells did significantly alter the tumour volume compared to the control condition, the intermediate dose (10 $\mu$ g/ml) of rNXPH1 caused a slight increase of the tumour weight (Figure 26C,D). The effects of this dose were thus studied more extensively, revealing that the addition of 10 $\mu$ g/ml of rNXPH1 increased by 62% and 82% the numbers of tumour (HuNu<sup>+</sup>) cells per section and per area quantified in tumour areas of similar size in the control grafts (Mean HuNu<sup>+</sup> cells per section: +rNXPH1= 2,689  $\pm$  719, Ctl=1,658  $\pm$  671; average cell density: +rNXPH1=1,847  $\pm$  599, Ctl=1,011  $\pm$  344; Figure 26E-H). These findings reveal that increasing NXPH1 activity promotes NB tumour growth *in vivo*.

Using a similar experimental set-up, we tested the effects of a commercial recombinant extracellular fragment of the rat  $\alpha$ -NRXN1 receptor, which is proposed to act as a decoy and thereby prevents the normal function of the endogenous  $\alpha$ -NRXN1 receptor (Figure 26I,J). Treating NB cells with different concentrations of the  $\alpha$ -NRXN1 decoy before grafting tended to decrease NB tumour growth (Figure 26K,L). In particular, the intermediate dose (15  $\mu$ g/ml) of decoy used to treat SK-N-SH cells reduced both the tumour volume and weight (Figure 26K,L). Unfortunately, its effects were not studied into further details. Nevertheless, these data suggest that blocking the endogenous activity of

$\alpha$ -NRXN1 is sufficient to reduce NB tumour growth *in vivo*.

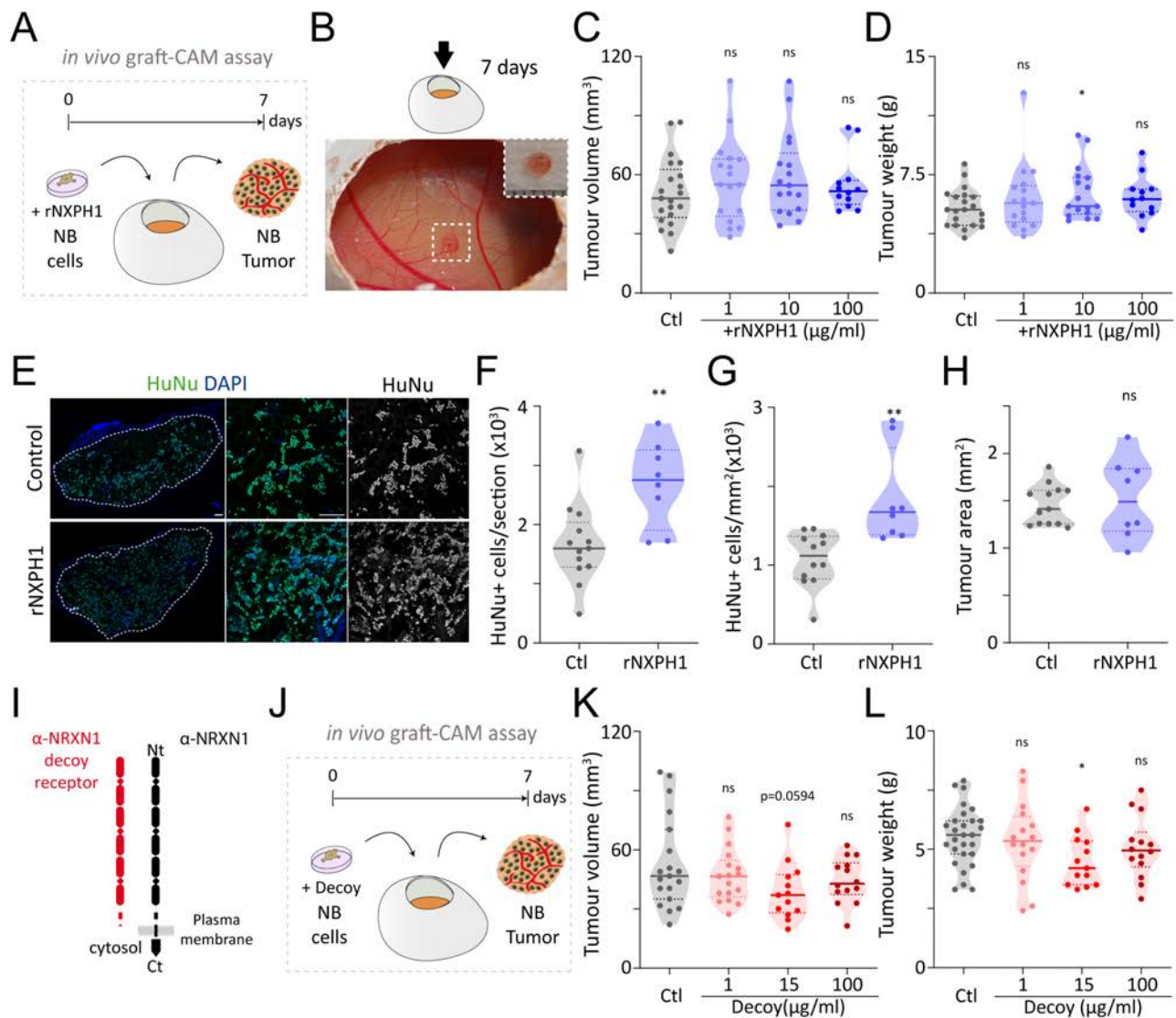


**Figure-26. Exogenous NXPH1 promotes NB growth in CAM assay**

(A-B) Methodology used for *in vivo* grafting of SK-N-SH cells in the presence of recombinant NXPH1 (rNXPH1) protein or its vehicle onto the CAM. Vascularised 7-days CAM-tumours were detected onto the CAM and were analysed by immunofluorescence (B). (C-D) The median tumour volume (C) and the median tumour weight (D) in rNXPH1- or vehicle-treated CAM tumours, obtained from 12-21 tumours per experimental condition. (E-H) The HuNu immunoreactivity in 10 $\mu$ g/ml rNXPH1- or vehicle-treated tumours (E) and the median HuNu+ cells per confocal section (F), the median HuNu+ cells per tumour area in mm<sup>2</sup> (G) and the median tumour area per confocal section (H) in 10 $\mu$ g/ml rNXPH1 or vehicle-treated CAM tumours. Each dot results from the quantification of 3-6 independent confocal sections obtained from 8-13 tumours per experimental condition. (I) Schematic representations of recombinant decoy  $\alpha$ -NRXN1 (Decoy) protein and full length  $\alpha$ -NRXN1 receptor. (J) Methodology used for *in vivo* grafting of SK-N-SH cells in the presence of Decoy or its vehicle onto the CAM. (K-L) The median tumour volume (K) and the median tumour weight (L) in Decoy- or vehicle-treated CAM tumours, obtained from 13-23 tumours per experimental condition. Significance was assessed with the parametric unpaired T-test (C-D, F-H, L) or the non-parametric Mann-Whitney test (C-D, G, K) in order to compare rNXPH1-treated versus vehicle-treated conditions. \* $p$ <0.05, \*\* $p$ <0.01. Scale bar: 100 $\mu$ m (E). Decoy: recombinant decoy  $\alpha$ -NRXN1 protein; NB: neuroblastoma; rNXPH1: recombinant NXPH1 protein.

#### 4.1.2. The addition of rNXPH1 increases p75NTR expression and stimulates proliferation

We further analysed the effects of rNPHX1 addition to gain insight into the mechanisms underlying its growth-promoting activity. Despite the increased number of HuNu+ NB cells found in the tumours treated with rNXPH1 (Figure 26E-H), we did not detect any effect of rNPHX1 addition on the proportions of cycling (Ki67+) or apoptotic (activated cleaved-Caspase 3, cCasp3+) HuNu+ cells present in the tumours after 7 days (Figure 27A-D). We reasoned that the effects caused by a single treatment with rNPHX1 administered at the beginning of the experiment might be transient and thus be masked when analysed at the end of the experimental window. Therefore, we conducted another experiment in which NB cells received a 24 hours pulse of BrdU *in vitro* prior to treatment with rNXPH1 or BSA and grafting. This allowed us to assess long-term BrdU retention and thereby determined whether rNXPH1 addition might have modulated NB cell proliferation over the course of the 7 days incubation (Figure 27E,F). The NB cells that had incorporated BrdU *in vitro* and had later undergone one or multiple rounds of division *in vivo*, thereby diluting partially the BrdU labelling, appeared as partially stained after BrdU immunodetection (<100% BrdU<sup>+</sup>). The proportion of these partially-stained BrdU<sup>+</sup> NB cells was increased by 1.5 folds in response to rNPHX1 treatment (Figure 27F,G), thus revealing that rNPHX1 had stimulated the proliferation of NB cells at some time point during the experimental window. The proportion of NB cells that had incorporated BrdU *in vitro* but did not divide during the 7 days incubation *in vivo*, thereby retaining 100% of BrdU labelling at the end of the experiment (100% BrdU<sup>+</sup>), did not appear altered by rNXPH1 (Figure 27F,G), suggesting that rNPHX1 had not stimulated the proliferation of slow-cycling NB cells or cell cycle-arrested NB cells. To explore whether the exposure of NB cells to rNXPH1 also affected their stem cell status, we carried out an immunostaining against the neural crest stem cell marker p75NTR. Interestingly, rNXPH1 addition doubled the proportion of NB cells expressing p75NTR (Figure 27H, I).

Collectively, these results demonstrate that NXPH1 is sufficient to increase NB growth *in vivo* in the CAM assay. Our findings further suggest that the growth-promoting activity of NXPH1 is due to its ability to stimulate the proliferation of actively dividing NB cells and/or to promote p75NTR expression. Whether these p75NTR<sup>+</sup> cells correspond to the actively dividing tumour cells remains to be defined.

#### 4.2. Inhibiting *NXPH1* and $\alpha$ -*NRXN1* expression impairs NB tumour formation and growth *in vivo*

In a second approach, we decided to investigate how the inhibition of NXPH1 or  $\alpha$ -NRXN1 activity would affect NB cell behaviour and malignancy, by generating clones of NB cells expressing sh-RNAs targeting specifically human *NXPH1* or  $\alpha$ -*NRXN1* mRNAs.



#### 4.2.1. Constitutive inhibition *NXPH1* or $\alpha$ -*NRXN1* impairs permanently SK-N-SH cell growth

First, we generated clones of SK-N-SH cells that produce short-hairpin RNAs targeting specifically human *NXPH1* or  $\alpha$ -*NRXN1* mRNAs in a stable and constitutive manner. To that end, 2 different specific target sequences were selected for each gene and specific sh-RNA sequences were cloned into the constitutive pLKO.1-puro plasmid, while a scramble sequence was used as a control (Figure 28A, see also the Material and Methods' section 4.1.1.1). After 3 days of selection in presence of puromycin, we assessed by RT-qPCR the efficiency of *NXPH1* and  $\alpha$ -*NRXN1* mRNA knockdown triggered by the respective sh-*NXPH1* and sh- $\alpha$ *NRXN1* clones and tested their putative effects on cell viability by an MTT assay (Figure 28B-E). Compared to the levels quantified in the sh-Ctl, the *NXPH1* mRNA levels were decreased by more than 70% in the sh1-*NXPH1* clone (Figure 28C). The *NXPH1* transcript levels quantified in the second shRNA sequence, sh2-*NXPH1*, were more variable, resulting in a less pronounced inhibition ( $\approx$ 30%, Figure 28C). However, the cell viability measured after 72 hours in both sh1-*NXPH1* and sh2-*NXPH1* clones was reduced to less than half the one measured in control cells (Figure 28E). Similarly, the sh1- $\alpha$ *NRXN1* and sh2- $\alpha$ *NRXN1* clones showed levels of  $\alpha$ -*NRXN1* transcripts reduced by 37% and 87% compared to control levels (Figure 28D), and presented a cell viability decreased by 66% and 33%, respectively (Figure 28E). The reduction in cell viability caused by both *NXPH1* and  $\alpha$ -*NRXN1* mRNA inhibition was maintained throughout the 3 weeks during which these clones were kept in culture. This reduced cell viability might result from an impairment of cell proliferation and/or cell survival. The latter option is supported by the presence of large amounts of cell debris that were observed in the culture dishes. Interestingly, changes in cellular morphology were also observed in all the sh-*NXPH1* and sh- $\alpha$ *NRXN1* clones (Figure 28F). Thus, we reasoned that constitutively reducing *NXPH1* or  $\alpha$ -*NRXN1* expression in NB cells impairs their growth to such an extent that it would likely have prevented us from getting clear conclusions in future studies.

#### 4.2.2. Inducible inhibition *NXPH1* or $\alpha$ -*NRXN1* impairs SK-N-SH cell growth

To overcome the cell viability issues caused by the constitutive inhibition of *NXPH1* and  $\alpha$ -*NRXN1* expression, we thought of generating clones of SK-N-SH that would express the sh-*NXPH1* or sh- $\alpha$ *NRXN1* in an inducible manner. To this aim, we used an inducible system that produces miR-shRNA sequences, together with EGFP, in an inducible and reversible manner upon doxycycline treatment (Figure 29A,B; see also Materials and Methods' section 4.1.1.2). The scramble and sh-RNA sequences previously inserted into the pLKO.1 plasmid and used to generate the constitutive sh-Ctl, sh1-*NXPH1* and sh1- $\alpha$ *NRXN1* clones, were selected and adapted to the inducible pSLIK-Neo platform. When grown without doxycycline and thus no sh-RNA was produced, the 3 transgenic clones generated (hereafter referred to as sh-Ctl, sh-*NXPH1* and sh- $\alpha$ *NRXN1*) showed similar cell viabilities (Figure 29C).

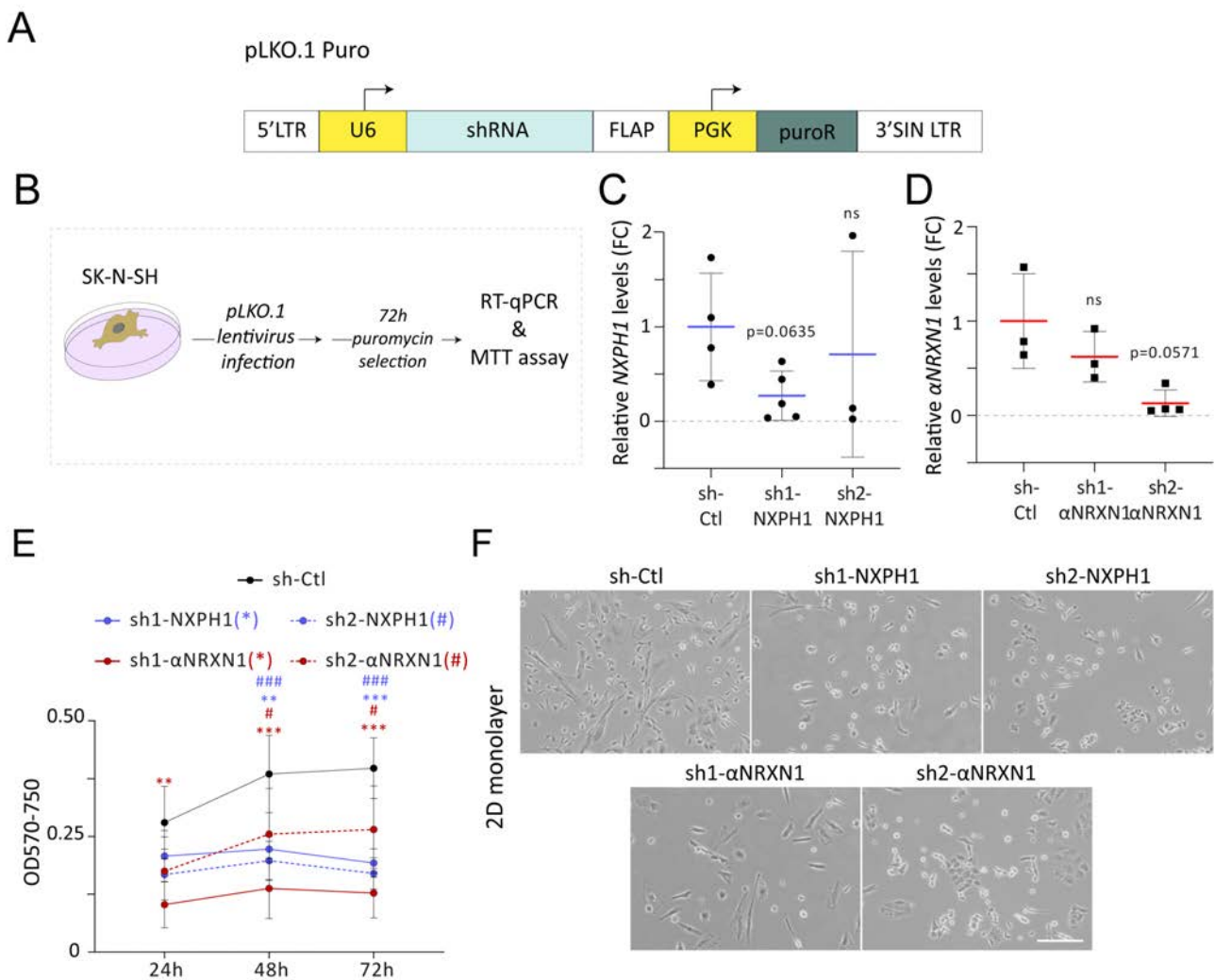


**Figure-28. The constitutive inhibition of *NXPH1* or  $\alpha$ -*NRXN1* expression prevents permanently NB cell growth *in vitro***

(A) Schematic representation of the pLKO.1-Puro vector driving a constitutive production of sh-RNAs (B) Methodology used to evaluate sh-RNA efficiency and cell viability after lentiviral infection of SK-N-SH cells with pLKO.1-Puro particles. (C-D) RT-qPCR quantification of the *NXPH1* (C) or  $\alpha$ -*NRXN1* (D) relative mRNA levels indicating the mean relative levels  $\pm$  SD in 3-4 independent sh-RNA clones. (E) The cell viability evolution in sh-RNA clones in terms of mean OD570-750  $\pm$  SD obtained from 4 independent sh-RNA clones. (G) Bright field images of sh-RNA clones 96h after puromycin selection. Significance was assessed with the non-parametric Mann-Whitney test (C-D) or the 2-way ANOVA + Dunnett's test (E). Scale bar: 100 $\mu$ m. 3'SIN LTR: 3' self-inactivating long terminal repeat; 5'LTR: 5' long terminal repeat; Ctl: control; PGK: Human phosphoglycerate kinase promoter; puroR: puromycine resistance gene; shRNA: short hairpin RNA; U6: human U6 promoter.

To specifically select the cells in which the sh-RNAs were induced, cells were grown for 3 days in presence of doxycycline (1 $\mu$ g/ml), purified by FACS based on EGFP expression and seeded at equal densities (Figure 29D). A time-course analysis conducted on these cells revealed a 15-20% reduction in the cell viability of the activated sh-*NXPH1* and sh- $\alpha$ *NRXN1* clones compared to the sh-Ctl, from 72 hours (Figure 29D). By comparing mRNA expression in the EGFP<sup>+</sup> subpopulation compared to their EGFP<sup>-</sup> sister cells by RT-qPCR, we could confirm that *NXPH1* and  $\alpha$ -*NRXN1* transcript levels were reduced by  $\approx$ 50% in the corresponding sh-*NXPH1* and sh- $\alpha$ *NRXN1* clones as compared to the levels quantified in sh-Ctl (Figure 29E,F).

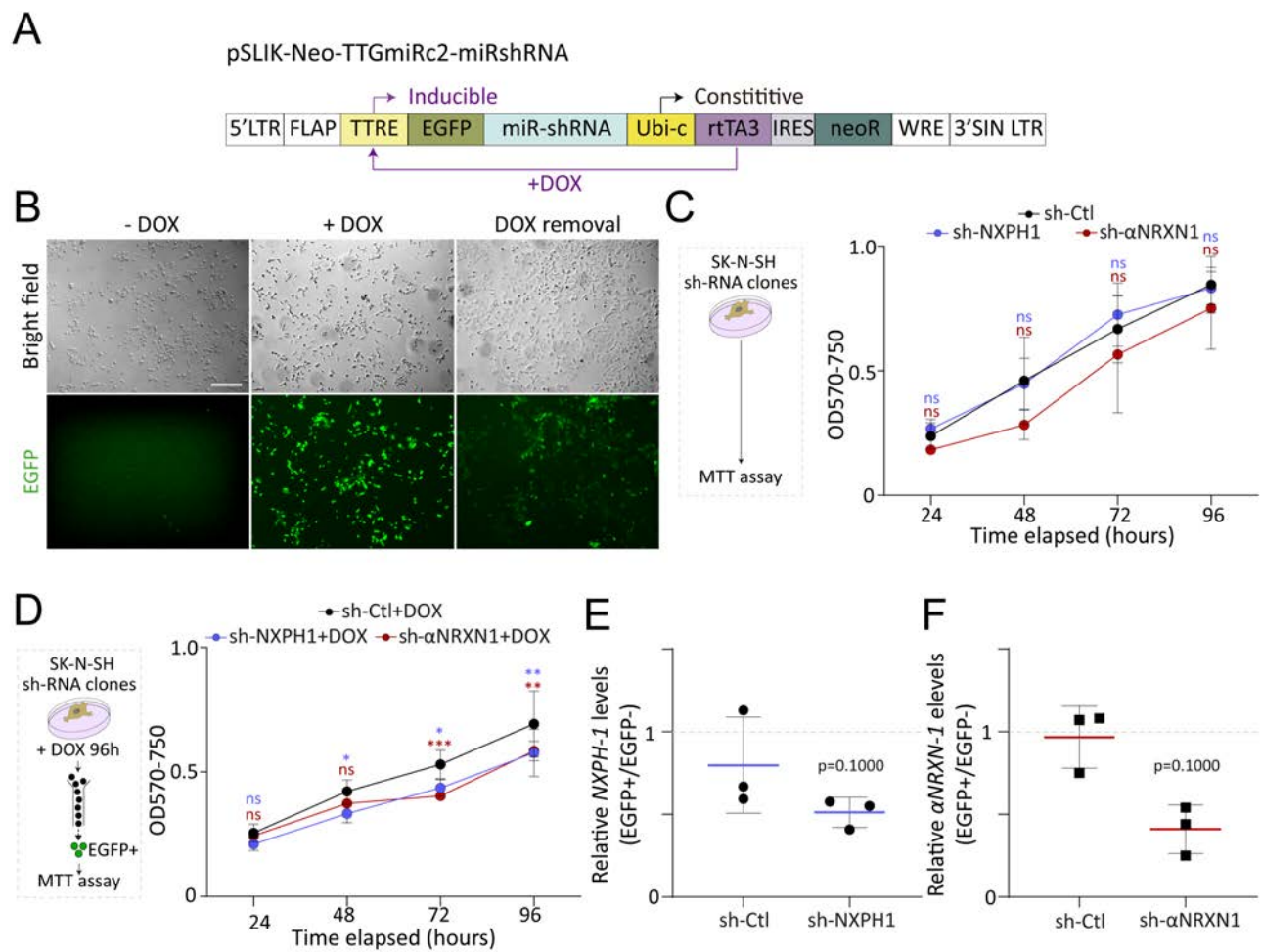


**Figure-29. The inducible inhibition of *NXPH1* or  $\alpha$ -*NRXN1* expression causes mild reduction of NB cell viability *in vitro***

(A) Schematic representation of the pSLIK-Neo-TTGmiRc2 vector driving an inducible and reversible production of sh-RNA. (B) SK-N-SH cells stably transfected with the pSLIK-Neo-TTGmiRc2 vector concomitantly produce EGFP and a shRNA only upon doxycycline treatment (+DOX vs -DOX), 2 days after initiation of the treatment. 3 days after DOX removal, most of the cells have lost or reduced EGFP fluorescence. (C) The cell viability evolution in non-induced SK-N-SH shRNA-clones in term of mean OD570-750  $\pm$  SD obtained from 2-4 independent sh-RNA clones. (D) The cell viability evolution in shRNA-(EGFP+)-producing SK-N-SH cells shRNA clones upon induction by doxycycline in term of mean OD570-750  $\pm$  SD obtained from 2-4 independent shRNA clones. (E-F) RT-qPCR quantification of the *NXPH1* (E) or  $\alpha$ -*NRXN1* (F) relative mRNA levels in the corresponding EGFP+-sorted cells compared to their EGFP- sisters cells, indicating the mean ratio  $\pm$  SD in 3 independent shRNA clones. Significance was assessed with the 2-way ANOVA + Dunnett's test (C-D) and the non-parametric Mann-Whitney test (E-F). \* $p < 0.05$ , \*\* $p < 0.01$ , \*\*\* $p < 0.001$ . Scale bar: 100 $\mu$ m. 3'SIN LTR: 3' self-inactivating long terminal repeat; 5'LTR: 5' long terminal repeat; DOX: doxycycline; EGFP: enhanced-green-fluorescent-protein; FLAP: region that contains central polypurine tract (cPPT/CTS); IRES: internal ribosome entry site; miR-sh-RNA: miR-like short hairpin RNA; neoR: neomycine/G418 resistance gene; rtTA3: 3rd generation reverse tetracycline transactivator element; TTRE: tight tetracycline repressor element; Ubi-c: Human ubiquitine-c promoter; WRE: Woodchuck hepatitis virus post-transcriptional regulatory element.

#### 4.2.3. Inhibiting *NXPH1* or $\alpha$ -*NRXN1* expression reduces NBcsc activation *in vitro*

To further test how *NXPH1* and  $\alpha$ -*NRXN1* inhibition impacts NB growth *in vitro*, SK-N-SH cells from the sh-NXPH1, sh- $\alpha$ NRXN1 and sh-Ctl clones were treated for 4 days with doxycycline to activate sh-

RNA production, sorted and purified by FACS based on EGFP expression. These purified cells with active sh-RNA production were further grown *in vitro* for 7 days in basal culture conditions in the presence of doxycycline to sustain *NXPH1* and  $\alpha$ -*NRXN1* inhibition (Figure 30A). In agreement with the results obtained with the MTT assay (Figure 29D), the number of EGFP+ cells quantified per image in both the sh-*NXPH1* and sh- $\alpha$ -*NRXN1* clones after 7 days was partially decreased compared to the number quantified in the sh-Ctl clone (Figure 30B,C), thereby confirming the partial reduction in cell viability in response to *NXPH1* and  $\alpha$ -*NRXN1* inhibition. The proportions of cycling (KI67<sup>+</sup>) and mitotic (pH3<sup>+</sup>) cells found in the sh-*NXPH1* and sh- $\alpha$ -*NRXN1* clones were comparable to the ones quantified in the control (Figure 30D-F). Unexpectedly, cells from sh-*NXPH1* clone showed an increase proportion of cells in S-phase, which was assessed after 2 hours of BrdU incorporation. S-phase index for sh- $\alpha$ -*NRXN1* clone did not differ to that of the control (Figures 30G,H). Together, these findings indicated that *NXPH1* and  $\alpha$ -*NRXN1* inhibition does not alter NB cell cycle kinetics in basal culture conditions. *NXPH1* and  $\alpha$ -*NRXN1* inhibition does not noticeably alter NB cell survival either, as suggested by the comparable proportions of pyknotic nuclei measured for cells of the sh-*NXPH1* and sh- $\alpha$ -*NRXN1* clones and their control (Figures 30G,I). Therefore, the inhibition of *NXPH1* or  $\alpha$ -*NRXN1* activity does not appear to primarily affect proliferation or survival, at least in basal culture conditions.

We previously defined that the NB cells expressing the  $\alpha$ -*NRXN1* receptor present CSC-like properties. We thus decided to test whether *NXPH1* or  $\alpha$ -*NRXN1* inhibition would affect NB stem cell activation *in vitro*. To this aim, SK-N-SH cells from the sh-*NXPH1*, sh- $\alpha$ -*NRXN1* and sh-Ctl clones were treated for 4 days with doxycycline to activate sh-RNA production, then sorted and purified by FACS based on EGFP expression. These purified cells with active sh-RNA production were further grown *in vitro* for 1 week in restrictive culture conditions to allow the formation of spheroids, and in the presence of doxycycline to sustain *NXPH1* and  $\alpha$ -*NRXN1* inhibition (Figure 30J). Compared to sh-Ctl cells, cells from the activated sh-*NXPH1* and sh- $\alpha$ -*NRXN1* clones generated remarkably fewer spheroids, especially the larger ones (Figure 30K,L). This last result suggested that the activation of NBcsc is diminished when *NXPH1* or  $\alpha$ -*NRXN1* activities are impaired.

#### 4.2.4. Inhibiting *NXPH1* or $\alpha$ -*NRXN1* expression impairs NB tumour formation and growth *in vivo*

Finally, we tested the consequences of *NXPH1* and  $\alpha$ -*NRXN1* inhibition on NB growth *in vivo*. To do so, cells from the sh-*NXPH1*, sh- $\alpha$ -*NRXN1* and sh-Ctl clones were treated for 4 days with doxycycline to activate sh-RNA production, then sorted and purified by FACS based on EGFP expression. The sorted cells were later injected sub-cutaneously in the flanks of immunodeprived NOD/SCID mice, which received doxycycline administration *ad libitum* to maintain the production of EGFP and sh-RNAs throughout the experiment (Figure 31A; see also the Materials and Methods' section 6.4.2).

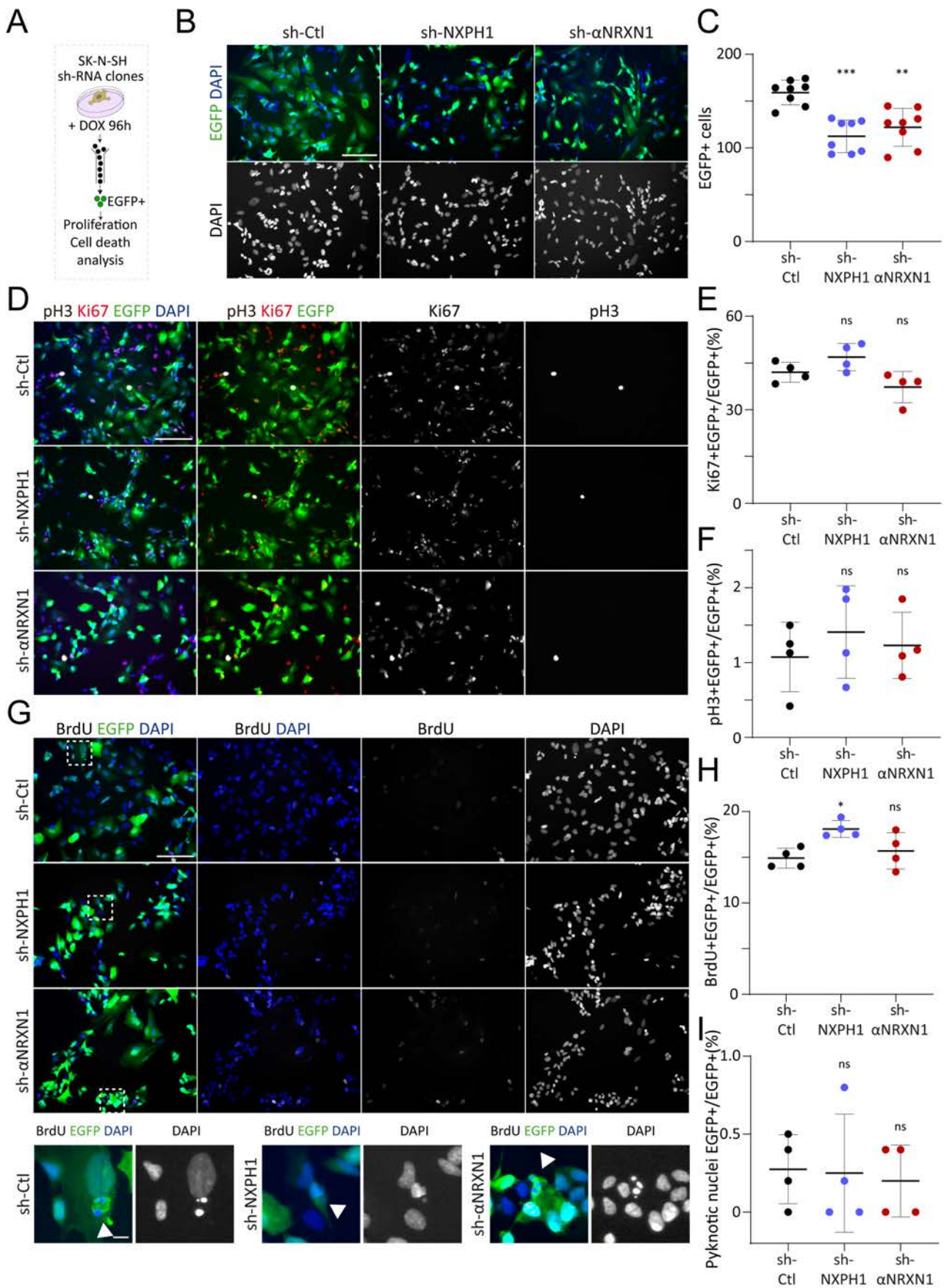
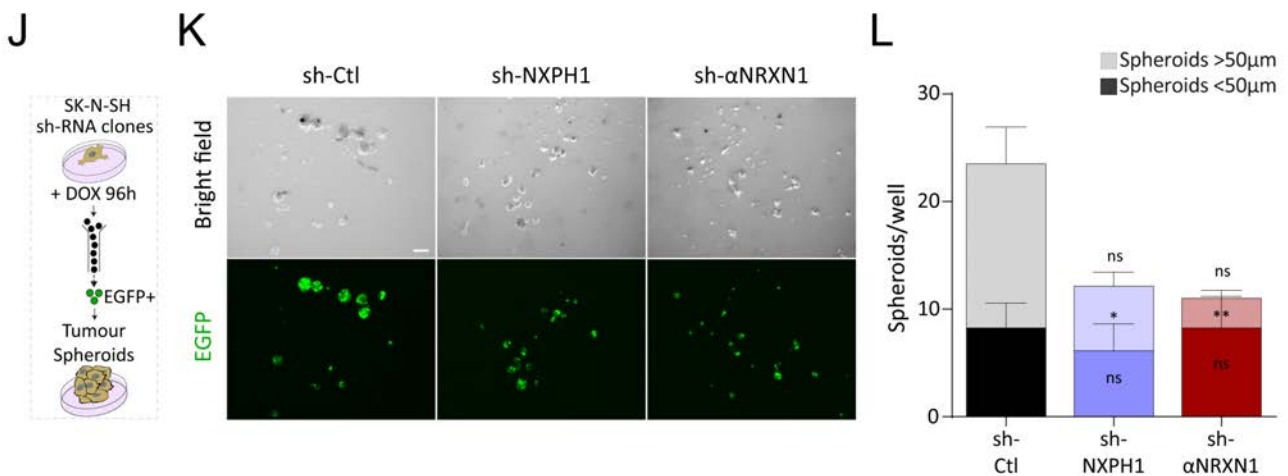


Figure-30. The inducible inhibition of *NXPH1* or  $\alpha$ -*NRXN1* expression reduces NB growth and tumorigenic potential *in vitro*



**Figure-30 continued. The inducible inhibition of *NXPH1* or  $\alpha$ -*NRXN1* expression reduces NB growth and tumorigenic potential *in vitro***

(A) Methodology used to FACS-sort shRNA (EGFP+)-producing SK-N-SH clones in order to evaluate proliferation and cell death upon doxycycline treatment. (B-C) Wide-field fluorescent imaging of shRNA (EGFP+)-producing SK-N-SH clones (B) and the mean number of EGFP+ cells  $\pm$  SD (C). (D-F) The Ki67 and phosphorylated-Histone 3 (pH3) immunoreactivity in shRNA (EGFP+)-producing SK-N-SH clones (D), the mean percentage of Ki67+EGFP+ cells  $\pm$  SD (E) and the mean percentage of pH3+EGFP+ cells  $\pm$  SD (F) in relation to the total number of EGFP+. (G-I) The BrdU immunoreactivity in shRNA (EGFP+)-producing SK-N-SH clones and high magnification images showing pyknotic nuclei (G), the mean percentage of BrdU+EGFP+ cells  $\pm$  SD (H) and the mean percentage of pyknotic nuclei EGFP+  $\pm$  SD (I) in relation to the total number of EGFP+. (J) Methodology used to FACS-sort shRNA (EGFP+)-producing SK-N-SH clones in order to evaluate tumorigenic potential upon doxycycline treatment. (K-L) Representative images of the EGFP+ spheroids generated by the sh-RNA clones (K) and the mean number of spheroids  $\pm$  SEM generated by the sh-RNA clones (L). Spheroid diameter (below or above 50µm) was taken into consideration during spheroid quantification. Error bars represent SEM interval of 8 technical replicates obtained from 2 independent experiments. Significance was assessed with the non-parametric Mann-Whitney test (E-F) or the Kruskal-Wallis test + Dunn's test (L). \* $p < 0.05$ , \*\* $p < 0.01$ , \*\*\* $p < 0.001$ . Each dot results from the quantification of 4-12 independent images obtained from 4 independent shRNA clones (C,E-F,H-I). Scale bar: 10µm (G, high magnification) and 100µm (B, D, G low magnification). DOX: doxycycline; EGFP: enhanced-green-fluorescent-protein; pH3: phosphorylated-Histone 3.

Cells from the sh-Ctl clone generated tumours that appeared palpable from the day 29 post-injection and which grew exponentially until the end of the experimental window (Figure 31B-D). By comparison, cells from both the sh-NXPH1 and sh- $\alpha$ NRXN1 clones generated fewer tumours, and the formation of these few tumours was delayed, thereby increasing the event-free survival (Figure 31B,C). Of note, the tumours generated by sh-NXPH1/sh- $\alpha$ NRXN1-derived cells appeared much less vascularized than the tumours derived from the sh-Ctl cells (Figure 31C). The average final volume of the tumours generated from sh-NXPH1 cells was reduced to 25% of the mean control volume, and their average weight decreased to 17% of the mean control value. The single sh- $\alpha$ NRXN1-derived tumour that was detected before day 53 showed a similar growth kinetic to that control tumours, but the average weight of the sh- $\alpha$ NRXN1-derived tumours decreased to 60% of the mean control value 53 days after grafting (Figure 31D,E). Therefore, inhibiting *NXPH1* or  $\alpha$ -*NRXN1* expression strongly impairs NB tumour formation and growth *in vivo*.

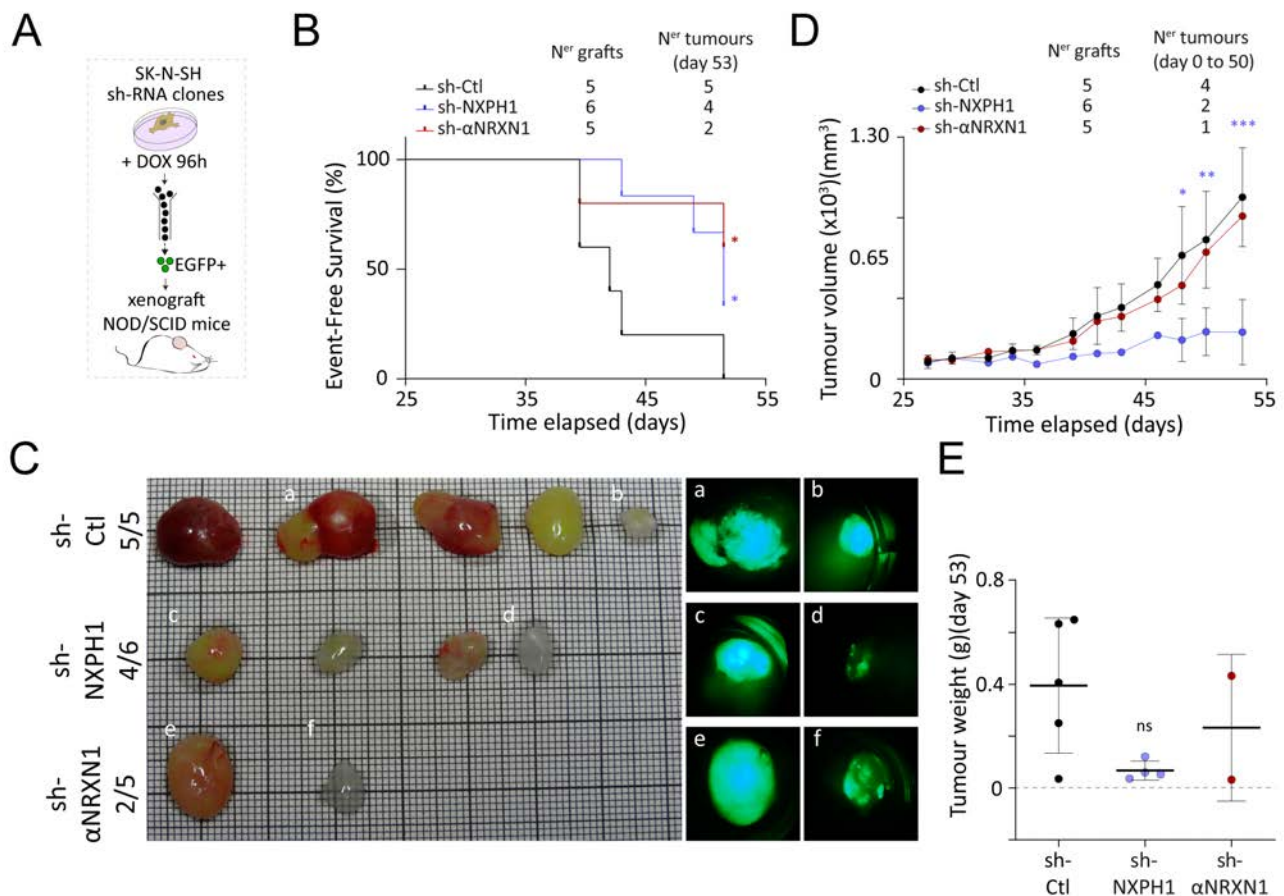


**Figure-31. The inducible inhibition of *NXPH1* or  $\alpha$ -*NRXN1* expression reduces subcutaneous NB burden and growth in mouse xenograft**

(A) Methodology used to FACS-sort shRNA (EGFP<sup>+</sup>)-producing SK-N-SH clones in order to evaluate in vivo tumorigenic potential by subcutaneous xenograft. (B-C) The event-free survival probability of NOD/SCID mouse injected with shCtl, sh-NXPH1 or sh- $\alpha$ NRXN1 clones (B) and the tumour appearance 53 days after grafting (C). (D-E) The kinetics of tumour growth in terms of mean volume  $\pm$  SD along 53 days (D) and mean weight  $\pm$  SD at day 53 (E). Significance was assessed with the Mantel-Cox logrank test (B), the 2-way ANOVA + Sidak's test (D) and the non-parametric Mann-Whitney test (E). \* $p < 0.05$ , \*\* $p < 0.01$ ; \*\*\* $p < 0.001$ . DOX: doxycycline; EGFP: enhanced-green-fluorescent-protein.

To test whether the reduction in tumour growth caused by *NXPH1* or  $\alpha$ -*NRXN1* inhibition could be related to stem cell activation and/or proliferation as our previous results suggested (see sections 4.2.1 to 4.2.3 from Results), we assessed the presence of cells expressing the NCC stem cell marker p75NTR in tumour sections by immunohistochemistry (Figure 32A,B). Considering the low number of tumours generated by either sh-NXPH1 and sh- $\alpha$ NRXN1 cells and their similar behaviour, the data obtained from these two experimental conditions were pooled together. No obvious difference in the proportion of p75NTR<sup>+</sup> cells among EGFP<sup>+</sup> tumour cells was detected between tumours derived from sh-Ctl and sh-NXPH1/sh- $\alpha$ NRXN1 cells (Figure 32A,B). The induction of an angiogenic response is essential for tumour burdening (Plaks *et al.*, 2015), and the macroscopic analysis of the resected tumours suggested that the sh-NXPH1/sh- $\alpha$ NRXN1-derived tumours were poorly vascularized compared to the control ones (Figure 31C). However, sections from the sh-Ctl-derived and sh-NXPH1/

sh- $\alpha$ NRXN1-derived tumours presented comparable numbers and densities of CD31<sup>+</sup> blood vessels (Figure 32C,D). The reduced vascularisation of the tumours derived from sh-NXPH1 and sh- $\alpha$ NRXN1 cells is thus likely to reflect the delayed and decreased growth of these tumours as compared to the control ones, rather than a more direct action of NXPH1/  $\alpha$ NRXN1 signalling on neoangiogenesis.

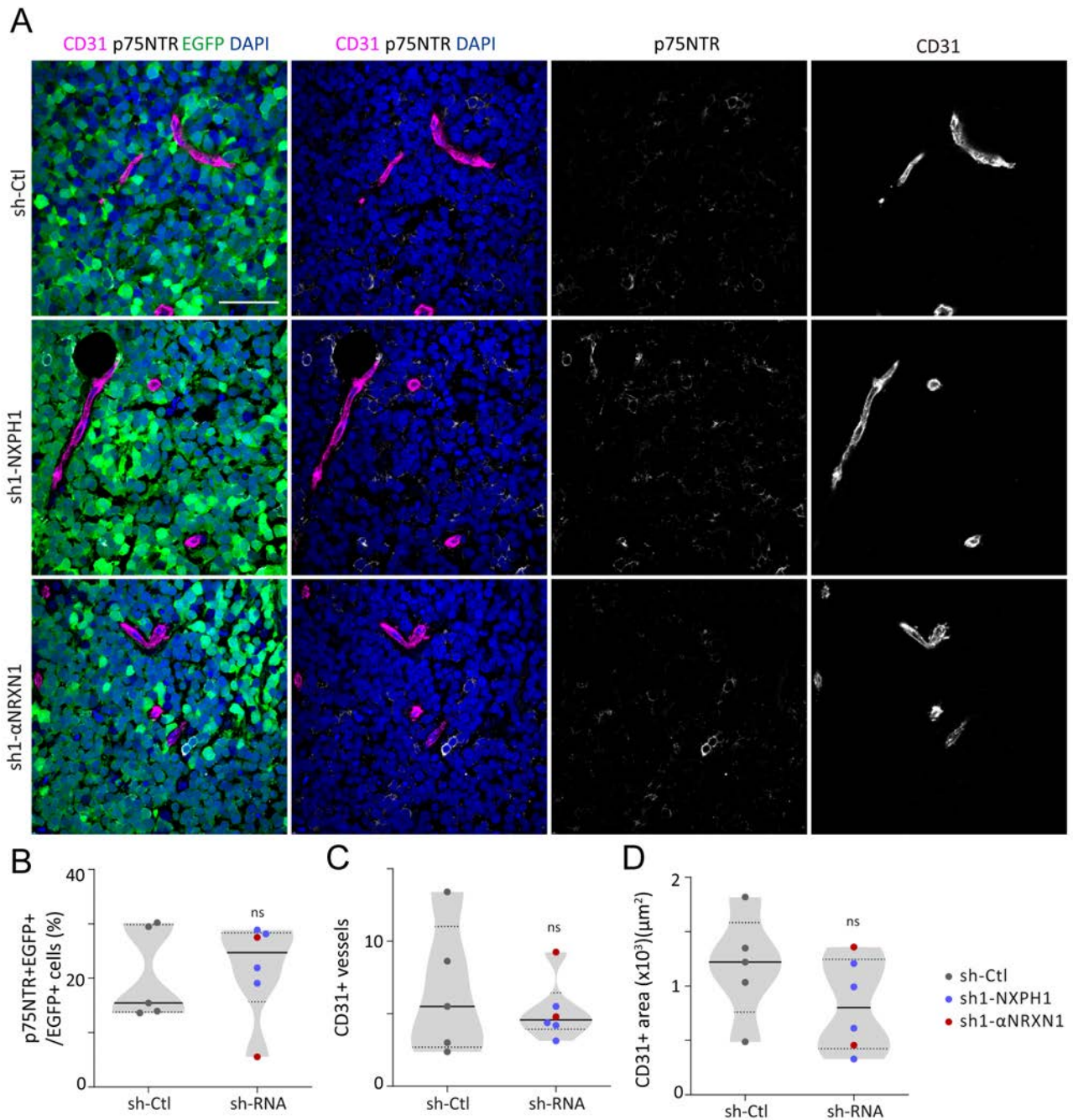


**Figure-32. The inducible inhibition of *NXPH1* or  $\alpha$ -*NRXN1* expression does not affect expression of p75NTR or neovascularization of NB tumours**

(A-D) The p75NTR and CD31 immunoreactivity in sh-RNA-derived xenograft tumours (A), the median percentage of p75NTR+EGFP+ (B), the median number of CD31+ vessels (C), and the median CD31+ area per image (D). Significance was assessed with the non-parametric Mann-Whitney test. Each dot results from the quantification of 6 images obtained from 4-6 tumours. Scale bar: 100 $\mu$ m.



## V. DISCUSSION

---



‘...the fittest will survive,  
and a race will be eventually produced adapted to the conditions in which it lives’

A. R. Wallace

NBs are devastating paediatric tumours that appear in organs derived from the developing SA lineage (Bolande, 1974; Tsubota and Kadomatsu, 2018). These tumours have an intriguing nature due to their heterogeneous clinical behaviour. In about 5 to 10% of the patients, the tumour will spontaneously regress despite a wide metastatic spreading, while half of the patients that present metastasis at diagnosis will succumb to the disease (Matthay *et al.*, 2016; Nakagawara *et al.*, 2018). Along the past decades major efforts have been done for the assessment and stratification of NB patients into risk groups, in order to optimize therapeutic approaches (Brodeur *et al.*, 1993; Brodeur *et al.*, 1988; Cohn *et al.*, 2009; Monclair *et al.*, 2009). According to the INRG, 36% of NB patients are diagnosed as HR (Cohn *et al.*, 2009). Despite aggressive multimodal therapeutic protocols, the 5 years overall survival for HR cases remains below 30-40% (Matthay *et al.*, 2016; Nakagawara *et al.*, 2018; Simon *et al.*, 2011). The therapeutic failure in these patients mainly results from metastatic dissemination and the development of therapy resistance. Recent studies suggest that the intra-tumour heterogeneity of NBs is a key factor contributing to tumour evolution and relapse following therapeutic failure (Boeva *et al.*, 2017; Eleveld *et al.*, 2015; Greaves, 2015; Schramm *et al.*, 2015; van Groningen *et al.*, 2017). The main sources of intra-tumour heterogeneity are genetic, due to mutations that are clonally expanded during tumour growth, and non-genetic, due to the persistence of epigenetic programs that assign a particular cellular identity to the tumour cells, or due to microenvironmental cues. The current data show that NB relapses present a reduction in the clonal heterogeneity as well as a divergent transcriptomic profile and an increased mutational burden, mainly causing activating mutation in *ALK*, loss of function mutation in *CHD5* and activating mutations in the RAS/MAPK pathway (Eleveld *et al.*, 2015; Schleiermacher *et al.*, 2014; Schramm *et al.*, 2015). However, the recurrence rate of most of the detected mutations remained low even after relapse, pointing towards a relevant role of non-genetic sources of tumour heterogeneity (Boeva *et al.*, 2017; Eleveld *et al.*, 2015; Schramm *et al.*, 2015; van Groningen *et al.*, 2017). Compelling evidences suggest the existence of cell subpopulations with tumour propagating capacity in NB tumours, called NBcsc (Boeva *et al.*, 2017; Ciccarone *et al.*, 1989; Hansford *et al.*, 2007; Hirschmann-Jax *et al.*, 2004; Hsu *et al.*, 2013; Newton *et al.*, 2010; Ross and Spengler, 2007; Ross *et al.*, 1983; Ross *et al.*, 2015; van Groningen *et al.*, 2017; Walton *et al.*, 2004). Whether NBs are hierarchically organized or not and the plasticity/shalowness of a putative hierarchy remain although controversial (Tomolonis *et al.*, 2018). Defining NB heterogeneity and stemness potential is fundamental to uncover new therapies that will target the driving force of the NBcsc: their self-renewal ability.

The general aim of this doctoral thesis was to identify a genetic signature for NBcsc, with the ultimate goal of providing new specific molecular markers of these cells and candidate genes that might be useful for the development of future therapeutic strategies targeting NBcsc in HR NBs. I studied the involvement of the secreted glycoprotein NXP1, one of the candidates identified by our double NB/NCC screening, in the regulation of NB malignancy. Our study established that NXP1, acting probably through its receptor  $\alpha$ -NRXN1, is a critical regulator of the tumour-propagating ability in human NB cells. The activities of both NXP1 and  $\alpha$ -NRXN1 are required for the primary growth of NB tumours *in vivo*. Importantly,  $\alpha$ -NRXN1 appears to be specifically expressed by a subpopulation of NB cells that present tumour-propagating properties *in vitro* and that are required to sustain primary NB growth *in vivo*. Nevertheless to fully uncover the role of NXP1 and of the  $\alpha$ -NRXN1<sup>+</sup> NB cells in tumour growth and progression, we need to carefully integrate the preclinical and clinical data.

## 1. NXP1 promotes primary NB growth through $\alpha$ -NRXN1<sup>+</sup> NBcsc-like cells, but might inhibit metastasis and tumour progression

### 1.1. $\alpha$ -NRXN1<sup>+</sup> NB cells are tumour-propagating cells.

Having identified novel molecular regulators of the tumour-propagating function made it possible to infer that the  $\alpha$ -NRXN1 receptor might act as a specific surface marker of the CSCs in NB. Using a fluorescence-conjugated antibody, we showed that  $\alpha$ -NRXN1<sup>+</sup> cells are detected in NB cell lines and PDX samples with low frequencies and that these cells are required to sustain NB growth. Our functional characterization determined that these  $\alpha$ -NRXN1<sup>+</sup> cells are actively-cycling cells with an increased self-renewal capacity and a higher probability to survive upon chemotherapeutic insults. Nevertheless, the functional characterization of this  $\alpha$ -NRXN1<sup>+</sup> subpopulation is not complete and the various caveats of our data need to be discussed.

First, our data revealed that the  $\alpha$ -NRXN1<sup>+</sup> cells present a higher self-renewal capacity, at least at short terms. Deciphering the extent of their capacity is required to understand whether these cells are truly NBcsc and are thus endowed with long-term self-renewal potential, or if they rather represent transient amplifying progenitors able to expand the tumour pool only for short terms. Elucidating this question requires to test their tumour-initiating capacity after serial transplantations of a limited number of tumour cells ( $\alpha$ -NRXN1<sup>+</sup> cells and  $\alpha$ -NRXN1<sup>-</sup>/bulk tumour cells) to ensure that the system is challenged and that the output of the most potent cells is measured. This type of transplantation is known as extreme limited dilution tumour-initiating cell assay (ELDA-TIC assay). To this aim, we

are currently conducting a pilot ELDA-TIC assay whereby 4 dilutions of  $\alpha$ -NRXN1<sup>+</sup> or  $\alpha$ -NRXN1<sup>-</sup> cells, previously purified by FACS, have been subcutaneously transplanted into immunodeficient Nod SCID Gamma (NSG) mice. This experimental setting aims to compare the tumorigenic potential of both cell subpopulations and should allow us to assess the number of tumour cells needed for a definitive assay.

Secondly, one conflicting aspect of our results might be to understand how  $\alpha$ -NRXN1<sup>+</sup> cells persist better upon chemotherapy despite their active cycling behaviour. Several evidences however suggest that a therapeutic treatment can induce the transition to a slow-cycling drug-tolerant state that protects the tumour cells from the drugs' cytotoxic effects (Rambow *et al.*, 2018). We have not explored the cycling profile of the  $\alpha$ -NRXN1<sup>+</sup> cells upon cisplatin or MTX exposure. It thus remains plausible that the  $\alpha$ -NRXN1<sup>+</sup> cells were not actively cycling during the treatment. Additionally, the CSCs as normal SCs frequently present self-guarding mechanisms to prevent DNA damage and the induction of apoptosis. The mechanisms described so far include a higher expression of pump transporters, an upregulation of pro-survival signals, an enhanced DNA repaired capacity or an upregulation of the detoxification pathways, among others (Cojoc *et al.*, 2015; Zhou *et al.*, 2009). Interestingly, lineage tracing experiments in a mouse model of SCC showed how TGF- $\beta$  signalling protects SCCcsc to cisplatin exposure via NRF2/p21, by enhancing the metabolic inactivation of the drug (Oshimori *et al.*, 2015). Interestingly, in a steady state the  $\alpha$ -NRXN1<sup>+</sup> cells show a higher expression of p21 than their negative counterparts. Although we do not know how the drug exposure changes the transcriptomic profile of these cells, it suggests that p21 might protect  $\alpha$ -NRXN1<sup>+</sup> cells from drug-induced DNA damage by a similar mechanism than the one described for SCCcsc.

Finally, it remains to be explored whether  $\alpha$ -NRXN1<sup>+</sup> cells, compared to  $\alpha$ -NRXN1<sup>-</sup> cells, possess a particular transcriptomic and/or epigenomic signature that endows them with a distinct functional behaviour. Identifying the transcriptomic/epigenomic profile of the  $\alpha$ -NRXN1<sup>+</sup> cells could be of clinical relevance since it might allow inferring which pathways are required to sustain their tumour-propagating potential. Unfortunately, our analysis of a panel of genes previously associated to a CSC/SC phenotype has been inconclusive. The use of genome-wide approaches such as full length RNA-sequencing or expression microarrays would be useful to define the transcriptome of this subpopulation in comparison to that of their negative counterparts.

## 1.2. *NXPH1* is required to sustain tumour growth in NB

Using lentiviral shRNA-mediated knockdown, we showed that NB cells are sensitive to modulations in the expression levels of *NXPH1* and  *$\alpha$ -NRXN1*. The reduction of both resulted in impaired tumour growth (*in vivo* & *in vitro*) and reduced short-term self-renewal capacity. Whether the long-term self-

renewal capacity of NB cells is also affected by the downregulation of *NXPH1* or  $\alpha$ -NRXN1 remains to be explored. As mentioned above, the evaluation of the long-term self-renewal potential requires the serial transplant of limited cell numbers into immunocompromised mice. Our results suggest that the downregulation of *NXPH1* or that of  $\alpha$ -NRXN1 did not cause exactly the same effect over tumour growth. Reducing *NXPH1* expression had a major impact over tumour growth and to a lesser extent on tumour incidence, as inferred from the EFS data. Conversely, the inhibition of  $\alpha$ -NRXN1 expression preferentially reduced the tumour incidence but, the few tumours that developed present growth kinetics comparable to the ones shown by the control tumours. This could be due to the  $\alpha$ -NRXN1 receptor responding to various ligands distinct to *NXPH1*, and/or *NXPH1* acting through other  $\alpha$ -NRXNs receptors also expressed by the NB cells. In this regard, the presence of  $\alpha$ -NRXN2 on the cell membrane of NB cells should not be discarded. Indeed, the expression of  $\alpha$ -NRXN2 was also markedly increased in the human NB cell lines grown in conditions of stem cell-enrichment. Unfortunately, the absence of an available fluorophore-conjugated anti- $\alpha$ -NRXN2 antibody prevented the analysis of its expression in live samples. Previous data from rat and mouse models suggest that  $\alpha$ -NRXN1 and  $\alpha$ -NRXN2 can be co-expressed in the same neuron where they play partially overlapping functions (Missler *et al.*, 2003; Ullrich *et al.*, 1995). Therefore, it is plausible that *NXPH1* is also acting through this receptor in NB cells. Elucidating the detailed mechanism by which *NXPH1*/ $\alpha$ -NRXN1 signalling targets the growth of NB xenografts would be informative. Our data suggest that *NXPH1* promotes NB growth by stimulating the proliferation of actively dividing cells and increasing the presence of p75NTR+ NB cells. p75NTR (also known as NGFR or CD271) is a surface marker of the pluripotent migratory NCCs in humans and other animals (Betters *et al.*, 2010; Morrison *et al.*, 1999). It codes for the Low Affinity Nerve Growth Factor Receptor that binds to NGF, BDNF, NT-3 and NT-4 (Dechant and Barde, 2002; Gentry *et al.*, 2004). Its role in NCC development remains unclear, although it might control cell survival and cell death in response to Nerve Growth Factor (Cortazzo *et al.*, 1996). Interestingly, the expression of p75NTR is increased in a transient drug-tolerant NCC-like population that appears during MRD in melanoma and that is responsible of tumour relapse (Rambow *et al.*, 2018). Of note, in our CAM assay, p75NTR+ NB cells appeared to be preferentially located close to the vascular niche. The preferential location of the CSCs in close contact with the capillary bed has already been described in other types of tumour (Bao *et al.*, 2006; Calabrese *et al.*, 2007; Charles *et al.*, 2010; Fessler *et al.*, 2015; Folkins *et al.*, 2009; Li *et al.*, 2009). Further experiments would be required to determine whether the growth-promoting activity of *NXPH1* is due to the activation of the  $\alpha$ -NRXN1+ NBcsc-like subpopulation. Repeating the *NXPH1* treatment in the presence of the decoy receptor might help answering this question. Additionally, it would be interesting to address whether  $\alpha$ -NRXN1+ and p75NTR+ cells correspond to the same cell subpopulation or not. To assess these questions, we could study by FACS whether  $\alpha$ -NRXN1 and p75NTR are expressed by the same cellular subpopulation. If it is the case, using the anti-p75NTR antibody will allow us to study the distribution of the p75NTR+/ $\alpha$ -NRXN1+ cells.

$\alpha$ -NRXN1+ NB cells within the tumour architecture. This data might be informative of the putative niche components of the  $\alpha$ -NRXN1+ NBcsc-like. Conversely, if they are expressed by different sub-populations, it would be interesting to clarify their causal relationship. In this scenario, the action of *NXPH1* on the  $\alpha$ -NRXN1+ cells might induce the proliferation of the neighbouring p75NTR+ subpopulation through paracrine signalling. Alternatively, *NXPH1* might promote the proliferation of  $\alpha$ -NRXN1+ cells and induce the expression of p75NTR as two concomitant events.

In conclusion, the revision of our preclinical data leads us to propose that *NXPH1* stimulates primary NB growth, probably by activating  $\alpha$ -NRXN1+ NBcsc-like cells (Figure 33A).

### 1.3. *NXPH1* expression inversely correlates with bad prognosis and tumour progression

*NXPH1* was retrieved by a double genetic screening aimed to recover genes involved in the regulation of the NBcsc phenotype. In order to do so, we compared the genes that were differentially expressed between clinically relevant NB subgroups with those differentially expressed by early chick NCCs. Our double screening strategy identified 6 genes that are enriched in the early NCC population and differentially expressed in the pair-wise NB comparison. Surprisingly our 6 candidates show a strong correlation with a favourable outcome in the HSJD cohort. Using this data to devise the role of *NXPH1* in NB requires reviewing the current model of tumour growth and progression.

The evolution towards a more aggressive tumour growth is characterized by the emergence of therapy-resistant relapses and metastasis, and depends on the selection and expansion of tumour cells with tumour propagating capacity. The tumour microenvironment has a prominent role in the regulation of the plasticity and the proliferative behaviour of these CSCs; however, the progressive accumulation of genetic/epigenetic changes along tumour progression promotes the acquisition of a cell-autonomous self-renewal behaviour that is expanded to most of the tumour cells. These genetic/epigenetic changes also cause the transient or steady acquisition of other malignant traits such as metastatic capacity or drug tolerance by different subsets of CSCs, turning the CSC phenotype progressively independent of the environmental control and favouring the metastatic dissemination and a more indolent tumour growth (Greaves, 2015; Kreso and Dick, 2014; Marjanovic *et al.*, 2013; Meacham and Morrison, 2013).

A overall perspective of our clinical and preclinical data leads us to question how *NXPH1* expression is inversely correlated with a bad prognosis if our results demonstrate that *NXPH1* promotes NB growth, probably by activating  $\alpha$ -NRXN1+ NBcsc-like cells. Considering the dynamic of tumour growth and the different constrains along tumour progression, our current hypothesis is that *NXPH1* might play an inhibitory role in the acquisition of an aggressive phenotype, probably by repressing metas-

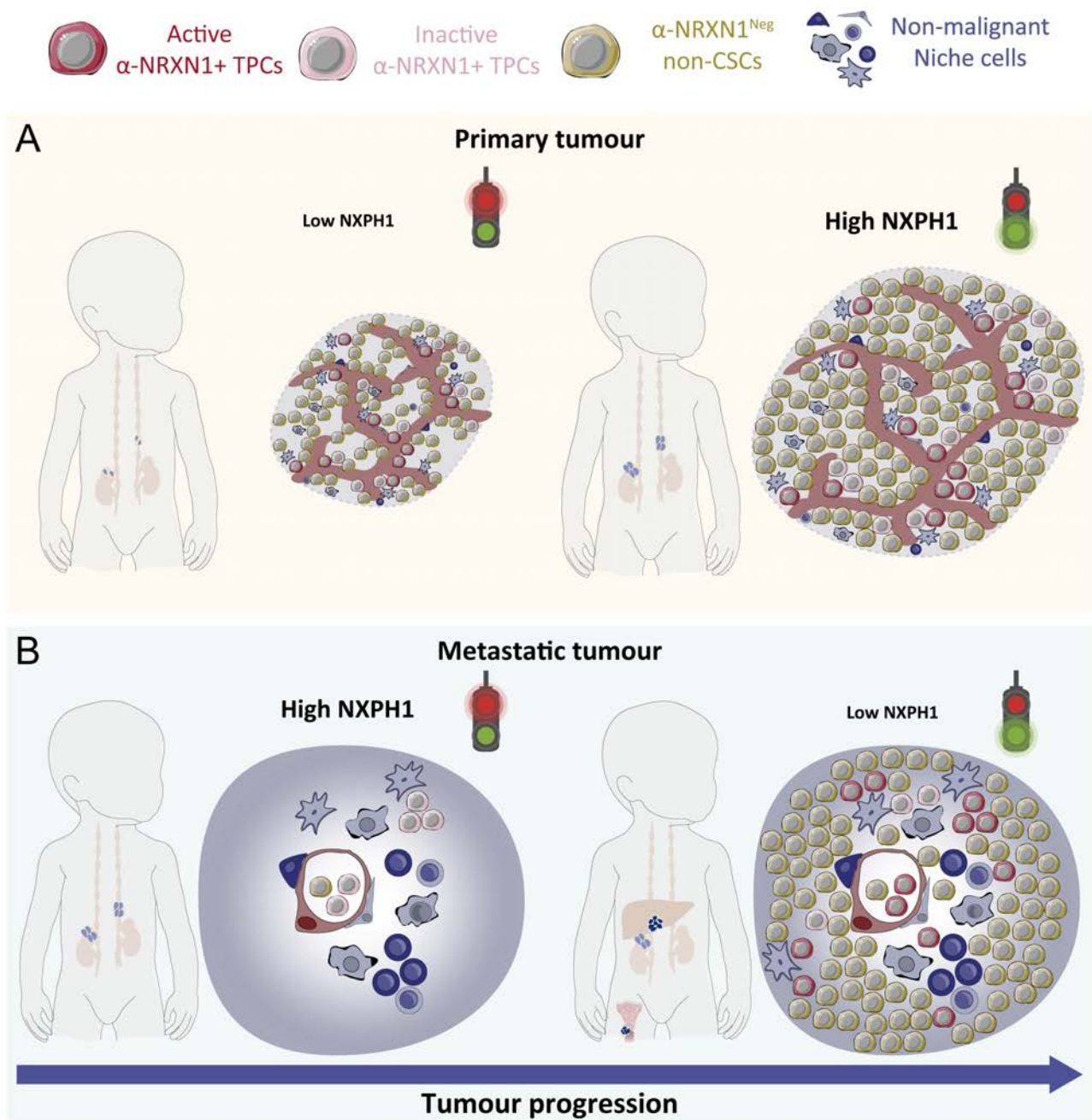


**Figure-33. *NXPH1*, through its receptor  $\alpha$ -*NRXN1*, might control the tumour propagating capacity of NB cells upon metastatic dissemination**

(A) Early in tumour evolution NB seems to have higher levels of *NXPH1* and the  $\alpha$ -*NRXN1*+ tumour propagating cells might contribute to tumour growth in the primitive location. The presence of high levels of *NXPH1* might avoid tumour dissemination and/or the effective engraftment of NB cells at secondary location (B) Along tumour evolution the progressive accumulation of genetic and epigenetic changes favours the acquisition of more malignant traits such as an increase in the tumour propagating potential or the acquisition of drug-tolerant or metastatic phenotypes. The downregulation of *NXPH1* expression along tumour progression might facilitate the metastatic burden of NB cells at secondary sites.

tasis (Figure 33B). Interestingly, the loss of *NXPH1* expression along tumour progression has already been described in breast cancer, pancreatic ductal adenocarcinoma and NB (Decock *et al.*, 2016a; Faryna *et al.*, 2012; Hong *et al.*, 2012; Jin and Tsai, 2016; Tommasi *et al.*, 2009; Warnat *et al.*, 2007). During the course of this doctoral thesis, the methylation of *NXPH1* promoter was proposed as a new

prognostic biomarker in NB since the extensive hypermethylation of the CpG promoter region of *NXPH1* gene largely correlates with a low OS and EFS of the patients (Decock *et al.*, 2016a). Thereby, if our working model were to be validated experimentally, the epigenetic silencing of *NXPH1* expression along NB progression might be related to the acquisition of certain malignant traits such as metastatic potential.

#### 1.4. *NXPH1* might inhibit NB metastasis and/or tumour dissemination

The relative *NXPH1* levels in the HSJD cohort suggest that patients with a good prognosis (normally non-metastatic and without *MYCN* amplification) present a higher expression of *NXPH1* than patients with a worst prognosis (normally metastatic and/or with *MYCN* amplification). To further validate our hypothesis we took advantage of the SEQC-498 dataset, a cohort of NB patients where the progression of the disease and the patients' survival has been reported (Su *et al.*, 2014). In the SEQC-498 cohort, *NXPH1* is differentially expressed between the group of patients that do not progress and those whose disease progress (FC:2.22,  $p < 0.001$ ; Figure 34A). The relative levels of *NXPH1* are independent of the patients' outcome when the NB does not progress (Figure 34B). However, high levels of *NXPH1* are associated with a better outcome in patients showing tumour progression (Figure 34C). These data support a model where the downregulation of *NXPH1* expression is induced or selected in the tumour cells during NB progression. Whenever NB cells with tumour propagating capacity (maybe the  $\alpha$ -NRXN1+ NBcsc-like) manage to escape the primary tumour and settle into distant organs, the levels of *NXPH1* might dictate whether these disseminated cells are able to self-renew outside of their original environment or not.

To test our working hypothesis, we are currently evaluating how reducing *NXPH1* or  $\alpha$ -NRXN1 expression affects the metastatic capacity of NB cells using an experimental model of metastasis in NSG mice. To this aim, we have engineered our sh-RNA clones to express a luciferase reporter, so that the metastatic seeding and the subsequent formation of "secondary" tumours can be monitored *in vivo*. Tumour cells are directly introduced into the systemic circulation via an injection into the left ventricle of the heart. The intra-cardiac injection allows assessing the homing of the tumour cells towards their preferential target organs and the metastatic growth. If our working model is correct, the downregulation of *NXPH1* should increase the metastatic growth of NB cells. Testing the behaviour of the sh- $\alpha$ NRXN1 cells will help us elucidating whether the expression of  $\alpha$ -NRXN1 is also required for metastatic dissemination.

To the best of our knowledge our work provides the first experimental evidence showing that *NXPH1* exerts a functional role in NB progression and malignancy. If our working model were to be validated experimentally, it would provide a framework for the development of new therapeutic ap-

proaches aimed at targeting the self-renewal potential of metastatic NBcsc and thereby improving the outcome of HR NB patients.

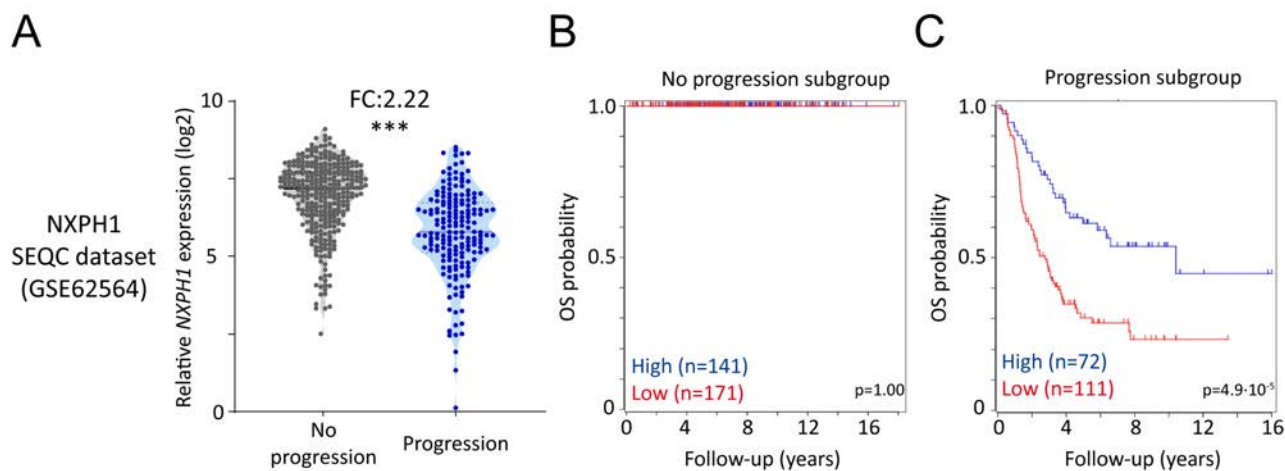


**Figure-34. NXP1 is downregulated along tumour progression**

(A) Violin plots showing NXP1 expression levels in SEQC cohort subgroups showing or not NB progression (B-C) Kaplan-meier overall survival curves in the SEQC cohort subdivided according to the absence of disease progression (B) or effective progression (C), based on high (above the average) and low (below the average) NXP1 expression. Statistical significance was assessed using Mann-Whitney test (A) or it was automatically assessed by R2-server using logrank test (B-C). OS: Overall survival.

## 2. A NCC-like program might have different roles during NB initiation and tumour progression

The fact that the CSCs and the normal SCs of their tissue of origin share many similarities has been exploited to identify CSC populations in different types of cancers (Dalerba *et al.*, 2011; Merlos-Suarez *et al.*, 2011; Pece *et al.*, 2010; Spike *et al.*, 2012). In the case of NB, a major handicap in performing a comparative transcriptomic analysis between NB tumours and their normal stem cell counterparts is the absence of the original tissue (the NCCs) at the moment of tumour diagnosis. The NCCs are a transient embryonic population that is specified very early during embryonic development. In the human embryo, the specification and the onset of migration of the NCCs occur as early as 2.5 to 4 weeks of gestation. Migration, proliferation and differentiation of committed SA precursors occur concomitantly from the week 4 until around birth; although some immature neuroblasts remain intermingled with the more differentiated sympathetic neurons/chromaffin cells during infancy (Bolande, 1974; Turkel and Itabashi, 1974). Hence, at the moment of tumour diagnosis the equivalent healthy stem cell population does not exist anymore. Cultures of NCCs derived from *in vitro* differentiation of human embryonic stem cells (hESCs) and of primary human NCC purified from early abortions have

been used as alternative sources (Bajpai *et al.*, 2010; Thomas *et al.*, 2008). This type of material has been used to unravel the epigenomic regulation of the NCC plasticity and migratory behaviour (Bajpai *et al.*, 2010; Rada-Iglesias *et al.*, 2012; Thomas *et al.*, 2008). During the course of this doctoral thesis, these models were used for the prospective identification of NCC-like cellular states in primary and cell line-derived NBs by two independent groups (Boeva *et al.*, 2017; van Groningen *et al.*, 2017). However, the long term *in vitro* culture of primary human NCCs or hESCs-derived NCCs might not faithfully reflect the endogenous NCC population, especially with regards to their relation with their physiological microenvironment.

In our study, we used freshly sorted embryonic NCCs to identify a transcriptome shared with NB cells. In order to do so, we took advantage of the early chick embryo as a source of NCCs. The analogy of human and chick embryos during early development is widely accepted and is especially relevant for the study of NCC development (Le Douarin, 2004; Zheng *et al.*, 2017). In a previous study fulfilled in our lab, *LMO4* was retrieved from a meta-analysis comparing our NCC signature and a NB signature accessible through the Neuroblastoma Gene Server. This study further demonstrated that the functional role of *LMO4* during NCC delamination as well as in the migratory and invasive behavior of NB cells (Ferronha *et al.*, 2013). To identify more specifically the genes that might be relevant for NB malignant progression, we took advantage of a pair-wise comparison between clinically and biologically relevant NB subgroups (Gomez *et al.*, 2015). Our double screening strategy identified 6 genes that are enriched in the early NCC population and differentially expressed in the pair-wise NB comparison.

## 2.1. The process of malignant transformation is accompanied by a re-activation of a NCC-like program

Despite the undeniable prognostic value of all the genes retrieved by our double screening, two major issues caught our attention. Firstly, the scarcity of the 'signature' retrieved by our screening and secondly, its unexpected correlation with a better patient outcome. The latter might be particularly counterintuitive; especially considering that we aimed to discover a CSC signature. Nevertheless, at least 2 distinct arguments might explain our findings.

The first possibility might be that we somehow recovered a 'differentiation' signature; a notion that would explain why all our candidates correlate with a better prognosis. Remarkably, 2 (*NXP1* and *PMP22*) out of the 6 genes retrieved, are induced during neuronal differentiation and play roles in neural development and synapse formation (Apostolova *et al.*, 2007; Petrenko *et al.*, 1996). However, all the tumour biopsies included in the expression array were carefully examined by a pathologist and only those with less than 30% of healthy neighbouring tissue were included for further profiling. It raises the possibility though that the 'differentiation' signature could result from the presence of

maturing NB cells naturally present in these tumour samples. NB tumours from the good prognosis groups present a favourable histology characterized by the presence a low proportion of maturing malignant neuroblasts (less than 5% of the total cancer cells) (Shimada *et al.*, 1999). We cannot discard that a strong expression coming from these cells contaminated our signature. Yet, it is intriguing to note that the same ‘differentiation’ genes were also enriched in the early migratory and pre-migratory NCC signature, considering that these cells are still pluripotent and do not present any prospective sign of lineage commitment at this early developmental stage (Baggiolini *et al.*, 2015; Furlan *et al.*, 2017; Soldatov *et al.*, 2019; Thomas *et al.*, 2008). Therefore, the recovery of a ‘differentiation’ signature appears unlikely and does probably not account for the complexity of our results.

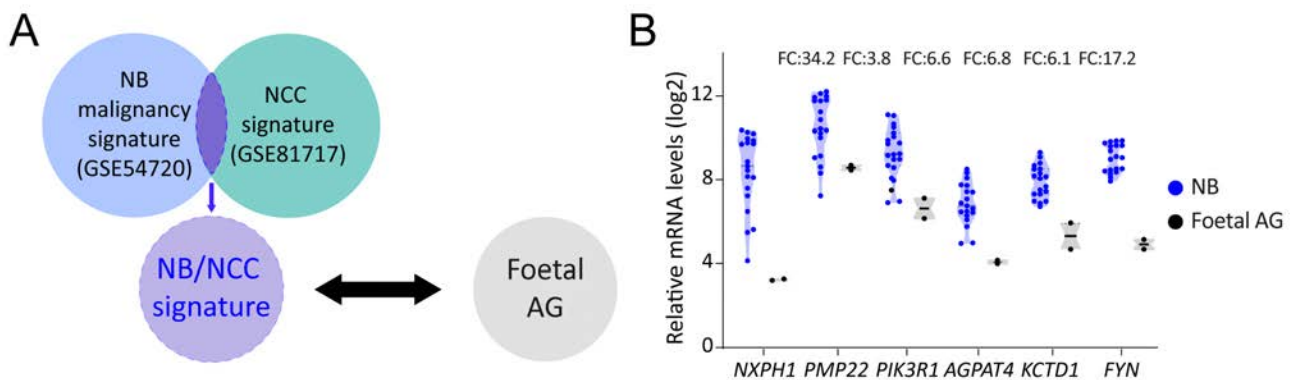


**Figure-35. Double genetic screening genes are downregulated along tumour progression**

(A) The relative expression of our candidate genes in the NB HSJD cohort was compared to their relative expression in human foetal adrenal gland. (B) Violin plot showing relative mRNA levels of each of our candidate genes in the HSJD cohort (purple) and in the human foetal adrenal gland (grey). AG: adrenal gland; DEGs: differentially expressed genes; FC: fold change; NB: Neuroblastoma.

The second possibility considers the nature of our double-screening and the dynamic of tumour growth and progression. We took for the double screening only those genes that were differentially expressed between clinically relevant NB subgroups. This implies that the genes were differentially expressed between the healthy tissue (for instance the adrenal gland or the sympathetic ganglia) and the tumour tissue (the NB) but that remained stable along tumour progression were initially discarded. However, the putative contribution of the latter to the deregulation of the self-renewal potential of the non-cancer or cancer cells cannot be neglected. Therefore, our stringent pre-requisite might have introduced a bias in our screening towards those genes whose expression is modulated along with tumour progression. To infer the putative relevance of our candidate genes in early NB disease, I have compared the expression of our 6 candidate genes in the HSJD cohort with two samples of human foetal adrenal gland that were included in the same expression microarray but discarded from further use (Figure 35A-B). Consistent with a putative role in malignant transformation or the initial tumour expansion, the expression of our 6 candidates is increased in the NB samples compared to the foetal adrenal gland (Figure 35B). These data suggest that the process of malignant transformation in NB appears to be accompanied by a re-activation of certain NCC features (Figure 36, left panel).

Nevertheless, it might be interesting to repeat the NB/NCC double screening using the broad transcriptome of the HSJD cohort in order to faithfully retrieve the complete NCC-like fingerprint of NB tumours.

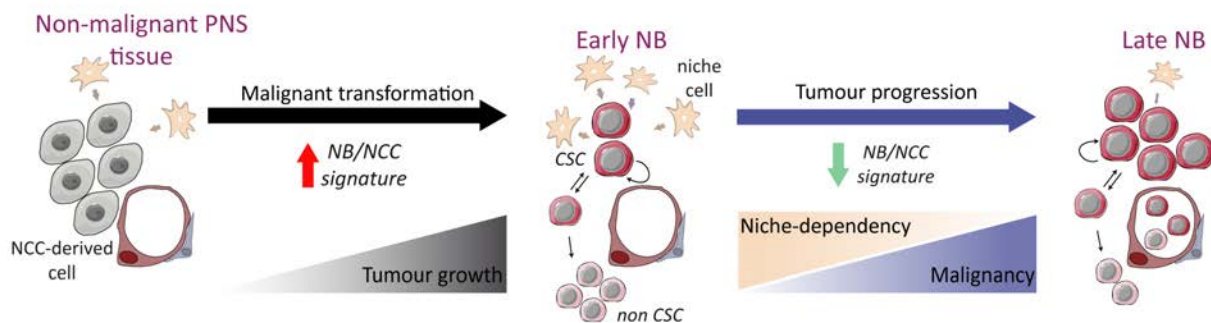


**Figure-36. Working model of NB initiation and progression where the loss of NB/NCC signature might be required for disease progression**

Timeline of neuroblastoma initiation and progression, showing the putative upregulation of the NB/NCC signature during malignant transformation or early tumour growth and how these genes are downregulated along tumour progression. These seem to occur concomitantly with the acquisition of other malignant traits such as an increase in the cell-autonomous tumour propagating capacity, the shallowness of the underlying developmental hierarchy or the acquisition of metastatic capacity. CSC: cancer stem cell; NCC: Neural crest cells; NB: Neuroblastoma.

## 2.2. The process of tumour progression is accompanied by a deactivation of certain NCC features and the loss of the niche-dependency

The control that the environment exerts over the NB tumour cells has been revealed in preclinical models. NB cells from cell lines and primary samples are able to respond to the embryonic cues that drive normal NCC development. Upon transplantation into their physiological environment in the chick embryo, NB cells integrate into the stereotypic migratory pathways of the NCCs to reach their ‘natural’ destination (Delloye-Bourgeois *et al.*, 2017). Once arrived at the presumptive adrenal gland and depending on the initial cell input, NB cells are able to integrate into the normal tissue architecture and even display morphological changes associated with an incipient differentiation (Carter *et al.*, 2012). When transplanted in substantial numbers, NB cells formed tumour masses in the adrenal primordia (Delloye-Bourgeois *et al.*, 2017). Interestingly, the embryonic environment, through SEMA3C/NRP/PLXNA4 signalling, ‘imposes’ a benign cohesive behaviour to the NB cells that in response form compact and well-defined tumours. Conversely, inhibiting the activity of this pathway induces the dispersion of the cells from the primary tumour and their metastatic spreading to local and distant secondary organs (Delloye-Bourgeois *et al.*, 2017). This elegant work highlights the plastic nature of the NB cells and the undeniable role of the tumour microenvironment in the regulation of NB malignancy. It also raised the question about whether the loss of the genes involved in the communication between the tumour cells and their microenvironment might contribute to the metastatic dissemination and tumour progression in the patients.

If the NB/NCC signature is truly associated with the CSC phenotype, we might have restricted the scope of our double screening to those genes plausibly involved in: 1) the maintenance of the hierarchical organization of the tumour, 2) the environmental control of the self-renewal potential, 3) the repression of the other malignant traits that are acquired by the self-replicative NBcsc along tumour growth such as the 'metastatic' phenotype. To be the case, the loss of these genes along tumour progression might: 1) expand the self-renewal capacity of the NB cells, increasing the number of NBcsc in the tumour, 2) render the NBcsc progressively independent of the environmental signals, 3) favour the acquisition of other malignant traits such as a 'metastatic' phenotype or drug tolerance by subpopulations of NBcsc. Either of these circumstances will contribute to a more virulent behaviour and the progression of the disease. Interestingly, when we check the expression of our candidate genes in relation with NB progression, all of them show a similar profile to that of *NXPH1* (Figure 34 and data not shown).

Collectively, our data together with the previous literature suggest that NB progression might be accompanied by a deactivation of certain NCC-related features such as the environmental control of the NBcsc phenotype/behaviour. If so, the downregulation of the expression of the NB/NCC candidate genes might 'lock' somehow the tumour cells in a cell-autonomous state with self-renewal potential and possibly metastatic/drug-tolerant properties at the expense of their capacity to respond to environmental cues (Figure 36, right panel). How the expression of these genes is lost or reduced remains unknown although their epigenetic silencing by DNA methylation appear to be a plausible possibility. Reinstating the environmental control over NB cells arises as a new and promising therapeutic approach to hamper tumour progression in high risk patients. Further research will be needed to validate this hypothesis.

### 2.3. What is known about these other candidate genes in the context of NB and cancer

A systematic review of the previous literature confirmed the role of some of our candidate genes in cancer progression, supporting the relevance of our approach to uncover genes potentially implicated in NB malignancy. A brief description of these candidates (other than *NXPH1*) is included hereafter:

- o The gene *PMP22* codes for the transmembrane protein Peripheral Myelin Protein 22, that is an important component of the myelin sheath. *PMP22* is expressed by the Schwann cells in the peripheral nervous system (PNS), where it participates in PNS development. It might also contribute to the regulation of cell growth in other tissues (Baechner *et al.*, 1995; Notterpek *et al.*, 2001;

Snipes *et al.*, 1992). A role for PMP22 in the proliferation and invasion of osteosarcoma and breast cancers has been described in preclinical models, but no clinical validation has been published to date (Tong *et al.*, 2010; van Dartel and Hulsebos, 2004; Winslow *et al.*, 2013).

- o The gene *PIK3R1* codes for the Regulatory Subunit 1 of the Phosphoinositide-3-Kinase (also known as p85 or p85 $\alpha$ ). PI3KR1 is one of the main intracellular components of the PI3K/AKT/mTOR pathway that controls cell polarity, growth, proliferation and survival in response to various extracellular signals (Bilanges *et al.*, 2019). Somatic mutations in *PIK3R1* have so far been reported in endometrial and bladder cancers (Ross *et al.*, 2013; Urick *et al.*, 2011). Detection of PI3KR1 levels together with those of 5 other PI3K isoforms were proposed to be predictive of the disease stage in NB (Fransson *et al.*, 2013).
- o The gene *FYN* codes for the proto-oncogene TKs FYN. FYN belongs to the Src family of non-receptor TKs and acts downstream of several TK surface receptors and integrins commonly involved in cell growth, axon guidance and neurite extension, and T and B-cell signalling (Saito *et al.*, 2010). In prostate and GB tumours, the overexpression of FYN is associated to cancer progression and metastasis (Gururajan *et al.*, 2015; Lu *et al.*, 2009; Posadas *et al.*, 2009). Conversely, its expression is reduced during NB progression and was proposed to be predictive of the long-term survival of NB patients independently of *MYCN* amplification (Berwanger *et al.*, 2002). As it maybe anticipated from its role in normal neural development, a role of FYN of NB differentiation was also suggested in experimental models (Berwanger *et al.*, 2002).
- o The gene *AGPAT4* codes for the 1-Acylglycerol-3-Phosphate O-Acyltransferase 4, one of the key enzymes involved in lipid metabolism. AGPAT4 resides in the endoplasmic reticulum where it catalyses the first steps of triacylglycerol synthesis, the conversion of glycerol-3-phosphate or acyl-CoA to 1-acylglycerol-3-phosphate (Takeuchi and Reue, 2009). A putative role of *AGPAT4* in cancer biology has not been reported to date.
- o The gene *KCTD1* codes for the Potassium Channel Tetramerization Domain Containing 1 protein, a poorly characterized transcriptional repressor. The direct repression of of the activity of the family of AP2 TFs by KCTD1 has been reported in experimental models, but whether it occurs physiologically is unknown (Ding *et al.*, 2009). Nevertheless, the AP2 TF family has an essential role in neural crest induction during early embryogenesis (de Croze *et al.*, 2011). A FGFR2-KCTD1 fusion protein was recently described in a genomic analysis of biliary tract cancer patients (Nakamura *et al.*, 2015). A putative role for KCTD1 in NB has not been reported to date.

### 3. The road ahead: unravelling tumour heterogeneity in the single cell genomics era

Tumours are complex ecosystems composed of multiple malignant and non-malignant cell populations that cooperate and compete to foster tumour growth (Greaves, 2015; Suva and Tirosh, 2019). Tumour growth has to be addressed in the context of an evolutionary framework, where the intra-tumour heterogeneity is the starting material for the evolution of the tumour. The ultimate goal of the dynamic of tumour growth will be thus to maximize the fitness of the tumour ecosystem (McGranahan and Swanton, 2017). The way towards new therapeutic approaches requires the integrative study of the different sources of intra-tumour heterogeneity and of the biological pathways that drive the different tumour growth dynamics (Hanahan and Weinberg, 2011; McGranahan and Swanton, 2017). A major criticism of the CSC model is that it over-simplifies a very complex genetic disease (Kreso, 2012). So far, most studies described the presence of CSCs without any reference to their genetic status, thus underestimating the intrinsic heterogeneity of these cells. The advent of single-cell genomics enables for the first time the profiling of the genetic and transcriptomic diversity of a tumour at a cellular level. The main advantages of single-cell profiling are that: 1) it enables the unbiased profiling of the different cellular populations that comprise the tumour; 2) it does not require prior population/cell type enrichment; 3) it requires a very low material input. Despite presenting several drawbacks such as its cost or the sub-optimal resolution of extremely rare cell populations and low expressed transcripts, the use of single-cell multi-OMICs should allow answering several complex questions in the coming years. Some relevant conundrums that might benefit from this approach could be:

- o To what extent does the cellular composition of a tumour correlate with the genetic alterations harboured by tumour cells?
- o What is the evolutionary relationship between the different genetic clonal populations and what is the relationship between the different cellular states?
- o How does the genetic and/or functional diversity of the tumour evolve throughout the progression of the disease?
- o Are the therapy-driven changes observed in the tumour population dependent on genetic changes or on the epigenetic reprogramming of pre-existing clones?

Up to now, single-cell genomics have already enabled the identification of new biologically meaningful markers of CSCs in GB and melanoma (Neftel *et al.*, 2019; Rambow *et al.*, 2018), the characterization of the functional diversity of non-malignant cell populations of the tumour microenvironment (Kumar *et al.*, 2018), the identification of transient and rare cell states previously undetected

---

in melanoma (Rambow *et al.*, 2018), to infer the putative cell of origin in H3K27M gliomas (Filbin *et al.*, 2018), to provide a definitive stratification of tumour subtypes in medulloblastoma (Hovestadt *et al.*, 2019) or to distinguish the contributions of the genetic and non-genetic mechanisms causing the intra-tumour heterogeneity in acute myeloid leukaemia, H3K27M-glioma, IDH-glioma and oligodendroglioma (Filbin *et al.*, 2018; Tirosh *et al.*, 2016; van Galen *et al.*, 2019; Venteicher *et al.*, 2017).

Regarding NB, no one has so far reported the tumour diversity at the single-cell level. The cellular composition of NB tumours has been only inferred from the analysis of primary samples and cell lines by bulk RNA-seq and Chip-seq, hence the authors could not evaluate the genetic status of the cellular states identified (Boeva *et al.*, 2017; van Groningen *et al.*, 2017). Therefore, uncovering NB heterogeneity at the light of the new single-cell multi-omics tools should allow a more comprehensive and nuanced understanding of NB complexity along tumour progression and should pave the way for the development of new therapeutic approaches that will tackle this fatal disease. In the present work, employing such techniques should allow us to define the specificity of the transcriptomic profile and the genetic status of  $\alpha$ -NRXN1+ cells, and might further help us determining whether  $\alpha$ -NRXN1+ cells indeed correspond to the bona fide NBcsc or if they rather represent a subpopulation of NBcsc.



## VI. CONCLUSIONS

---



---

The work realized during the course of this doctoral thesis led to the main following conclusions:

1. We identified 6 genes (*NXPH1*, *PMP22*, *FYN*, *AGPAT4*, *PIK3R1* and *KCTD1*) that are both differentially expressed between clinically-relevant NB subgroups and enriched in early NCCs, and which might thus be relevant to NB tumour propagating potential and malignancy.
2. The expression of our candidate gene *NXPH1* and that of its receptors  $\alpha$ -*NRXN1/2* positively correlates with NB stemness *in vitro*.
3. The expression of the *NXPH1* receptor,  $\alpha$ -*NRXN1*, identifies a subpopulation of NB cells that present stem cell-like properties in NB cell lines and PDXs.
4. This subpopulation of  $\alpha$ -*NRXN1*+ NB cells is required for NB growth *in vivo*.
5. The activity of *NXPH1* and  $\alpha$ -*NRXN1* sustains NB growth *in vivo*.
6. *NXPH1* seems to promote NB growth by stimulating the activation or proliferation of NB cells with tumour propagating potential.



## VII. REFERENCES

---



## REFERENCES

- Al-Hajj, M., Wicha, M.S., Benito-Hernandez, A., Morrison, S.J., and Clarke, M.F. (2003). Prospective identification of tumorigenic breast cancer cells. *Proc Natl Acad Sci U S A* 100, 3983-3988.
- Alaminos, M., Davalos, V., Cheung, N.K., Gerald, W.L., and Esteller, M. (2004). Clustering of gene hypermethylation associated with clinical risk groups in neuroblastoma. *J Natl Cancer Inst* 96, 1208-1219.
- Alvero, A.B., Chen, R., Fu, H.H., Montagna, M., Schwartz, P.E., Rutherford, T., Silasi, D.A., Steffensen, K.D., Waldstrom, M., Visintin, I., *et al.* (2009). Molecular phenotyping of human ovarian cancer stem cells unravels the mechanisms for repair and chemoresistance. *Cell Cycle* 8, 158-166.
- Amler, L.C., and Schwab, M. (1989). Amplified N-myc in human neuroblastoma cells is often arranged as clustered tandem repeats of differently recombined DNA. *Mol Cell Biol* 9, 4903-4913.
- Anderson, K., Lutz, C., van Delft, F.W., Bateman, C.M., Guo, Y., Colman, S.M., Kempinski, H., Moorman, A.V., Tittley, I., Swansbury, J., *et al.* (2011). Genetic variegation of clonal architecture and propagating cells in leukaemia. *Nature* 469, 356-361.
- Ando, K., Ohira, M., Ozaki, T., Nakagawa, A., Akazawa, K., Suenaga, Y., Nakamura, Y., Koda, T., Kamijo, T., Murakami, Y., *et al.* (2008). Expression of TSLC1, a candidate tumor suppressor gene mapped to chromosome 11q23, is downregulated in unfavorable neuroblastoma without promoter hypermethylation. *Int J Cancer* 123, 2087-2094.
- Apostolova, G., Dorn, R., Ka, S., Hallbook, F., Lundeberg, J., Liser, K., Hakim, V., Brodski, C., Michaelidis, T.M., and Dechant, G. (2007). Neurotransmitter phenotype-specific expression changes in developing sympathetic neurons. *Mol Cell Neurosci* 35, 397-408.
- Askanazy, M. (1907). Die Teratome nach ihrem Bau, ihrem Verlauf, ihrer Genese und im Vergleich zum experimentellen Teratoid. *Verhandl Deutsch Pathol* 11, 39-82.
- Attiyeh, E.F., London, W.B., Mosse, Y.P., Wang, Q., Winter, C., Khazi, D., McGrady, P.W., Seeger, R.C., Look, A.T., Shimada, H., *et al.* (2005). Chromosome 1p and 11q deletions and outcome in neuroblastoma. *N Engl J Med* 353, 2243-2253.
- Avantaggiato, V., Dathan, N.A., Grieco, M., Fabien, N., Lazzaro, D., Fusco, A., Simeone, A., and Santoro, M. (1994). Developmental expression of the RET protooncogene. *Cell Growth Differ* 5, 305-311.
- Bacelli, I., Schneeweiss, A., Riethdorf, S., Stenzinger, A., Schillert, A., Vogel, V., Klein, C., Saini, M., Bauerle, T., Wallwiener, M., *et al.* (2013). Identification of a population of blood circulating tumor cells from breast cancer patients that initiates metastasis in a xenograft assay. *Nat Biotechnol* 31, 539-544.
- Bachetti, T., and Ceccherini, I. (2019). Causative and common PHOX2B variants define a broad phenotypic spectrum. *Clin Genet*.
- Baechner, D., Liehr, T., Hameister, H., Altenberger, H., Grehl, H., Suter, U., and Rautenstrauss, B. (1995). Widespread expression of the peripheral myelin protein-22 gene (PMP22) in neural and non-neural tissues during murine development. *J Neurosci Res* 42, 733-741.
- Bagchi, A., Papazoglu, C., Wu, Y., Capurso, D., Brodt, M., Francis, D., Bredel, M., Vogel, H., and Mills, A.A. (2007). CHD5 is a tumor suppressor at human 1p36. *Cell* 128, 459-475.

- Baggiolini, A., Varum, S., Mateos, J.M., Bettosini, D., John, N., Bonalli, M., Ziegler, U., Dimou, L., Clevers, H., Furrer, R., *et al.* (2015). Premigratory and migratory neural crest cells are multipotent in vivo. *Cell Stem Cell* 16, 314-322.
- Bahena-Ocampo, I., Espinosa, M., Ceballos-Cancino, G., Lizarraga, F., Campos-Arroyo, D., Schwarz, A., Maldonado, V., Melendez-Zajgla, J., and Garcia-Lopez, P. (2016). miR-10b expression in breast cancer stem cells supports self-renewal through negative PTEN regulation and sustained AKT activation. *EMBO Rep* 17, 648-658.
- Bajpai, R., Chen, D.A., Rada-Iglesias, A., Zhang, J., Xiong, Y., Helms, J., Chang, C.P., Zhao, Y., Swigut, T., and Wysocka, J. (2010). CHD7 cooperates with PBAF to control multipotent neural crest formation. *Nature* 463, 958-962.
- Ball, C.R., Oppel, F., Ehrenberg, K.R., Dubash, T.D., Dieter, S.M., Hoffmann, C.M., Abel, U., Herbst, F., Koch, M., Werner, J., *et al.* (2017). Succession of transiently active tumor-initiating cell clones in human pancreatic cancer xenografts. *EMBO Mol Med* 9, 918-932.
- Bao, S., Wu, Q., McLendon, R.E., Hao, Y., Shi, Q., Hjelmeland, A.B., Dewhirst, M.W., Bigner, D.D., and Rich, J.N. (2006). Glioma stem cells promote radioresistance by preferential activation of the DNA damage response. *Nature* 444, 756-760.
- Barriga, E.H., Trainor, P.A., Bronner, M., and Mayor, R. (2015). Animal models for studying neural crest development: is the mouse different? *Development* 142, 1555-1560.
- Batlle, E., and Clevers, H. (2017). Cancer stem cells revisited. *Nat Med* 23, 1124-1134.
- Beck, B., and Blanpain, C. (2013). Unravelling cancer stem cell potential. *Nat Rev Cancer* 13, 727-738.
- Beerling, E., Seinstra, D., de Wit, E., Kester, L., van der Velden, D., Maynard, C., Schafer, R., van Diest, P., Voest, E., van Oudenaarden, A., *et al.* (2016). Plasticity between Epithelial and Mesenchymal States Unlinks EMT from Metastasis-Enhancing Stem Cell Capacity. *Cell Rep* 14, 2281-2288.
- Benard, J., Raguenez, G., Kauffmann, A., Valent, A., Ripoche, H., Joulin, V., Job, B., Danglot, G., Cantais, S., Robert, T., *et al.* (2008). MYCN-non-amplified metastatic neuroblastoma with good prognosis and spontaneous regression: a molecular portrait of stage 4S. *Mol Oncol* 2, 261-271.
- Berwanger, B., Hartmann, O., Bergmann, E., Bernard, S., Nielsen, D., Krause, M., Kartal, A., Flynn, D., Wiedemeyer, R., Schwab, M., *et al.* (2002). Loss of a FYN-regulated differentiation and growth arrest pathway in advanced stage neuroblastoma. *Cancer Cell* 2, 377-386.
- Bettorsini, D., Liu, Y., Kjaeldgaard, A., Sundstrom, E., and Garcia-Castro, M.I. (2010). Analysis of early human neural crest development. *Dev Biol* 344, 578-592.
- Biederer, T., and Sudhof, T.C. (2000). Mints as adaptors. Direct binding to neurexins and recruitment of munc18. *J Biol Chem* 275, 39803-39806.
- Biederer, T., and Sudhof, T.C. (2001). CASK and protein 4.1 support F-actin nucleation on neurexins. *J Biol Chem* 276, 47869-47876.
- Biedler, J.L., Helson, L., and Spengler, B.A. (1973). Morphology and growth, tumorigenicity, and cytogenetics of human neuroblastoma cells in continuous culture. *Cancer Res* 33, 2643-2652.
- Bilanges, B., Posor, Y., and Vanhaesebroeck, B. (2019). PI3K isoforms in cell signalling and vesicle trafficking. *Nat Rev Mol Cell Biol* 20, 515-534.

- Binda, E., Visioli, A., Giani, F., Lamorte, G., Copetti, M., Pitter, K.L., Huse, J.T., Cajola, L., Zanetti, N., DiMeco, F., *et al.* (2012). The EphA2 receptor drives self-renewal and tumorigenicity in stem-like tumor-propagating cells from human glioblastomas. *Cancer Cell* 22, 765-780.
- Blanpain, C. (2013). Tracing the cellular origin of cancer. *Nat Cell Biol* 15, 126-134.
- Blanpain, C., and Simons, B.D. (2013). Unravelling stem cell dynamics by lineage tracing. *Nat Rev Mol Cell Biol* 14, 489-502.
- Bleau, A.M., Hambarzumyan, D., Ozawa, T., Fomchenko, E.I., Huse, J.T., Brennan, C.W., and Holland, E.C. (2009). PTEN/PI3K/Akt pathway regulates the side population phenotype and ABCG2 activity in glioma tumor stem-like cells. *Cell Stem Cell* 4, 226-235.
- Boesch, M., Sopper, S., Zeimet, A.G., Reimer, D., Gastl, G., Ludewig, B., and Wolf, D. (2016). Heterogeneity of Cancer Stem Cells: Rationale for Targeting the Stem Cell Niche. *Biochim Biophys Acta* 1866, 276-289.
- Boeva, V., Jouannet, S., Daveau, R., Combaret, V., Pierre-Eugene, C., Cazes, A., Louis-Brennetot, C., Schleiermacher, G., Ferrand, S., Pierron, G., *et al.* (2013). Breakpoint features of genomic rearrangements in neuroblastoma with unbalanced translocations and chromothripsis. *PLoS One* 8, e72182.
- Boeva, V., Louis-Brennetot, C., Peltier, A., Durand, S., Pierre-Eugene, C., Raynal, V., Etchevers, H.C., Thomas, S., Lermine, A., Daudigeos-Dubus, E., *et al.* (2017). Heterogeneity of neuroblastoma cell identity defined by transcriptional circuitries. *Nat Genet* 49, 1408-1413.
- Bolande, R. (1974). THE NEUROCRISTOPATHIES: A Unifying Concept of Disease Arising in Neural Crest Maldevelopment. *Human Pathology* 5, 409-429.
- Bonnet, D., and Dick, J.E. (1997). Human acute myeloid leukemia is organized as a hierarchy that originates from a primitive hematopoietic cell. *Nat Med* 3, 730-737.
- Bookout, A.L., Cummins, C.L., Mangelsdorf, D.J., Pesola, J.M., and Kramer, M.F. (2006). High-throughput real-time quantitative reverse transcription PCR. *Curr Protoc Mol Biol* Chapter 15, Unit 15 18.
- Born, G., Breuer, D., Wang, S., Rohlmann, A., Coulon, P., Vakili, P., Reissner, C., Kiefer, F., Heine, M., Pape, H.C., *et al.* (2014). Modulation of synaptic function through the alpha-neurexin-specific ligand neurexophilin-1. *Proc Natl Acad Sci U S A* 111, E1274-1283.
- Borowicz, S., Van Scoyk, M., Avasarala, S., Karuppusamy Rathinam, M.K., Tauler, J., Bikkavilli, R.K., and Winn, R.A. (2014). The soft agar colony formation assay. *J Vis Exp*, e51998.
- Boucard, A.A., Ko, J., and Sudhof, T.C. (2012). High affinity neurexin binding to cell adhesion G-protein-coupled receptor CIRL1/latrophilin-1 produces an intercellular adhesion complex. *J Biol Chem* 287, 9399-9413.
- Boumahdi, S., Driessens, G., Lapouge, G., Rorive, S., Nassar, D., Le Mercier, M., Delatte, B., Caauwe, A., Lenglez, S., Nkusi, E., *et al.* (2014). SOX2 controls tumour initiation and cancer stem-cell functions in squamous-cell carcinoma. *Nature* 511, 246-250.
- Bown, N., Cotterill, S., Lastowska, M., O'Neill, S., Pearson, A.D., Plantaz, D., Meddeb, M., Danglot, G., Brinkschmidt, C., Christiansen, H., *et al.* (1999). Gain of chromosome arm 17q and adverse outcome in patients with neuroblastoma. *N Engl J Med* 340, 1954-1961.
- Brabletz, T. (2012). EMT and MET in metastasis: where are the cancer stem cells? *Cancer Cell* 22, 699-701.
- Brabletz, T., Jung, A., Reu, S., Porzner, M., Hlubek, F., Kunz-Schughart, L.A., Knuechel, R., and Kirchner, T. (2001).

- Variable beta-catenin expression in colorectal cancers indicates tumor progression driven by the tumor environment. *Proc Natl Acad Sci U S A* 98, 10356-10361.
- Braekeveldt, N., Wigerup, C., Gisselsson, D., Mohlin, S., Merselius, M., Beckman, S., Jonson, T., Borjesson, A., Backman, T., Tadeo, I., *et al.* (2015). Neuroblastoma patient-derived orthotopic xenografts retain metastatic patterns and geno- and phenotypes of patient tumours. *Int J Cancer* 136, E252-261.
- Breitman, T.R., Collins, S.J., and Keene, B.R. (1981). Terminal differentiation of human promyelocytic leukemic cells in primary culture in response to retinoic acid. *Blood* 57, 1000-1004.
- Bridge, A.J., Pebernard, S., Ducraux, A., Nicoulaz, A.L., and Iggo, R. (2003). Induction of an interferon response by RNAi vectors in mammalian cells. *Nat Genet* 34, 263-264.
- Brodeur, G.M. (2003). Neuroblastoma: biological insights into a clinical enigma. *Nat Rev Cancer* 3, 203-216.
- Brodeur, G.M. (2018). Spontaneous regression of neuroblastoma. *Cell Tissue Res* 372, 277-286.
- Brodeur, G.M., and Bagatell, R. (2014). Mechanisms of neuroblastoma regression. *Nat Rev Clin Oncol* 11, 704-713.
- Brodeur, G.M., Pritchard, J., Berthold, F., Carlsen, N.L., Castel, V., Castelberry, R.P., De Bernardi, B., Evans, A.E., Favrot, M., Hedborg, F., *et al.* (1993). Revisions of the international criteria for neuroblastoma diagnosis, staging, and response to treatment. *J Clin Oncol* 11, 1466-1477.
- Brodeur, G.M., and Seeger, R.C. (1986). Gene amplification in human neuroblastomas: basic mechanisms and clinical implications. *Cancer Genet Cytogenet* 19, 101-111.
- Brodeur, G.M., Seeger, R.C., Barrett, A., Berthold, F., Castleberry, R.P., D'Angio, G., De Bernardi, B., Evans, A.E., Favrot, M., Freeman, A.I., *et al.* (1988). International criteria for diagnosis, staging, and response to treatment in patients with neuroblastoma. *J Clin Oncol* 6, 1874-1881.
- Bronner-Fraser, M., and Fraser, S.E. (1988). Cell lineage analysis reveals multipotency of some avian neural crest cells. *Nature* 335, 161-164.
- Bronner, M.E., and LeDouarin, N.M. (2012). Development and evolution of the neural crest: an overview. *Dev Biol* 366, 2-9.
- Bruce, W.R., and Van Der Gaag, H. (1963). A Quantitative Assay for the Number of Murine Lymphoma Cells Capable of Proliferation in Vivo. *Nature* 199, 79-80.
- Buganim, Y., Goldstein, I., Lipson, D., Milyavsky, M., Polak-Charcon, S., Mardoukh, C., Solomon, H., Kalo, E., Madar, S., Brosh, R., *et al.* (2010). A novel translocation breakpoint within the BPTF gene is associated with a pre-malignant phenotype. *PLoS One* 5, e9657.
- Buitrago-Delgado, E., Nordin, K., Rao, A., Geary, L., and LaBonne, C. (2015). NEURODEVELOPMENT. Shared regulatory programs suggest retention of blastula-stage potential in neural crest cells. *Science* 348, 1332-1335.
- Cairns, J. (1975). Mutation selection and the natural history of cancer. *Nature* 255, 197-200.
- Calabrese, C., Poppleton, H., Kocak, M., Hogg, T.L., Fuller, C., Hamner, B., Oh, E.Y., Gaber, M.W., Finklestein, D., Allen, M., *et al.* (2007). A perivascular niche for brain tumor stem cells. *Cancer Cell* 11, 69-82.
- Cantilena, S., Pastorino, F., Pezzolo, A., Chayka, O., Pistoia, V., Ponzoni, M., and Sala, A. (2011). Frizzled receptor 6 marks rare, highly tumorigenic stem-like cells in mouse and human neuroblastomas. *Oncotarget* 2,

976-983.

- Capasso, M., Devoto, M., Hou, C., Asgharzadeh, S., Glessner, J.T., Attiyeh, E.F., Mosse, Y.P., Kim, C., Diskin, S.J., Cole, K.A., *et al.* (2009). Common variations in BARD1 influence susceptibility to high-risk neuroblastoma. *Nat Genet* *41*, 718-723.
- Carter, R., Mullassery, D., See, V., Theocharatos, S., Pizer, B., Losty, P.D., Jesudason, E., and Moss, D.J. (2012). Exploitation of chick embryo environments to reprogram MYCN-amplified neuroblastoma cells to a benign phenotype, lacking detectable MYCN expression. *Oncogenesis* *1*, e24.
- Cellosaurus (2019). Cellosaurus.
- Chaffer, C.L., Brueckmann, I., Scheel, C., Kaestli, A.J., Wiggins, P.A., Rodrigues, L.O., Brooks, M., Reinhardt, F., Su, Y., Polyak, K., *et al.* (2011). Normal and neoplastic nonstem cells can spontaneously convert to a stem-like state. *Proc Natl Acad Sci U S A* *108*, 7950-7955.
- Chaffer, C.L., Marjanovic, N.D., Lee, T., Bell, G., Kleer, C.G., Reinhardt, F., D'Alessio, A.C., Young, R.A., and Weinberg, R.A. (2013). Poised chromatin at the ZEB1 promoter enables breast cancer cell plasticity and enhances tumorigenicity. *Cell* *154*, 61-74.
- Challen, G.A., and Little, M.H. (2006). A side order of stem cells: the SP phenotype. *Stem Cells* *24*, 3-12.
- Charles, N., Ozawa, T., Squatrito, M., Bleau, A.M., Brennan, C.W., Hambardzumyan, D., and Holland, E.C. (2010). Perivascular nitric oxide activates notch signaling and promotes stem-like character in PDGF-induced glioma cells. *Cell Stem Cell* *6*, 141-152.
- Chen, J., Li, Y., Yu, T.S., McKay, R.M., Burns, D.K., Kernie, S.G., and Parada, L.F. (2012a). A restricted cell population propagates glioblastoma growth after chemotherapy. *Nature* *488*, 522-526.
- Chen, L.Y., Jiang, M., Zhang, B., Gokce, O., and Sudhof, T.C. (2017). Conditional Deletion of All Neurexins Defines Diversity of Essential Synaptic Organizer Functions for Neurexins. *Neuron* *94*, 611-625 e614.
- Chen, R., Nishimura, M.C., Bumbaca, S.M., Kharbanda, S., Forrest, W.F., Kasman, I.M., Greve, J.M., Soriano, R.H., Gilmour, L.L., Rivers, C.S., *et al.* (2010). A hierarchy of self-renewing tumor-initiating cell types in glioblastoma. *Cancer Cell* *17*, 362-375.
- Chen, T., Yang, K., Yu, J., Meng, W., Yuan, D., Bi, F., Liu, F., Liu, J., Dai, B., Chen, X., *et al.* (2012b). Identification and expansion of cancer stem cells in tumor tissues and peripheral blood derived from gastric adenocarcinoma patients. *Cell Res* *22*, 248-258.
- Chen, W.J., Ho, C.C., Chang, Y.L., Chen, H.Y., Lin, C.A., Ling, T.Y., Yu, S.L., Yuan, S.S., Chen, Y.J., Lin, C.Y., *et al.* (2014). Cancer-associated fibroblasts regulate the plasticity of lung cancer stemness via paracrine signalling. *Nat Commun* *5*, 3472.
- Chen, Y., Takita, J., Choi, Y.L., Kato, M., Ohira, M., Sanada, M., Wang, L., Soda, M., Kikuchi, A., Igarashi, T., *et al.* (2008). Oncogenic mutations of ALK kinase in neuroblastoma. *Nature* *455*, 971-974.
- Chen, Z., Shi, T., Zhang, L., Zhu, P., Deng, M., Huang, C., Hu, T., Jiang, L., and Li, J. (2016). Mammalian drug efflux transporters of the ATP binding cassette (ABC) family in multidrug resistance: A review of the past decade. *Cancer Lett* *370*, 153-164.
- Cheung, N.K., and Dyer, M.A. (2013). Neuroblastoma: developmental biology, cancer genomics and immunotherapy. *Nat Rev Cancer* *13*, 397-411.

- Cheung, N.K., Zhang, J., Lu, C., Parker, M., Bahrami, A., Tickoo, S.K., Heguy, A., Pappo, A.S., Federico, S., Dalton, J., *et al.* (2012). Association of age at diagnosis and genetic mutations in patients with neuroblastoma. *JAMA* *307*, 1062-1071.
- Ciccarone, V., Spengler, B.A., Meyers, M.B., Biedler, J.L., and Ross, R.A. (1989). Phenotypic diversification in human neuroblastoma cells: expression of distinct neural crest lineages. *Cancer Res* *49*, 219-225.
- Clarkson, B., Fried, J., Strife, A., Sakai, Y., Ota, K., and Okita, T. (1970). Studies of cellular proliferation in human leukemia. 3. Behavior of leukemic cells in three adults with acute leukemia given continuous infusions of 3H-thymidine for 8 or 10 days. *Cancer* *25*, 1237-1260.
- Clarkson, B.D. (1969). Review of recent studies of cellular proliferation in acute leukemia. *Natl Cancer Inst Monogr* *30*, 81-120.
- Clevers, H. (2011). The cancer stem cell: premises, promises and challenges. *Nat Med* *17*, 313-319.
- Clevers, H. (2015). STEM CELLS. What is an adult stem cell? *Science* *350*, 1319-1320.
- Cohn, S.L., Pearson, A.D., London, W.B., Monclair, T., Ambros, P.F., Brodeur, G.M., Faldum, A., Hero, B., Iehara, T., Machin, D., *et al.* (2009). The International Neuroblastoma Risk Group (INRG) classification system: an INRG Task Force report. *J Clin Oncol* *27*, 289-297.
- Cojoc, M., Mabert, K., Muders, M.H., and Dubrovskaja, A. (2015). A role for cancer stem cells in therapy resistance: cellular and molecular mechanisms. *Semin Cancer Biol* *31*, 16-27.
- Cole, K.A., Huggins, J., Laquaglia, M., Hulderman, C.E., Russell, M.R., Bosse, K., Diskin, S.J., Attiyeh, E.F., Sennett, R., Norris, G., *et al.* (2011). RNAi screen of the protein kinome identifies checkpoint kinase 1 (CHK1) as a therapeutic target in neuroblastoma. *Proc Natl Acad Sci U S A* *108*, 3336-3341.
- Collins, A.T., Berry, P.A., Hyde, C., Stower, M.J., and Maitland, N.J. (2005). Prospective identification of tumorigenic prostate cancer stem cells. *Cancer Res* *65*, 10946-10951.
- Cortazzo, M.H., Kassis, E.S., Sproul, K.A., and Schor, N.F. (1996). Nerve growth factor (NGF)-mediated protection of neural crest cells from antimetabolic agent-induced apoptosis: the role of the low-affinity NGF receptor. *J Neurosci* *16*, 3895-3899.
- Cournoyer, S., Nyalendo, C., Addioui, A., Belounis, A., Beaunoyer, M., Aumont, A., Teira, P., Duval, M., Fernandes, K., Fetni, R., *et al.* (2012). Genotype analysis of tumor-initiating cells expressing CD133 in neuroblastoma. *Genes Chromosomes Cancer* *51*, 792-804.
- Crane, J.F., and Trainor, P.A. (2006). Neural crest stem and progenitor cells. *Annu Rev Cell Dev Biol* *22*, 267-286.
- Cui, H., Hu, B., Li, T., Ma, J., Alam, G., Gunning, W.T., and Ding, H.F. (2007). Bmi-1 is essential for the tumorigenicity of neuroblastoma cells. *Am J Pathol* *170*, 1370-1378.
- Curley, M.D., Therrien, V.A., Cummings, C.L., Sergent, P.A., Koulouris, C.R., Friel, A.M., Roberts, D.J., Seiden, M.V., Scadden, D.T., Rueda, B.R., *et al.* (2009). CD133 expression defines a tumor initiating cell population in primary human ovarian cancer. *Stem Cells* *27*, 2875-2883.
- D'Angio, G.J., Evans, A.E., and Koop, C.E. (1971). Special pattern of widespread neuroblastoma with a favourable prognosis. *Lancet* *1*, 1046-1049.
- Daenen, S., Vellenga, E., van Dobbenburgh, O.A., and Halie, M.R. (1986). Retinoic acid as antileukemic therapy in a patient with acute promyelocytic leukemia and Aspergillus pneumonia. *Blood* *67*, 559-561.

- Dalerba, P., Dylla, S.J., Park, I.K., Liu, R., Wang, X., Cho, R.W., Hoey, T., Gurney, A., Huang, E.H., Simeone, D.M., *et al.* (2007). Phenotypic characterization of human colorectal cancer stem cells. *Proc Natl Acad Sci U S A* *104*, 10158-10163.
- Dalerba, P., Kalisky, T., Sahoo, D., Rajendran, P.S., Rothenberg, M.E., Leyrat, A.A., Sim, S., Okamoto, J., Johnston, D.M., Qian, D., *et al.* (2011). Single-cell dissection of transcriptional heterogeneity in human colon tumors. *Nat Biotechnol* *29*, 1120-1127.
- Day, B.W., Stringer, B.W., Al-Ejeh, F., Ting, M.J., Wilson, J., Ensbey, K.S., Jamieson, P.R., Bruce, Z.C., Lim, Y.C., Offenhauser, C., *et al.* (2013). EphA3 maintains tumorigenicity and is a therapeutic target in glioblastoma multiforme. *Cancer Cell* *23*, 238-248.
- de Croze, N., Maczkowiak, F., and Monsoro-Burq, A.H. (2011). Reiterative AP2a activity controls sequential steps in the neural crest gene regulatory network. *Proc Natl Acad Sci U S A* *108*, 155-160.
- de Goeij, B.E., and Lambert, J.M. (2016). New developments for antibody-drug conjugate-based therapeutic approaches. *Curr Opin Immunol* *40*, 14-23.
- de Sousa e Melo, F., Kurtova, A.V., Harnoss, J.M., Kljavin, N., Hoeck, J.D., Hung, J., Anderson, J.E., Storm, E.E., Modrusan, Z., Koeppen, H., *et al.* (2017). A distinct role for Lgr5(+) stem cells in primary and metastatic colon cancer. *Nature* *543*, 676-680.
- de Wit, J., Sylwestrak, E., O'Sullivan, M.L., Otto, S., Tiglio, K., Savas, J.N., Yates, J.R., 3rd, Comoletti, D., Taylor, P., and Ghosh, A. (2009). LRRTM2 interacts with Neurexin1 and regulates excitatory synapse formation. *Neuron* *64*, 799-806.
- Dechant, G., and Barde, Y.A. (2002). The neurotrophin receptor p75(NTR): novel functions and implications for diseases of the nervous system. *Nat Neurosci* *5*, 1131-1136.
- Decock, A., Ongenaert, M., Cannoodt, R., Verniers, K., De Wilde, B., Laureys, G., Van Roy, N., Berbegall, A.P., Bienertova-Vasku, J., Bown, N., *et al.* (2016a). Methyl-CpG-binding domain sequencing reveals a prognostic methylation signature in neuroblastoma. *Oncotarget* *7*, 1960-1972.
- Decock, A., Ongenaert, M., De Wilde, B., Brichard, B., Noguera, R., Speleman, F., and Vandesompele, J. (2016b). Stage 4S neuroblastoma tumors show a characteristic DNA methylation portrait. *Epigenetics* *11*, 761-771.
- Decock, A., Ongenaert, M., Van Criekinge, W., Speleman, F., and Vandesompele, J. (2016c). DNA methylation profiling of primary neuroblastoma tumors using methyl-CpG-binding domain sequencing. *Sci Data* *3*, 160004.
- Decock, A., Ongenaert, M., Vandesompele, J., and Speleman, F. (2011). Neuroblastoma epigenetics: from candidate gene approaches to genome-wide screenings. *Epigenetics* *6*, 962-970.
- Delloye-Bourgeois, C., Bertin, L., Thoinet, K., Jarrosson, L., Kindbeiter, K., Buffet, T., Tauszig-Delamasure, S., Bozon, M., Marabelle, A., Combaret, V., *et al.* (2017). Microenvironment-Driven Shift of Cohesion/Detachment Balance within Tumors Induces a Switch toward Metastasis in Neuroblastoma. *Cancer Cell* *32*, 427-443 e428.
- Delloye-Bourgeois, C., and Castellani, V. (2019). Hijacking of Embryonic Programs by Neural Crest-Derived Neuroblastoma: From Physiological Migration to Metastatic Dissemination. *Front Mol Neurosci* *12*, 52.
- Dick, J.E., Bhatia, M., Gan, O., Kapp, U., and Wang, J.C. (1997). Assay of human stem cells by repopulation of NOD/SCID mice. *Stem Cells* *15 Suppl 1*, 199-203; discussion 204-197.

- Diehn, M., Cho, R.W., Lobo, N.A., Kalisky, T., Dorie, M.J., Kulp, A.N., Qian, D., Lam, J.S., Ailles, L.E., Wong, M., *et al.* (2009). Association of reactive oxygen species levels and radioresistance in cancer stem cells. *Nature* *458*, 780-783.
- Ding, X., Luo, C., Zhou, J., Zhong, Y., Hu, X., Zhou, F., Ren, K., Gan, L., He, A., Zhu, J., *et al.* (2009). The interaction of KCTD1 with transcription factor AP-2alpha inhibits its transactivation. *J Cell Biochem* *106*, 285-295.
- Diskin, S.J., Capasso, M., Schnepf, R.W., Cole, K.A., Attiyeh, E.F., Hou, C., Diamond, M., Carpenter, E.L., Winter, C., Lee, H., *et al.* (2012). Common variation at 6q16 within HACE1 and LIN28B influences susceptibility to neuroblastoma. *Nat Genet* *44*, 1126-1130.
- Doupe, D.P., Klein, A.M., Simons, B.D., and Jones, P.H. (2010). The ordered architecture of murine ear epidermis is maintained by progenitor cells with random fate. *Dev Cell* *18*, 317-323.
- Driessens, G., Beck, B., Caauwe, A., Simons, B.D., and Blanpain, C. (2012). Defining the mode of tumour growth by clonal analysis. *Nature* *488*, 527-530.
- DuBois, S.G., Kalika, Y., Lukens, J.N., Brodeur, G.M., Seeger, R.C., Atkinson, J.B., Haase, G.M., Black, C.T., Perez, C., Shimada, H., *et al.* (1999). Metastatic sites in stage IV and IVS neuroblastoma correlate with age, tumor biology, and survival. *J Pediatr Hematol Oncol* *21*, 181-189.
- Durinck, K., and Speleman, F. (2018). Epigenetic regulation of neuroblastoma development. *Cell Tissue Res* *372*, 309-324.
- Eleveld, T.F., Oldridge, D.A., Bernard, V., Koster, J., Colmet Daage, L., Diskin, S.J., Schild, L., Bentahar, N.B., Bellini, A., Chicard, M., *et al.* (2015). Relapsed neuroblastomas show frequent RAS-MAPK pathway mutations. *Nat Genet* *47*, 864-871.
- Eramo, A., Lotti, F., Sette, G., Pillozzi, E., Biffoni, M., Di Virgilio, A., Conticello, C., Ruco, L., Peschle, C., and De Maria, R. (2008). Identification and expansion of the tumorigenic lung cancer stem cell population. *Cell Death Differ* *15*, 504-514.
- Etchevers, H.C., Amiel, J., and Lyonnet, S. (2006). Molecular bases of human neurocristopathies. *Adv Exp Med Biol* *589*, 213-234.
- Evans, A.E., D'Angio, G.J., and Randolph, J. (1971). A proposed staging for children with neuroblastoma. Children's cancer study group A. *Cancer* *27*, 374-378.
- Fabian, J., Lodrini, M., Oehme, I., Schier, M.C., Thole, T.M., Hielscher, T., Kopp-Schneider, A., Opitz, L., Capper, D., von Deimling, A., *et al.* (2014). GRHL1 acts as tumor suppressor in neuroblastoma and is negatively regulated by MYCN and HDAC3. *Cancer Res* *74*, 2604-2616.
- Fabian, J., Opitz, D., Althoff, K., Lodrini, M., Hero, B., Volland, R., Beckers, A., de Preter, K., Decock, A., Patil, N., *et al.* (2016). MYCN and HDAC5 transcriptionally repress CD9 to trigger invasion and metastasis in neuroblastoma. *Oncotarget* *7*, 66344-66359.
- Faryna, M., Konermann, C., Aulmann, S., Bermejo, J.L., Brugger, M., Diederichs, S., Rom, J., Weichenhan, D., Claus, R., Rehli, M., *et al.* (2012). Genome-wide methylation screen in low-grade breast cancer identifies novel epigenetically altered genes as potential biomarkers for tumor diagnosis. *FASEB J* *26*, 4937-4950.
- Feoktistova, M., Geserick, P., and Leverkus, M. (2016). Crystal Violet Assay for Determining Viability of Cultured Cells. *Cold Spring Harb Protoc* *2016*, pdb prot087379.
- Ferronha, T., Rabadan, M.A., Gil-Guinon, E., Le Dreau, G., de Torres, C., and Marti, E. (2013). LMO4 is an es-

- sential cofactor in the Snail2-mediated epithelial-to-mesenchymal transition of neuroblastoma and neural crest cells. *J Neurosci* *33*, 2773-2783.
- Fessler, E., Borovski, T., and Medema, J.P. (2015). Endothelial cells induce cancer stem cell features in differentiated glioblastoma cells via bFGF. *Mol Cancer* *14*, 157.
- Filbin, M.G., Tirosch, I., Hovestadt, V., Shaw, M.L., Escalante, L.E., Mathewson, N.D., Neftel, C., Frank, N., Pelton, K., Hebert, C.M., *et al.* (2018). Developmental and oncogenic programs in H3K27M gliomas dissected by single-cell RNA-seq. *Science* *360*, 331-335.
- Fish, R.J., and Kruihof, E.K. (2004). Short-term cytotoxic effects and long-term instability of RNAi delivered using lentiviral vectors. *BMC Mol Biol* *5*, 9.
- Flavahan, W.A., Gaskell, E., and Bernstein, B.E. (2017). Epigenetic plasticity and the hallmarks of cancer. *Science* *357*.
- Folkins, C., Shaked, Y., Man, S., Tang, T., Lee, C.R., Zhu, Z., Hoffman, R.M., and Kerbel, R.S. (2009). Glioma tumor stem-like cells promote tumor angiogenesis and vasculogenesis via vascular endothelial growth factor and stromal-derived factor 1. *Cancer Res* *69*, 7243-7251.
- Foster, B.M., Zaidi, D., Young, T.R., Mobley, M.E., and Kerr, B.A. (2018). CD117/c-kit in Cancer Stem Cell-Mediated Progression and Therapeutic Resistance. *Biomedicines* *6*.
- Francis, J.M., Zhang, C.Z., Maire, C.L., Jung, J., Manzo, V.E., Adalsteinsson, V.A., Homer, H., Haidar, S., Blumenstiel, B., Peadarallu, C.S., *et al.* (2014). EGFR variant heterogeneity in glioblastoma resolved through single-nucleus sequencing. *Cancer Discov* *4*, 956-971.
- Fransson, S., Abel, F., Kogner, P., Martinsson, T., and Ejeskar, K. (2013). Stage-dependent expression of PI3K/Akt pathway genes in neuroblastoma. *Int J Oncol* *42*, 609-616.
- Friedmann-Morvinski, D., Bushong, E.A., Ke, E., Soda, Y., Marumoto, T., Singer, O., Ellisman, M.H., and Verma, I.M. (2012). Dedifferentiation of neurons and astrocytes by oncogenes can induce gliomas in mice. *Science* *338*, 1080-1084.
- Frisch, S.M., and Francis, H. (1994). Disruption of epithelial cell-matrix interactions induces apoptosis. *J Cell Biol* *124*, 619-626.
- Furlan, A., and Adameyko, I. (2018). Schwann cell precursor: a neural crest cell in disguise? *Dev Biol* *444 Suppl 1*, S25-S35.
- Furlan, A., Dyachuk, V., Kastriti, M.E., Calvo-Enrique, L., Abdo, H., Hadjab, S., Chontorotzea, T., Akkuratova, N., Usoskin, D., Kamenev, D., *et al.* (2017). Multipotent peripheral glial cells generate neuroendocrine cells of the adrenal medulla. *Science* *357*.
- Furth, J.K., M.C.; Breedis, C. (1937). The transmission of leukemia of mice with a single cell. *Cancer Res* *31*, 276-282.
- Gammill, L.S., and Bronner-Fraser, M. (2003). Neural crest specification: migrating into genomics. *Nat Rev Neurosci* *4*, 795-805.
- Gammill, L.S., and Roffers-Agarwal, J. (2010). Division of labor during trunk neural crest development. *Dev Biol* *344*, 555-565.
- Gans, C., and Northcutt, R.G. (1983). Neural crest and the origin of vertebrates: a new head. *Science* *220*, 268-

273.

- Gao, R., Davis, A., McDonald, T.O., Sei, E., Shi, X., Wang, Y., Tsai, P.C., Casasent, A., Waters, J., Zhang, H., *et al.* (2016). Punctuated copy number evolution and clonal stasis in triple-negative breast cancer. *Nat Genet* *48*, 1119-1130.
- Garcia, I., Mayol, G., Rios, J., Domenech, G., Cheung, N.K., Oberthuer, A., Fischer, M., Maris, J.M., Brodeur, G.M., Hero, B., *et al.* (2012). A three-gene expression signature model for risk stratification of patients with neuroblastoma. *Clin Cancer Res* *18*, 2012-2023.
- Gautier, L., Cope, L., Bolstad, B.M., and Irizarry, R.A. (2004). affy--analysis of Affymetrix GeneChip data at the probe level. *Bioinformatics* *20*, 307-315.
- Geary, L.A., Nash, K.A., Adisetiyo, H., Liang, M., Liao, C.P., Jeong, J.H., Zandi, E., and Roy-Burman, P. (2014). CAF-secreted annexin A1 induces prostate cancer cells to gain stem cell-like features. *Mol Cancer Res* *12*, 607-621.
- Gentry, J.J., Barker, P.A., and Carter, B.D. (2004). The p75 neurotrophin receptor: multiple interactors and numerous functions. *Prog Brain Res* *146*, 25-39.
- George, R.E., Sanda, T., Hanna, M., Frohling, S., Luther, W., 2nd, Zhang, J., Ahn, Y., Zhou, W., London, W.B., McGrady, P., *et al.* (2008). Activating mutations in ALK provide a therapeutic target in neuroblastoma. *Nature* *455*, 975-978.
- Geppert, M., Ushkaryov, Y.A., Hata, Y., Davletov, B., Petrenko, A.G., and Sudhof, T.C. (1992). Neurexins. *Cold Spring Harb Symp Quant Biol* *57*, 483-490.
- Giancotti, F.G. (2013). Mechanisms governing metastatic dormancy and reactivation. *Cell* *155*, 750-764.
- Ginestier, C., Hur, M.H., Charafe-Jauffret, E., Monville, F., Dutcher, J., Brown, M., Jacquemier, J., Viens, P., Kleer, C.G., Liu, S., *et al.* (2007). ALDH1 is a marker of normal and malignant human mammary stem cells and a predictor of poor clinical outcome. *Cell Stem Cell* *1*, 555-567.
- Godfried, M.B., Veenstra, M., v Sluis, P., Boon, K., v Asperen, R., Hermus, M.C., v Schaik, B.D., Voute, T.P., Schwab, M., Versteeg, R., *et al.* (2002). The N-myc and c-myc downstream pathways include the chromosome 17q genes nm23-H1 and nm23-H2. *Oncogene* *21*, 2097-2101.
- Golebiewska, A., Brons, N.H., Bjerkvig, R., and Niclou, S.P. (2011). Critical appraisal of the side population assay in stem cell and cancer stem cell research. *Cell Stem Cell* *8*, 136-147.
- Gomez, S., Castellano, G., Mayol, G., Sunol, M., Queiros, A., Bibikova, M., Nazor, K.L., Loring, J.F., Lemos, I., Rodriguez, E., *et al.* (2015). DNA methylation fingerprint of neuroblastoma reveals new biological and clinical insights. *Epigenomics* *7*, 1137-1153.
- Gonzalez-Roca, E., Garcia-Albeniz, X., Rodriguez-Mulero, S., Gomis, R.R., Kornacker, K., and Auer, H. (2010). Accurate expression profiling of very small cell populations. *PLoS One* *5*, e14418.
- Goodell, M.A., Brose, K., Paradis, G., Conner, A.S., and Mulligan, R.C. (1996). Isolation and functional properties of murine hematopoietic stem cells that are replicating in vivo. *J Exp Med* *183*, 1797-1806.
- Goodman, M.T.G., J.G.; Smith, M.A.; Olshan, A.F. (1999). Sympathetic nervous system tumors. In: *Cancer Incidence and Survival among Children and Adolescents: United States SEER Program, 1975-1995*. In *Cancer Incidence and Survival among Children and Adolescents: United States*

- SEER Program 1975-1995, L.A.G.S. Ries, M.A.; Gurney, J.G.; Linet, M. Tamra, T. Young, J.L. Bunin, G.R., ed. (Bethesda, MD: National Cancer Institute, SEER Program.), pp. 65-72.
- Greaves, M. (2013). Cancer stem cells as 'units of selection'. *Evol Appl* 6, 102-108.
- Greaves, M. (2015). Evolutionary determinants of cancer. *Cancer Discov* 5, 806-820.
- Greaves, M., and Maley, C.C. (2012). Clonal evolution in cancer. *Nature* 481, 306-313.
- Gregoire, D., and Kmita, M. (2014). Genetic cell ablation. *Methods Mol Biol* 1092, 421-436.
- Gupta, P.B., Fillmore, C.M., Jiang, G., Shapira, S.D., Tao, K., Kuperwasser, C., and Lander, E.S. (2011). Stochastic state transitions give rise to phenotypic equilibrium in populations of cancer cells. *Cell* 146, 633-644.
- Gururajan, M., Cavassani, K.A., Sievert, M., Duan, P., Lichterman, J., Huang, J.M., Smith, B., You, S., Nandana, S., Chu, G.C., *et al.* (2015). SRC family kinase FYN promotes the neuroendocrine phenotype and visceral metastasis in advanced prostate cancer. *Oncotarget* 6, 44072-44083.
- Hall, B.K. (1999). *The Neural Crest in Development and Evolution*, 1st edition edn (New York: Springer Science+Business Media).
- Hamburger, A.W., and Salmon, S.E. (1977). Primary bioassay of human tumor stem cells. *Science* 197, 461-463.
- Hamburger, V., and Hamilton, H.L. (1951). A series of normal stages in the development of the chick embryo. *J Morphol* 88, 49-92.
- Hanahan, D., and Weinberg, R.A. (2011). Hallmarks of cancer: the next generation. *Cell* 144, 646-674.
- Hansford, L.M., McKee, A.E., Zhang, L., George, R.E., Gerstle, J.T., Thorner, P.S., Smith, K.M., Look, A.T., Yeger, H., Miller, F.D., *et al.* (2007). Neuroblastoma cells isolated from bone marrow metastases contain a naturally enriched tumor-initiating cell. *Cancer Res* 67, 11234-11243.
- Hansford, L.M., Thomas, W.D., Keating, J.M., Burkhart, C.A., Peaston, A.E., Norris, M.D., Haber, M., Armati, P.J., Weiss, W.A., and Marshall, G.M. (2004). Mechanisms of embryonal tumor initiation: distinct roles for MycN expression and MYCN amplification. *Proc Natl Acad Sci U S A* 101, 12664-12669.
- Hartomo, T.B., Van Huyen Pham, T., Yamamoto, N., Hirase, S., Hasegawa, D., Kosaka, Y., Matsuo, M., Hayakawa, A., Takeshima, Y., Iijima, K., *et al.* (2015). Involvement of aldehyde dehydrogenase 1A2 in the regulation of cancer stem cell properties in neuroblastoma. *Int J Oncol* 46, 1089-1098.
- Hata, Y., Butz, S., and Sudhof, T.C. (1996). CASK: a novel dlg/PSD95 homolog with an N-terminal calmodulin-dependent protein kinase domain identified by interaction with neurexins. *J Neurosci* 16, 2488-2494.
- Held, M.A., Curley, D.P., Dankort, D., McMahan, M., Muthusamy, V., and Bosenberg, M.W. (2010). Characterization of melanoma cells capable of propagating tumors from a single cell. *Cancer Res* 70, 388-397.
- Henrich, K.O., Schwab, M., and Westermann, F. (2012). 1p36 tumor suppression--a matter of dosage? *Cancer Res* 72, 6079-6088.
- Hermann, P.C., Huber, S.L., Herrler, T., Aicher, A., Ellwart, J.W., Guba, M., Bruns, C.J., and Heeschen, C. (2007). Distinct populations of cancer stem cells determine tumor growth and metastatic activity in human pancreatic cancer. *Cell Stem Cell* 1, 313-323.
- Hewitt, H.B. (1958). Studies of the dissemination and quantitative transplantation of a lymphocytic leukaemia of CBA mice. *Br J Cancer* 12, 378-401.

- Hidalgo, M., Amant, F., Biankin, A.V., Budinska, E., Byrne, A.T., Caldas, C., Clarke, R.B., de Jong, S., Jonkers, J., Maelandsmo, G.M., *et al.* (2014). Patient-derived xenograft models: an emerging platform for translational cancer research. *Cancer Discov* 4, 998-1013.
- Hilton, J. (1984). Role of aldehyde dehydrogenase in cyclophosphamide-resistant L1210 leukemia. *Cancer Res* 44, 5156-5160.
- Hirschmann-Jax, C., Foster, A.E., Wulf, G.G., Nuchtern, J.G., Jax, T.W., Gobel, U., Goodell, M.A., and Brenner, M.K. (2004). A distinct "side population" of cells with high drug efflux capacity in human tumor cells. *Proc Natl Acad Sci U S A* 101, 14228-14233.
- Hong, S.M., Omura, N., Vincent, A., Li, A., Knight, S., Yu, J., Hruban, R.H., and Goggins, M. (2012). Genome-wide CpG island profiling of intraductal papillary mucinous neoplasms of the pancreas. *Clin Cancer Res* 18, 700-712.
- Hovestadt, V., Smith, K.S., Bihannic, L., Filbin, M.G., Shaw, M.L., Baumgartner, A., DeWitt, J.C., Groves, A., Mayr, L., Weisman, H.R., *et al.* (2019). Resolving medulloblastoma cellular architecture by single-cell genomics. *Nature* 572, 74-79.
- Hsu, D.M., Agarwal, S., Benham, A., Coarfa, C., Trahan, D.N., Chen, Z., Stowers, P.N., Courtney, A.N., Lakoma, A., Barbieri, E., *et al.* (2013). G-CSF receptor positive neuroblastoma subpopulations are enriched in chemotherapy-resistant or relapsed tumors and are highly tumorigenic. *Cancer Res* 73, 4134-4146.
- Hu, Y., Yan, C., Mu, L., Huang, K., Li, X., Tao, D., Wu, Y., and Qin, J. (2015). Fibroblast-Derived Exosomes Contribute to Chemoresistance through Priming Cancer Stem Cells in Colorectal Cancer. *PLoS One* 10, e0125625.
- Huang, C.P., Tsai, M.F., Chang, T.H., Tang, W.C., Chen, S.Y., Lai, H.H., Lin, T.Y., Yang, J.C., Yang, P.C., Shih, J.Y., *et al.* (2013a). ALDH-positive lung cancer stem cells confer resistance to epidermal growth factor receptor tyrosine kinase inhibitors. *Cancer Lett* 328, 144-151.
- Huang, J., Li, C., Wang, Y., Lv, H., Guo, Y., Dai, H., Wicha, M.S., Chang, A.E., and Li, Q. (2013b). Cytokine-induced killer (CIK) cells bound with anti-CD3/anti-CD133 bispecific antibodies target CD133(high) cancer stem cells in vitro and in vivo. *Clin Immunol* 149, 156-168.
- Huang, M., and Weiss, W.A. (2013). Neuroblastoma and MYCN. *Cold Spring Harb Perspect Med* 3, a014415.
- Huang, M.E., Ye, Y.C., Chen, S.R., Zhao, J.C., Gu, L.J., Cai, J.R., Zhao, L., Xie, J.X., Shen, Z.X., and Wang, Z.Y. (1987). All-trans retinoic acid with or without low dose cytosine arabinoside in acute promyelocytic leukemia. Report of 6 cases. *Chin Med J (Engl)* 100, 949-953.
- Huang, R., Cheung, N.K., Vider, J., Cheung, I.Y., Gerald, W.L., Tickoo, S.K., Holland, E.C., and Blasberg, R.G. (2011). MYCN and MYC regulate tumor proliferation and tumorigenesis directly through BMI1 in human neuroblastomas. *FASEB J* 25, 4138-4149.
- Huber, K. (2006). The sympathoadrenal cell lineage: specification, diversification, and new perspectives. *Dev Biol* 298, 335-343.
- Huber, K., Kalcheim, C., and Unsicker, K. (2009). The development of the chromaffin cell lineage from the neural crest. *Auton Neurosci* 151, 10-16.
- Huynh, P.T., Beswick, E.J., Coronado, Y.A., Johnson, P., O'Connell, M.R., Watts, T., Singh, P., Qiu, S., Morris, K., Powell, D.W., *et al.* (2016). CD90(+) stromal cells are the major source of IL-6, which supports cancer stem-like cells and inflammation in colorectal cancer. *Int J Cancer* 138, 1971-1981.

- Ichtchenko, K., Hata, Y., Nguyen, T., Ullrich, B., Missler, M., Moomaw, C., and Sudhof, T.C. (1995). Neuroligin 1: a splice site-specific ligand for beta-neurexins. *Cell* *81*, 435-443.
- Ichtchenko, K., Nguyen, T., and Sudhof, T.C. (1996). Structures, alternative splicing, and neurexin binding of multiple neuroligins. *J Biol Chem* *271*, 2676-2682.
- Ikegaki, N., Shimada, H., Fox, A.M., Regan, P.L., Jacobs, J.R., Hicks, S.L., Rappaport, E.F., and Tang, X.X. (2013). Transient treatment with epigenetic modifiers yields stable neuroblastoma stem cells resembling aggressive large-cell neuroblastomas. *Proc Natl Acad Sci U S A* *110*, 6097-6102.
- Islam, A., Kageyama, H., Takada, N., Kawamoto, T., Takayasu, H., Isogai, E., Ohira, M., Hashizume, K., Kobayashi, H., Kaneko, Y., *et al.* (2000). High expression of Survivin, mapped to 17q25, is significantly associated with poor prognostic factors and promotes cell survival in human neuroblastoma. *Oncogene* *19*, 617-623.
- Jang, J.W., Song, Y., Kim, S.H., Kim, J., and Seo, H.R. (2017). Potential mechanisms of CD133 in cancer stem cells. *Life Sci* *184*, 25-29.
- Janoueix-Lerosey, I., Lequin, D., Brugieres, L., Ribeiro, A., de Pontual, L., Combaret, V., Raynal, V., Puisieux, A., Schleiermacher, G., Pierron, G., *et al.* (2008). Somatic and germline activating mutations of the ALK kinase receptor in neuroblastoma. *Nature* *455*, 967-970.
- Jiang, M., Stanke, J., and Lahti, J.M. (2011). The connections between neural crest development and neuroblastoma. *Curr Top Dev Biol* *94*, 77-127.
- Jin, J.S., and Tsai, W.C. (2016). The detection of tumor location and lymph node metastasis by aberrant NXP1 and NXP2 expressions in pancreatic ductal adenocarcinomas. *Chin J Physiol* *59*, 348-354.
- Johnson, J.R., Ning, Y.M., Farrell, A., Justice, R., Keegan, P., and Pazdur, R. (2011). Accelerated approval of oncology products: the food and drug administration experience. *J Natl Cancer Inst* *103*, 636-644.
- Joyce, J.A., and Pollard, J.W. (2009). Microenvironmental regulation of metastasis. *Nat Rev Cancer* *9*, 239-252.
- Kastriti, M.E., Kameneva, P., Kamenev, D., Dyachuk, V., Furlan, A., Hampl, M., Memic, F., Marklund, U., Lallemend, F., Hadjab, S., *et al.* (2019). Schwann Cell Precursors Generate the Majority of Chromaffin Cells in Zuckerkandl Organ and Some Sympathetic Neurons in Paraganglia. *Front Mol Neurosci* *12*, 6.
- Killmann, S.A., Cronkite, E.P., Robertson, J.S., Fliedner, T.M., and Bond, V.P. (1963). Estimation of phases of the life cycle of leukemic cells from labeling in human beings in vivo with tritiated thymidine. *Lab Invest* *12*, 671-684.
- Kim, E., Kim, M., Woo, D.H., Shin, Y., Shin, J., Chang, N., Oh, Y.T., Kim, H., Rhee, J., Nakano, I., *et al.* (2013). Phosphorylation of EZH2 activates STAT3 signaling via STAT3 methylation and promotes tumorigenicity of glioblastoma stem-like cells. *Cancer Cell* *23*, 839-852.
- Kinzfogel, J., Hangoc, G., and Broxmeyer, H.E. (2011). Neurexophilin 1 suppresses the proliferation of hematopoietic progenitor cells. *Blood* *118*, 565-575.
- Kleinsmith, L.J., and Pierce, G.B., Jr. (1964). Multipotentiality of Single Embryonal Carcinoma Cells. *Cancer Res* *24*, 1544-1551.
- Ko, J., Fuccillo, M.V., Malenka, R.C., and Sudhof, T.C. (2009). LRRTM2 functions as a neurexin ligand in promoting excitatory synapse formation. *Neuron* *64*, 791-798.
- Kocak, H., Ackermann, S., Hero, B., Kahlert, Y., Oberthuer, A., Juraeva, D., Roels, F., Theissen, J., Westermann, F.,

- Deubzer, H., *et al.* (2013). Hox-C9 activates the intrinsic pathway of apoptosis and is associated with spontaneous regression in neuroblastoma. *Cell Death Dis* 4, e586.
- Komuro, H., Saihara, R., Shinya, M., Takita, J., Kaneko, S., Kaneko, M., and Hayashi, Y. (2007). Identification of side population cells (stem-like cell population) in pediatric solid tumor cell lines. *J Pediatr Surg* 42, 2040-2045.
- Kondo, T., Setoguchi, T., and Taga, T. (2004). Persistence of a small subpopulation of cancer stem-like cells in the C6 glioma cell line. *Proc Natl Acad Sci U S A* 101, 781-786.
- Koyama, H., Zhuang, T., Light, J.E., Kolla, V., Higashi, M., McGrady, P.W., London, W.B., and Brodeur, G.M. (2012). Mechanisms of CHD5 Inactivation in neuroblastomas. *Clin Cancer Res* 18, 1588-1597.
- Kreso, A. (2012). Characterization of Tumour-initiating Cells in Human Colorectal Cancer. In Department of Molecular Genetics (University of Toronto), pp. 156.
- Kreso, A., and Dick, J.E. (2014). Evolution of the cancer stem cell model. *Cell Stem Cell* 14, 275-291.
- Kreso, A., O'Brien, C.A., van Galen, P., Gan, O.I., Notta, F., Brown, A.M., Ng, K., Ma, J., Wienholds, E., Dunant, C., *et al.* (2013). Variable clonal repopulation dynamics influence chemotherapy response in colorectal cancer. *Science* 339, 543-548.
- Kretzschmar, K., and Watt, F.M. (2012). Lineage tracing. *Cell* 148, 33-45.
- Kulis, M., Heath, S., Bibikova, M., Queiros, A.C., Navarro, A., Clot, G., Martinez-Trillos, A., Castellano, G., Brun-Heath, I., Pinyol, M., *et al.* (2012). Epigenomic analysis detects widespread gene-body DNA hypomethylation in chronic lymphocytic leukemia. *Nat Genet* 44, 1236-1242.
- Kumar, K.K., Burgess, A.W., and Gulbis, J.M. (2014). Structure and function of LGR5: an enigmatic G-protein coupled receptor marking stem cells. *Protein Sci* 23, 551-565.
- Kumar, M.P., Du, J., Lagoudas, G., Jiao, Y., Sawyer, A., Drummond, D.C., Lauffenburger, D.A., and Raue, A. (2018). Analysis of Single-Cell RNA-Seq Identifies Cell-Cell Communication Associated with Tumor Characteristics. *Cell Rep* 25, 1458-1468 e1454.
- Kurtova, A.V., Xiao, J., Mo, Q., Pazhanisamy, S., Krasnow, R., Lerner, S.P., Chen, F., Roh, T.T., Lay, E., Ho, P.L., *et al.* (2015). Blocking PGE2-induced tumour repopulation abrogates bladder cancer chemoresistance. *Nature* 517, 209-213.
- Kushner, B.H., Gilbert, F., and Helson, L. (1986). Familial neuroblastoma. Case reports, literature review, and etiologic considerations. *Cancer* 57, 1887-1893.
- Lapidot, T., Sirard, C., Vormoor, J., Murdoch, B., Hoang, T., Caceres-Cortes, J., Minden, M., Paterson, B., Caligiuri, M.A., and Dick, J.E. (1994). A cell initiating human acute myeloid leukaemia after transplantation into SCID mice. *Nature* 367, 645-648.
- Laszlo, G.S., Estey, E.H., and Walter, R.B. (2014). The past and future of CD33 as therapeutic target in acute myeloid leukemia. *Blood Rev* 28, 143-153.
- Lau, E.Y., Lo, J., Cheng, B.Y., Ma, M.K., Lee, J.M., Ng, J.K., Chai, S., Lin, C.H., Tsang, S.Y., Ma, S., *et al.* (2016). Cancer-Associated Fibroblasts Regulate Tumor-Initiating Cell Plasticity in Hepatocellular Carcinoma through c-Met/FRA1/HEY1 Signaling. *Cell Rep* 15, 1175-1189.
- Lavarino, C., Cheung, N.K., Garcia, I., Domenech, G., de Torres, C., Alaminos, M., Rios, J., Gerald, W.L., Kushner,

- B., LaQuaglia, M., *et al.* (2009). Specific gene expression profiles and chromosomal abnormalities are associated with infant disseminated neuroblastoma. *BMC Cancer* 9, 44.
- Lavarino, C., Garcia, I., Mackintosh, C., Cheung, N.K., Domenech, G., Rios, J., Perez, N., Rodriguez, E., de Torres, C., Gerald, W.L., *et al.* (2008). Differential expression of genes mapping to recurrently abnormal chromosomal regions characterize neuroblastic tumours with distinct ploidy status. *BMC Med Genomics* 1, 36.
- Le Douarin, N.M. (2004). The avian embryo as a model to study the development of the neural crest: a long and still ongoing story. *Mech Dev* 121, 1089-1102.
- Le Dreau, G., Garcia-Campmany, L., Rabadan, M.A., Ferronha, T., Tozer, S., Briscoe, J., and Marti, E. (2012). Canonical BMP7 activity is required for the generation of discrete neuronal populations in the dorsal spinal cord. *Development* 139, 259-268.
- Lee, S.H., Kim, J.S., Zheng, S., Huse, J.T., Bae, J.S., Lee, J.W., Yoo, K.H., Koo, H.H., Kyung, S., Park, W.Y., *et al.* (2017). ARID1B alterations identify aggressive tumors in neuroblastoma. *Oncotarget* 8, 45943-45950.
- Lessard, J., and Sauvageau, G. (2003). Bmi-1 determines the proliferative capacity of normal and leukaemic stem cells. *Nature* 423, 255-260.
- Leushacke, M., Ng, A., Galle, J., Loeffler, M., and Barker, N. (2013). Lgr5(+) gastric stem cells divide symmetrically to effect epithelial homeostasis in the pylorus. *Cell Rep* 5, 349-356.
- Li, C., Heidt, D.G., Dalerba, P., Burant, C.F., Zhang, L., Adsay, V., Wicha, M., Clarke, M.F., and Simeone, D.M. (2007). Identification of pancreatic cancer stem cells. *Cancer Res* 67, 1030-1037.
- Li, H.J., Reinhardt, F., Herschman, H.R., and Weinberg, R.A. (2012). Cancer-stimulated mesenchymal stem cells create a carcinoma stem cell niche via prostaglandin E2 signaling. *Cancer Discov* 2, 840-855.
- Li, Z., Bao, S., Wu, Q., Wang, H., Eyler, C., Sathornsumetee, S., Shi, Q., Cao, Y., Lathia, J., McLendon, R.E., *et al.* (2009). Hypoxia-inducible factors regulate tumorigenic capacity of glioma stem cells. *Cancer Cell* 15, 501-513.
- Liau, B.B., Sievers, C., Donohue, L.K., Gillespie, S.M., Flavahan, W.A., Miller, T.E., Venteicher, A.S., Hebert, C.H., Carey, C.D., Rodig, S.J., *et al.* (2017). Adaptive Chromatin Remodeling Drives Glioblastoma Stem Cell Plasticity and Drug Tolerance. *Cell Stem Cell* 20, 233-246 e237.
- Linabery, A.M., and Ross, J.A. (2008). Trends in childhood cancer incidence in the U.S. (1992-2004). *Cancer* 112, 416-432.
- Lodrini, M., Oehme, I., Schroeder, C., Milde, T., Schier, M.C., Kopp-Schneider, A., Schulte, J.H., Fischer, M., De Preter, K., Pattyn, F., *et al.* (2013). MYCN and HDAC2 cooperate to repress miR-183 signaling in neuroblastoma. *Nucleic Acids Res* 41, 6018-6033.
- London, W.B., Castleberry, R.P., Matthay, K.K., Look, A.T., Seeger, R.C., Shimada, H., Thorner, P., Brodeur, G., Maris, J.M., Reynolds, C.P., *et al.* (2005). Evidence for an age cutoff greater than 365 days for neuroblastoma risk group stratification in the Children's Oncology Group. *J Clin Oncol* 23, 6459-6465.
- Lopez-Garcia, C., Klein, A.M., Simons, B.D., and Winton, D.J. (2010). Intestinal stem cell replacement follows a pattern of neutral drift. *Science* 330, 822-825.
- Lotti, F., Jarrar, A.M., Pai, R.K., Hitomi, M., Lathia, J., Mace, A., Gantt, G.A., Jr., Sukhdeo, K., DeVecchio, J., Vasanji, A., *et al.* (2013). Chemotherapy activates cancer-associated fibroblasts to maintain colorectal cancer-initiating cells by IL-17A. *J Exp Med* 210, 2851-2872.

- Lu, K.V., Zhu, S., Cvrljevic, A., Huang, T.T., Sarkaria, S., Ahkavan, D., Dang, J., Dinca, E.B., Plaisier, S.B., Oderberg, I., *et al.* (2009). Fyn and SRC are effectors of oncogenic epidermal growth factor receptor signaling in glioblastoma patients. *Cancer Res* 69, 6889-6898.
- Ma, S., Chan, K.W., Lee, T.K., Tang, K.H., Wo, J.Y., Zheng, B.J., and Guan, X.Y. (2008). Aldehyde dehydrogenase discriminates the CD133 liver cancer stem cell populations. *Mol Cancer Res* 6, 1146-1153.
- Maehle, A.H. (2011). Ambiguous cells: the emergence of the stem cell concept in the nineteenth and twentieth centuries. *Notes Rec R Soc Lond* 65, 359-378.
- Magee, J.A., Piskounova, E., and Morrison, S.J. (2012). Cancer stem cells: impact, heterogeneity, and uncertainty. *Cancer Cell* 21, 283-296.
- Mahller, Y.Y., Williams, J.P., Baird, W.H., Mitton, B., Grossheim, J., Saeki, Y., Cancelas, J.A., Ratner, N., and Cripe, T.P. (2009). Neuroblastoma cell lines contain pluripotent tumor initiating cells that are susceptible to a targeted oncolytic virus. *PLoS One* 4, e4235.
- Makino, S. (1956). Further evidence favoring the concept of the stem cell in ascites tumors of rats. *Ann N Y Acad Sci* 63, 818-830.
- Malanchi, I., Peinado, H., Kassen, D., Hussenet, T., Metzger, D., Chambon, P., Huber, M., Hohl, D., Cano, A., Birchmeier, W., *et al.* (2008). Cutaneous cancer stem cell maintenance is dependent on beta-catenin signalling. *Nature* 452, 650-653.
- Mani, S.A., Guo, W., Liao, M.J., Eaton, E.N., Ayyanan, A., Zhou, A.Y., Brooks, M., Reinhard, F., Zhang, C.C., Shipitsin, M., *et al.* (2008). The epithelial-mesenchymal transition generates cells with properties of stem cells. *Cell* 133, 704-715.
- Marcato, P., Dean, C.A., Pan, D., Araslanova, R., Gillis, M., Joshi, M., Helyer, L., Pan, L., Leidal, A., Gujar, S., *et al.* (2011). Aldehyde dehydrogenase activity of breast cancer stem cells is primarily due to isoform ALDH1A3 and its expression is predictive of metastasis. *Stem Cells* 29, 32-45.
- Maris, J.M., and Denny, C.T. (2002). Focus on embryonal malignancies. *Cancer Cell* 2, 447-450.
- Maris, J.M., Hogarty, M.D., Bagatell, R., and Cohn, S.L. (2007). Neuroblastoma. *Lancet* 369, 2106-2120.
- Marjanovic, N.D., Weinberg, R.A., and Chaffer, C.L. (2013). Cell plasticity and heterogeneity in cancer. *Clin Chem* 59, 168-179.
- Matsuda, K., Budisantoso, T., Mitakidis, N., Sugaya, Y., Miura, E., Kakegawa, W., Yamasaki, M., Konno, K., Uchigashima, M., Abe, M., *et al.* (2016). Transsynaptic Modulation of Kainate Receptor Functions by C1q-like Proteins. *Neuron* 90, 752-767.
- Matsui, W.H. (2016). Cancer stem cell signaling pathways. *Medicine (Baltimore)* 95, S8-S19.
- Matthay, K.K., Maris, J.M., Schleiermacher, G., Nakagawara, A., Mackall, C.L., Diller, L., and Weiss, W.A. (2016). Neuroblastoma. *Nat Rev Dis Primers* 2, 16078.
- Matthay, K.K., Villablanca, J.G., Seeger, R.C., Stram, D.O., Harris, R.E., Ramsay, N.K., Swift, P., Shimada, H., Black, C.T., Brodeur, G.M., *et al.* (1999). Treatment of high-risk neuroblastoma with intensive chemotherapy, radiotherapy, autologous bone marrow transplantation, and 13-cis-retinoic acid. Children's Cancer Group. *N Engl J Med* 341, 1165-1173.
- Mayol, G., Martin-Subero, J.I., Rios, J., Queiros, A., Kulis, M., Sunol, M., Esteller, M., Gomez, S., Garcia, I., de Tor-

- res, C., *et al.* (2012). DNA hypomethylation affects cancer-related biological functions and genes relevant in neuroblastoma pathogenesis. *PLoS One* 7, e48401.
- McGranahan, N., and Swanton, C. (2017). Clonal Heterogeneity and Tumor Evolution: Past, Present, and the Future. *Cell* 168, 613-628.
- Meacham, C.E., and Morrison, S.J. (2013). Tumour heterogeneity and cancer cell plasticity. *Nature* 501, 328-337.
- Meads, M.B., Gatenby, R.A., and Dalton, W.S. (2009). Environment-mediated drug resistance: a major contributor to minimal residual disease. *Nat Rev Cancer* 9, 665-674.
- Medema, J.P. (2013). Cancer stem cells: the challenges ahead. *Nat Cell Biol* 15, 338-344.
- Merlos-Suarez, A., Barriga, F.M., Jung, P., Iglesias, M., Cespedes, M.V., Rossell, D., Sevillano, M., Hernando-Mombona, X., da Silva-Diz, V., Munoz, P., *et al.* (2011). The intestinal stem cell signature identifies colorectal cancer stem cells and predicts disease relapse. *Cell Stem Cell* 8, 511-524.
- Missler, M., Hammer, R.E., and Sudhof, T.C. (1998). Neurexophilin binding to alpha-neurexins. A single LNS domain functions as an independently folding ligand-binding unit. *J Biol Chem* 273, 34716-34723.
- Missler, M., and Sudhof, T.C. (1998). Neurexophilins form a conserved family of neuropeptide-like glycoproteins. *J Neurosci* 18, 3630-3638.
- Missler, M., Zhang, W., Rohlmann, A., Kattenstroth, G., Hammer, R.E., Gottmann, K., and Sudhof, T.C. (2003). Alpha-neurexins couple Ca<sup>2+</sup> channels to synaptic vesicle exocytosis. *Nature* 423, 939-948.
- Mobley, B.C., Kwon, M., Kraemer, B.R., Hickman, F.E., Qiao, J., Chung, D.H., and Carter, B.D. (2015). Expression of MYCN in Multipotent Sympathoadrenal Progenitors Induces Proliferation and Neural Differentiation, but Is Not Sufficient for Tumorigenesis. *PLoS One* 10, e0133897.
- Moffat, J., Grueneberg, D.A., Yang, X., Kim, S.Y., Kloepfer, A.M., Hinkle, G., Piqani, B., Eisenhaure, T.M., Luo, B., Grenier, J.K., *et al.* (2006). A lentiviral RNAi library for human and mouse genes applied to an arrayed viral high-content screen. *Cell* 124, 1283-1298.
- Molenaar, J.J., Koster, J., Zwijnenburg, D.A., van Sluis, P., Valentijn, L.J., van der Ploeg, I., Hamdi, M., van Nes, J., Westerman, B.A., van Arkel, J., *et al.* (2012). Sequencing of neuroblastoma identifies chromothripsis and defects in neuritogenesis genes. *Nature* 483, 589-593.
- Monclair, T., Brodeur, G.M., Ambros, P.F., Brisse, H.J., Cecchetto, G., Holmes, K., Kaneko, M., London, W.B., Matthay, K.K., Nuchtern, J.G., *et al.* (2009). The International Neuroblastoma Risk Group (INRG) staging system: an INRG Task Force report. *J Clin Oncol* 27, 298-303.
- Monterrubio, C., Paco, S., Olaciregui, N.G., Pascual-Pasto, G., Vila-Ubach, M., Cuadrado-Vilanova, M., Ferrandiz, M.M., Castillo-Ecija, H., Glisoni, R., Kuplennik, N., *et al.* (2017). Targeted drug distribution in tumor extracellular fluid of GD2-expressing neuroblastoma patient-derived xenografts using SN-38-loaded nanoparticles conjugated to the monoclonal antibody 3F8. *J Control Release* 255, 108-119.
- Monterrubio, C., Paco, S., Vila-Ubach, M., Rodriguez, E., Glisoni, R., Lavarino, C., Schaiquevich, P., Sosnik, A., Mora, J., and Carcaboso, A.M. (2015). Combined Microdialysis-Tumor Homogenate Method for the Study of the Steady State Compartmental Distribution of a Hydrophobic Anticancer Drug in Patient-Derived Xenografts. *Pharm Res* 32, 2889-2900.
- Mora, J., Cheung, N.K., Chen, L., Qin, J., and Gerald, W. (2001). Survival analysis of clinical, pathologic, and genetic features in neuroblastoma presenting as locoregional disease. *Cancer* 91, 435-442.

- Mora, J., and Gerald, W.L. (2004). Origin of neuroblastic tumors: clues for future therapeutics. *Expert Rev Mol Diagn* 4, 293-302.
- Mora, J., Lavarino, C., Alaminos, M., Cheung, N.K., Rios, J., de Torres, C., Illei, P., Juan, G., and Gerald, W.L. (2007). Comprehensive analysis of tumoral DNA content reveals clonal ploidy heterogeneity as a marker with prognostic significance in locoregional neuroblastoma. *Genes Chromosomes Cancer* 46, 385-396.
- Morgenstern, D.A., Bagatell, R., Cohn, S.L., Hogarty, M.D., Maris, J.M., Moreno, L., Park, J.R., Pearson, A.D., Schleiermacher, G., Valteau-Couanet, D., *et al.* (2019). The challenge of defining “ultra-high-risk” neuroblastoma. *Pediatr Blood Cancer* 66, e27556.
- Morrison, S.J., and Spradling, A.C. (2008). Stem cells and niches: mechanisms that promote stem cell maintenance throughout life. *Cell* 132, 598-611.
- Morrison, S.J., White, P.M., Zock, C., and Anderson, D.J. (1999). Prospective identification, isolation by flow cytometry, and in vivo self-renewal of multipotent mammalian neural crest stem cells. *Cell* 96, 737-749.
- Mosedale, M., Egodage, S., Calma, R.C., Chi, N.W., and Chessler, S.D. (2012). Neurexin-1alpha contributes to insulin-containing secretory granule docking. *J Biol Chem* 287, 6350-6361.
- Mosse, Y.P., Laudenslager, M., Khazi, D., Carlisle, A.J., Winter, C.L., Rappaport, E., and Maris, J.M. (2004). Germ-line PHOX2B mutation in hereditary neuroblastoma. *Am J Hum Genet* 75, 727-730.
- Mosse, Y.P., Laudenslager, M., Longo, L., Cole, K.A., Wood, A., Attiyeh, E.F., Laquaglia, M.J., Sennett, R., Lynch, J.E., Perri, P., *et al.* (2008). Identification of ALK as a major familial neuroblastoma predisposition gene. *Nature* 455, 930-935.
- Mukherjee, K., Sharma, M., Urlaub, H., Bourenkov, G.P., Jahn, R., Sudhof, T.C., and Wahl, M.C. (2008). CASK Functions as a Mg<sup>2+</sup>-independent neurexin kinase. *Cell* 133, 328-339.
- Nagoshi, N., Shibata, S., Kubota, Y., Nakamura, M., Nagai, Y., Satoh, E., Morikawa, S., Okada, Y., Mabuchi, Y., Kato, H., *et al.* (2008). Ontogeny and multipotency of neural crest-derived stem cells in mouse bone marrow, dorsal root ganglia, and whisker pad. *Cell Stem Cell* 2, 392-403.
- Nakagawara, A., Li, Y., Izumi, H., Muramori, K., Inada, H., and Nishi, M. (2018). Neuroblastoma. *Jpn J Clin Oncol* 48, 214-241.
- Nakamura, H., Arai, Y., Totoki, Y., Shirota, T., Elzawahry, A., Kato, M., Hama, N., Hosoda, F., Urushidate, T., Ohashi, S., *et al.* (2015). Genomic spectra of biliary tract cancer. *Nat Genet* 47, 1003-1010.
- Nassar, D., and Blanpain, C. (2016). Cancer Stem Cells: Basic Concepts and Therapeutic Implications. *Annu Rev Pathol* 11, 47-76.
- Neftel, C., Laffy, J., Filbin, M.G., Hara, T., Shore, M.E., Rahme, G.J., Richman, A.R., Silverbush, D., Shaw, M.L., Hebert, C.M., *et al.* (2019). An Integrative Model of Cellular States, Plasticity, and Genetics for Glioblastoma. *Cell* 178, 835-849 e821.
- Newton, T.C., Wolcott, K., and Roberts, S.S. (2010). Comparison of the side populations in pretreatment and postrelapse neuroblastoma cell lines. *Transl Oncol* 3, 246-251.
- Nguyen le, B., Diskin, S.J., Capasso, M., Wang, K., Diamond, M.A., Glessner, J., Kim, C., Attiyeh, E.F., Mosse, Y.P., Cole, K., *et al.* (2011). Phenotype restricted genome-wide association study using a gene-centric approach identifies three low-risk neuroblastoma susceptibility Loci. *PLoS Genet* 7, e1002026.

- Niemoller, C., Renz, N., Bleul, S., Blagitko-Dorfs, N., Greil, C., Yoshida, K., Pfeifer, D., Follo, M., Duyster, J., Claus, R., *et al.* (2016). Single cell genotyping of exome sequencing-identified mutations to characterize the clonal composition and evolution of inv(16) AML in a CBL mutated clonal hematopoiesis. *Leuk Res* 47, 41-46.
- Nilsson, B. (1984). Probable in vivo induction of differentiation by retinoic acid of promyelocytes in acute promyelocytic leukaemia. *Br J Haematol* 57, 365-371.
- Northcutt, R.G. (2005). The new head hypothesis revisited. *J Exp Zool B Mol Dev Evol* 304, 274-297.
- Notterpek, L., Roux, K.J., Amici, S.A., Yazdanpour, A., Rahner, C., and Fletcher, B.S. (2001). Peripheral myelin protein 22 is a constituent of intercellular junctions in epithelia. *Proc Natl Acad Sci U S A* 98, 14404-14409.
- Nowak, D., Stewart, D., and Koeffler, H.P. (2009). Differentiation therapy of leukemia: 3 decades of development. *Blood* 113, 3655-3665.
- Nowell, P.C. (1976). The clonal evolution of tumor cell populations. *Science* 194, 23-28.
- O'Brien, C.A., Pollett, A., Gallinger, S., and Dick, J.E. (2007). A human colon cancer cell capable of initiating tumour growth in immunodeficient mice. *Nature* 445, 106-110.
- Ocana, O.H., Corcoles, R., Fabra, A., Moreno-Bueno, G., Acloque, H., Vega, S., Barrallo-Gimeno, A., Cano, A., and Nieto, M.A. (2012). Metastatic colonization requires the repression of the epithelial-mesenchymal transition inducer Prrx1. *Cancer Cell* 22, 709-724.
- Oehme, I., Deubzer, H.E., Lodrini, M., Milde, T., and Witt, O. (2009a). Targeting of HDAC8 and investigational inhibitors in neuroblastoma. *Expert Opin Investig Drugs* 18, 1605-1617.
- Oehme, I., Deubzer, H.E., Wegener, D., Pickert, D., Linke, J.P., Hero, B., Kopp-Schneider, A., Westermann, F., Ulrich, S.M., von Deimling, A., *et al.* (2009b). Histone deacetylase 8 in neuroblastoma tumorigenesis. *Clin Cancer Res* 15, 91-99.
- Oldridge, D.A., Wood, A.C., Weichert-Leahey, N., Crimmins, I., Sussman, R., Winter, C., McDaniel, L.D., Diamond, M., Hart, L.S., Zhu, S., *et al.* (2015). Genetic predisposition to neuroblastoma mediated by a LMO1 super-enhancer polymorphism. *Nature* 528, 418-421.
- Olsson, M., Beck, S., Kogner, P., Martinsson, T., and Caren, H. (2016). Genome-wide methylation profiling identifies novel methylated genes in neuroblastoma tumors. *Epigenetics* 11, 74-84.
- OMIM (2019). Online Mendelian Inheritance in Man.
- Oshimori, N., Oristian, D., and Fuchs, E. (2015). TGF-beta promotes heterogeneity and drug resistance in squamous cell carcinoma. *Cell* 160, 963-976.
- Oskarsson, T., Acharyya, S., Zhang, X.H., Vanharanta, S., Tavazoie, S.F., Morris, P.G., Downey, R.J., Manova-Todorova, K., Brogi, E., and Massague, J. (2011). Breast cancer cells produce tenascin C as a metastatic niche component to colonize the lungs. *Nat Med* 17, 867-874.
- Oskarsson, T., Batlle, E., and Massague, J. (2014). Metastatic stem cells: sources, niches, and vital pathways. *Cell Stem Cell* 14, 306-321.
- Pardo Romaguera, E.M.L., A., Valero Poveda, S.; Porta Cebolla, S.; Fernández-Delgado, R.; Barreda Reines, M. S.; Peris Bonet, R. (2018). Cáncer infantil en España. Estadísticas 1980-2017. Registro Español de Tumores Infantiles (RETI-SEHOP). (Valencia:: Universitat de València).

- Park, I.K., Qian, D., Kiel, M., Becker, M.W., Pihalja, M., Weissman, I.L., Morrison, S.J., and Clarke, M.F. (2003). Bmi-1 is required for maintenance of adult self-renewing haematopoietic stem cells. *Nature* 423, 302-305.
- Park, J.R., Bagatell, R., Cohn, S.L., Pearson, A.D., Villablanca, J.G., Berthold, F., Burchill, S., Boubaker, A., McHugh, K., Nuchtern, J.G., *et al.* (2017). Revisions to the International Neuroblastoma Response Criteria: A Consensus Statement From the National Cancer Institute Clinical Trials Planning Meeting. *J Clin Oncol* 35, 2580-2587.
- Pascual, G., Avgustinova, A., Mejetta, S., Martin, M., Castellanos, A., Attolini, C.S., Berenguer, A., Prats, N., Toll, A., Hueto, J.A., *et al.* (2017). Targeting metastasis-initiating cells through the fatty acid receptor CD36. *Nature* 541, 41-45.
- Patrawala, L., Calhoun, T., Schneider-Broussard, R., Li, H., Bhatia, B., Tang, S., Reilly, J.G., Chandra, D., Zhou, J., Claypool, K., *et al.* (2006). Highly purified CD44+ prostate cancer cells from xenograft human tumors are enriched in tumorigenic and metastatic progenitor cells. *Oncogene* 25, 1696-1708.
- Patrawala, L., Calhoun, T., Schneider-Broussard, R., Zhou, J., Claypool, K., and Tang, D.G. (2005). Side population is enriched in tumorigenic, stem-like cancer cells, whereas ABCG2+ and ABCG2- cancer cells are similarly tumorigenic. *Cancer Res* 65, 6207-6219.
- Pece, S., Tosoni, D., Confalonieri, S., Mazzarol, G., Vecchi, M., Ronzoni, S., Bernard, L., Viale, G., Pelicci, P.G., and Di Fiore, P.P. (2010). Biological and molecular heterogeneity of breast cancers correlates with their cancer stem cell content. *Cell* 140, 62-73.
- Peifer, M., Hertwig, F., Roels, F., Dreidax, D., Gartlgruber, M., Menon, R., Kramer, A., Roncaioli, J.L., Sand, F., Heuckmann, J.M., *et al.* (2015). Telomerase activation by genomic rearrangements in high-risk neuroblastoma. *Nature* 526, 700-704.
- Petrenko, A.G., Perin, M.S., Davletov, B.A., Ushkaryov, Y.A., Geppert, M., and Sudhof, T.C. (1991). Binding of synaptotagmin to the alpha-latrotoxin receptor implicates both in synaptic vesicle exocytosis. *Nature* 353, 65-68.
- Petrenko, A.G., Ullrich, B., Missler, M., Krasnoperov, V., Rosahl, T.W., and Sudhof, T.C. (1996). Structure and evolution of neurexophilin. *J Neurosci* 16, 4360-4369.
- Pettem, K.L., Yokomaku, D., Luo, L., Linhoff, M.W., Prasad, T., Connor, S.A., Siddiqui, T.J., Kawabe, H., Chen, F., Zhang, L., *et al.* (2013). The specific alpha-neurexin interactor calsynenin-3 promotes excitatory and inhibitory synapse development. *Neuron* 80, 113-128.
- Pezzolo, A., Parodi, F., Corrias, M.V., Cinti, R., Gambini, C., and Pistoia, V. (2007). Tumor origin of endothelial cells in human neuroblastoma. *J Clin Oncol* 25, 376-383.
- Piccirillo, S.G., Spiteri, I., Sottoriva, A., Touloumis, A., Ber, S., Price, S.J., Heywood, R., Francis, N.J., Howarth, K.D., Collins, V.P., *et al.* (2015). Contributions to drug resistance in glioblastoma derived from malignant cells in the sub-ependymal zone. *Cancer Res* 75, 194-202.
- Pierce, G.B. (1974). Neoplasms, differentiations and mutations. *Am J Pathol* 77, 103-118.
- Pierce, G.B., and Wallace, C. (1971). Differentiation of malignant to benign cells. *Cancer Res* 31, 127-134.
- Plaks, V., Kong, N., and Werb, Z. (2015). The cancer stem cell niche: how essential is the niche in regulating stemness of tumor cells? *Cell Stem Cell* 16, 225-238.
- Plantaz, D., Mohapatra, G., Matthay, K.K., Pellarin, M., Seeger, R.C., and Feuerstein, B.G. (1997). Gain of chromosome 17 is the most frequent abnormality detected in neuroblastoma by comparative genomic hybridiza-

- tion. *Am J Pathol* 150, 81-89.
- Podberezin, M., Wen, J., and Chang, C.C. (2013). Cancer stem cells: a review of potential clinical applications. *Arch Pathol Lab Med* 137, 1111-1116.
- Posadas, E.M., Al-Ahmadie, H., Robinson, V.L., Jagadeeswaran, R., Otto, K., Kasza, K.E., Tretiakov, M., Siddiqui, J., Pienta, K.J., Stadler, W.M., *et al.* (2009). FYN is overexpressed in human prostate cancer. *BJU Int* 103, 171-177.
- Pott, S., and Lieb, J.D. (2015). What are super-enhancers? *Nat Genet* 47, 8-12.
- Prince, M.E., Sivanandan, R., Kaczorowski, A., Wolf, G.T., Kaplan, M.J., Dalerba, P., Weissman, I.L., Clarke, M.F., and Ailles, L.E. (2007). Identification of a subpopulation of cells with cancer stem cell properties in head and neck squamous cell carcinoma. *Proc Natl Acad Sci U S A* 104, 973-978.
- Program, S. (2019). SEER Cancer Statistics Review, 1975-2016, N.N. Howlander, A. M.; Krapcho, M.; Miller, D.; Brest, A.; Yu, M.; Ruhl, J.; Tatalovich, Z.; Mariotto, A.; Lewis, D. R.; Chen, H.S.; Feuer, E.J.; Cronin, K. A., ed. (Bethesda, MD: National Cancer Institute).
- Puck, T.T., and Marcus, P.I. (1956). Action of x-rays on mammalian cells. *J Exp Med* 103, 653-666.
- Pugh, T.J., Morozova, O., Attiyeh, E.F., Asgharzadeh, S., Wei, J.S., Auclair, D., Carter, S.L., Cibulskis, K., Hanna, M., Kiezun, A., *et al.* (2013). The genetic landscape of high-risk neuroblastoma. *Nat Genet* 45, 279-284.
- Puisieux, A., Brabletz, T., and Caramel, J. (2014). Oncogenic roles of EMT-inducing transcription factors. *Nat Cell Biol* 16, 488-494.
- Quintana, E., Shackleton, M., Foster, H.R., Fullen, D.R., Sabel, M.S., Johnson, T.M., and Morrison, S.J. (2010). Phenotypic heterogeneity among tumorigenic melanoma cells from patients that is reversible and not hierarchically organized. *Cancer Cell* 18, 510-523.
- Quintana, E., Shackleton, M., Sabel, M.S., Fullen, D.R., Johnson, T.M., and Morrison, S.J. (2008). Efficient tumour formation by single human melanoma cells. *Nature* 456, 593-598.
- R2-server (2019). R2: Genomic Analysis and Visualization Platform.
- Rabadan, M.A., Usieto, S., Lavarino, C., and Marti, E. (2013). Identification of a putative transcriptome signature common to neuroblastoma and neural crest cells. *Dev Neurobiol* 73, 815-827.
- Rada-Iglesias, A., Bajpai, R., Prescott, S., Brugmann, S.A., Swigut, T., and Wysocka, J. (2012). Epigenomic annotation of enhancers predicts transcriptional regulators of human neural crest. *Cell Stem Cell* 11, 633-648.
- Rafehi, H., Orłowski, C., Georgiadis, G.T., Ververis, K., El-Osta, A., and Karagiannis, T.C. (2011). Clonogenic assay: adherent cells. *J Vis Exp*.
- Rajendran, V., and Jain, M.V. (2018). In Vitro Tumorigenic Assay: Colony Forming Assay for Cancer Stem Cells. *Methods Mol Biol* 1692, 89-95.
- Rambow, F., Rogiers, A., Marin-Bejar, O., Aibar, S., Femel, J., Dewaele, M., Karras, P., Brown, D., Chang, Y.H., Debiec-Rychter, M., *et al.* (2018). Toward Minimal Residual Disease-Directed Therapy in Melanoma. *Cell* 174, 843-855 e819.
- Ramos, E.K., Hoffmann, A.D., Gerson, S.L., and Liu, H. (2017). New Opportunities and Challenges to Defeat Cancer Stem Cells. *Trends Cancer* 3, 780-796.

- Rashidi, H., and Sottile, V. (2009). The chick embryo: hatching a model for contemporary biomedical research. *Bioessays* 31, 459-465.
- Reissner, C., Stahn, J., Breuer, D., Klose, M., Pohlentz, G., Mormann, M., and Missler, M. (2014). Dystroglycan binding to alpha-neurexin competes with neurexophilin-1 and neuroligin in the brain. *J Biol Chem* 289, 27585-27603.
- Reya, T., Morrison, S.J., Clarke, M.F., and Weissman, I.L. (2001). Stem cells, cancer, and cancer stem cells. *Nature* 414, 105-111.
- Reynolds, B.A., Tetzlaff, W., and Weiss, S. (1992). A multipotent EGF-responsive striatal embryonic progenitor cell produces neurons and astrocytes. *J Neurosci* 12, 4565-4574.
- Reynolds, B.A., and Weiss, S. (1992). Generation of neurons and astrocytes from isolated cells of the adult mammalian central nervous system. *Science* 255, 1707-1710.
- Ribatti, D., Nico, B., Pezzolo, A., Vacca, A., Meazza, R., Cinti, R., Carlini, B., Parodi, F., Pistoia, V., and Corrias, M.V. (2006). Angiogenesis in a human neuroblastoma xenograft model: mechanisms and inhibition by tumour-derived interferon-gamma. *Br J Cancer* 94, 1845-1852.
- Ricci-Vitiani, L., Lombardi, D.G., Pilozzi, E., Biffoni, M., Todaro, M., Peschle, C., and De Maria, R. (2007). Identification and expansion of human colon-cancer-initiating cells. *Nature* 445, 111-115.
- Ricci-Vitiani, L., Pallini, R., Biffoni, M., Todaro, M., Invernici, G., Cenci, T., Maira, G., Parati, E.A., Stassi, G., Larocca, L.M., *et al.* (2010). Tumour vascularization via endothelial differentiation of glioblastoma stem-like cells. *Nature* 468, 824-828.
- Roesch, A., Fukunaga-Kalabis, M., Schmidt, E.C., Zabierowski, S.E., Brafford, P.A., Vultur, A., Basu, D., Gimotty, P., Vogt, T., and Herlyn, M. (2010). A temporarily distinct subpopulation of slow-cycling melanoma cells is required for continuous tumor growth. *Cell* 141, 583-594.
- Ross, R.A., and Spengler, B.A. (2007). Human neuroblastoma stem cells. *Semin Cancer Biol* 17, 241-247.
- Ross, R.A., Spengler, B.A., and Biedler, J.L. (1983). Coordinate morphological and biochemical interconversion of human neuroblastoma cells. *J Natl Cancer Inst* 71, 741-747.
- Ross, R.A., Spengler, B.A., Domenech, C., Porubcin, M., Rettig, W.J., and Biedler, J.L. (1995). Human neuroblastoma I-type cells are malignant neural crest stem cells. *Cell Growth Differ* 6, 449-456.
- Ross, R.A., Walton, J.D., Han, D., Guo, H.F., and Cheung, N.K. (2015). A distinct gene expression signature characterizes human neuroblastoma cancer stem cells. *Stem Cell Res* 15, 419-426.
- Ross, R.L., Burns, J.E., Taylor, C.F., Mellor, P., Anderson, D.H., and Knowles, M.A. (2013). Identification of mutations in distinct regions of p85 alpha in urothelial cancer. *PLoS One* 8, e84411.
- Saito, Y.D., Jensen, A.R., Salgia, R., and Posadas, E.M. (2010). Fyn: a novel molecular target in cancer. *Cancer* 116, 1629-1637.
- Sauka-Spengler, T., and Bronner-Fraser, M. (2008). A gene regulatory network orchestrates neural crest formation. *Nat Rev Mol Cell Biol* 9, 557-568.
- Sausen, M., Leary, R.J., Jones, S., Wu, J., Reynolds, C.P., Liu, X., Blackford, A., Parmigiani, G., Diaz, L.A., Jr., Papadopoulos, N., *et al.* (2013). Integrated genomic analyses identify ARID1A and ARID1B alterations in the childhood cancer neuroblastoma. *Nat Genet* 45, 12-17.

- Schepers, A.G., Snippert, H.J., Stange, D.E., van den Born, M., van Es, J.H., van de Wetering, M., and Clevers, H. (2012). Lineage tracing reveals Lgr5+ stem cell activity in mouse intestinal adenomas. *Science* 337, 730-735.
- Schleiermacher, G., Javanmardi, N., Bernard, V., Leroy, Q., Cappo, J., Rio Frio, T., Pierron, G., Lapouble, E., Combaret, V., Speleman, F., *et al.* (2014). Emergence of new ALK mutations at relapse of neuroblastoma. *J Clin Oncol* 32, 2727-2734.
- Schramm, A., Koster, J., Assenov, Y., Althoff, K., Peifer, M., Mahlow, E., Odersky, A., Beisser, D., Ernst, C., Henssen, A.G., *et al.* (2015). Mutational dynamics between primary and relapse neuroblastomas. *Nat Genet* 47, 872-877.
- Schreiner, D., Nguyen, T.M., Russo, G., Heber, S., Patrignani, A., Ahrne, E., and Scheiffele, P. (2014). Targeted combinatorial alternative splicing generates brain region-specific repertoires of neurexins. *Neuron* 84, 386-398.
- Shackleton, M., Quintana, E., Fearon, E.R., and Morrison, S.J. (2009). Heterogeneity in cancer: cancer stem cells versus clonal evolution. *Cell* 138, 822-829.
- Shimada, H., Ambros, I.M., Dehner, L.P., Hata, J., Joshi, V.V., and Roald, B. (1999). Terminology and morphologic criteria of neuroblastic tumors: recommendations by the International Neuroblastoma Pathology Committee. *Cancer* 86, 349-363.
- Shimokawa, M., Ohta, Y., Nishikori, S., Matano, M., Takano, A., Fujii, M., Date, S., Sugimoto, S., Kanai, T., and Sato, T. (2017). Visualization and targeting of LGR5(+) human colon cancer stem cells. *Nature* 545, 187-192.
- Shin, K.J., Wall, E.A., Zavzavadjian, J.R., Santat, L.A., Liu, J., Hwang, J.I., Rebres, R., Roach, T., Seaman, W., Simon, M.I., *et al.* (2006). A single lentiviral vector platform for microRNA-based conditional RNA interference and coordinated transgene expression. *Proc Natl Acad Sci U S A* 103, 13759-13764.
- Shultz, L.D., Schweitzer, P.A., Christianson, S.W., Gott, B., Schweitzer, I.B., Tennent, B., McKenna, S., Mobraaten, L., Rajan, T.V., Greiner, D.L., *et al.* (1995). Multiple defects in innate and adaptive immunologic function in NOD/LtSz-scid mice. *J Immunol* 154, 180-191.
- Simoës-Costa, M., and Bronner, M.E. (2015). Establishing neural crest identity: a gene regulatory recipe. *Development* 142, 242-257.
- Simon, T., Berthold, F., Borkhardt, A., Kremens, B., De Carolis, B., and Hero, B. (2011). Treatment and outcomes of patients with relapsed, high-risk neuroblastoma: results of German trials. *Pediatr Blood Cancer* 56, 578-583.
- Singh, S.K., Hawkins, C., Clarke, I.D., Squire, J.A., Bayani, J., Hide, T., Henkelman, R.M., Cusimano, M.D., and Dirks, P.B. (2004). Identification of human brain tumour initiating cells. *Nature* 432, 396-401.
- Skene, J.H., Jacobson, R.D., Snipes, G.J., McGuire, C.B., Norden, J.J., and Freeman, J.A. (1986). A protein induced during nerve growth (GAP-43) is a major component of growth-cone membranes. *Science* 233, 783-786.
- Sledz, C.A., Holko, M., de Veer, M.J., Silverman, R.H., and Williams, B.R. (2003). Activation of the interferon system by short-interfering RNAs. *Nat Cell Biol* 5, 834-839.
- Snipes, G.J., Suter, U., Welcher, A.A., and Shooter, E.M. (1992). Characterization of a novel peripheral nervous system myelin protein (PMP-22/SR13). *J Cell Biol* 117, 225-238.
- Snippert, H.J., van der Flier, L.G., Sato, T., van Es, J.H., van den Born, M., Kroon-Veenboer, C., Barker, N., Klein, A.M., van Rheenen, J., Simons, B.D., *et al.* (2010). Intestinal crypt homeostasis results from neutral competi-

- tion between symmetrically dividing Lgr5 stem cells. *Cell* *143*, 134-144.
- Soeda, A., Park, M., Lee, D., Mintz, A., Androutsellis-Theotokis, A., McKay, R.D., Engh, J., Iwama, T., Kunisada, T., Kassam, A.B., *et al.* (2009). Hypoxia promotes expansion of the CD133-positive glioma stem cells through activation of HIF-1alpha. *Oncogene* *28*, 3949-3959.
- Soldatov, R., Kaucka, M., Kastriti, M.E., Petersen, J., Chontorotzea, T., Englmaier, L., Akkuratova, N., Yang, Y., Haring, M., Dyachuk, V., *et al.* (2019). Spatiotemporal structure of cell fate decisions in murine neural crest. *Science* *364*.
- Son, M.J., Woolard, K., Nam, D.H., Lee, J., and Fine, H.A. (2009). SSEA-1 is an enrichment marker for tumor-initiating cells in human glioblastoma. *Cell Stem Cell* *4*, 440-452.
- Spike, B.T., Engle, D.D., Lin, J.C., Cheung, S.K., La, J., and Wahl, G.M. (2012). A mammary stem cell population identified and characterized in late embryogenesis reveals similarities to human breast cancer. *Cell Stem Cell* *10*, 183-197.
- Stahl, M., Kohrman, N., Gore, S.D., Kim, T.K., Zeidan, A.M., and Prebet, T. (2016). Epigenetics in Cancer: A Hematological Perspective. *PLoS Genet* *12*, e1006193.
- Sterky, F.H., Trotter, J.H., Lee, S.J., Recktenwald, C.V., Du, X., Zhou, B., Zhou, P., Schwenk, J., Fakler, B., and Sudhof, T.C. (2017). Carbonic anhydrase-related protein CA10 is an evolutionarily conserved pan-neurexin ligand. *Proc Natl Acad Sci U S A* *114*, E1253-E1262.
- Stewart, E., Federico, S.M., Chen, X., Shelat, A.A., Bradley, C., Gordon, B., Karlstrom, A., Twarog, N.R., Clay, M.R., Bahrami, A., *et al.* (2017). Orthotopic patient-derived xenografts of paediatric solid tumours. *Nature* *549*, 96-100.
- Stewart, J.M., Shaw, P.A., Gedye, C., Bernardini, M.Q., Neel, B.G., and Ailles, L.E. (2011). Phenotypic heterogeneity and instability of human ovarian tumor-initiating cells. *Proc Natl Acad Sci U S A* *108*, 6468-6473.
- Stine, R.R., and Matunis, E.L. (2013). Stem cell competition: finding balance in the niche. *Trends Cell Biol* *23*, 357-364.
- Su, Z., Fang, H., Hong, H., Shi, L., Zhang, W., Zhang, W., Zhang, Y., Dong, Z., Lancashire, L.J., Bessarabova, M., *et al.* (2014). An investigation of biomarkers derived from legacy microarray data for their utility in the RNA-seq era. *Genome Biol* *15*, 523.
- Suckow, A.T., Comoletti, D., Waldrop, M.A., Mosedale, M., Egodage, S., Taylor, P., and Chessler, S.D. (2008). Expression of neurexin, neuroligin, and their cytoplasmic binding partners in the pancreatic beta-cells and the involvement of neuroligin in insulin secretion. *Endocrinology* *149*, 6006-6017.
- Sudhof, T.C. (2017). Synaptic Neurexin Complexes: A Molecular Code for the Logic of Neural Circuits. *Cell* *171*, 745-769.
- Suenaga, Y., Islam, S.M., Alagu, J., Kaneko, Y., Kato, M., Tanaka, Y., Kawana, H., Hossain, S., Matsumoto, D., Yamamoto, M., *et al.* (2014). NCYM, a Cis-antisense gene of MYCN, encodes a de novo evolved protein that inhibits GSK3beta resulting in the stabilization of MYCN in human neuroblastomas. *PLoS Genet* *10*, e1003996.
- Sugita, S., Saito, F., Tang, J., Satz, J., Campbell, K., and Sudhof, T.C. (2001). A stoichiometric complex of neurexins and dystroglycan in brain. *J Cell Biol* *154*, 435-445.
- Sun, R., Hu, Z., and Curtis, C. (2018). Big Bang Tumor Growth and Clonal Evolution. *Cold Spring Harb Perspect Med* *8*.

- Sun, Y., Bell, J.L., Carter, D., Gherardi, S., Poulos, R.C., Milazzo, G., Wong, J.W., Al-Awar, R., Tee, A.E., Liu, P.Y., *et al.* (2015). WDR5 Supports an N-Myc Transcriptional Complex That Drives a Protumorigenic Gene Expression Signature in Neuroblastoma. *Cancer Res* 75, 5143-5154.
- Suva, M.L., Rheinbay, E., Gillespie, S.M., Patel, A.P., Wakimoto, H., Rabkin, S.D., Riggi, N., Chi, A.S., Cahill, D.P., Nashed, B.V., *et al.* (2014). Reconstructing and reprogramming the tumor-propagating potential of glioblastoma stem-like cells. *Cell* 157, 580-594.
- Suva, M.L., and Tirosh, I. (2019). Single-Cell RNA Sequencing in Cancer: Lessons Learned and Emerging Challenges. *Mol Cell* 75, 7-12.
- Szotek, P.P., Pieretti-Vanmarcke, R., Masiakos, P.T., Dinulescu, D.M., Connolly, D., Foster, R., Dombkowski, D., Preffer, F., Maclaughlin, D.T., and Donahoe, P.K. (2006). Ovarian cancer side population defines cells with stem cell-like characteristics and Mullerian Inhibiting Substance responsiveness. *Proc Natl Acad Sci U S A* 103, 11154-11159.
- Taddei, M.L., Giannoni, E., Fiaschi, T., and Chiarugi, P. (2012). Anoikis: an emerging hallmark in health and diseases. *J Pathol* 226, 380-393.
- Tahira, T., Ishizaka, Y., Itoh, F., Nakayasu, M., Sugimura, T., and Nagao, M. (1991). Expression of the ret proto-oncogene in human neuroblastoma cell lines and its increase during neuronal differentiation induced by retinoic acid. *Oncogene* 6, 2333-2338.
- Takeishi, S., Matsumoto, A., Onoyama, I., Naka, K., Hirao, A., and Nakayama, K.I. (2013). Ablation of Fbxw7 eliminates leukemia-initiating cells by preventing quiescence. *Cancer Cell* 23, 347-361.
- Takenobu, H., Shimosato, O., Nakamura, T., Ochiai, H., Yamaguchi, Y., Ohira, M., Nakagawara, A., and Kamijo, T. (2011). CD133 suppresses neuroblastoma cell differentiation via signal pathway modification. *Oncogene* 30, 97-105.
- Takeuchi, K., and Reue, K. (2009). Biochemistry, physiology, and genetics of GPAT, AGPAT, and lipin enzymes in triglyceride synthesis. *Am J Physiol Endocrinol Metab* 296, E1195-1209.
- Talukdar, S., Emdad, L., Das, S.K., Sarkar, D., and Fisher, P.B. (2016). Evolving Strategies for Therapeutically Targeting Cancer Stem Cells. *Adv Cancer Res* 131, 159-191.
- Theveneau, E., and Mayor, R. (2012). Neural crest delamination and migration: from epithelium-to-mesenchyme transition to collective cell migration. *Dev Biol* 366, 34-54.
- Thiele, C.J. (1998). Neuroblastoma. In *Human Cell Culture J. Masters, ed.* (Lancaster, UK: Kluwer Academic Publishers), pp. 21-53.
- Thiery, J.P., Acloque, H., Huang, R.Y., and Nieto, M.A. (2009). Epithelial-mesenchymal transitions in development and disease. *Cell* 139, 871-890.
- Thomas, S., Thomas, M., Wincker, P., Babarit, C., Xu, P., Speer, M.C., Munnich, A., Lyonnet, S., Vekemans, M., and Etchevers, H.C. (2008). Human neural crest cells display molecular and phenotypic hallmarks of stem cells. *Hum Mol Genet* 17, 3411-3425.
- Tirosh, I., Venteicher, A.S., Hebert, C., Escalante, L.E., Patel, A.P., Yizhak, K., Fisher, J.M., Rodman, C., Mount, C., Filbin, M.G., *et al.* (2016). Single-cell RNA-seq supports a developmental hierarchy in human oligodendroglioma. *Nature* 539, 309-313.
- Tolbert, V.P., Coggins, G.E., and Maris, J.M. (2017). Genetic susceptibility to neuroblastoma. *Curr Opin Genet*

- Dev 42, 81-90.
- Tolbert, V.P., and Matthay, K.K. (2018). Neuroblastoma: clinical and biological approach to risk stratification and treatment. *Cell Tissue Res* 372, 195-209.
- Tommasi, S., Karm, D.L., Wu, X., Yen, Y., and Pfeifer, G.P. (2009). Methylation of homeobox genes is a frequent and early epigenetic event in breast cancer. *Breast Cancer Res* 11, R14.
- Tomolonis, J.A., Agarwal, S., and Shohet, J.M. (2018). Neuroblastoma pathogenesis: deregulation of embryonic neural crest development. *Cell Tissue Res* 372, 245-262.
- Tong, D., Heinze, G., Pils, D., Wolf, A., Singer, C.F., Concin, N., Hofstetter, G., Schiebel, I., Rudas, M., and Zeillinger, R. (2010). Gene expression of PMP22 is an independent prognostic factor for disease-free and overall survival in breast cancer patients. *BMC Cancer* 10, 682.
- Treutlein, B., Gokce, O., Quake, S.R., and Sudhof, T.C. (2014). Cartography of neurexin alternative splicing mapped by single-molecule long-read mRNA sequencing. *Proc Natl Acad Sci U S A* 111, E1291-1299.
- Trochet, D., Bourdeaut, F., Janoueix-Lerosey, I., Deville, A., de Pontual, L., Schleiermacher, G., Coze, C., Philip, N., Frebourg, T., Munnich, A., *et al.* (2004). Germline mutations of the paired-like homeobox 2B (PHOX2B) gene in neuroblastoma. *Am J Hum Genet* 74, 761-764.
- Tsubota, S., and Kadomatsu, K. (2018). Origin and initiation mechanisms of neuroblastoma. *Cell Tissue Res* 372, 211-221.
- Tsuyada, A., Chow, A., Wu, J., Somlo, G., Chu, P., Loera, S., Luu, T., Li, A.X., Wu, X., Ye, W., *et al.* (2012). CCL2 mediates cross-talk between cancer cells and stromal fibroblasts that regulates breast cancer stem cells. *Cancer Res* 72, 2768-2779.
- Turkel, S.B., and Itabashi, H.H. (1974). The natural history of neuroblastic cells in the fetal adrenal gland. *Am J Pathol* 76, 225-244.
- Uckun, F.M., Sather, H., Reaman, G., Shuster, J., Land, V., Trigg, M., Gunther, R., Chelstrom, L., Bleyer, A., Gaynon, P., *et al.* (1995). Leukemic cell growth in SCID mice as a predictor of relapse in high-risk B-lineage acute lymphoblastic leukemia. *Blood* 85, 873-878.
- Uemura, T., Lee, S.J., Yasumura, M., Takeuchi, T., Yoshida, T., Ra, M., Taguchi, R., Sakimura, K., and Mishina, M. (2010). Trans-synaptic interaction of GluRdelta2 and Neurexin through Cbln1 mediates synapse formation in the cerebellum. *Cell* 141, 1068-1079.
- Ullrich, B., Ushkaryov, Y.A., and Sudhof, T.C. (1995). Cartography of neurexins: more than 1000 isoforms generated by alternative splicing and expressed in distinct subsets of neurons. *Neuron* 14, 497-507.
- Unsicker, K., Huber, K., Schober, A., and Kalcheim, C. (2013). Resolved and open issues in chromaffin cell development. *Mech Dev* 130, 324-329.
- Urick, M.E., Rudd, M.L., Godwin, A.K., Sgroi, D., Merino, M., and Bell, D.W. (2011). PIK3R1 (p85alpha) is somatically mutated at high frequency in primary endometrial cancer. *Cancer Res* 71, 4061-4067.
- Ushkaryov, Y.A., Hata, Y., Ichtchenko, K., Moomaw, C., Afendis, S., Slaughter, C.A., and Sudhof, T.C. (1994). Conserved domain structure of beta-neurexins. Unusual cleaved signal sequences in receptor-like neuronal cell-surface proteins. *J Biol Chem* 269, 11987-11992.
- Ushkaryov, Y.A., Petrenko, A.G., Geppert, M., and Sudhof, T.C. (1992). Neurexins: synaptic cell surface proteins

- related to the alpha-latrotoxin receptor and laminin. *Science* 257, 50-56.
- Ushkaryov, Y.A., and Sudhof, T.C. (1993). Neurexin III alpha: extensive alternative splicing generates membrane-bound and soluble forms. *Proc Natl Acad Sci U S A* 90, 6410-6414.
- Valenti, G., Quinn, H.M., Heynen, G., Lan, L., Holland, J.D., Vogel, R., Wulf-Goldenberg, A., and Birchmeier, W. (2017). Cancer Stem Cells Regulate Cancer-Associated Fibroblasts via Activation of Hedgehog Signaling in Mammary Gland Tumors. *Cancer Res* 77, 2134-2147.
- Valentijn, L.J., Koster, J., Zwijnenburg, D.A., Hasselt, N.E., van Sluis, P., Volckmann, R., van Noesel, M.M., George, R.E., Tytgat, G.A., Molenaar, J.J., *et al.* (2015). TERT rearrangements are frequent in neuroblastoma and identify aggressive tumors. *Nat Genet* 47, 1411-1414.
- van Dartel, M., and Hulsebos, T.J. (2004). Characterization of PMP22 expression in osteosarcoma. *Cancer Genet Cytogenet* 152, 113-118.
- van Galen, P., Hovestadt, V., Wadsworth li, M.H., Hughes, T.K., Griffin, G.K., Battaglia, S., Verga, J.A., Stephansky, J., Pastika, T.J., Lombardi Story, J., *et al.* (2019). Single-Cell RNA-Seq Reveals AML Hierarchies Relevant to Disease Progression and Immunity. *Cell* 176, 1265-1281 e1224.
- van Groningen, T., Koster, J., Valentijn, L.J., Zwijnenburg, D.A., Akogul, N., Hasselt, N.E., Broekmans, M., Haneveld, F., Nowakowska, N.E., Bras, J., *et al.* (2017). Neuroblastoma is composed of two super-enhancer-associated differentiation states. *Nat Genet* 49, 1261-1266.
- van Noesel, M.M. (2012). Neuroblastoma stage 4S: a multifocal stem-cell disease of the developing neural crest. *Lancet Oncol* 13, 229-230.
- Vasiliou, V., and Nebert, D.W. (2005). Analysis and update of the human aldehyde dehydrogenase (ALDH) gene family. *Hum Genomics* 2, 138-143.
- Vega-Lopez, G.A., Cerrizuela, S., Tribulo, C., and Aybar, M.J. (2018). Neurocristopathies: New insights 150 years after the neural crest discovery. *Dev Biol* 444 Suppl 1, S110-S143.
- Venteicher, A.S., Tirosh, I., Hebert, C., Yizhak, K., Neftel, C., Filbin, M.G., Hovestadt, V., Escalante, L.E., Shaw, M.L., Rodman, C., *et al.* (2017). Decoupling genetics, lineages, and microenvironment in IDH-mutant gliomas by single-cell RNA-seq. *Science* 355.
- Vermeulen, L., De Sousa, E.M.F., van der Heijden, M., Cameron, K., de Jong, J.H., Borovski, T., Tuynman, J.B., Todaro, M., Merz, C., Rodermond, H., *et al.* (2010). Wnt activity defines colon cancer stem cells and is regulated by the microenvironment. *Nat Cell Biol* 12, 468-476.
- Vik, T.A., Pfluger, T., Kadota, R., Castel, V., Tulchinsky, M., Farto, J.C., Heiba, S., Serafini, A., Tume, S., Khutoryansky, N., *et al.* (2009). (123)I-mIBG scintigraphy in patients with known or suspected neuroblastoma: Results from a prospective multicenter trial. *Pediatr Blood Cancer* 52, 784-790.
- Virchow, R. (1864,1865). Hyperplasie der Zirbel und der Nebennieren in die Krankhaften Geschwülste. *A Hirschwald, Berlin* 2, 149-150.
- Visvader, J.E. (2011). Cells of origin in cancer. *Nature* 469, 314-322.
- Vo, K.T., Matthay, K.K., Neuhaus, J., London, W.B., Hero, B., Ambros, P.F., Nakagawara, A., Miniati, D., Wheeler, K., Pearson, A.D., *et al.* (2014). Clinical, biologic, and prognostic differences on the basis of primary tumor site in neuroblastoma: a report from the international neuroblastoma risk group project. *J Clin Oncol* 32, 3169-3176.

- Walton, J.D., Kattan, D.R., Thomas, S.K., Spengler, B.A., Guo, H.F., Biedler, J.L., Cheung, N.K., and Ross, R.A. (2004). Characteristics of stem cells from human neuroblastoma cell lines and in tumors. *Neoplasia* 6, 838-845.
- Wang, J.C., and Dick, J.E. (2005). Cancer stem cells: lessons from leukemia. *Trends Cell Biol* 15, 494-501.
- Wang, X., Kruihof-de Julio, M., Economides, K.D., Walker, D., Yu, H., Halili, M.V., Hu, Y.P., Price, S.M., Abate-Shen, C., and Shen, M.M. (2009). A luminal epithelial stem cell that is a cell of origin for prostate cancer. *Nature* 461, 495-500.
- Wang, Y., Waters, J., Leung, M.L., Unruh, A., Roh, W., Shi, X., Chen, K., Scheet, P., Vattathil, S., Liang, H., *et al.* (2014). Clonal evolution in breast cancer revealed by single nucleus genome sequencing. *Nature* 512, 155-160.
- Warnat, P., Oberthuer, A., Fischer, M., Westermann, F., Eils, R., and Brors, B. (2007). Cross-study analysis of gene expression data for intermediate neuroblastoma identifies two biological subtypes. *BMC Cancer* 7, 89.
- Watt, K.E.N.T., P.A. (2014). Neurocristopathies: The Etiology and Pathogenesis of Disorders Arising from Defects in Neural Crest Cell Development. In *Neural Crest Cells Evolution, Development and Disease* (Elsevier), pp. 361-394.
- Weiss, W.A., Aldape, K., Mohapatra, G., Feuerstein, B.G., and Bishop, J.M. (1997). Targeted expression of MYCN causes neuroblastoma in transgenic mice. *EMBO J* 16, 2985-2995.
- Weiswald, L.B., Bellet, D., and Dangles-Marie, V. (2015). Spherical cancer models in tumor biology. *Neoplasia* 17, 1-15.
- Winslow, S., Leandersson, K., and Larsson, C. (2013). Regulation of PMP22 mRNA by G3BP1 affects cell proliferation in breast cancer cells. *Mol Cancer* 12, 156.
- Wong, C.E., Paratore, C., Dours-Zimmermann, M.T., Rochat, A., Pietri, T., Suter, U., Zimmermann, D.R., Dufour, S., Thiery, J.P., Meijer, D., *et al.* (2006). Neural crest-derived cells with stem cell features can be traced back to multiple lineages in the adult skin. *J Cell Biol* 175, 1005-1015.
- Wong, M., Tee, A.E.L., Milazzo, G., Bell, J.L., Poulos, R.C., Atmadibrata, B., Sun, Y., Jing, D., Ho, N., Ling, D., *et al.* (2017). The Histone Methyltransferase DOT1L Promotes Neuroblastoma by Regulating Gene Transcription. *Cancer Res* 77, 2522-2533.
- Wright, J.H. (1910). Neurocytoma or Neuroblastoma, a Kind of Tumor Not Generally Recognized. *J Exp Med* 12, 556-561.
- Wu, C., and Alman, B.A. (2008). Side population cells in human cancers. *Cancer Lett* 268, 1-9.
- Wu, C., Wei, Q., Utomo, V., Nadesan, P., Whetstone, H., Kandel, R., Wunder, J.S., and Alman, B.A. (2007). Side population cells isolated from mesenchymal neoplasms have tumor initiating potential. *Cancer Res* 67, 8216-8222.
- Xing, L.L., Sha, Y.L., Wu, Y.M., Hu, J.M., Zhang, M., and Lv, F. (2015). Preliminary analysis of stem cell-like cells in human neuroblastoma. *World J Pediatr* 11, 54-60.
- Yasuda, K., Torigoe, T., Mariya, T., Asano, T., Kuroda, T., Matsuzaki, J., Ikeda, K., Yamauchi, M., Emori, M., Asanuma, H., *et al.* (2014). Fibroblasts induce expression of FGF4 in ovarian cancer stem-like cells/cancer-initiating cells and upregulate their tumor initiation capacity. *Lab Invest* 94, 1355-1369.

- Yoshimoto, M., Caminada De Toledo, S.R., Monteiro Caran, E.M., de Seixas, M.T., de Martino Lee, M.L., de Campos Vieira Abib, S., Vianna, S.M., Schettini, S.T., and Anderson Duffles Andrade, J. (1999). MYCN gene amplification. Identification of cell populations containing double minutes and homogeneously staining regions in neuroblastoma tumors. *Am J Pathol* *155*, 1439-1443.
- Yu, C., Yu, J., Yao, X., Wu, W.K., Lu, Y., Tang, S., Li, X., Bao, L., Li, X., Hou, Y., *et al.* (2014). Discovery of biclonal origin and a novel oncogene SLC12A5 in colon cancer by single-cell sequencing. *Cell Res* *24*, 701-712.
- Zhang, C., Atasoy, D., Arac, D., Yang, X., Fucillo, M.V., Robison, A.J., Ko, J., Brunger, A.T., and Sudhof, T.C. (2010a). Neurexins physically and functionally interact with GABA(A) receptors. *Neuron* *66*, 403-416.
- Zhang, M., Atkinson, R.L., and Rosen, J.M. (2010b). Selective targeting of radiation-resistant tumor-initiating cells. *Proc Natl Acad Sci U S A* *107*, 3522-3527.
- Zhang, S., Balch, C., Chan, M.W., Lai, H.C., Matei, D., Schilder, J.M., Yan, P.S., Huang, T.H., and Nephew, K.P. (2008). Identification and characterization of ovarian cancer-initiating cells from primary human tumors. *Cancer Res* *68*, 4311-4320.
- Zhao, C., Blum, J., Chen, A., Kwon, H.Y., Jung, S.H., Cook, J.M., Lagoo, A., and Reya, T. (2007). Loss of beta-catenin impairs the renewal of normal and CML stem cells in vivo. *Cancer Cell* *12*, 528-541.
- Zheng, T., Menard, M., and Weiss, W.A. (2017). Neuroblastoma Metastases: Leveraging the Avian Neural Crest. *Cancer Cell* *32*, 395-397.
- Zhong, Z.Y., Shi, B.J., Zhou, H., and Wang, W.B. (2018). CD133 expression and MYCN amplification induce chemoresistance and reduce average survival time in pediatric neuroblastoma. *J Int Med Res* *46*, 1209-1220.
- Zhou, B.B., Zhang, H., Damelin, M., Geles, K.G., Grindley, J.C., and Dirks, P.B. (2009). Tumour-initiating cells: challenges and opportunities for anticancer drug discovery. *Nat Rev Drug Discov* *8*, 806-823.
- Zhu, S., Lee, J.S., Guo, F., Shin, J., Perez-Atayde, A.R., Kutok, J.L., Rodig, S.J., Neuberg, D.S., Helman, D., Feng, H., *et al.* (2012). Activated ALK collaborates with MYCN in neuroblastoma pathogenesis. *Cancer Cell* *21*, 362-373.
- Zomer, A., Ellenbroek, S.I., Ritsma, L., Beerling, E., Vrisekoop, N., and Van Rheenen, J. (2013). Intravital imaging of cancer stem cell plasticity in mammary tumors. *Stem Cells* *31*, 602-606. APPENDIX I



## VIII. APPENDICES

---



---

## APPENDIX I

### LIST OF TABLES

**Table-A.** Formulations of the home-made buffers, growth media and reagents used in this doctoral thesis

**Table-B.** Sequences used to generate target specific sh-RNA using a constitutive (pLKO-1-puro) and an inducible (pSLIK-neo) strategy.

**Table-C.** List of sequencing qPCR primers used in this doctoral thesis

**Table D.** List of antibodies used in this doctoral thesis

**Table E.** List of commercial reagents used in this doctoral thesis

<table border="1"> <thead> <tr> <th colspan="2">ACK Lysis buffer</th> </tr> </thead> <tbody> <tr> <td>0.1mM</td> <td>Na<sub>2</sub>EDTA</td> </tr> <tr> <td>10mM</td> <td>KHCO<sub>3</sub></td> </tr> <tr> <td>150mM</td> <td>NH<sub>4</sub>Cl</td> </tr> <tr> <td></td> <td>H<sub>2</sub>O MQ</td> </tr> <tr> <td></td> <td>pH 7.2-7.4</td> </tr> <tr> <td colspan="2">Store at RT</td> </tr> </tbody> </table>	ACK Lysis buffer		0.1mM	Na <sub>2</sub> EDTA	10mM	KHCO <sub>3</sub>	150mM	NH <sub>4</sub> Cl		H <sub>2</sub> O MQ		pH 7.2-7.4	Store at RT		<table border="1"> <thead> <tr> <th colspan="2">Annealing buffer</th> </tr> </thead> <tbody> <tr> <td>2mM</td> <td>MgAc (CH<sub>3</sub>CO<sub>2</sub>Mg<sub>2</sub>)</td> </tr> <tr> <td>10mM</td> <td>KAc (CH<sub>3</sub>CO<sub>2</sub>K)</td> </tr> <tr> <td>30mM</td> <td>HepesKOH 1M, pH 7.9</td> </tr> <tr> <td></td> <td>H<sub>2</sub>O MQ</td> </tr> <tr> <td colspan="2">Store at RT</td> </tr> </tbody> </table>	Annealing buffer		2mM	MgAc (CH <sub>3</sub> CO <sub>2</sub> Mg <sub>2</sub> )	10mM	KAc (CH <sub>3</sub> CO <sub>2</sub> K)	30mM	HepesKOH 1M, pH 7.9		H <sub>2</sub> O MQ	Store at RT		<table border="1"> <thead> <tr> <th colspan="2">0.5% Crystal violet</th> </tr> </thead> <tbody> <tr> <td>0.5%</td> <td>Crystal Violet</td> </tr> <tr> <td>20%</td> <td>Methanol (CH<sub>3</sub>OH)</td> </tr> <tr> <td></td> <td>H<sub>2</sub>O MQ</td> </tr> <tr> <td colspan="2">Store at RT</td> </tr> </tbody> </table>	0.5% Crystal violet		0.5%	Crystal Violet	20%	Methanol (CH <sub>3</sub> OH)		H <sub>2</sub> O MQ	Store at RT									
ACK Lysis buffer																																														
0.1mM	Na <sub>2</sub> EDTA																																													
10mM	KHCO <sub>3</sub>																																													
150mM	NH <sub>4</sub> Cl																																													
	H <sub>2</sub> O MQ																																													
	pH 7.2-7.4																																													
Store at RT																																														
Annealing buffer																																														
2mM	MgAc (CH <sub>3</sub> CO <sub>2</sub> Mg <sub>2</sub> )																																													
10mM	KAc (CH <sub>3</sub> CO <sub>2</sub> K)																																													
30mM	HepesKOH 1M, pH 7.9																																													
	H <sub>2</sub> O MQ																																													
Store at RT																																														
0.5% Crystal violet																																														
0.5%	Crystal Violet																																													
20%	Methanol (CH <sub>3</sub> OH)																																													
	H <sub>2</sub> O MQ																																													
Store at RT																																														
<table border="1"> <thead> <tr> <th colspan="2">DNase buffer</th> </tr> </thead> <tbody> <tr> <td>10mM</td> <td>Tris</td> </tr> <tr> <td>2.5mM</td> <td>MgCl<sub>2</sub></td> </tr> <tr> <td>0.1mM</td> <td>CaCl<sub>2</sub></td> </tr> <tr> <td></td> <td>H<sub>2</sub>O MQ</td> </tr> <tr> <td></td> <td>pH 7.4</td> </tr> <tr> <td colspan="2">Store at 4°C</td> </tr> </tbody> </table>	DNase buffer		10mM	Tris	2.5mM	MgCl <sub>2</sub>	0.1mM	CaCl <sub>2</sub>		H <sub>2</sub> O MQ		pH 7.4	Store at 4°C		<table border="1"> <thead> <tr> <th colspan="2">FACS buffer</th> </tr> </thead> <tbody> <tr> <td>10%</td> <td>FBS</td> </tr> <tr> <td>10µM</td> <td>Rock Inhibitor (when needed)</td> </tr> <tr> <td></td> <td>ice-cold DMEM</td> </tr> <tr> <td colspan="2">Prepare fresh</td> </tr> <tr> <td colspan="2">Store at 4°C</td> </tr> </tbody> </table>	FACS buffer		10%	FBS	10µM	Rock Inhibitor (when needed)		ice-cold DMEM	Prepare fresh		Store at 4°C		<table border="1"> <thead> <tr> <th colspan="2">Grafting media</th> </tr> </thead> <tbody> <tr> <td>7mg/ml</td> <td>Matrigel® matrix</td> </tr> <tr> <td></td> <td>DMEM:F12</td> </tr> <tr> <td colspan="2">Prepare fresh</td> </tr> <tr> <td colspan="2">Store at 4°C</td> </tr> </tbody> </table>	Grafting media		7mg/ml	Matrigel® matrix		DMEM:F12	Prepare fresh		Store at 4°C									
DNase buffer																																														
10mM	Tris																																													
2.5mM	MgCl <sub>2</sub>																																													
0.1mM	CaCl <sub>2</sub>																																													
	H <sub>2</sub> O MQ																																													
	pH 7.4																																													
Store at 4°C																																														
FACS buffer																																														
10%	FBS																																													
10µM	Rock Inhibitor (when needed)																																													
	ice-cold DMEM																																													
Prepare fresh																																														
Store at 4°C																																														
Grafting media																																														
7mg/ml	Matrigel® matrix																																													
	DMEM:F12																																													
Prepare fresh																																														
Store at 4°C																																														
<table border="1"> <thead> <tr> <th colspan="2">Immunostaining blocking buffer</th> </tr> </thead> <tbody> <tr> <td>1%</td> <td>BSA</td> </tr> <tr> <td>0.3%</td> <td>Glycine</td> </tr> <tr> <td>10%</td> <td>Horse Serum</td> </tr> <tr> <td></td> <td>0.1% PBT buffer</td> </tr> <tr> <td colspan="2">Prepare fresh</td> </tr> </tbody> </table>	Immunostaining blocking buffer		1%	BSA	0.3%	Glycine	10%	Horse Serum		0.1% PBT buffer	Prepare fresh		<table border="1"> <thead> <tr> <th colspan="2">Mowiol</th> </tr> </thead> <tbody> <tr> <td>2,4g</td> <td>Mowiol</td> </tr> <tr> <td>6g</td> <td>Glycerol</td> </tr> <tr> <td>0,12M</td> <td>Tris-HCl, pH 8.5</td> </tr> <tr> <td></td> <td>H<sub>2</sub>OMQ</td> </tr> <tr> <td colspan="2">Store at -20°C</td> </tr> </tbody> </table>	Mowiol		2,4g	Mowiol	6g	Glycerol	0,12M	Tris-HCl, pH 8.5		H <sub>2</sub> OMQ	Store at -20°C		<table border="1"> <thead> <tr> <th colspan="2">P1 resuspension buffer</th> </tr> </thead> <tbody> <tr> <td>100mg/ml</td> <td>Rnase A</td> </tr> <tr> <td>50 mM</td> <td>Tris-HCl</td> </tr> <tr> <td>10mM</td> <td>Na<sub>2</sub>EDTA, pH 8.0</td> </tr> <tr> <td></td> <td>H<sub>2</sub>O MQ</td> </tr> <tr> <td colspan="2">Store at 4°C</td> </tr> </tbody> </table>	P1 resuspension buffer		100mg/ml	Rnase A	50 mM	Tris-HCl	10mM	Na <sub>2</sub> EDTA, pH 8.0		H <sub>2</sub> O MQ	Store at 4°C									
Immunostaining blocking buffer																																														
1%	BSA																																													
0.3%	Glycine																																													
10%	Horse Serum																																													
	0.1% PBT buffer																																													
Prepare fresh																																														
Mowiol																																														
2,4g	Mowiol																																													
6g	Glycerol																																													
0,12M	Tris-HCl, pH 8.5																																													
	H <sub>2</sub> OMQ																																													
Store at -20°C																																														
P1 resuspension buffer																																														
100mg/ml	Rnase A																																													
50 mM	Tris-HCl																																													
10mM	Na <sub>2</sub> EDTA, pH 8.0																																													
	H <sub>2</sub> O MQ																																													
Store at 4°C																																														
<table border="1"> <thead> <tr> <th colspan="2">P2 lysis buffer</th> </tr> </thead> <tbody> <tr> <td>200 mM</td> <td>NaOH</td> </tr> <tr> <td>1%</td> <td>SDS</td> </tr> <tr> <td></td> <td>H<sub>2</sub>O MQ</td> </tr> <tr> <td colspan="2">Store at RT</td> </tr> </tbody> </table>	P2 lysis buffer		200 mM	NaOH	1%	SDS		H <sub>2</sub> O MQ	Store at RT		<table border="1"> <thead> <tr> <th colspan="2">P3 neutralization buffer</th> </tr> </thead> <tbody> <tr> <td>3.0 M</td> <td>KAc (CH<sub>3</sub>CO<sub>2</sub>K)</td> </tr> <tr> <td></td> <td>H<sub>2</sub>O MQ</td> </tr> <tr> <td></td> <td>pH 5.5</td> </tr> <tr> <td colspan="2">Store at 4°C</td> </tr> </tbody> </table>	P3 neutralization buffer		3.0 M	KAc (CH <sub>3</sub> CO <sub>2</sub> K)		H <sub>2</sub> O MQ		pH 5.5	Store at 4°C		<table border="1"> <thead> <tr> <th colspan="2">PBS10x</th> </tr> </thead> <tbody> <tr> <td>137mM</td> <td>NaCl</td> </tr> <tr> <td>2,7mM</td> <td>KCl</td> </tr> <tr> <td>10mM</td> <td>Na<sub>2</sub>HPO<sub>4</sub></td> </tr> <tr> <td>2mM</td> <td>KH<sub>2</sub>PO<sub>4</sub></td> </tr> <tr> <td></td> <td>pH 7.4</td> </tr> <tr> <td colspan="2">Store at RT</td> </tr> </tbody> </table>	PBS10x		137mM	NaCl	2,7mM	KCl	10mM	Na <sub>2</sub> HPO <sub>4</sub>	2mM	KH <sub>2</sub> PO <sub>4</sub>		pH 7.4	Store at RT											
P2 lysis buffer																																														
200 mM	NaOH																																													
1%	SDS																																													
	H <sub>2</sub> O MQ																																													
Store at RT																																														
P3 neutralization buffer																																														
3.0 M	KAc (CH <sub>3</sub> CO <sub>2</sub> K)																																													
	H <sub>2</sub> O MQ																																													
	pH 5.5																																													
Store at 4°C																																														
PBS10x																																														
137mM	NaCl																																													
2,7mM	KCl																																													
10mM	Na <sub>2</sub> HPO <sub>4</sub>																																													
2mM	KH <sub>2</sub> PO <sub>4</sub>																																													
	pH 7.4																																													
Store at RT																																														
<table border="1"> <thead> <tr> <th colspan="2">0.1% PBT buffer</th> </tr> </thead> <tbody> <tr> <td>0.1%</td> <td>Triton-X100</td> </tr> <tr> <td></td> <td>PBS1x</td> </tr> <tr> <td colspan="2">Store at RT</td> </tr> </tbody> </table>	0.1% PBT buffer		0.1%	Triton-X100		PBS1x	Store at RT		<table border="1"> <thead> <tr> <th colspan="2">Sphere-forming-media (SFM)</th> </tr> </thead> <tbody> <tr> <td>10%</td> <td>Knock-out serum replacement</td> </tr> <tr> <td>2mM</td> <td>Glutamax™</td> </tr> <tr> <td>1%</td> <td>Non-essential aminoacids</td> </tr> <tr> <td>1%</td> <td>Penicillin/Streptomycin</td> </tr> <tr> <td>0.1mM</td> <td>β-mercaptoethanol</td> </tr> <tr> <td>10ng/ml</td> <td>bFGF, added just before use</td> </tr> <tr> <td></td> <td>DMEM:F12 with 15mM HEPES</td> </tr> <tr> <td colspan="2">Prepare fresh</td> </tr> <tr> <td colspan="2">Store at 4°C</td> </tr> </tbody> </table>	Sphere-forming-media (SFM)		10%	Knock-out serum replacement	2mM	Glutamax™	1%	Non-essential aminoacids	1%	Penicillin/Streptomycin	0.1mM	β-mercaptoethanol	10ng/ml	bFGF, added just before use		DMEM:F12 with 15mM HEPES	Prepare fresh		Store at 4°C		<table border="1"> <thead> <tr> <th colspan="2">Xenograft dissociation buffer</th> </tr> </thead> <tbody> <tr> <td>0.6mg/ml</td> <td>Collagenase II</td> </tr> <tr> <td>0.05mg/ml</td> <td>Elastase</td> </tr> <tr> <td>0.3mg/ml</td> <td>Trypsin</td> </tr> <tr> <td>0.32mg/ml</td> <td>Dnase I type II</td> </tr> <tr> <td></td> <td>HBSS with Ca<sup>2+</sup>/Mg<sup>2+</sup></td> </tr> <tr> <td colspan="2">Prepare fresh</td> </tr> <tr> <td colspan="2">Store at 4°C</td> </tr> </tbody> </table>	Xenograft dissociation buffer		0.6mg/ml	Collagenase II	0.05mg/ml	Elastase	0.3mg/ml	Trypsin	0.32mg/ml	Dnase I type II		HBSS with Ca <sup>2+</sup> /Mg <sup>2+</sup>	Prepare fresh		Store at 4°C	
0.1% PBT buffer																																														
0.1%	Triton-X100																																													
	PBS1x																																													
Store at RT																																														
Sphere-forming-media (SFM)																																														
10%	Knock-out serum replacement																																													
2mM	Glutamax™																																													
1%	Non-essential aminoacids																																													
1%	Penicillin/Streptomycin																																													
0.1mM	β-mercaptoethanol																																													
10ng/ml	bFGF, added just before use																																													
	DMEM:F12 with 15mM HEPES																																													
Prepare fresh																																														
Store at 4°C																																														
Xenograft dissociation buffer																																														
0.6mg/ml	Collagenase II																																													
0.05mg/ml	Elastase																																													
0.3mg/ml	Trypsin																																													
0.32mg/ml	Dnase I type II																																													
	HBSS with Ca <sup>2+</sup> /Mg <sup>2+</sup>																																													
Prepare fresh																																														
Store at 4°C																																														

Table-A. Formulations of home-made buffers, growth media and reagents used in this doctoral thesis

pLKO.1-puro system		
Primer	Sequence	
oligo_shCtl	Fw	5'-CCGGCCTAAGGTTAAGTCGCCCTCGCTGCAGCGAGGGCGACTTAACCTTAGGTTTTG-3'
	Rv	5'-AATTCAAAAACCTAAGGTTAAGTCGCCCTCGCTGCAGCGAGGGCGACTTAACCTTAGG-3'
oligo_sh1Nxph1	Fw	5'-CCGGGCCCTTTAAGGTGATCTGTATCTGCAGATACAGATCACCTTAAAGGGCTTTTTG-3'
	Rv	5'-AATTCAAAAAGCCCTTTAAGGTGATCTGTATCTGCAGATACAGATCACCTTAAAGGGC-3'
oligo_sh3Nxph1	Fw	5'-CCGGATGGGACATTTAGTGTTTATTCTGCAGAATAAACACTAAATGTCCCATTTTTG-3'
	Rv	5'-AATTCAAAAATGGGACATTTAGTGTTTATTCTGCAGAATAAACACTAAATGTCCCAT-3'
oligo_sh2NRXN1a	Fw	5'-CCGGGGCTATAACCTCAATGATAACCTGCAGGTTATCATTGAGGTTATAGCCTTTTG-3'
	Rv	5'-AATTCAAAAAGGCTATAACCTCAATGATAACCTGCAGGTTATCATTGAGGTTATAGCC-3'
oligo_sh3NRXN1a	Fw	5'-CCGGTGTGAGAATGTTGCAACTTACTGCAGTAAAGTTGCAACATTCTCACATTTTTG-3'
	Rv	5'-AATTCAAAAATGTGAGAATGTTGCAACTTACTGCAGTAAAGTTGCAACATTCTCACA-3'
pSLIK-neo system		
Primer	Sequence	
oligo_shCtl	Fw	5'-AGCGCCCTAAGGTTAAGTCGCCCTCTTAGTGAAGCCACGATGTAAGAGGGCGACTTAACCTTAGGT-3'
	Rv	5'-GGCAACCTAAGGTTAAGTCGCCCTCTTAGTGAAGCCACGATGTAAGAGGGCGACTTAACCTTAGGG-3'
oligo_sh1Nxph1	Fw	5'-AGCGACCCCTTTAAGGTGATCTGTATTAGTGAAGCCACGATGTAATACAGATCACCTTAAAGGGC-3'
	Rv	5'-GGCAGCCCTTTAAGGTGATCTGTATTAGTGAAGCCACGATGTAATACAGATCACCTTAAAGGGT-3'
oligo_sh2NRXN1a	Fw	5'-AGCGAGGCTATAACCTCAATGATAATTAGTGAAGCCACGATGTAATTATCATTGAGGTTATAGCCG-3'
	Rv	5'-GGCAGGGCTATAACCTCAATGATAATTAGTGAAGCCACGATGTAATTATCATTGAGGTTATAGCCT-3'

Table -B. Sequences used to generate target -specific sh-RNA sequences using a constitutive (pLKO.1-puro) and an inducible (pSLIK-neo) strategy. Target-specific sequence in seen in black, adaptor sequences are light in dark blue, loop sequences in light green. At the bottom, mismatched nucleotides are lighted in red

Sequencing primers				
Name	Primers	Target sequence	Design	
EGFP-C Fw	5'-CATGGTCCTGCTGGAGTTCGTG-3'	3' end of EGFP, forward primer	Addgene	
pLKO.1 puro Fw	5'-CAAGGCTGTTAGAGAGATAATTGGA-3'	shRNA insert in pLKO.1	This project	
RT-qPCR primers				
Gene	Primers	Amplified exons	Amplicon size	Design
<i>ALK</i>	Hs_ALK_1_SG QuantiTect Primer Assay	2/3	105	QIAGEN-QT00028847
<i>CD133</i>	5'-GTCGGAAACTGGCAGATAGC-3'	5/6	110	This project
	5'-CGCCTTGTCTTGGTAGTGT-3'			
<i>CDKN1A/P21</i>	5'-GACTCTCAGGGTCGAAAACG-3'	2/3	90	This project
	5'-TTAGGGCTTCTCTTGGAGAA-3'			
<i>CHD5</i>	Hs_CHD5_1_SG QuantiTect Primer Assay	11/12	124	QIAGEN-QT00088683
<i>CXCR4</i>	Hs_CXCR4_1_SG QuantiTect Primer Assay	not available	106	QIAGEN-QT00223188
<i>FYN</i>	5'-GGTCACCAAAGGAAGAGTGC-3'	11/12	145	This project
	5'-AGGGTCCTTTTCCAGCAGT-3'			
<i>GAP43</i>	5'-AGAGCAGCCAAGCTGAAGAG-3'	2/3	106	This project
	5'-TCTTGGTCAGCCTCAGGTTC-3'			
<i>KIT/CD117</i>	5'-GATGCAGATCCCCTAAAAAGA-3'	20/21	109	This project
	5'-GGCTGCAGTTTGCTAAGTTG-3'			
<i>MDR1/ABCB1</i>	5'-ACATGCCTTCATCGAGTCAC-3'	18/19	118	This project
	5'-CTGTCTAACAAGGGCAGAG-3'			
<i>MYCN</i>	Hs_MYCN_1_SG QuantiTect Primer Assay	not available	113	QIAGEN-QT00201404
<i>NANOG</i>	Hs_NANOG_2_SG QuantiTect Primer Assay	1/2	164	QIAGEN-QT01844808
$\alpha$ - <i>NRXN1</i>	5'-GTCTGGCGCACCTGATGAT-3'	3/4/5	113	This project
	5'-ACTGCTGCTTTGAATGGGGT-3'			
$\alpha$ - <i>NRXN2</i>	5'-GACGGCCACCTCTATCTTCT-3'	8/9	148	This project
	5'-TGCTGCGACTATCACTGAG-3'			
$\alpha$ - <i>NRXN3</i>	5'-CAGAAGAAAGCCAATGATGG-3'	4/5	140	This project
	5'-ATGTCTCCTTCCAGGTCCA-3'			
<i>TRKA</i>	5'-GATCTTCACCTACGGCAAGC-3'	16/17	123	This project
	5'-ATGATGGCGTAGACCTCTGG-3'			
<i>NXPH1</i>	Hs_NXPH1_2_SG QuantiTect Primer Assay	2/3	115	QIAGEN-QT02317259
<i>OCT4A</i>	5'-AAACCCACACTGCAGCAGAT-3'	4/5	116	This project
	5'-TAGTCGCTGCTTGATCGCTT-3'			
<i>p75NTR</i>	5'-ACAGCGACAGTGGCATCTC-3'	5/6	215	This project
	5'-TATGTGCTCGGGCTGGTAG-3'			
<i>PI3KR1/p85 alpha</i>	5'-AAAATCTCGCTCCACACC-3'	1/2	119	This project
	5'-TCTGCAAGATCCGGGAGAGT-3'			
<i>RET</i>	5'-TCCTGGGAGAAGCTCAGTGT-3'	2/3	79	This project
	5'-ATGTGGGTGACAGGAAGACC-3'			
<i>SOX2</i>	5'-ACTTTTGTCCGGAGACGGAGA-3'	unique exon	99	This project
	5'-CGGGGCCGGTATTTATAATC-3'			
<i>SOX9</i>	5'-GTACCCGCACTGCACAAC-3'	1/2	74	This project
	5'-TCTCGCTCTCGTTCAGAAGTC-3'			
<i>18SrRNA</i>	5'-GGAGAGGGAGCCTGAGAAAC-3'	-	69	This project
	5'-TCGGGAGTGGTAATTTGC-3'			
<i>TBP</i>	Hs_TBP_1_SG QuantiTect Primer Assay	4/5/6	132	QIAGEN-QT00000721

Table-C. List of sequencing and qPCR primers used in this doctoral thesis

Primary antibodies						
Antigen	Antibody	Vendor	Catalog number	RRID identifier	Working concentration	Application
BrdU	anti-BrdU, clone BU1/75 (ICR1)	BIO RAD	MCA 2060	AB_323427	1:250	IF
cCaspase-3	anti- active-Caspase-3, clone C92-605	BD PharMingen	559565	AB_397274	1:500	IF
CD11b	PE-Cy™7 anti-CD11b , clone M1/70	BD PharMingen	561098	AB_2033994	1: 400	FC
CD31	PE-Cy7 anti-CD31, clone 390	BD PharMingen	561410	AB_10612003	1:400	FC
Gangliside GD2	Alexa Fluor® 647 anti-Disialoganglioside GD2, clone 14.G2a	BD PharMingen	562096	AB_11154051	1: 400	FC
phospho-Histone 3	polyclonal anti-phospho-Histone H3 (Ser10)	UPSTATE	06-570	AB_310177	1:500	IF
phospho-Histone 3	anti-phospho-Histone H3 (pSer28), clone HTA28	SIGMA	H9908	AB_260096	1:500-1000	IF
Human nuclei antigen	anti-Human Nuclear Antigen clone 235-1	Abcam	ab191181	not available	1:500	IF
Ki67	polyclonal anti-Ki67	Abcam	ab66155	AB_1140752	1:500	IF
α-Neurexin1	polyclonal ATTO488 anti-Neurexin 1α	Alomone	ANR-031-AG	not available	1:100	FC
p75 NTR	anti-p75NTR, clone ME20.4	Millipore	05-446	AB_309737	1:1000	IF
Polysialil (PSA)-NCAM	anti-PSA NCAM, clone 2-2B	AbCys	AbC0019	AB_2313692	1:1000	IF
Secondary antibodies and isotype controls						
Antigen	Antibody	Vendor	Catalog number	RRID identifier	Working concentration	Application
Isotype control	Alexa Fluor® 647 Mouse IgG2a, κ Isotype Control, clone G155-178	BD PharMingen	557715	AB_396824	1: 400	FC
Alexa Fluor®-conjugated secondary antibodies	Alexa Fluor® (488, 555, 647) donkey anti-(IgG or IgM), monoclonal	Life Technologies	various	various	1:1000	IF

Table-D. List of antibodies used in this doctoral thesis

Reagent	Vendor	Catalog number	Materials and Methods sections
Commercial name			
StemPro® Accutase® Cell Dissociation Reagent	ThermoFisher SCIENTIFIC	A1110501	5
AMBION® DNA-free™ DNase Treatment and Removal Reagents	Fisher Scientific	AM1906	7
Ampicillin sodium salt 5G SIGMA	SIGMA	A9518-5G	4
Agarosa D-1 Low EEO 250 g	LAB.CONDISA	8014	4
BfuAI, 250 u	Werfen	R0701S	4
bis-Benzimide H 33342 trihydrochloride (Hoescht 33342)	SIGMA	B2261-100MG	5
Bovine Serum Albumin	SIGMA	A7906-100G	3,6 and 8
Brain Tumor Dissociation Kit (P), human	Miltenyi Biotec	130-095-942	6
BrdU (5-Bromo-2'-deoxyuridine)	SIGMA	858811	2
Cisplatin	SIGMA	BP809	2
Cloroformo (Triclorometano) PA ISO 99% (GLC) 1 l.	Carlo erba	438601	7
Collagenase II	SIGMA	C6885-100mg	6
Crystal violet solution 1%, aqueous solution	SIGMA	V5265-250ML	2
Cryogenic Vial, Ext-Thread, 2.0 mL, Plug Seal, Round	CULTEK	15430289	2
DAPI 4',6-Diamidino-2-phenylindole dihydrochloride, 1 mg	SIGMA	D9542	2, 5 and 8
Dish 60mm ultra low attachment surface, S, BK, 5/20	Cultek	153261	2
DMEM, high glucose, GlutaMAX™ Supplement, 500ml	Lifetechnologies	61965-026	2, 5 and 6
DMEM/F-12, HEPES	ThermoFisher SCIENTIFIC	11330-032	2 and 6
Dimethyl sulfoxide Hybri-Max™, sterile-filtered, BioReagent, suitable for hybridoma, ≥99.7% (DMSO)	SIGMA	D2650-100ML	2
DNase I type II	SIGMA	D4527-10KU	6 and 8
Doxycycline Hiclate BioChemica (CAS:24390-14-5)[25 g]	ACEFESA	PAA29510025	5 and 6
Elastase, Porcine Pancreas, High Purity, Crystallized	Merck	324682-250U	6
Ethanol, molecular grade PA-ACS-ISO, 1L	PCB	131086.1611	7
Falcon 70µm Cell Strainer, White, Sterile, Individually Packaged, 50_Case	Cultek	4532350	6
FastAP Thermosensitive Alkaline Phosphatase (1 U/µL)	ThermoFisher SCIENTIFIC	EF0654	4
Fetal Bovine Serum	Cultek	16SV30160.03RYB35908	2
FGF-Basic (AA 10-155) Recombinant Human Protein; 100 ug (bFGF)	ThermoFisher SCIENTIFIC	PHG0021	2
G 418 disulfate salt (neomycine)	SIGMA	A1720-1G	4
GlutaMAX™, 100 ml	ThermoFisher SCIENTIFIC	35050038	2
Glycylglycina (25 g)	SIGMA	G1002	8
HBSS, calcium, magnesium, no phenol red	ThermoFisher SCIENTIFIC	14025092	6
HBSS, no calcium, no magnesium (Gibco)	ThermoFisher SCIENTIFIC	14170088	6
High-Capacity cDNA Reverse Transcription Kit	Life Technologies	4368814	7
Horse serum 100 ml	ThermoFisher SCIENTIFIC	16050-130	8
Illustra™ GFX™ PCR DNA and Gel Band Purification kit (GE Healthcare Life Science™)	ACEFE	28903470	4
Isopropanol ACS Normapur para analisis 2.5 l	VWR	20.842.323	7
KnockOut Serum Replacement	ThermoFisher SCIENTIFIC	10828010	2
Lab-Tek Chamber Slide System, 8 well, Permax™ (16u/pack)	Fisher Scientific	177445	2 and 8
LIGHTCYCLER 480 SYBR GREEN 2x MASTER. ROCHE	ROCHE	04 887 352 001	7
Lipofectamine® 2000 Transfection Reagent, 1,5 ml	ThermoFisher SCIENTIFIC	11668019	4
LR CLONASE II ENZYME MIX	Fisher Scientific	11791-020	4
Matrigel™ Membrane Matrix HC. Sin LDEV. 10 ml. CORNING 354248.	Fisher Scientific	10365602	6
MEM Non-Essential Amino Acids Solution (100X)	ThermoFisher SCIENTIFIC	11140035	2
2-Mercaptoethanol	SIGMA-ALDRICH	M3148-25ML	2
45µm Millex-HV PVDF syringe filter	Merck-Millipore	SLHV033RS	4
Mitoxantrone dihydrochloride	SIGMA	M6545-10MG	2
Mowiol 4-88 (250g) (Polyvinyl alcohol 4-88)	SIGMA	81381	8
Multiwell plates and culture dishes, (polysterene-coated)	Cultek	various	2
Multiwell plates and culture dishes, (uncoated)	ThermoFisher SCIENTIFIC	various	2
Rat Neurexin 1 alpha Recombinant Protein, CF (R and D System)	R&D Systems	4485-Nx	2 and 6
Human Neurexophilin 1/NXPH1 Recombinant Protein, CF(R and D System)	R&D Systems	4957-NX-050	2 and 6
NucleoBond® Xtra Midi. (midi-preps kits)	Cultek	740410.50	4
Optical Seal Film LightCycler 480 100 u	ATTENDBIO	GK480K-OS	7
Opti-MEM™ I Reduced Serum Medium	ThermoFisher SCIENTIFIC	31985070	4
Paraformaldehyde	SIGMA	16005	2, 6 and 8
PCR-Plates, white KISKER (PCR plates LightCycler)	ATTENDBIO	GK480K-50	7
Pellet Paint Co-precipitant 125 rxn	Merck Millipore	69049-3	7
Penicillin/streptomycin	ThermoFisher SCIENTIFIC	15140-122	2
Puromycin dihydrochloride from Streptomyces alboniger	SIGMA	p8833-10mg	4
Pyronin Y	SIGMA	P9172-1G	2
Restriction enzymes	ThermoFisher SCIENTIFIC	various	4
Retinoic acid	SIGMA	R2625-50MG	2
Rock inhibitor (Y-27632 DIHYDROCHLORIDE, POWDER, ≥98%)	SIGMA	Y0503-1MG	2, 5 and 6
RPMI 1640 Medium, GlutaMAX™. Supplement (no HEPES) 500 ML	ThermoFisher SCIENTIFIC	61870010	2
sucrose 99.7%	SIGMA	84100	8
TESPA (3-Aminopropyl)triethoxysilane 100 ml	SIGMA	A3648	8
Thiazolyl Blue Tetrazolium Bromide (MTT)	SIGMA	M2128-500MG	2
Tissue-tek® OCT™ Compound	Sakura FineTek	4583	8
T4 PNK 10u/µL	Fisher scientific	EK0031	4
T4 DNA Ligase 1000u.	Fisher scientific	EL0011	4
TRITON X-100, 500ml	SIGMA	x100	8
TRizol® Reagent, 200ml	ThermoFisher SCIENTIFIC	15596-018	7
Trypan Blue solution 0.4%, liquid, sterile-filtered, suitable for cell culture	SIGMA	T8154-100ML	2
0.25% Trypsin-EDTA (1X), Phenol Red, 100 ml; GIBCO	Lifetechnologies	25200-056	2
Trypsin	SIGMA	T8003-100mg	6
H2O MQ molecular grade (water)	SIGMA	W4502-1L	4 and 7

Table-E. List of commercial reagents used in this doctoral thesis

---

## APPENDIX II

The technical experience acquired in the course of this doctoral thesis has allowed me to collaborate in the following peer-reviewed articles:

Garreta E, Prado P, Tarantino C, Oria R, **Fanlo L**, Martí E, Zalvídea D, Trepát X, Roca-Cusachs P, Gavaldà-Navarro A, Cozzuto L, Campistol JM, Izpisúa-Belmonte JC, Hurtado Del Pozo C, & Montserrat N. (2019). Fine tuning the extracellular environment accelerates the derivation of kidney organoids from human pluripotent stem cells. *Nat Materials*, 18 (4):397-405.

Bruguera D, Marquez Y, Racioppi C, Permanyer J, Torres-Mendez A, Esposito R, Albuixech-Crespo B, **Fanlo-Escudero L**, D'Agostino Y, Gohr A, Návas-Pérez E, Riesgo A, Cuomo C, Benvenuto G, Christian L, Martí E, D'Aniello S, Spagnuolo A, Risoratore F, Arnone M, García-Fernández J, Irimia M. (2017). Evolutionary recruitment of flexible *Esrp*-dependent splicing programs into diverse embryonic morphogenetic processes. *Nature Communications*, 8: 1799.

Rabadán MA, Herrera A, **Fanlo L**, Usieto S, Carmona-Fontaine C, Barriga EH, Mayor R, Pons S, Martí E. (2016). Delamination of neural crest cells requires transient and reversible Wnt inhibition mediated by DACT1/2. *Development*, 143: 2194-2205.

Richardson J, Gauert A, Briones-Montecinos L, **Fanlo L**, Alhashem ZM, Assar R, Martí E, Kabla A, Härtel S, Linker C. (2016). Leader Cells Define Directionality of Trunk, but Not Cranial, Neural Crest Cell Migration. *Cell Reports*, 15: 1-13.



---

## ACKNOWLEDGEMENTS

En estas páginas están condensadas buena parte de mi día a día de los últimos 5 años y medio. Es por ello que he decidido que estas líneas cierren la tesis, porque con ellas también cierro un “capítulo” no menor en mi vida. Un capítulo que empezó con una mudanza a Barcelona casi por casualidad (porque no encontré labo para hacer la tesis en Madrid ni en las otras 5 ó 6 ciudades donde lo solicité...). Aunque para ser justos y entender por qué decidí lanzarme a hacer una tesis (sin tener ni idea de en qué consistía por supuesto) y qué me ha permitido terminarla, si no con éxito científico sí con satisfacción personal, hay que empezar por el principio.

Y lo primero son mis padres, que son un ejemplo personal y profesional y han sabido darnos alas sin hacernos perder de vista el suelo. Gracias por quererme y acompañarme en mi camino, aunque no siempre me haya dejado acompañar. Mi maldita curiosidad, causante de algún disgusto y alguna alegría durante esta tesis, es completamente “culpa” vuestra. Y gracias por darme a los mejores compañeros de vida que puedo tener, mis hermanos. Sobra decir que no se expresan lo que significáis para mí, quizá baste con decir que mi hogar está y siempre estará donde estéis vosotros. Y una parte integral del hogar son los abuelos, los que están y los que ya no están. Sois una fuente inagotable de cariño. Gracias especiales a mi abuela Conchita, que en cada llamada telefónica me pregunta por cuando nos vamos a volver a ver y que me ha recordado durante todo el verano que “está convencida de que no me van a suspender”. Gracias a Álvaro, que es uno más de casa y por hacer un esfuerzo por entender mi trabajo y compartir los buenos y los malos ratos. Este apartado de familia lo tiene que cerrar Kitty, compañera infatigable de este largo verano. Gracias por aportar sensatez a mis horarios, por arrancarme sonrisas y por dormir en la dura mesa sobre tesis y artículos teniendo a un paso el cojín.

La etapa riojana no la puedo cerrar sin mencionar a Danae, Elena, Jorge, Alex, Lorena y Clavijo. Gracias por vuestro interés y apoyo estos años. Danae merece mención especial porque después de mi familia creo que nadie me conoce desde hace tanto tiempo como tú. Estoy encantada de haber compartido tanto contigo. Gracias por estar siempre disponible. ¡Sabes que eres mi médica favorita!

El viaje continúa hacia Madrid. Aquí aparecen unas cuantas personas que me conocieron antes de que la tesis se cruzara en mi camino: Sara, María, Javi, Martha y otros cuantos biólogos. Madrid no es Madrid sin vosotros. Gracias por ser capaces de mantener esta amistad que ya empieza a ser vieja a pesar del tiempo, la distancia y mi alergia al teléfono móvil. Gracias por vuestro cariño y vuestro apoyo. Gracias por lo que me habéis cuidado este verano. No sabéis lo feliz que me hacéis cada vez que nos vemos, espero que sigamos compartiendo el camino muchos años más.

Y ahora sí que toca Barcelona y la suerte que tuve en conseguir aquella JAE-Intro para el verano de 4º de carrera. Ahí aparecieron Chelo y Blanca, a las que sin saberlo seguiría ligada durante todos estos años. Gracias a Chelo y a su familia, que con sus viajes de Dresden a Pontevedra, han ido marcando el paso de las estaciones y los años. Es un placer compartir esos ratos contigo y espero poder seguir haciéndolo estemos las dos donde estemos. A Blanca y a Ángela, porque fuimos capaces de formar una pequeña familia en un entorno nuevo para las tres. Fuisteis un pilar en mi vida durante los primeros años aquí. Estoy realmente orgullosa de las mujeres en las que os habéis convertido y espero sinceramente poder seguir compartiendo camino con vosotras. Tengo que hacer mención especial a Ángela. Gracias por estar siempre ahí, por tu cariño, por tu amistad, por ser de otro planeta. Siento una admiración profunda por tu energía inagotable, tu tesón, tu inteligencia y tu buen humor. Sigo sin creerme lo de que eres seismesina, apuesto a que en realidad te caíste en una marmita como Obelix XD. Un trocito de esta tesis es tuyo.

No puedo olvidar a Afri, Santos, Mertxe, Borja, Leire y algunos más que han sido también protagonistas de la historia barcelonesa y a los que les debo no pocas risas y cervezas. Muchas y sinceras gracias chicos.

Al llegar a Barcelona tuve la suerte de encontrar a gente estupenda, que me hizo no extrañar Madrid (o extrañarlo solo un poquito) y con los que siempre es genial compartir un rato: Ester, Oriol, Laura, Marlies, Pablo, Gemma, Ester Valls, Yenny y el resto de gente del Clinic. Gracias especiales a Ester y Oriol, por ayudarme y darme vuestra opinión sincera en momentos que para mí eran difíciles. Me encanta ver como habéis tirado para delante y os deseo lo mejor a los dos.

La casualidad y la ciencia hicieron que me reencontrara con Saray en el Ateneu de Barcelona allá por 2013. ¡Quién me iba a decir lo que iba a venir después! Gracias por llevarme de paseo a la montaña. Y por hacer que aparecieran Pablo, Mar, María, Marcos, Marc, Bea, Irene, David y Ricard. ¡Gracias chicos por compartir montaña, teatro, cervezas y algo de ciencia durante estos años!

Pablo fue el causante de mi aterrizaje en Vilanova y no puedo olvidar a Pili, Miguel y Maria, que me han hecho sentir una más de la familia desde el primer día. Gracias por vuestro cariño y atenciones y por hacer que me sienta una vilanovina más.

Y ahora llegan los que realmente han estado afectados por el día a día de esta tesis, algunos a nivel profesional y otros a nivel personal. A Elisa, que me conquistó el primer día con su energía arrolladora y que me dio una segunda oportunidad en la ciencia. A Gwen, por tu generosidad infinita. Gracias por tu esfuerzo, tu dedicación y tus fuerzas para tirar de este proyecto. Gracias por poner orden al caos y hacerlo con la mayor tranquilidad y lógica posible. Gracias por ser el culpable de to-

das las buenas ideas que ha habido en este proyecto. Eres un grandísimo investigador. Te debo gran parte de esta tesis. A mis compis de labo durante estos años: Sus, Ele, Jose, Mu, Ireni, René y Angie. A Sus, sin la cual el 80% de los experimentos de esta tesis hubieran fracasado. Gracias por tu amabilidad, por tu disponibilidad y por tu ayuda inestimable. Y por ayudarme a mantener la calma cuando yo no podía. A Ele, qué contenta estoy de terminar contigo amiga! Gracias por tu energía y alegría, por tus canciones, tus infinitos “¿Qué preferirías?”, por llevarme a bailar y por enseñarme a disfrutar un poquito más de las cosas. A Jose, que siempre está a mano para ofrecer buenas ideas, buena conversación o demostrarnos que nunca es tarde para ser joven. Ánimo amigo, eres un crack! A Mu, siempre disponible para animar el labo, te deseo muchísima suerte en la nueva etapa que empiezas. A los pollitos que ya volaron del nido pero que también han sido fundamentales en esta historia Irene, René y Angie. A Irene, que es una amiga genial, llena de buenas ideas y consejos. A René con el que compartí mi llegada al labo y gracias amigo por los ratos juntos. A Angie y su sonrisa contagiosa, de la que heredé parcialmente el proyecto cuando llegué. Mi día a día no hubiera sido igual sin todos vosotros, ¡Muchísimas gracias!

Al grupo de Cinzia Lavarino en el Sant Joan de Dèu, muy especialmente a Cinzia, Sole y Mònica, que han dedicado parte de su tiempo a esta tesis. Muchas gracias por vuestra disponibilidad y amabilidad. Unos cuantos experimentos de esta tesis son totalmente vuestros. A la gente de los labos de Sebastián, Marian y Mariona: Toni, Blanca, Anhara, Andrea, Raquel, Stella, Simona, Marta, Mariajo, Sonia, Isa, Alex y a los jefes. Por estar siempre disponibles para resolver dudas científicas y por compartir cervezas, alegrías y algún disgusto durante estos años. Gracias a Mariajo por su generosidad infinita, por ser una gran científica y por dejarme compartir ese proyecto tan bonito que es Biocomunicat. ¡Os deseo mucha suerte a todos! Finalmente al resto de miembros del IBMB sobre todo a Elena y Jaume, cuya ayuda en el servicio de microscopía es inestimable, y a los miembros del servicio de citometría de la UB (Jaume y Sonia).

A Pablo, con el que he compartido casi todo este viaje y con el que compartiré el que vendrá. Gràcies per ballar amb mi des del primer dia, encara que la música no sempre sigui bonica. Gràcies per fer-me agafar la lluna amb un cove. Només em queda desitjar allò que diu la cançó: [...] si véns amb mi, no demanis un camí planer, ni estels d'argent, ni un demà ple de promeses, sols un poc de sort, i que la vida ens doni un camí ben llarg. Gràcies!

PD. Estas líneas también están escondidas por una razón más práctica y es que es imposible no desnudarse un poquito en ellas y como saben algunas de las personas que aparecen, me puede la timidez ☺





